**Politechnika Gdańska**

**Wydział Elektroniki,
Telekomunikacji i Informatyki**

| | |
|---|---|
| **Katedra:** | Microwave and Antenna Technique |
| **Imię i nazwisko dyplomanta:** | Ana Hernández Martínez |
| **Nr albumu:** | 159138 |
| **Forma i poziom studiów:** | Title of Telecommunication Engineering |
| **Kierunek studiów:** | Informatyka |

# Praca dyplomowa magisterska

**Temat pracy:**
Finite Difference Method in Electromagnetic Problems

**Kierujący pracą:**
dr. inz Piotr Kowalczyk

**Zakres pracy:**
Electromagnetic Theory

Gdańsk, 2014-15

# Contents

# Gratitude

En primer lugar, hacer una mención especial a mi supervisor, dc. Piotr Kowalzcyk, quien me ha ayudado y aconsejado durante todo el proyecto.

A Jose Luis Gómez Tornero, mi director de proyecto, al que quiero agradecer su tiempo, sus consejos y su cercanía durante toda la carrera.

Asimismo, agradecer a todos y cada uno de los docentes con los que he coincidido durante mi trayectoria universitaria, de los que me llevo algo que me ha ayudado a mejorar.

Por supuesto, mencionar a quien me ha aportado su ayuda y sus conocimientos durante todo este año y a quien le debo gran parte de lo conseguido, Javier Díaz.

A mis padres y a mi hermana que han sabido apoyarme y decirme las palabras exactas para no rendirme. A ellos les debo estar donde estoy y ser lo que soy.

Y, por último, a ti Antonio, por ser mi apoyo cada día, por ayudarme, por quererme y por darme la fuerza necesaria para conseguir llegar hasta el final.

# Chapter 1

# Introduction

## 1.1 History and origin of this project

This document is concerning the final project of telecommunication engineering. The problem which will be presented is focused on Finite Difference Method (FDM). This method is one of the most flexible and general techniques, so it is commonly used in analysis and designing of microwave and optical devices (also in comercial softwares).

Firstly, it is important to know that the theory of electromagnetic field is a very wide area and each region must be studied with specific tools. Although it should be explained each electromagnetic wave, it will be presented the concept of microwave. The field of radio frequency (RF) and Microwave engineering generally covers the behaviour of alternating current signals with frequencies in the range of 100 MHz to 1000 GHz . RF frequencies range from very high frequency (VHF) (30-300 MHz) to ultra high frequency and (UHF) (300-3000 MHz), while the term microwave is typycally used for frequencies between 3 and 300 GHz, with a corresponding electrical wavelength between $\lambda$ , respectively. Because of the high frequencies (and short wavelengths), standard circuit theory often cannot be used directly to solve microwave network problems. In a sense, standard circuit theory is an approximation, or special case, of the broader theory of electromagnetics as described by Maxwell's equations. This is due to the fact that, in general, the lumped circuit element approximations of circuit theory may not be valid at high RF and microwave frequencies. microwave components often act as distributed elements, where the phase of the voltage or current changes significantly over the physical extent of the device because the device dimensions are on the order of the electrical wavelength. At much lower frequencies the wavelength is large enough that there is insignificant phase variation across the dimensions of a component. In RF and microwave engineering, then, one must often work with Maxwell's equations and their solutions. It is in the nature of these equations that mathematical complexity arises since Maxwell's equations involve vector differential or integral operations on vector field quantities, and these fields are functions of spatial coordinates. In such problems numerical analysis is convenient. A field theory solution generally provides a complete description of the electromagnetic field at every point in space, which is usually much more information than we need for most practical purposes. It is this complexity that adds to the challenge, as well as the rewards, of microwave engineering. [4]

For a brief description of what is this kind of analysis, numerical analysis is considered a branch of mathematics whose boundaries are not entirely accurate. Firmly, it can be defined as the discipline employed to describe, analyze and create some numerical algorithms that allow us to solve mathematical problems in which numerical quantities are involved , with a given (determined) accuracy.

In the context of numerical calculation, an algorithm is a procedure that can lead us to an approximate solution of a problem by a finite number of steps that can be performed logically.

In some cases, the name given is constructive methods numerical algorithms. The numerical analysis is particulary important with the advent of computers. Computers are useful for complex mathematical calculations but ultimately operate with binary numbers and simple mathematical operations.

From this point of view, the numerical analysis is necessary to carry out all those mathematical procedures to express algorithmicaly numerical analysis based on algorithms that allow simulation or calculation using simpler processes with numbers. From here an additional concept,the error, appears in consequence of the finite nature of computers which only can operate with finite numbers, therefore it is the difference between identical results and results closest that is possible to obtain with the discrete numerical system in a computer. In general, these methods are applied when a numeric value is required as a solution of a mathematical problem. In this case, analytical or accurate procedures (theory of differential equations, integration methods, etc) are unable to get a response. Due to this,the procedures are frequently used by engineers and physicists which progress has been fortunate because of need to obtain solutions although they are not completely accurate. On the other hand, the rise of numerical analysis has been due to the development of computers. The large increase in computing power has done possible to use efficient algorithms which are difficult by hand. [5]

The problems can be classified into many types. If the classification is according to the size:

- Finite dimension: those whose response is a finite set of numbers, like a algebraic equation, eigenvalue problems, etc.
- Infinite dimension: problems whose solution or approach involved elements described by an infinite amount of numbers, as numerical integration and derivation, interpolation, etc.

There are different numerical methods, among which include:

- Generalized Method of Moments (GMM)

  Today, the method of moments is one of the most used numerical methods to determine fields emitted o received by radiating structures. In the first case, an external source provides a current variable over time in the antenna conductors, and the fields generated are calculated by them (transmitting antenna) whereas in the second case, it is assumed a wave that incident on a structure and which produces inducing variable currents on time. So, in this case, it may be analyzed from the perspective of useful fem induced on the conductors (receiving antenna). The part important of this method is the linearity of Maxwell's equations is that from mathematical point of view may be represented by lineal operators who are applied to functions of spatial and time coordinates.

- Transmission Line Matrix Method

  This method was developed in 1970 to analize problems of propagation of sound waves and electromagnetics. It is a simple, intuitive and unconditionally method for modeling wave propagations due to the model is related to the physical process of propagation. In this case, the space for modeling is represented by a cartesian mesh whose nodes are connected by some electrical transmission lines. Each node of mesh represents a electrical node where must carry out the circuital equations. The model of propagation is accurate because is a passive network.

- Finite Element Method (FEM)

  This method is a general numerical method to approximate solutions of partial differential equations which are widely used in various engineering and physical problems. This method is designed to be used in computers and allows to solve differential equations associated to a physical problem of complicated geometries. This method is used to the pattern and improvement of industrial products, applications and in the simulation of complex physical

and biologic systems.The variety of problems that can be applied has increased enormously, and in this case the basic requirement is that the constitutive equations and equations of time evolution of the problem to be considered must be known in advance.

- Finite Difference Method (FD)

  Among all numerical techniques which solve the Maxwell's equations with help of a computer, the finite difference method is the one of the oldest techniques and with less analytical content. Especially, the application of this method consist of calculate the solution of original differential problem in a discrete set of points. In the finite difference method, the process of discretization is done by approximating the partial derivatives which appear in Maxwell equations in any of its versions, temporary or frecuencial, by somo finite difference operators. As a result a system of linear equations relating the fields in different network nodes is obtained.

## 1.2 Objectives

The objective of this project is to present the FDM and their numerical properties. Various programs in the Matlab environment will be presented. Firstly, it will be demostrated the validity of this method to analyse waveguides and resonant cavities of various geometries and loaded with different media. This work reviews and compares different methods of solving electromagnetic problems by means of the FDM.

The plan of this project can be specified in the following points:

- Go over the concepts of Maxwell's equations.
- Implementation of FDM in one and two dimensions using Matlab environment.
- Verification of the algorithms for a few structrures ( field distributions, resonant frequencies, cutoff frequencies, dispersion characteristics, etc ).
- Analysis of possibilities of acceleration of the method in some special courses.

Objectives:

- Both understanding electromagnetic phenomenon in microwave and optical structures due to direct solution of Maxwell (in FDM).
- Full acces to all variables and procedures.
- Possibility of arbitrary modifications of the method (dedicated software can be faster and more accurate than the commercial one).

## 1.3 Model description

At present, the comercial software for simulation of applied electromagnetics problems is an important tool for designers of any electrical device or high-speed optical. In fact, its use greatly goes down the progress time and allows savings of resources because in the past, the prototypes had to be made and at the same time were perfomed numerous experimental tests. In such a way that the simulators have become an essential element in any research project, design and development. Nowadays, the advance of optical engineering and radiofrequency are inconceivable without these tools. That simulators are supported by electromagnetic computing machines which are based on numerical methods to solve Maxwell's equations.

The importante of knowledge about this type of numerical methods is linked to the ability to create a wide variety of specific software tools which can be perfectly adapted to needs of any project due to in comercial programs usually are not concerning problems with very particular characteristics. In addition, another advantage of studying numerical methods is that the overview about how to perform the commercial programs has been increased and how to make numerical approximations and error sources have allowed an more efficient use. Noticing their weakness and limitations, the correct choice of calculation tools is reached and its potential is massively increased in according with requirements of each application. By having detailed knowledge of the bases, as the numerical algorithms and their programming, the current tools will be improved and it will be generated national original technology.

Finite Difference allow solving in an intuitive way the equations that govern most of the physical behavior, in mechanic and so as in electromagnetic. The aim of this project is to solve the algebraic equations remaining after the implementation of the method, and in that way to achieve the results which provides the solution that can be used to solve different electromagnetic magnitudes, such as electrical field, electromagnetic problems. The aim of being able to calculate is being capable of kwon the right measures that pass the required specifications. The main task of the project consist of adapt the equations that model the electromagnetic behavior, into a solution that a program like MATLAB can solve. After a first period of a learning about the mathematics that describe the finite difference method, it is decided how the formulation will be done in order to get the results that best fits into they are expected, no in the point of view of the accuracy, but the computational efficiency and save time, so to achieve that you must to choose the sort of element in that the problem will be divided. That will be a great help to those that want to take advantage of this project to implement other functions based on post procces that allows evaluating the solutions of the problems.

### 1.3.1 Maxwell equations

The whole subject of electromagnetic unfolds as a logical deduction from eight postulated equations, namely, Maxwell's four field equations and four medium-depedent equations. Before we review these equations, it may be hepful to state two important theorems commonly used in electromagnetics.

- The divergence or Gauss's theorem

$$\oint_{\vec{S}} \vec{F} \cdot d\vec{S} = \int_v \nabla \cdot \vec{F}\, dv \tag{1.1}$$

  where $S$ is a closed surface and surrounding volume $V$.

- Stokes's theorem

$$\oint_L \vec{F} \cdot d\vec{l} = \int_S \nabla \times \vec{F} \cdot d\vec{S} \tag{1.2}$$

  where L is a boundary of surface.

The best way to review electromagnetic theory is by using the fundamental concept of electric charge. Electromagnetic theory can be regarded as the study of fields produced by electric charges at rest and in motion. Electrostatic fields are usually produced by static electric charges, whereas magnetostatic fields are due to motion of electric charges with uniform velocity (direct current). Dynamic or time-varying fields are usually due to accelerated charges or time-varying currents.

### Electrostatic fields

The two fundamental laws governing these electrostatic fields are Gauss's law,

$$\oint_S \vec{D} \cdot d\vec{S} = \int_V \rho_v \, dV \tag{1.3}$$

which is a direct consequence of Coulomb's force law, and the law describing electrostatic fields as conservative,

$$\oint_L \vec{E} \cdot d\vec{l} = 0 \tag{1.4}$$

In equations (1.3) and (1.4) there are different letters which are defined as:

- $\vec{D}$ is the electric flux density, in coulombs per meter squared ($C/m^2$).
- $\rho_v$ is the electric charge density, in coulombs per meter cubed ($C/m^3$).
- $\vec{E}$ is the electric field, in volts per meter (V/m).

The integral form of the laws in equations (1.3) and (1.4) can be expressed in the differential form by applying equation (1.1) to equation (1.3) and equation (1.2) to (1.4). Due to this, it is obtained:

$$\nabla \cdot \vec{D} = \rho_v \tag{1.5}$$

and

$$\nabla \times \vec{E} = 0 \tag{1.6}$$

The vector fields $\vec{D}$ and $\vec{E}$ are related as

$$\vec{D} = \epsilon \vec{E} \tag{1.7}$$

where $\epsilon$ is the dielectric permitivity (in F/m) of the medium. If case of free space, $\epsilon_0 = 8,85 \cdot 10^{-}12$ F/m . In terms of the electrical potential (V), $\vec{E}$ is expressed as

$$\vec{E} = -\nabla V \tag{1.8}$$

or in the same case as

$$V = -\int \vec{E} \cdot d\vec{l} \tag{1.9}$$

Combining equations (1.5), (1.7), and (1.8) is given Poisson's equation:

$$\nabla \cdot \epsilon \nabla V = -\rho_v \tag{1.10}$$

or, if $\epsilon$ is constant,

$$\nabla^2 V = -\frac{\rho_v}{\epsilon} \tag{1.11}$$

When $\rho_v = 0$ , equation (1.10) becomes Laplace's equation:

$$\nabla \cdot \epsilon \nabla V = 0 \tag{1.12}$$

or for constant $\epsilon$

$$\nabla^2 V = 0 \tag{1.13}$$

**Magnetostatic fields**

The basic laws of magnetostatic fields are Ampere's law

$$\oint_L \vec{H} \cdot \vec{dl} = \int_S \vec{J} \cdot \vec{dS} \tag{1.14}$$

which is related to Biot-Savart law and the law of conservation of magnetic flux:

$$\oint_S \vec{B} \cdot \vec{dS} = 0 \tag{1.15}$$

In the same way, we can defined different letters like:

- $\vec{H}$ is the magnetic field, in amperes per meter (A/m).
- $\vec{J}$ is the electric current density, in amperes per meter squared (A/m2).
- $\vec{B}$ is the magnetic flux density, in webers per meter squared (Wb/m2).

Applying equation (1.2) to (1.12) and equation (1.1) to (1.13) yields their differential form as

$$\nabla \times \vec{H} = \vec{J_e} \tag{1.16}$$

and

$$\nabla \cdot \vec{B} = 0 \tag{1.17}$$

The vector fields $\vec{B}$ and $\vec{H}$ are related through the permeability $\mu$ (in H/m) of the medium as

$$\vec{B} = \mu \vec{H} \tag{1.18}$$

If it is related to free space, the equation (1.18) should be

$$\vec{B} = \mu_0 \vec{H} \tag{1.19}$$

where $\mu_0 = 4\pi \cdot 10^7$ H/m is the permeability of free-space.
In addition, $\vec{J}$ is related to $\vec{E}$ through the conductivity $\sigma$ (in $\Omega$/m) of the medium as

$$\vec{J} = \sigma \vec{E} \tag{1.20}$$

This is usually referred to as point form of Ohm's law. In terms of the magnetic vector potential $\vec{A}$ in Wb/m

$$\vec{B} = \nabla \times \vec{A} \tag{1.21}$$

Applying the vector identity

$$\nabla \times (\nabla \times \vec{F}) = \nabla(\nabla \cdot \vec{F}) - \nabla^2 \vec{F} \tag{1.22}$$

to equations (1.16) and (1.21) and assuming Coulomb gauge condition ( $\nabla \cdot \vec{A} = 0$ ) leads to Poisson's equation for magnetostatic fields: [1]

$$\nabla^2 \vec{A} = -\mu \vec{J} \tag{1.23}$$

When J = 0, equation (1.20) becomes Laplace's equation

$$\nabla^2 \vec{A} = 0 \tag{1.24}$$

**Time-varying Fields**

In this case, electric and magnetic fields exist simultaneously. After we review all magnetic and electrical equations, we can focus on Maxwell's equations with the objective to understand all previous equations. It is necessary to incorporate Faraday's law so equations (1.5) and (1.15) remain the same whereas equations (1.6) and (1.14) requires some modification for dynamic fields. In case of equation (1.6) Faraday's law of induction and in equation (1.14) is warranted to allow for displacement current. The time-varying electromagnetic fields are governed by physical laws expressed mathematically as

$$\nabla \cdot \vec{D} = \rho v \tag{1.25}$$

$$\nabla \cdot \vec{B} = 0 \tag{1.26}$$

$$\nabla \times \vec{E} = -\frac{\partial \vec{B}}{\partial t} - \vec{J_m} \tag{1.27}$$

$$\nabla \times \vec{H} = \vec{J_e} + \frac{\partial \vec{D}}{\partial t} \tag{1.28}$$

where $\vec{J_m} = \sigma * \vec{H}$ is the magnetic conductive current density (in $\mathrm{V}/m^2$ and $\sigma*$ is the magnetic resistivity (in $Omega$/meter). These equations are referred to as Maxwell's equations in the generalized form. They are first-order linear coupled differential equations relating the vector field quantities to each other. The equivalent integral form of equations (1.25) to (1.28) are

$$\oint_S \vec{D} \cdot d\vec{S} = \int_v \rho_v \, dV \tag{1.29}$$

$$\oint_S \vec{B} \cdot d\vec{S} = 0 \tag{1.30}$$

$$\oint_L \vec{E} \cdot d\vec{l} = -\int_S (\frac{\partial \vec{B}}{\partial t} + \vec{J_m}) \cdot d\vec{S} \tag{1.31}$$

$$\oint_L \vec{H} \cdot d\vec{l} = \int_S (\vec{J_e} + \frac{\partial \vec{D}}{\partial t}) \cdot d\vec{S} \tag{1.32}$$

In addition to these four Maxwell's equations, there are four medium-dpendent equations

[1] there are also others gauges as eq.Lorentz

$$\vec{D} = \epsilon \vec{E} \tag{1.33}$$

$$\vec{B} = \mu \vec{H} \tag{1.34}$$

$$\vec{J_e} = \sigma \vec{E} \tag{1.35}$$

$$\vec{J_m} = \sigma * \vec{M} \tag{1.36}$$

There are called constitutive relations for the medium in which the fields exist. Equations (1.22) and (1.24) form the eight postulated equations on which electromagnetic theory unfolds itself. On the other hand it is necessary to review an important concept in electromagnetism which is related with Maxwell equations. This is Lorentz force equation

$$\vec{F} = Q(\vec{E} + \vec{u} \times \vec{B}) \tag{1.37}$$

where $\vec{F}$ is the force experienced by a particle with charge Q moving with velocity $\vec{u}$ in an electromagnetic field; the Lorentz force equation constitutes a link between electromagnetic and mechanics. The other is the continuity equation:

$$\nabla \cdot \vec{J} = -\frac{\partial \rho_v}{\partial t} \tag{1.38}$$

which expresses the conservation of electric charge. The continuity equation is implicit in Maxwell's equations. [2]

### 1.3.2 Fields in media and boundary conditions

In the preceding section it was assumed that the electric and magnetic fields were in free space, with no materials bodies present. In practice, material bodies are often present,this complicates the analysis but also allows the useful application of material properties to microwave components. When electromagnetic fields exist in material media, the field vectors are related to each other by the constitutive relations. For a dielectric material, an applied electric field $\vec{E}$ causes the polarization of the atoms or molecules of the material to create electric dipole moments that augment the total displacement flux, $\vec{D}$ . This additional polariation vector is called $\vec{P}_e$ , the electric polarization, where

$$\vec{D} = \epsilon_0 \vec{E} + \vec{P}_e \tag{1.39}$$

In a linear medium the electric polarization is linearly related to the applied electric field as

$$\vec{P}_e = \epsilon_0 \chi_e \vec{E} \tag{1.40}$$

where $\chi_e$, which may be complex, is called the electric susceptibility. Then,

$$\vec{D} = \epsilon_0 \vec{E} + \vec{P}_e = \epsilon_0 (1 + \chi_e) \vec{E} = \epsilon \vec{E} \tag{1.41}$$

where

[2] In fluid mechanics, where $\vec{J}$ corresponds with velocity and $\rho_v$ with mass, equation (1.26) expresses the law of conservation of mass

$$\epsilon = \epsilon_0(1 + \chi_e) \tag{1.42}$$

which is Ohm's law as we know.

On the other hand, it was assumed that $\vec{P}_e$ was a vector in the same direction as $\vec{E}$. Such materials are called isotropic materials, but not all materials have this property. Some materials are anisotropic and are characterized by a more complicated relation between $\vec{P}_e$ and $\vec{E}$ , or $\vec{D}$ and $\vec{E}$. The most general linear relation between these vectors takes the form of a tensor of rank two, which can be written in matrix form as

$$\begin{bmatrix} D_x \\ D_y \\ D_z \end{bmatrix} = \begin{bmatrix} \epsilon_x x & \epsilon_x y & \epsilon_x z \\ \epsilon_y x & \epsilon_y y & \epsilon_y z \\ \epsilon_z x & \epsilon_z y & \epsilon_z z \end{bmatrix} \begin{bmatrix} E_x \\ E_y \\ E_z \end{bmatrix} = \begin{bmatrix} \epsilon \end{bmatrix} \begin{bmatrix} E_x \\ E_y \\ E_z \end{bmatrix}$$

It thus seen that a given vector component of $\vec{E}$ gives rise, in general, to three components of $\vec{D}$. Crystal structures and ionized gases are examples of anisotropic dielectrics. For a linear isotropic material, the matrix of () reduces to a diagonal matrix with elements $\epsilon$.

An analogous situation occurs for magnetic materials. An applied magnetic field may align magnetic dipole moments in a magnetic material to produce a magnetic polarization ( or magnetization ) $\vec{P}_m$. Then,

$$\vec{B} = \mu_0(\vec{H} + \vec{P}_m) \tag{1.43}$$

For a linear magnetic material, $\vec{P}_m$ is linearly related to $\vec{H}$ as

$$\vec{P}_m = \chi_m \vec{H} \tag{1.44}$$

where $\chi_m$ is a complex magnetic susceptibility. Then,

$$\vec{B} = \mu_0(1 + \chi_m)\vec{H} = \mu\vec{H} \tag{1.45}$$

where $\mu = \mu_0(1 + \chi_m)$ is the permeability of the medium. As in the electric case, magnetic materials may be anisotropic, in wich case a tensor permeability can be written as

$$\begin{bmatrix} B_x \\ B_y \\ B_z \end{bmatrix} = \begin{bmatrix} \mu_x x & \mu_x y & \mu_x z \\ \mu_y x & \mu_y y & \mu_y z \\ \mu_z x & \mu_z y & \mu_z z \end{bmatrix} \begin{bmatrix} H_x \\ H_y \\ H_z \end{bmatrix} = \begin{bmatrix} \mu \end{bmatrix} \begin{bmatrix} H_x \\ H_y \\ H_z \end{bmatrix}$$

An important example of anisotropic magnetic materials in microwave engineering is the class of ferromagnetic materials known as ferrites.

### Fields at General Material Interface

It is considered a plane interface between two media, as shown in Figure 1.1. Maxwell's equations in integral form can be usea to deduce conditions involving the normal and tangential fields at this interface.

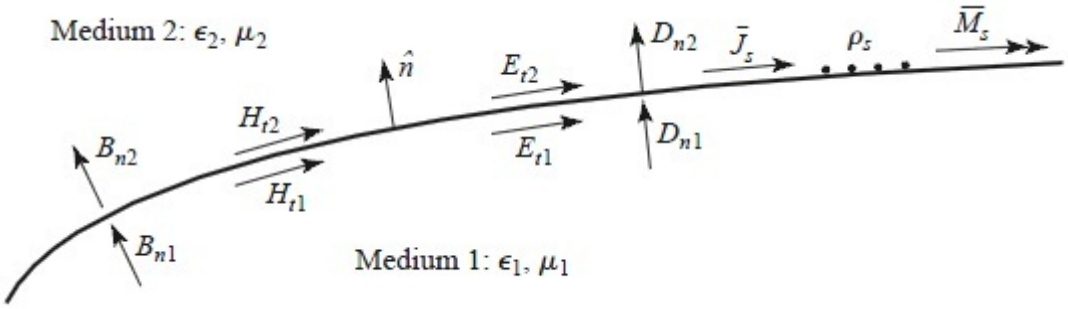


Figure 1.1: Fields, currents and surface charge at a general interface between two media

Let us start from equation (1.3), where S is the closed "pillbox" surface shown in Figure 1.2,

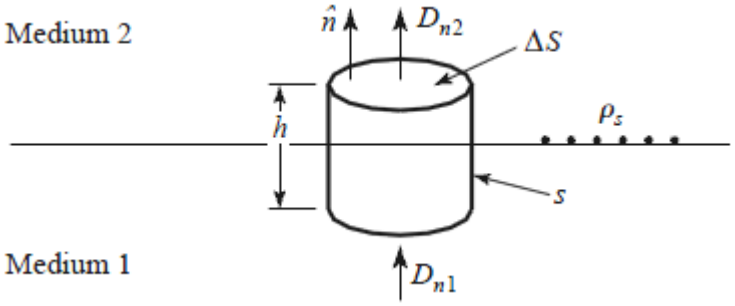


Figure 1.2: Closed surface S for equation 1.47

$$\oint_S \vec{D} \cdot \vec{ds} = \int_V \rho \, dv \tag{1.46}$$

In the limit as h $\rightarrow$ 0, the contribution of electrical flux through the sidewalls goes to zero, so (1.47) reduces to

$$\vec{D_2} \cdot \triangle S\hat{n} + \vec{D_1} \cdot (- \triangle S\hat{n}) = \triangle S \cdot \rho_s \tag{1.47}$$

or

$$D_{2n} - D_{1n} = \rho_s \tag{1.48}$$

where $\rho_s$ is the surface charge density on the interface and $\hat{n}$ is a vector directed for medium 1 to medium 2. $D_{1n}$ and $D_{2n}$ are normal components of the field in 1 and 2 medium, respectively. In vector form, we can writer

$$\hat{n} \cdot (\vec{D}_2 - \vec{D}_1) = \rho_s \tag{1.49}$$

A similar argument for $\vec{B}$ leads to the result that

$$\hat{n} \cdot \vec{B}_2 = \hat{n} \cdot \vec{B}_1 \tag{1.50}$$

or

$$B_{2n} - B_{1n} = 0 \tag{1.51}$$

because there is no free magnetic charge.

For the tangencial components of electric field, we can look at this figure (1.3). It will be better to understand the next equations.

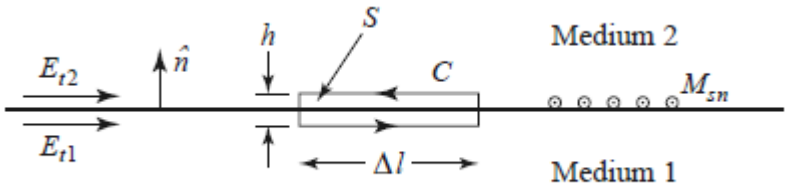


Figure 1.3: Closed contour C

From equation (1.31) boundary conditions for tangencial components of electric field interface can be obtained as

$$E_{t1} - E_{t2} = -M_s \tag{1.52}$$

which can be generalized in vector form as

$$(\vec{E}_2 - \vec{E}_1) \times \hat{n} = \vec{M}_s \tag{1.53}$$

A similar argument for the magnetic field can be obtained from equation (1.32)

$$\hat{n} \times (\vec{H}_2 - \vec{H}_1) = \vec{J}_s \tag{1.54}$$

where $\vec{J}_s$ is an electric surface current density that may exist at the interface.

### Fields at a Dielectric Interface

At an interface between two lossless dielectric materials, no charge or surface current densities will ordinarily exist. Equations (1.50), (1.51), (1.53), and (1.54) then reduce to

$$\hat{n} \cdot \vec{D}_1 = \hat{n} \cdot \vec{D}_2 \tag{1.55}$$

$$\hat{n} \cdot \vec{B}_1 = \hat{n} \cdot \vec{B}_2 \tag{1.56}$$

$$\hat{n} \times \vec{E}_1 = \hat{n} \times \vec{E}_2 \tag{1.57}$$

$$\hat{n} \times \vec{H}_1 = \hat{n} \times \vec{H}_2 \tag{1.58}$$

In words, these equations state that the normal components of $\vec{D}$ and $\vec{B}$ are continuous across the interface, and the tangential components of $\vec{E}$ and $\vec{H}$ are continuous across the interface. Because Maxwell's equations are not all linearly independent, the six boundary conditions contained in the above equations are not all linearly independent. Thus, the enforcement of (1.57) and (1.58) for the four tangential field components, for example, will automatically force the satisfaction of the equations for the continuity of the normal components.

**Fields at the interface of Perfect Electrical Conductor (PEC)**

Many problems in microwave engineering involve boundaries with good conductors (e.g., metals), which can often be assumed as lossless $\sigma \to \infty$ . In case of a perfect conductor, all electric field components must be zero inside the conducting region. This result can be seen by considering a conductor with finite conductivity $\sigma < \infty$ and noting that the skin depth (the depth to which most of the microwave power penetrates) goes to zero as $\sigma \to \infty$. If we also assume here that $\vec{M}_s = 0$, which would be the case if the perfect conductor filled all the space on one side of the boundary, then (1.50), (1.51), (1.53), and (1.54) reduce to the following:

$$\hat{n} \cdot \vec{D} = \rho_s \tag{1.59}$$

$$\hat{n} \times \vec{E} = 0 \tag{1.60}$$

where $\rho_s$ is the electric surface charge density, on the interface, and $\hat{n}$ is the normal unit vector pointing out of the perfect conductor. Such a boundary is also know as an electric wall because the tangential components of $\vec{E}$ are "shorted out," as seen from (1.61), and must vanish at the surface of the conductor.

**Fields at the interface of Perfect Magnetic Conductor (PMC)**

Dual to the preceding boundary condition is the magnetic wall boundary condition, where the tangential components of $\vec{H}$ must vanish. Such a boundary does not really exist in practice but may be approximated by a corrugated surface or in certain planar transmission line problems. In addition, the idealization that $\hat{n} \times \vec{H} = 0$ at an interface is often a convenient simplification. It is important to know that the magnetic wall boundary condition is analogous to the relations between the voltage and current at the end of an open-circuited transmission line, while the electric wall boundary condition is analogous to the voltage and current at the end of a short-circuited transmission line. The magnetic wall condition, then, provides a degree of completeness in our formulation of boundary conditions and is a useful approximation in several cases of practical interest.

The fileds at a magnetic wall satify the following conditions:

$$\hat{n} \cdot \vec{B} = 0 \tag{1.61}$$

$$\hat{n} \times \vec{H} = 0 \tag{1.62}$$

where $\hat{n}$ is the normal unit vector pointng out of the magnetic wall region.

### 1.3.3 Wave Equations

As mentioned earlier, Maxwell's equations are coupled first-orden differential equations which are difficult to apply when solving boundary-value problems. The first-order differential equations which are difficulty is overcome by decoupling the first-order equations, thereby obtaining the wave equation, a second-order differential equation which is useful for solving problems.

To obtain the wave equation for a linear, isotropic, homogeneus, source-free medium ( $\rho_v = 0$ , $\vec{J}_s = 0$ ) from equations (1.25), (1.26), (1.27) and (1.28), we take the curl of both sides of equation (1.27). This gives

$$\nabla \times \nabla \times \vec{E} = -\mu \frac{\partial}{\partial t}(\nabla \times \vec{H}) \tag{1.63}$$

From (1.28)

$$\nabla \times \vec{H} = -\epsilon \frac{\partial \vec{E}}{\partial t} \tag{1.64}$$

since $\vec{J_s} = 0$, so that equation becomes

$$\nabla \times \nabla \times \vec{E} = -\mu \frac{\partial^2 \vec{E}}{\partial t^2} \tag{1.65}$$

Applying the vector identity in equation (1.69)

$$\nabla(\nabla \cdot \vec{E}) - \nabla^2 \vec{E} = -\mu\epsilon \frac{\partial^2 \vec{E}}{\partial t^2} \tag{1.66}$$

Since $\nabla \cdot \vec{E} = 0$ from equation (1.25), and hence we obtain

$$\nabla^2 \vec{E} - \mu\epsilon \frac{\partial^2 \vec{E}}{\partial^2 t} = 0 \tag{1.67}$$

In other case, we would obtain the wave equation for H

$$\nabla^2 \vec{H} - \mu\epsilon \frac{\partial^2 \vec{H}}{\partial t^2} = 0 \tag{1.68}$$

Equations (1.71) and (1.72) are the equations of motion of electromagnetic waves in the medium under consideration. The velocity (in m/s) of wave propagation is

$$u = \frac{1}{\sqrt{\mu\epsilon}} \tag{1.69}$$

where $u = c = \frac{1}{\sqrt{\mu_0 \epsilon_0}} \approx 3 \cdot 10^8$ m/s in free space. It should be noted that each of the vector equations (1.71) and (1.72) has three scalar components, so that altogether we have six scalar equations for $E_x, E_y, E_z, H_x, H_y$ and $H_z$. Thus each component of the wave equation has the form

$$\nabla^2 \psi - \frac{1}{u^2} \frac{\partial^2 \psi}{\partial t^2} = 0 \tag{1.70}$$

which is the scalar wave equation.

### Time-varying Potentials

Although we are often interested in electric and magnetic field intensities ( E and H ), which are physically measurable quantities, it is often convenient to use auxiliary functions in analyzing an electromagnetic field. These auxiliary functions are the scalar electric potential V and vector magnetic potential $\vec{A}$. These are required to satisfy Maxwell's equations. Their derivation is based on two fundamental vector identities,

$$\nabla \times \nabla\phi = 0 \tag{1.71}$$

and

$$\nabla \cdot \nabla \times \vec{F} = 0 \tag{1.72}$$

which an arbitrary scalar field $\phi$ and vector field F must satisfy. Maxwell's equation (1.26) along with equation (1.75) is satisfied if we define A such that

$$\vec{B} = \nabla \times \vec{A} \tag{1.73}$$

Substituting this equation in (1.27) and being compatible with equation (1.35), we can choose the scalar field V such that

$$\vec{E} = -\nabla V - \frac{\partial \vec{A}}{\partial t} \tag{1.74}$$

We still need to find the solution for the potential functions. Substituting equations (1.76) and (1.77) into (1.28) and assuming a linear, homogeneus medium and applying the vector identity leads to

$$\nabla^2 \vec{A} - \nabla(\nabla \cdot \vec{A}) = -\mu \vec{J} + \mu\epsilon \frac{\partial^2 \vec{A}}{\partial^2 t} + \mu\epsilon \nabla \frac{\partial V}{\partial t} \tag{1.75}$$

Finally, we obtain

$$\nabla^2 V + \frac{\partial}{\partial t} \nabla \cdot \vec{A} = -\frac{\rho_v}{\epsilon} \tag{1.76}$$

According to the Helmholtz theorem of vector analysis, a vector is uniquely defined if and oly if both its curl and divergence are specified. If we use the Lorentz condition

$$\nabla \cdot \vec{A} = -\mu\epsilon \frac{\partial V}{\partial t} \tag{1.77}$$

Incorporating this condition with these equations, the results are

$$\nabla^2 \vec{A} - \mu\epsilon \frac{\partial^2 \vec{A}}{\partial t^2} = -\mu \vec{J} \tag{1.78}$$

and

$$\nabla^2 V - \mu\epsilon \frac{\partial^2 V}{\partial t^2} = -\frac{\rho_v}{\epsilon} \tag{1.79}$$

which are inhomogeneous wave equations.

### 1.3.4 Applications in microwave and optical engineering

The method of this project is a general technique which can be appiled to solve different electromagnetic structures as can be: cylyndrical, rectangular waveguide and optical fibers, resonators.

Among optical waveguides, only a few structures such as slab waveguides and step-index optical fibers can be solved analytically. For more complex waveguide structures, rigorous numerical methods have been proposed including both finite element methods and finite difference (FD) methods.

For instance, propagation of light through Optical fiber is governed by Partial Differential Equations (PDEs). Numerical solution to Partial Differential Equations has drawn a lot of research interest recently. Multiwavelet based methods are among the latest techniques in such problems. FDM, powered by its simplicity is considered as one among the popular methods available for the numerical solution of PDEs. But this technique fails to produce better result in problems like propagation of light pulses in a fiber medium, due to the presence of sharp variation in the intensity

of light over a small section of the fiber. In such cases, to achieve a given accuracy FDM techniques require very small grid size throughout the region of interest. This results in high computational overhead.

A class of dielectric waveguide structures using a rectangular dielectric strip in conjunction with one or more layered dielectrics is analyzed with a finite-difference method formulated directly in terms of the wave equation for the transverse components of the magnetic field. It leads to an eigenvalue problem where the nonphysical, spurions modes do not appear. Moreover, the analysis includes hybrid-mode conversion effects, such as complex waves, at frequencies where the modes are not yet completely bonnd to the core of the highest dielectric constant, as well as at frequencies below cutoff. Dispersion characteristic examples are calculated for structures suitable for millimeter-wave and optical integrated circuits, such as dielectric image lines, shielded dielectric waveguides, insulated image guides, ridge guides, and inverted strip, channel, strip-slab, and indiffused inverted ridge guides. The numerical examples are verified by results available from other methods.

Analysis of EM fields is required in designing microwave/optical devices/components (waveguides, resonators, filters, couplers, phase shifters, etc). As it shown in previous paragraph PDE must be considered circuit model theory can not describe full such phenomenon. Only simple structures can be analyzed analytically in general numerical methods which must be performed.

FDM is based directly on Maxwell equations so it is very flexible and universal, therefore it is commonly used also in commercial software. Moreover, educational aspect of this method can not be omitted.

# Chapter 2

# Fundamental concept of Finite Difference Method

## 2.1 Introduction

It is rare for real-life electromagnetics problems to fall neatly into a class that can be solved by the analytical methods presented in the preceding chapter. Classical approaches may fail if:

- The PDE is not linear and cannot be linearized without seriously affecting the result.
- The solution region is complex.
- The boundary conditions are of mixed types.
- The medium is inhomogeneous or anisotropic.

Whenever a problem with such complexity arises, numerical solutions must be employed. Of the numerical methods available for solving PDEs, those employing finite differences are more easily understood, more frequently used, and more universally applicable than any other. The finite difference method was first developed by A. Thom in the 1920s under the title "the method of squares" to solve nonlinear hydrodynamic equations. Since then, the method has found applications in solving different field problems. The finite difference techniques are based upon approximations which permit replacing differential equations by finite difference equations. These finite difference approximations are algebraic in form; they relate the value of the dependent variable at a point in the solution to the values at some neighboring points. Thus a finite difference solution basically involves three steps:

1. Dividing the solution region into a grid of nodes.
2. Approximating the given differencial equation by finite difference equivalent that relates the dependent variable at a point in the solution region to its values at the neighboring points.
3. Solving the difference equations subject to the prescribed boundary conditions and/or initial conditions.

Before finding the finite difference solutions to specific PDEs, we will look at how one constructs finite difference approximations form a given differential equation. This essentially involves derivatives numerically. Given a function f(x), we can approximate its derivative, slope or the tangent at P by the slope of the arc PB, giving the forward- difference formula,

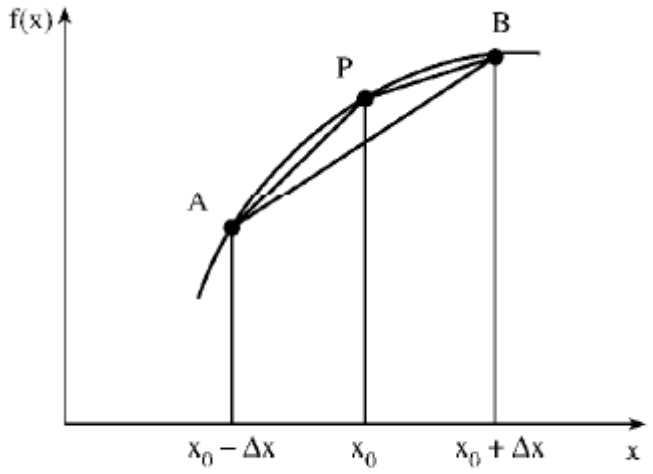


Figure 2.1: Estimates for the derivative of f(x) at P using forward, backward, and central differences

$$f'(x_o) \simeq \frac{f(x_o + \triangle x) - f(x_o)}{\triangle x} \tag{2.1}$$

We can also estimate the second derivative of f(x) at P as

$$f"(x_o) \simeq \frac{f(x_o + \triangle x) - 2f(x_o) + f(x_o - \triangle x)}{(\triangle x)^2} \tag{2.2}$$

Any approximation of a derivative in terms of values at a discrete set of points is called finite difference approximation.

The approach used above in obtaining finite difference approximations is rather intuitive. A more general approach is using Taylor's series. According to the well-known expansion,

$$f(x_o + \triangle x) = f(x_o) + \triangle x f'(x_o) + \frac{1}{2!}(\triangle x)^2 f"(x_o) + \ldots \tag{2.3}$$

and

$$f(x_o - \triangle x) = f(x_o) - \triangle x f'(x_o) + \frac{1}{2!}(\triangle x)^2 f"(x_o) - \ldots \tag{2.4}$$

Upon adding these expansions,

$$f(x_o + \triangle x) + f(x_o - \triangle x) = 2f(x_o) + (\triangle x f'(x_o))^2 f"(x_o) + O(\triangle x)^4 \tag{2.5}$$

where $O(\triangle x)^4$ is the error introduced by truncating the series. We say that this error is of the order $(\triangle x)^4$. Assuming these terms:

$$f'(x_o) \simeq \frac{f(x_o + \triangle x) - f(x_o - \triangle x)}{2 \triangle x}, \triangle x << 1 \tag{2.6}$$

## 2.2 Finite Differencing of PDEs

There are some Finite Difference for each type of PDE as parabolic which is considered a simple example of a parabolic partial equation with one spatial independent variable,

$$k\frac{\partial\phi}{\partial t} = \frac{\partial^2\phi}{\partial x^2} \tag{2.7}$$

where k is a constant.

In a second case, it is considered Finite Difference of Hyberbolic PDEs as the simplest hyperbolic partial differential equation which is the wave equation of the form

$$u^2\frac{\partial^2\phi}{\partial x^2} = \frac{\partial^2\phi}{\partial t^2} \tag{2.8}$$

where u is the speed of the wave.

And the last form of finite difference are elliptic PDEs which are caracterized as Poisson's equation, which in two dimensions is given by

$$V^2\phi = \frac{\partial^2\phi}{\partial x^2} + \frac{\partial^2\phi}{\partial y^2} \tag{2.9}$$

Within the context of Finite differencing of PDEs, it has to know that there are two methods for solving the numerical solutions which are Explicit and Implicit methods. These are approaches used in numerical analysis for obtaining numerical solutions of time-dependent ordinary and partial differential equations, as is required in computer simulations of physical processes.

Explicit methods calculate the state of a system at a later time from the state of the system at the current time, while implicit methods find a solution by solving an equation involving both the current state of the system and the later one.

It is clear that implicit methods require an extra computation (solving the above equation), and they can be much harder to implement. Implicit methods are used because many problems arising in practice are stiff, for which the use of an explicit method requires impractically small time steps $\triangle t$ to keep the error in the result bounded. As a consequence, one should use an explicit or implicit method depends upon the problem to be solved.

## 2.3 Maxwell equations for harmonic amplitudes

As we know, Finite Difference Methods are based on Maxwell's equations. In this thesis Maxwell equations for harmonic amplitudes are applied.

#### Time-harmonic Fields

Previously to this point, in the first chapert, we have considered the general case of arbitrary time variation of electromagnetic fields. In many practical situations, especially at low frequencies, it is sufficent to deal with only steady-state solution of electromagnetic fields when produced by sinusoidal currents. Such fields are said o be sinusoidal time-varying or time-harmonic, that, they are vary at sinusoidal frequency $\omega$ . An arbitrary time-dependent field $\vec{F}(x,y,z,t)$ or $\vec{F}(\vec{r},t)$ can be expressed as

$$\vec{F}(\vec{r},t) = Re[\vec{F}_s(\vec{r})e^{j\omega t}] \tag{2.10}$$

where $\vec{F}_s = \vec{F}_s(x, y, z)$ is the phasor form of F(r,t) and is in general complex, Re() indicates "taking a real part of" quantity in brackets, and $\omega$ is the angular frequency (in rad/s) of the sinusoidal excitation. The electromagnetic field quatities can be represented in phasor notation as

$$\begin{bmatrix} E(r,t) \\ D(r,t) \\ H(r,t) \\ B(r,t) \end{bmatrix} = Re\left( e^{j\omega t} \begin{bmatrix} E_s(r) \\ D_s(r) \\ H_s(r) \\ B_s(r) \end{bmatrix} \right)$$

Using the phasor representation allows us to replace the time derivations $\frac{\partial}{\partial t}$ by $j\omega$ since

$$\frac{\partial e^{j\omega t}}{\partial t} = j\omega e^{j\omega t} \tag{2.11}$$

Thus Maxwell's equations, in sinusoidal steady state, become

$$\nabla \cdot \vec{D}_s(r) = \rho_{vs} \tag{2.12}$$

$$\nabla \cdot \vec{B}_s(r) = 0 \tag{2.13}$$

$$\nabla \times \vec{E}_s(r) = -j\omega \vec{B}_s(r) \tag{2.14}$$

$$\nabla \times \vec{H}_s(r) = \vec{J}_s(r) + j\omega \vec{D}_s(r) \tag{2.15}$$

where $\vec{D}_s(r) = \epsilon \vec{E}_s(r)$ and $\vec{B}_s(r) = \mu \vec{H}_s(r)$.

The effect of the time-harmonic assumption is to eliminate the time dependence from Maxwell's equations, thereby reducing the time-space dependence to space dependence only. This simplification does not exclude more general time-varying fields if we consider $\omega$ to be one element of an entire frequency spectrum, with all the Fourier components superposed.

Replacing the time derivative in equation (1.74) by $(j\omega)^2$ yields the scalar wave equation in phasor representation as

$$\nabla^2 \psi + k^2 \psi = 0 \tag{2.16}$$

where k is the propagation constant (in rad/m), given by

$$k = \frac{\omega}{u} = \frac{2\pi f}{u} = \frac{2\pi}{\lambda} \tag{2.17}$$

We recall that equations (1.71) to (1.74) were obtained assuming that $\rho_v = 0 = \vec{J}$. If $\rho_v \neq 0 \neq J$, equation (2.16) will have the general form as

$$\nabla^2 \psi + k^2 \psi = g \tag{2.18}$$

We notice that this Helmholtz equation reduces to

1. Poisson's equation

$$\nabla^2 \psi = g \tag{2.19}$$

when k = 0.

2. Laplace's equation

$$\nabla^2\psi = 0 \tag{2.20}$$

when k = 0 = g.

Thus Poisson's and Laplace's equations are special cases of Helmholtz equation. Note that function $\psi$ is said to be harmonic if it satisfies Laplace's equation.

In this paper, the notion of electric or magnetic field is meant is often only the harmonic amplitude. Although this convention is widely accepted, but it is worth noting again that the physical scenario versus field is derived from the product of the real part of the amplitude of the harmonic factor $e^{j\omega t}$. In the cartesian coordinate system, Maxwell equations $\triangle \cdot \vec{D} = \rho_v$ and $\triangle \cdot \vec{B} = 0$ can be written in the form

$$\begin{bmatrix} 0 & -\frac{\partial}{\partial z} & \frac{\partial}{\partial y} \\ \frac{\partial}{\partial z} & 0 & -\frac{\partial}{\partial x} \\ -\frac{\partial}{\partial y} & \frac{\partial}{\partial x} & 0 \end{bmatrix} \begin{bmatrix} E_x \\ E_y \\ E_z \end{bmatrix} = -j\omega\mu_0 \begin{bmatrix} \mu_x & 0 & 0 \\ 0 & \mu_y & 0 \\ 0 & 0 & \mu_z \end{bmatrix} \begin{bmatrix} H_x \\ H_y \\ H_z \end{bmatrix} \tag{2.21}$$

$$\begin{bmatrix} 0 & -\frac{\partial}{\partial z} & \frac{\partial}{\partial y} \\ \frac{\partial}{\partial z} & 0 & -\frac{\partial}{\partial x} \\ -\frac{\partial}{\partial y} & \frac{\partial}{\partial x} & 0 \end{bmatrix} \begin{bmatrix} H_x \\ H_y \\ H_z \end{bmatrix} = j\omega\epsilon_0 \begin{bmatrix} \epsilon_x & 0 & 0 \\ 0 & \epsilon_y & 0 \\ 0 & 0 & \epsilon_z \end{bmatrix} \begin{bmatrix} E_x \\ E_y \\ E_z \end{bmatrix} + \begin{bmatrix} J_x \\ J_y \\ J_z \end{bmatrix} \tag{2.22}$$

The above form is the starting point for application of the finite difference methods.

# Chapter 3

# Finite Difference Method in one Dimension

Firstly, it will be considered the dielectric plate arranged parallel to the plane of Oyz. It is possible to suppose that the dielectric plate is $\epsilon(x)$, an the magnetic is $\mu(x)$. The system according to the imposed boundary conditions can be treated either as plano-parallel waveguide and a planar optical fiber. Supposing that the wave is carried out therein the positive direction Oz, then we can assume that the volatility of the fields in this direction represents a factor of $e^{\gamma z}$, where $\gamma = \alpha + j\beta$ ( $\alpha$ damping factor and $\beta$ coefficient of propagation).

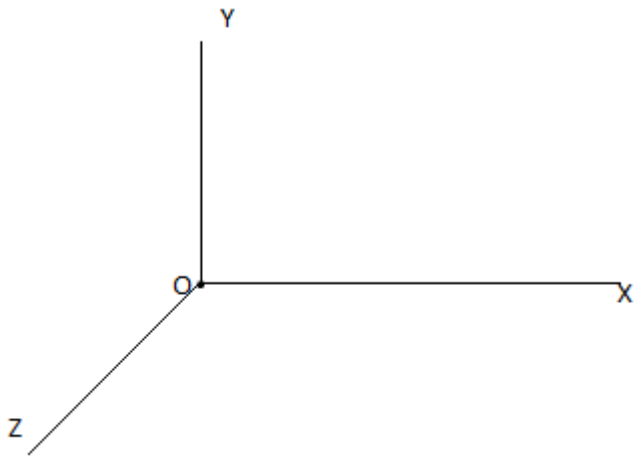


Figure 3.1: Axis

Postulating the lack of variation in the Oy axis direction fields which do not flow conduction currents ($\sigma = 0$), the above matrices can be written as:

$$\begin{bmatrix} 0 & \gamma & 0 \\ -\gamma & 0 & -\frac{\partial}{\partial x} \\ 0 & \frac{\partial}{\partial x} & 0 \end{bmatrix} \begin{bmatrix} E_x \\ E_y \\ E_z \end{bmatrix} = -j\omega\mu_0 \begin{bmatrix} \mu_x & 0 & 0 \\ 0 & \mu_y & 0 \\ 0 & 0 & \mu_z \end{bmatrix} \begin{bmatrix} H_x \\ H_y \\ H_z \end{bmatrix} \tag{3.1}$$

$$\begin{bmatrix} 0 & \gamma & 0 \\ -\gamma & 0 & -\frac{\partial}{\partial x} \\ 0 & \frac{\partial}{\partial x} & 0 \end{bmatrix} \begin{bmatrix} H_x \\ H_y \\ H_z \end{bmatrix} = j\omega\epsilon_0 \begin{bmatrix} \epsilon_x & 0 & 0 \\ 0 & \epsilon_y & 0 \\ 0 & 0 & \epsilon_z \end{bmatrix} \begin{bmatrix} E_x \\ E_y \\ E_z \end{bmatrix} \tag{3.2}$$

Obtained in this way, the system of differential equations are separated into two independent systems which include $TE$ and $TM$ polarization. In the TE one it will be taken into account that only some fields will be acceptable as $E_y$, $H_x$, $H_z$ and a special chacarteristic of TE is that $E_z = 0$. In case of TM modes, it will be taken into account only $E_x$, $E_z$ and $H_y$ will be acceptable and in this case $H_z = 0$.

- $E_x$, $H_x$ and $H_z$ $(TE)$

$$\begin{cases} -\gamma E_y = -j\omega\mu_0\mu_x H_x \\ \frac{\partial E_y}{\partial x} = -j\omega\mu_0\mu_z H_z \\ -\gamma H_x - \frac{\partial H_z}{\partial x} = j\omega\epsilon_0\epsilon_y E_y \end{cases} \tag{3.3}$$

- $E_x$, $E_z$ and $H_y$ $(TM)$

$$\begin{cases} -\gamma E_x - \frac{\partial E_z}{\partial x} = -j\omega\mu_0\mu_z H_y \\ \gamma H_y = j\omega\epsilon_0\epsilon_x E_x \\ \frac{\partial H_y}{\partial x} = j\omega\epsilon_0\epsilon_z E_z \end{cases} \tag{3.4}$$

In both cases, the problem comes down to solve their eigenvalue problems for second-order differential operator. Sometimes it is possible to solve it analytically. However, in the general case, when the $\epsilon(x)$ is arbitrary, the Finite difference method can be used. There are a lot of applications of this method in the analysis of waveguides, resonant cavities, etc ( dispersion characteristics, cutoff and resonant frequencies ($\gamma = 0$), field distributions ).

## 3.1 TE Polarization

In order to present the basic assumptions of finite difference method, it is necessary to consider a special case of the issues discussed in the previous paragraph. Assuming that the material from which the layer is formed, is non-magnetic, the solution of the TE fields generated in the structure are considered by removing the $H_x$ component of the above system. In this way, the equations (3.3) will be:

$$\begin{cases} \frac{\partial E_y}{\partial x} = -j\omega\mu_0 H_z \\ -\frac{\partial H_z}{\partial x} = (-\frac{\gamma^2}{j\omega\mu_0} + j\omega\epsilon_0\epsilon_y)E_y \end{cases} \tag{3.5}$$

The first step of the method is based on the finite difference discretization space calculation. In this case, for Ox axis is the selection of the points which will be sampled electric and magnetic field. The distance between successive points of discretization of the field will be called discretization step Figure 3.2 This concept was first proposed in 1966 by KS Yee.

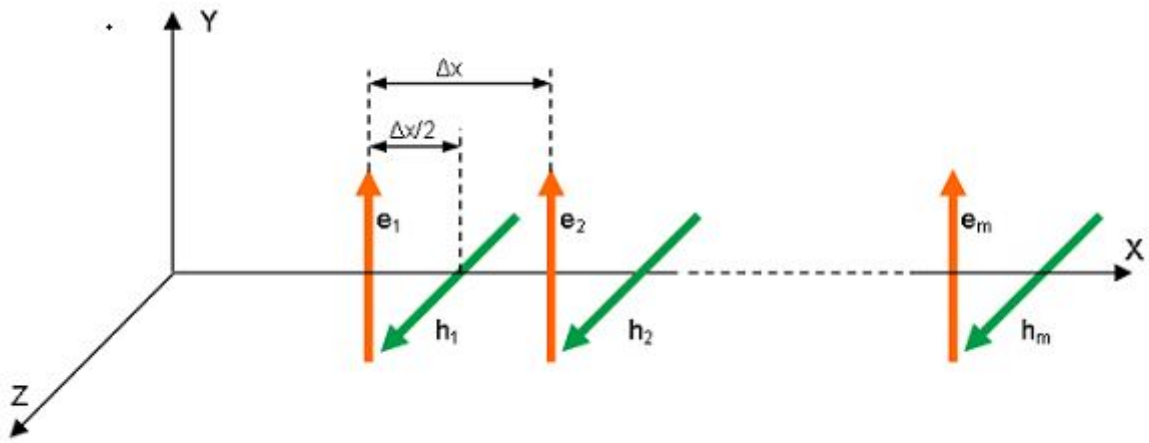


Figure 3.2: Field distribution for TE mode

The essence of the method is the finite difference approximation to the derivative of the function of the differential quotient. As it has been explained in the previous chapter, for a given function f(x), we can approximate its derivative as:

$$f'(x_o) \simeq \frac{f(x_o + \triangle x/2) - f(x_o - \triangle x/2)}{\triangle x}, \triangle x << 1 \tag{3.6}$$

Firstly, we focus our attention on TE modes which are obtained through the Maxwell's equations. If we take into account the equation (3.5) and we look at the Figure 3.2, it is possible to see that can have many electric and magnetic fields, because of this, applying the above algorithm, let us to introduce the following notation:

$$\frac{E_2 - E_1}{\triangle x} = -j\omega\mu H_1 \tag{3.7}$$

$$\frac{E_3 - E_2}{\triangle x} = -j\omega\mu H_2 \tag{3.8}$$

$$\frac{E_4 - E_3}{\triangle x} = -j\omega\mu H_3 \tag{3.9}$$

$$\frac{E_5 - E_4}{\triangle x} = -j\omega\mu H_4 \tag{3.10}$$

where the group is,

$$\frac{E_{m+1} - E_m}{\triangle x} = -j\omega\mu H_m \tag{3.11}$$

while, in case of $H_z$ the equations would be:

$$-\frac{H_1 - H_0}{\triangle x} = (-\frac{\gamma^2}{j\omega\mu_0} + j\omega\epsilon_0 P_1)E_1 \tag{3.12}$$

$$-\frac{H_2 - H_1}{\triangle x} = (-\frac{\gamma^2}{j\omega\mu_0} + j\omega\epsilon_0 P_2)E_2 \tag{3.13}$$

$$-\frac{H_3 - H_2}{\triangle x} = (-\frac{\gamma^2}{j\omega\mu_0} + j\omega\epsilon_0 P_3)E_3 \tag{3.14}$$

$$-\frac{H_4 - H_3}{\triangle x} = (-\frac{\gamma^2}{j\omega\mu_0} + j\omega\epsilon_0 P_4)E_4 \tag{3.15}$$

where $P_m = \epsilon_y(M \triangle x)$ when m=1, 2, ... and

$$-\frac{H_m - H_{m-1}}{\triangle x} = (-\frac{\gamma^2}{j\omega\mu_0} + j\omega\epsilon_0 P_m)E_m \tag{3.16}$$

In the same way, if we base on equations (3.11) and (3.16) will be presented as:

$$\begin{cases} C_{zy}^{(e)}\mathbf{e} = -j\omega\mu_0\mathbf{h} \\ C_{yz}^{(h)}\mathbf{h} = (-\frac{\gamma^2}{j\omega\mu_0} + j\omega\epsilon_0 P)\mathbf{e} \end{cases} \tag{3.17}$$

where $C_{zy}^{(e)}$ , $C_{yz}^{(h)}$ and P are square matrices of dimension M x M which are based on equations (3.7) to (3.10) and (3.12) to (3.15).

$$[C_{zy}^{(e)}]_{mn} = \triangle x^{-1} \begin{cases} -1, m = n, \\ 1, m = n+1, \\ 0, rest \end{cases} \tag{3.18}$$

$$C_{zy}^{(h)} = C_{zy}^{(e)^T} \tag{3.19}$$

$$P = diag[P_1, \ldots, P_M] \tag{3.20}$$

where P is defined as the permittivity matrix $P_m = \epsilon_r((m-1) \triangle x)$ and it can be show as:

$$P_m = \begin{bmatrix} \epsilon_r((m-1) \triangle x) & 0 & 0 & \ldots & 0 \\ 0 & \epsilon_r((m-1) \triangle x) & 0 & \ldots & 0 \\ 0 & 0 & \epsilon_r((m-1) \triangle x) & \ldots & 0 \\ \vdots & & & & \\ 0 & 0 & 0 & \ldots & \epsilon_r((m-1) \triangle x) \end{bmatrix} \tag{3.21}$$

and vectors **e** and **h** are

$$\mathbf{e} = \begin{bmatrix} E_1 \\ E_2 \\ \vdots \\ E_M \end{bmatrix} \mathbf{h} = \begin{bmatrix} H_1 \\ H_2 \\ \vdots \\ H_M \end{bmatrix}$$

If we focus on equations (3.18) and (3.19), the matrices of equations (3.17) can be presented as $C_{zy}^{(e)}$ and $C_{yz}^{(h)}$ as:

$$C_{zy}^{(e)} = \frac{1}{\triangle X} \begin{bmatrix} -1 & 1 & 0 & 0 & 0 & \ldots \\ 0 & -1 & 1 & 0 & 0 & \ldots \\ 0 & 0 & -1 & 1 & 0 & \ldots \\ 0 & 0 & 0 & -1 & 1 & \ldots \\ \vdots & & & & \ddots & \\ 0 & 0 & 0 & 0 & 0 & -1 \end{bmatrix} \tag{3.22}$$

$$C_{yz}^{(h)} = \frac{1}{\triangle Y}\begin{bmatrix} 1 & 0 & 0 & 0 & 0 & \dots \\ -1 & 1 & 0 & 0 & 0 & \dots \\ 0 & -1 & 1 & 0 & 0 & \dots \\ 0 & 0 & -1 & 1 & 0 & \dots \\ \vdots & & & & \ddots & \\ 0 & 0 & 0 & 0 & -1 & 1 \end{bmatrix} \tag{3.23}$$

The equations (3.17) can be reorganised to obtain the eigenvalue problem for determining the types of TE propagation constant,

$$[C_{yz}^{(h)} C_{zy}^{(e)} - \omega^2 \mu_0 \epsilon_0 P]e = \gamma^2 e \tag{3.24}$$

or in case of $\gamma = 0$ cuttof frequency of a waveguide (or resonant frequency of a cavity) can be obtained from the analogous equation:

$$[\mu_0^{-1}\epsilon_0^{-1}P^{-1}C_{yz}^{(h)}C_{zy}^{(e)}]e = \omega^2 e \tag{3.25}$$

In both cases it does not take into account the boundary conditions so far, however they are necessary to complete the formulation of the problem (either in the form or discrete and continuous). The simplest implementation of the wall, is by forcing to zero the tangential component, respectively, of the electric or magnetic fields. In practice, it means restoring or removing the column of the matrix $C_{zy}^{(e)}$ and (or row $C_{yz}^{(h)}$) for the electric wall (PEC). Simultaneously, columns $C_{zy}^{(h)}$ (or row $C_{yz}^{(e)}$), in the case of a magnetic wall (PMC).

It is necessary to mention that the problems (3.24) and (3.25) are implemented naturally with boundary conditions which are for magnetic wall at $x = -\frac{1}{2}\triangle x$ and for electric wall at $x = M\triangle x$.

## 3.2 Boundary conditions in one dimension

Due to boundary conditions, it is possible to create some transformation matrix which reduces the computer time, by elimination all field samples at the boundary. This new matrix is changed by boundary conditions but it will not affect the main equations. Thus, the equation (3.17) is modified by $e = T_e\tilde{e}$ and $h = T_h\tilde{h}$,

$$\begin{cases} C^e T_e \tilde{e} = -j\omega\mu T_h \tilde{h} \\ C^h T_h \tilde{h} = j\omega\epsilon P \tilde{e} \end{cases} \tag{3.26}$$

where taking into account the condition of perfect electrical conductor (PEC) in case of $T_e$ will be eye matrix with elimination of the first and the last column as:

$$T_e = \begin{bmatrix} 0 & 0 & 0 & \dots & 0 \\ 1 & 0 & 0 & \dots & 0 \\ 0 & 1 & 0 & \dots & 0 \\ 0 & 0 & 1 & \dots & 0 \\ \vdots & & & & \\ 0 & 0 & 0 & \dots & 1 \\ 0 & 0 & 0 & \dots & 0 \end{bmatrix} \tag{3.27}$$

and in case of $T_m$ will be eliminated the last column as

$$T_h = \begin{bmatrix} 1 & 0 & 0 & 0 & \dots & 0 \\ 0 & 1 & 0 & 0 & \dots & 0 \\ 0 & 0 & 1 & 0 & \dots & 0 \\ 0 & 0 & 0 & 1 & \dots & 0 \\ \vdots & & & & & \\ 0 & 0 & 0 & 0 & \dots & 1 \\ 0 & 0 & 0 & 0 & \dots & 0 \end{bmatrix} \tag{3.28}$$

Since $T_h^T \cdot T_h = I$ and $T_e^T \cdot T_e = I$, the changed equations are

$$\begin{cases} T_h^T C^e T_e \tilde{e} = -j\omega\mu\tilde{h} \\ T_e^T C^h T_h \tilde{h} = j\omega\epsilon T_e^T P T_e \tilde{e} \end{cases} \tag{3.29}$$

or shorter,

$$\begin{cases} \tilde{C^e}\tilde{e} = -j\omega\mu\tilde{h} \\ \tilde{C^h}\tilde{h} = j\omega\epsilon\tilde{P}\tilde{e} \end{cases} \tag{3.30}$$

where $\tilde{C^e} = T_h^T C^e T_e$, $\tilde{C^h} = T_e^T C^h T_h$ and $\tilde{P} = T_e^T P T_e$.

## 3.3 Dielectric permittivity

There are many different techniques of dielectric permittivity implementation in FDM. In this thesis the simplest-staircase approximation is applied as equation (3.21) but it can be simply upgraded to more complex algorithms. More accurate results can be obtained by using of Kaneda, Itoh [9] approximation. It is found that the FDM is well suited for these types of problems. Apart of this, dielectric resonators have been analyzed by the finite-difference time-domain (FDTD) method too. The contour-path integral FDTD (CFDTD) method has been successfully applied to curved surfaces of conducting and dielectric bodies. However, this method needs special treatment for those E-fields across the boundary such as the borrowing of neighboring fields and the interpolation of fields. These procedures cause additional complexity and computation time. Finite-volume time-domain (FVTD) techniques and the non-orthogonal FDTD method have improved accuracy for the approximation of curved surfaces at the expense of complex operation and increased computation time and memory.

## 3.4 TM Polarization

Similarly to TE modes, TM modes will be solved in the same way but we focus on another group of equations. In this case, we are going to start with propagation problem and then go to cuttof frequency $\gamma = 0$. Remembering the TM concept which $H_z = 0$ and $E_z \neq 0$ and the group of equations (3.4), now the equations will be,

$$\begin{cases} \frac{\partial H_y}{\partial x} = j\omega\epsilon E_z \\ -\frac{\partial E_z}{\partial x} = (-\frac{\gamma^2}{j\omega\epsilon_0\epsilon_x} + j\omega\mu_0\mu_z)H_y \end{cases} \tag{3.31}$$

Likewise that TE mode, in the TM mode representation is taken into account the magnetic field is transverse to the direction of propagation $z$.

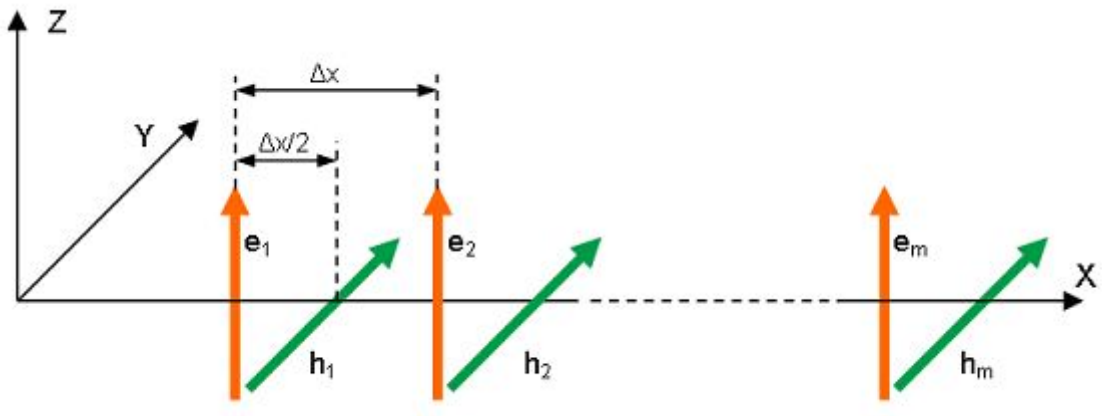


Figure 3.3: Field distribution for TM mode

Basing on equation (3.31), it will be obtained this group of equations for electric field,

$$-\frac{E_2 - E_1}{\triangle x} = (-\frac{\gamma^2}{j\omega\epsilon_0\epsilon_x} + j\omega\mu_0\mu_z)H_1 \tag{3.32}$$

$$-\frac{E_3 - E_2}{\triangle x} = (-\frac{\gamma^2}{j\omega\epsilon_0\epsilon_x} + j\omega\mu_0\mu_z)H_2 \tag{3.33}$$

$$-\frac{E_4 - E_3}{\triangle x} = (-\frac{\gamma^2}{j\omega\epsilon_0\epsilon_x} + j\omega\mu_0\mu_z)H_3 \tag{3.34}$$

$$-\frac{E_5 - E_4}{\triangle x} = (-\frac{\gamma^2}{j\omega\epsilon_0\epsilon_x} + j\omega\mu_0\mu_z)H_4 \tag{3.35}$$

where$P_m = \epsilon_x(M \triangle x)$ and

$$-\frac{E_{m+1} - E_m}{\triangle x} = (-\frac{\gamma^2}{j\omega\epsilon_0}P^{-1} + j\omega\mu_0\mu_z)H_m \tag{3.36}$$

and for magnetic field,

$$-\frac{H_1 - H_0}{\triangle x} = -j\omega\mu E_1 \tag{3.37}$$

$$-\frac{H_2 - H_1}{\triangle x} = -j\omega\mu E_2 \tag{3.38}$$

$$-\frac{H_3 - H_2}{\triangle x} = -j\omega\mu E_3 \tag{3.39}$$

$$-\frac{H_4 - H_3}{\triangle x} = -j\omega\mu E_4 \tag{3.40}$$

where the group is,

$$-\frac{H_m - H_{m-1}}{\triangle x} = -j\omega\mu E_m \tag{3.41}$$

In contract with TE modes, the equations will be a little different and can be group together as

$$\begin{cases} C_{yz}^{(e)}\mathbf{e} = (-\frac{\gamma^2}{j\omega\epsilon} + j\omega\mu_z)\mathbf{h} \\ C_{zy}^{(h)}\mathbf{h} = j\omega\epsilon\mathbf{e} \end{cases} \tag{3.42}$$

where $C_{zy}^{(e)}$, $C_{yz}^{(h)}$ and P are square matrices of dimension M x M.

$$[C_{yz}^{(e)}]_{mn} = \triangle x^{-1} \begin{cases} -1, m = n, \\ 1, m = n+1, \\ 0, rest \end{cases} \tag{3.43}$$

$$C_{zy}^{(h)} = C_{yz}^{(e)^T} \tag{3.44}$$

$$P = diag[P_1, \ldots, P_M] \tag{3.45}$$

where P is defined as the permittivity matrix $P_m = \epsilon_r((m-1) \triangle x$ and it can be show as:

$$P_m = \begin{bmatrix} \epsilon_r((m-1)\triangle x) & 0 & 0 & \ldots & 0 \\ 0 & \epsilon_r((m-1)\triangle x) & 0 & \ldots & 0 \\ 0 & 0 & \epsilon_r((m-1)\triangle x) & \ldots & 0 \\ \vdots & & & & \\ 0 & 0 & 0 & \ldots & \epsilon_r((m-1)\triangle x) \end{bmatrix} \tag{3.46}$$

If we focus on equations (3.43) and (3.44), the equation (3.42) will be presented as two matrix which will belong to $C_{yz}^{(e)}$ and $C_{zy}^{(h)}$ as:

$$C_{yz}^{(e)} = -\frac{1}{\triangle X} \begin{bmatrix} -1 & 0 & 0 & \ldots & \\ 1 & -1 & 0 & \ldots & \\ 0 & 1 & -1 & 0 & \\ 0 & 0 & 1 & -1 & \\ \vdots & & & & \\ 0 & 0 & 0 & 1 & \ldots \end{bmatrix} \tag{3.47}$$

$$C_{zy}^{(h)} = -\frac{1}{\triangle Y} \begin{bmatrix} 1 & 0 & 0 & 0 & \ldots \\ -1 & 1 & 0 & 0 & \ldots \\ 0 & -1 & 1 & 0 & \ldots \\ 0 & 0 & -1 & 1 & \ldots \\ \vdots & & & & \\ \ldots & 0 & 0 & -1 & 1 \end{bmatrix} \tag{3.48}$$

Likewise in TE mode, it can be obtained the propagation characteristics and cutoff frequency in the same way explained previously.

If the equation (3.42) is reorganised, it is going to obtain the eigenvalue problem for determining the types of TM propagation constant,

$$[C_{zy}^{(h)}C_{yz}^{(e)} - \omega^2\mu_0\epsilon_0 P]e = \gamma^2 e \tag{3.49}$$

or in case of $\gamma = 0$ (cuttof frequency of a waveguide or resonant frequency of a cavity can be obtained from the simultaneous equation:

$$[\mu_0^{-1}\epsilon_0^{-1}P^{-1}C_{zy}^{(h)}C_{yz}^{(e)}]e = \omega^2 e \tag{3.50}$$

As it has been explained previously, in both cases it does not take into account the boundary conditions so far as they are necessary to complete the formulation of the problem. The simplest in terms of the implementation of the wall, is the superposition of networks of electrical and magnetic mesh. It is accomplished by forcing to zero the tangential component, respectively, of the electric or magnetic fields. In practice, it means restoring (or removing) the column of the matrix $C_{yz}^{(e)}$ and (or row $C_{zy}^{(h)}$) of the electric wall.

The new equations which have been included the boundary conditions will be the same but the calculation time will be fewer. These boundary conditions are explained in section 3.2. These conditions will be the same for TE and TM polarization in unidimensional problem.

## 3.5 Numerical tests

During whole the project, many tests have been done with the goal of comparing or demostrating that this method is valid. It has been carried out by Matlab environmental. As a result it will be exposed the different results for each polarization TE and TM. On the one hand, it will be exposed the results for cutoff frequency and on the other hand the propagation characteristics.

To verify that method, it will be introduce one dielectric of permittivity $\epsilon_{r1} = 9$. Shilded with parallel-plate waveguide of width a = 22.86mm.

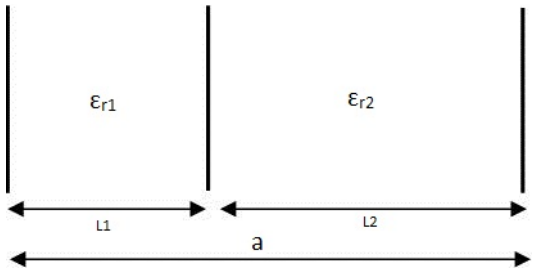


Figure 3.4: Waveguide with a relative permitivity $\epsilon_r$

As it is shown in Figure 3.4, it has one dielectric with a permittivity of $\epsilon_{r1} = 9$ and the rest of waveguide is empty $\epsilon_{r2} = 1$.

Conducting bodies are often idealized as perfect electric conductors (PEC), characterized by vanishing tangential electric field at the conducting surface, and zero total electric field inside. In setting up equivalent field problems the concept of a perfect magnetic conductor (PMC) is useful, characterized by a tangential magnetic field at the surface. Both are described by an infinite conductivity, and the vanishing fields can be argued on the physical grounds that the current density inside remain finite as $\sigma \dashrightarrow \infty$. From Faraday's law, zero electric field in a PEC implies that the time-varying component of the magnetic field also vanish. Similar arguments also hold for a PMC. Thus for radiation problems we assume all fields to be zero everywhere inside of both the PEC and PMC.

It must be remembered that $\epsilon_r$ belong to P matrix which will be a square matrix M x M. In this way the new matrix P will be formed by a diagonal of values of different dielectrics. We have choosen $\epsilon_r = 9$ but it is possible to choose any permitivity. Finally, P matrix should be as:

$$P = \begin{bmatrix} 9 & 0 & \dots & 0 & 0 & 0 & 0 \\ 0 & 9 & \dots & 0 & 0 & 0 & 0 \\ \vdots & & \ddots & 0 & 0 & 0 & \vdots \\ 0 & 0 & 0 & 9 & 0 & 0 & \dots \\ 0 & 0 & 0 & 0 & 1 & 0 & \dots \\ \vdots & 0 & 0 & 0 & 0 & \ddots & \\ & & & & & & \\ 0 & 0 & 0 & 0 & 0 & 0 & 1 \end{bmatrix}$$

In the waveguide depending on the distance that is taken up by the dielectric, the diagonal of matrix will have more or less values of the permitivity. In our case, it was decided that the distance would be 10mm and the rest of the waveguide air.

### 3.5.1 TE Polarization

#### Obtaining cutoff frequencies in one dimension

First of all, we have studied how to obtain the cutoff frequecies of the structure. Now, we are going to obtain the cuttof frequencies in a conditions which are $\epsilon_0 = 8.854187818 \cdot 10^{-12}$ , $c = 299792458$ m/s $\simeq 3 \cdot 10^8$ m/s. All of results have been implemented by Matlab environment. In this case, $\gamma = 0$, therefore it will not take into account the equation (3.24) but it will be used the equation (3.25) which is a standard matrix of eigenvalue problem.

Combining terms of equation (3.25), we have the eigenvalue problem

$$AX = \lambda X \tag{3.51}$$

where $A = \frac{1}{\mu_0 \epsilon_0} P^{-1} C_{yz}^{(h)} C_{zy}^{(e)}$, $\lambda = \omega^2$ which represents the cutoff frequency and vector X represents the corresponding field distribution.

#### Results of $TE_{m0}$ modes in WR90 waveguide

The next data table show the cutoff frequencies of first five modes for TE polarization. It is shown the numerical solutions which have been obtained by Matlab environment and the analytical solutions which are obtained by equations in appendix A.

| | TE10 | TE20 | TE30 | TE40 | TE50 |
|---|---|---|---|---|---|
| Value | fc1(GHz) | fc2(GHz) | fc3(GHz) | fc4(GHz) | fc5(GHz) |
| Numerical N=10 | 3,1952 | 7,5269 | 10,279 | 11,585 | 19,106 |
| Error(%) | 6,76 | 3,35 | 5,6 | 13,6 | 9,18 |
| Numerical N=100 | 2,9838 | 7,2558 | 10,883 | 13,378 | 17,398 |
| Error(%) | 0,29 | 0,37 | 0,10 | 0,30 | 0,58 |
| Numerical N=1000 | 2,9949 | 7,2891 | 10,897 | 13,426 | 17,515 |
| Error(%) | 0,07 | 0,08 | 0,01 | 0,04 | 0,08 |
| Numerical N=10000 | 2,9929 | 7,2835 | 10,895 | 13,420 | 17,501 |
| Error(%) | 0,007 | 0,008 | 0,0009 | 0,04 0,003 | 0,008 |
| Analytical | 2,9927 | 7,2829 | 10,895 | 13,420 | 17,500 |

Table 3.1: Cutoff frequency data table for $TE_m0$ obtained for different meshes

It is possible to see in the Table 3.1 the comparison between numerical and analytical results.

With these approximations, we can have an idea about the validity of this method. The accuracy of the results increase for denser mesh (number of samples N) and lower modes (smoother function).

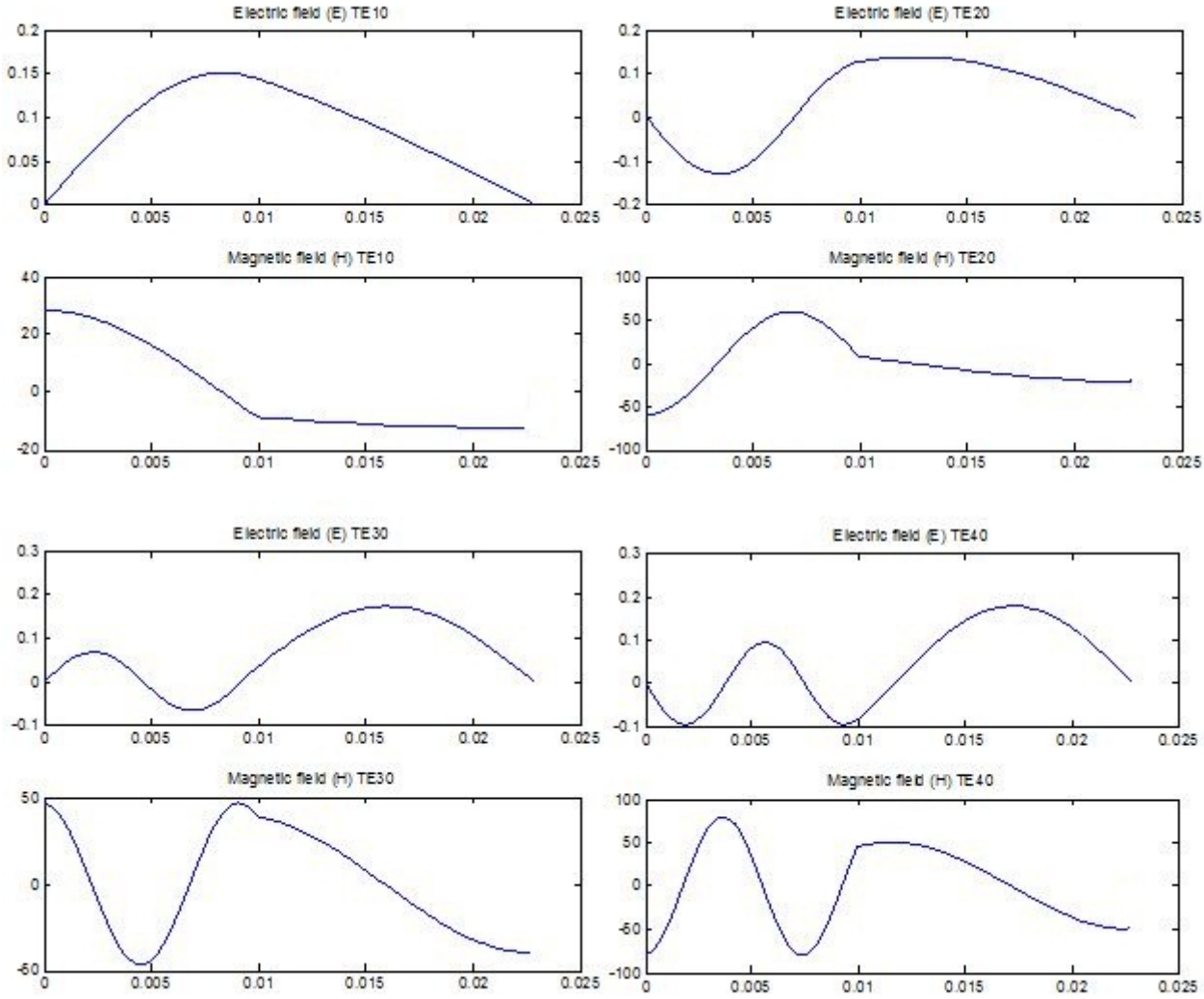


Figure 3.5: Representation of cutoff frequencies for TE modes in one dimension

In the Figure 3.5, it is shown the variation of electric and magnetic fields in the first four modes. These results have been obtained by a mesh $N = 100$.

### Results of propagation coefficients for TE modes

Likewise in case of cutof frequencies, it will be obtained the propagation constants. Therefore, we will focus on equation (3.24). In the same way, we will have a problem which presents

$$AX = \lambda X \tag{3.52}$$

where, in case of propagation coefficients $A = C_{zy}^{(h)} C_{zy}^{(e)} - \omega^2 \mu_0 \epsilon_0 P$, $\lambda = \gamma^2$ and X represents field distribution correspondin to propagation coefficient $\gamma$.

In the Figure 3.8, it is shown the propagation coefficients of TE modes. As it was commented previously, if the frequency mode is lower than the cutoff frequency, it will be obtained a real propagation constant as in this case, which is not presented here.

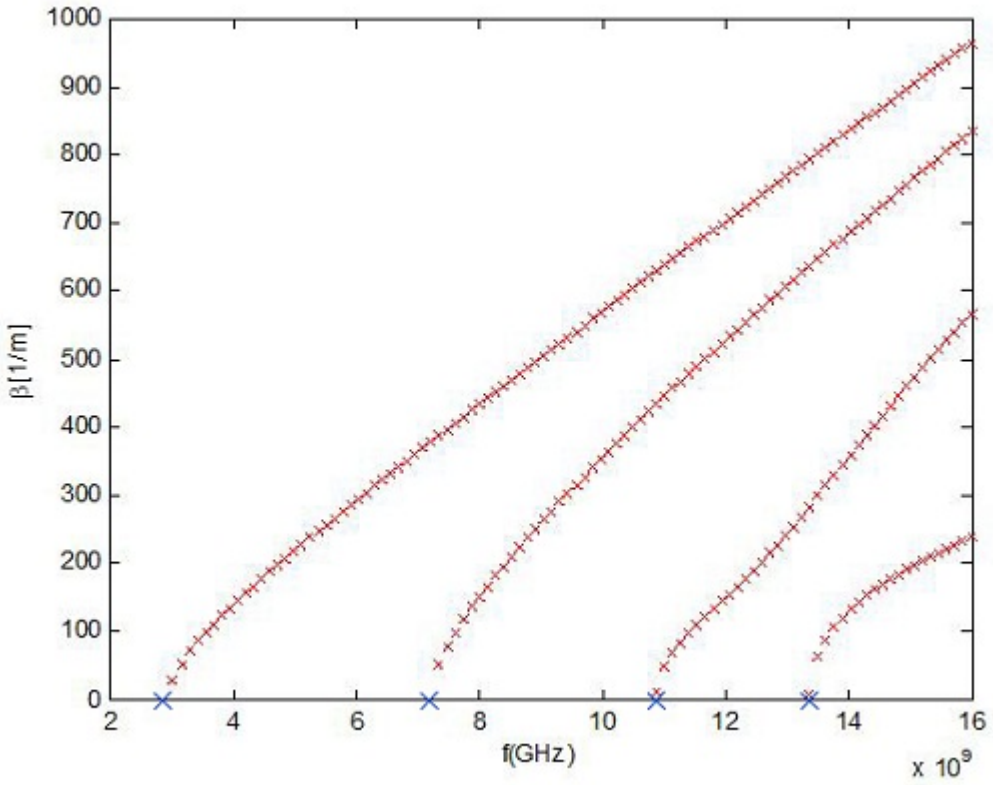


Figure 3.6: Propagation coefficients for $TE_{m0}$ modes

This figure is composed by a group of lines which show the propagation coefficients of TE modes that have been obtained in the program. This grafhic shows the first four modes which are propagated in the waveguide. This waveguide presents the same conditions that it has been taken into account to obtain the cutoff frequencies. It has been used the same mesh $N = 100$. The cutoff frequency have been demonstrated in the chart by big blue crosses. That crosses indicate the beginning of the mode which is propagated.

### 3.5.2 TM Polarization

#### Obtaining cutoff frequencies in one dimension

It will be used the same conditions to obtain the cutoff frequency that in TE modes. In addition, as we have explained, it will be taken into account that $\gamma = 0$, thus it will be used the equation (3.50).The conditions are $\epsilon_0 = 8.854187818 \cdot 10^{-12}$ , $c = 299792458$ m/s $\simeq 3 \cdot 10^8$ m/s. It has been used the same set of meshes $N = 100$.

Also this time, equation (3.50) can be tested as eigenvalue problem as,

$$AX = \lambda X \tag{3.53}$$

where $A = \frac{1}{\mu_0 \epsilon_0} C_{zy}^{(h)} C_{yz}^{(e}$, $\lambda = \omega^2$, which represents the cutoff frequency and vector X the field distributions, analoge to TE polarization.

#### Results of $TM_{m0}$ modes in WR90 waveguide

Similarly, it will be used a rectangular waveguide with dimensions $a = 22.86mm$ and permittivity $\epsilon_{r1} = 9$ and another $\epsilon_{r2} = 1$ which is the air. These permittivities values have been chosen by us, but it can be chosen any value of permittivy. Obviously, in that way the results will be different.

In the following table (3.2) is shown the different cutoff frequencies of different TM modes which have been obtained by Matlab environmental and compared with analytical results. These analytical results are shown in appendix A. A very good agreement was achieved.

The Figure 3.7 shows, in the same way that TE polarization, the variation of electric and magnetic field por TM modes. This representation is four the first four modes, which have been obtained in the same conditions that TE.

| | TM10 | TM20 | TM30 | TM40 | TM50 |
|---|---|---|---|---|---|
| Value | fc1 | fc2 | fc3 | fc4 | fc5 |
| Numerical N10 | 3,1952 | 7,5269 | 10,279 | 11,585 | 19,106 |
| Error(%) | 6,76 | 3,35 | 5,6 | 13,6 | 9,18 |
| Numerical N100 | 2,9838 | 7,2558 | 10,883 | 13,378 | 17,398 |
| Error(%) | 0,30 | 0,36 | 0,11 | 0,30 | 0,57 |
| Numerical N1000 | 2,9949 | 7,2891 | 10,897 | 13,426 | 17,515 |
| Error(%) | 0,07 | 0,08 | 0,01 | 0,05 | 0,09 |
| Numerical N10000 | 2,9929 | 7,2835 | 10,895 | 13,420 | 17,501 |
| Error(%) | 0,003 | 0,01 | 0,001 | 0,04 0,007 | 0,01 |
| Analytical | 2,9928 | 7,2827 | 10,895 | 13,419 | 17,499 |

Table 3.2: Cutoff frequency data table for $TM_m0$ obtained for different meshes

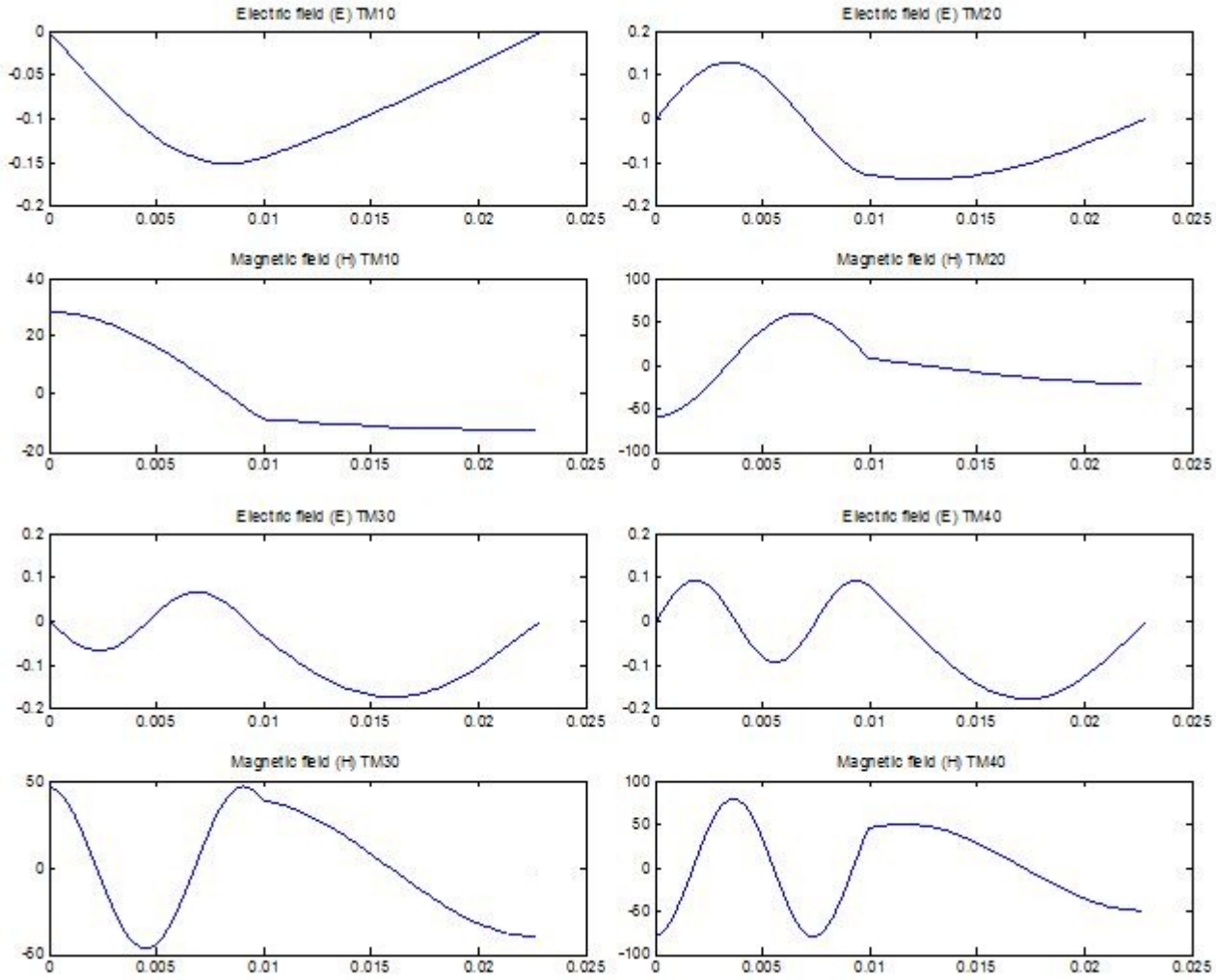


Figure 3.7: Representation of cutoff frequencies for TM modes in one dimension

### Results of propagation coefficients for TM modes

If it is remembered the cutoff frequencies which have been obtained in above section, we can show the propagation constant of TM modes in the Figure 3.8. Likewise in case of cutof frequencies, it will be obtained the propagation constants. Therefore, we will focus on equation (3.50). In the same way, we will have a problem which presents

$$AX = \lambda X \tag{3.54}$$

where, in case of propagation coefficients $A = C_{zy}^{(h)} C_{zy}^{(e)} - \omega^2 \mu_0 \epsilon_0 P$ and $\lambda = \gamma^2$.

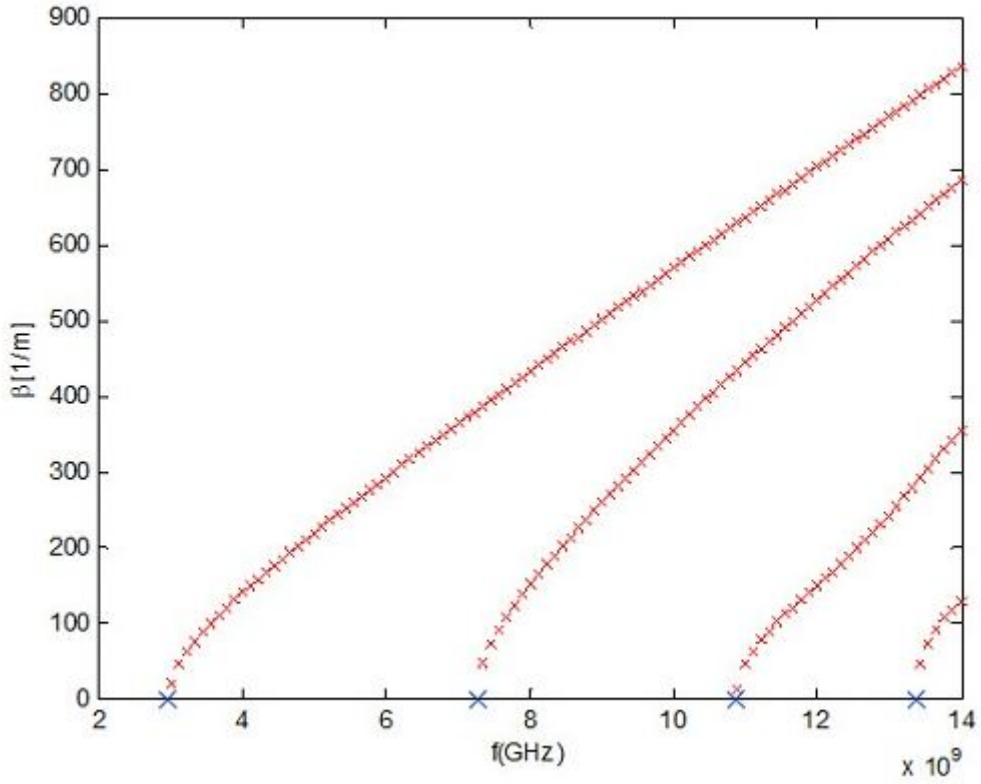


Figure 3.8: Propagation coefficients for $TM_{m0}$ modes

As it is shown in the Figure 3.9, the propagation coefficents are for first four TM modes which their cutoff frequency has been solved previously. As it is possible to see in the Figure, it has been show the point which these modes start to propagate by the waveguide. We can compare the results which have been obtained in the cutoff frequencies table (Table 3.2). The cutoff frequency have been demonstrated in the chart by big blue crosses. That crosses indicate the beginning of the mode which is propagated.

# Chapter 4

# Finite Difference Method in two dimensions

In the previous section, it has been presented an analysis of only a particular group of closed surface. This type of structures have a rather narrow practice application, however, their analysis helps to understand the idea of the finite difference method.

## 4.1 Maxwell equations in two dimensional problems

In the general case, considering the types of either polarity (including hybrid units) is necessary to include all components of the electrical and magnetic fields. Assuming that the relevant structure is uniform along the z-axis, it is possible to assume that each of the components of both fields is represented by the variation in the z-direction by the factor $e^{-\gamma z}$. In addition, assuming that it is a non-magnetic medium in which no currents flow conductivity ($\sigma = 0$) and the spatial charge density is equal to zero ($\rho_v = 0$), equations (2.12-2.15) can be written as:

$$\begin{bmatrix} 0 & \gamma & \frac{\partial}{\partial y} \\ -\gamma & 0 & -\frac{\partial}{\partial x} \\ -\frac{\partial}{\partial y} & \frac{\partial}{\partial x} & 0 \end{bmatrix} \begin{bmatrix} E_x \\ E_y \\ E_z \end{bmatrix} = -j\omega\mu_0 \begin{bmatrix} H_x \\ H_y \\ H_z \end{bmatrix} \tag{4.1}$$

$$\begin{bmatrix} 0 & \gamma & \frac{\partial}{\partial y} \\ -\gamma & 0 & -\frac{\partial}{\partial x} \\ -\frac{\partial}{\partial y} & \frac{\partial}{\partial x} & 0 \end{bmatrix} \begin{bmatrix} H_x \\ H_y \\ H_z \end{bmatrix} = j\omega\epsilon_0 \begin{bmatrix} \epsilon_x & 0 & 0 \\ 0 & \epsilon_y & 0 \\ 0 & 0 & \epsilon_z \end{bmatrix} \begin{bmatrix} E_x \\ E_y \\ E_z \end{bmatrix} \tag{4.2}$$

$$\begin{bmatrix} \frac{\partial}{\partial x} & \frac{\partial}{\partial y} - \gamma \end{bmatrix} \begin{bmatrix} \epsilon_x & 0 & 0 \\ 0 & \epsilon_y & 0 \\ 0 & 0 & \epsilon_z \end{bmatrix} \begin{bmatrix} E_x \\ E_y \\ E_z \end{bmatrix} = 0 \tag{4.3}$$

$$\begin{bmatrix} \frac{\partial}{\partial x} & \frac{\partial}{\partial y} - \gamma \end{bmatrix} \begin{bmatrix} H_x \\ H_y \\ H_z \end{bmatrix} = 0 \tag{4.4}$$

The system of equations described above can be analyzed, similarly, as in the unidimensional case. The sets of points, in which electrical components and transverse magnetic fields are sampled are shown in Figure 4.1.

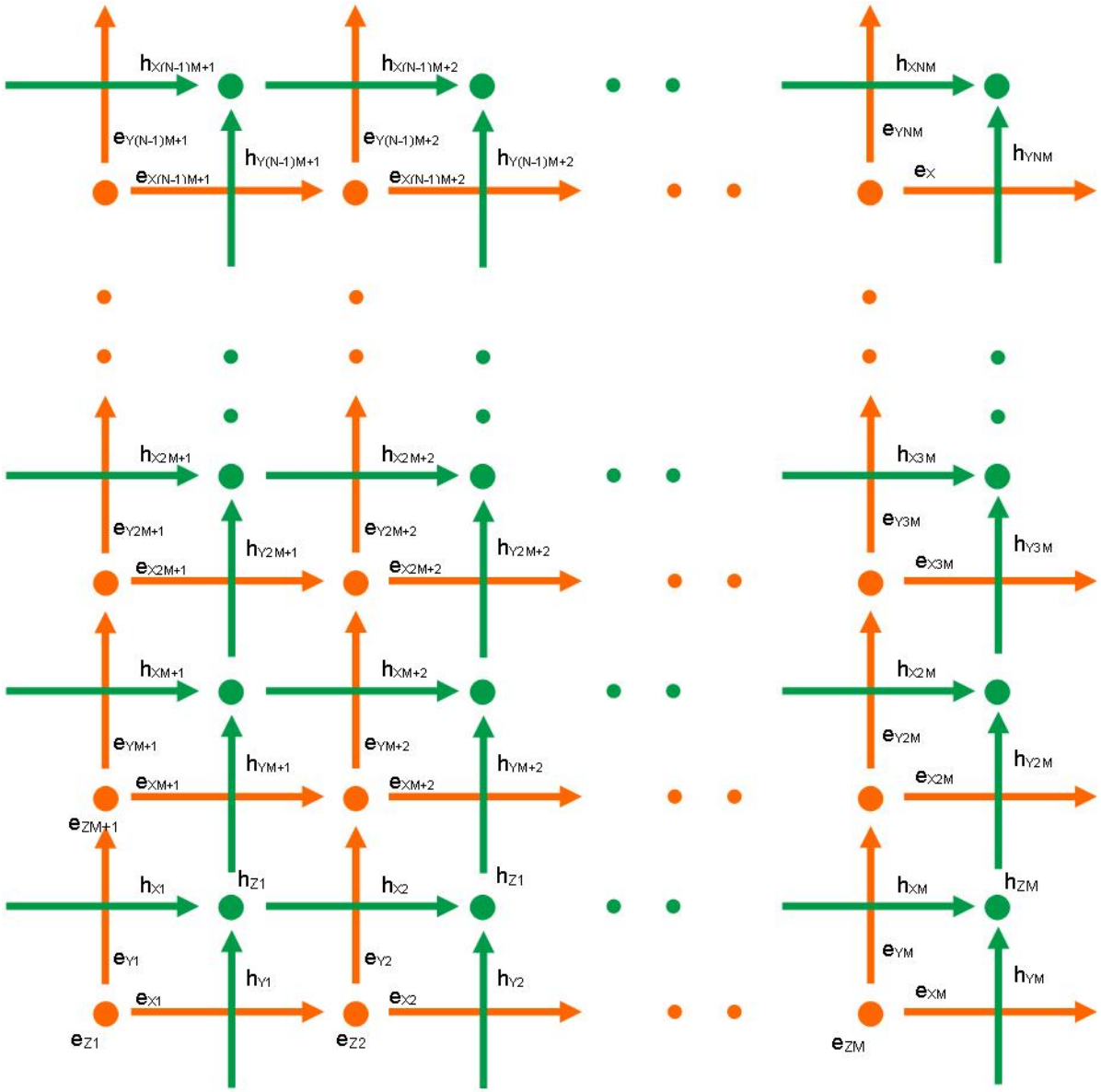


Figure 4.1: The set of points, which are sampled electric and magnetic fields

It will be named as M of the sample in the X-axis direction and N in the Y-axis direction,thus the set of samples K will be obtained as $K = M \cdot N$ for each of the field components. Simplifying the discussion, to sample only a numbered index is desirable. This is allowed in the map below:

$$k = (n-1)M + m \tag{4.5}$$

where k=1,. . ., K, m=1,. . ., M and n=1,. . ., N. The vector $\mathbf{e}_i$ which contains the samples of the i-th component of the electric field can be written as:

$$[e_x]_k = E_x((m - \frac{1}{2}) \triangle x, (n-1) \triangle y) \tag{4.6}$$

$$[e_y]_k = E_y((m-1) \triangle x, (n - \frac{1}{2}) \triangle y) \tag{4.7}$$

$$[e_z]_k = E_z((m-1) \triangle x, (n-1) \triangle y) \tag{4.8}$$

and in case of $h_i$ elements:

$$[h_x]_k = E_x((m-1) \triangle x, (n-\frac{1}{2}) \triangle y) \tag{4.9}$$

$$[h_y]_k = E_y((m-\frac{1}{2}) \triangle x, (n-1) \triangle y) \tag{4.10}$$

$$[h_z]_k = E_z((m-\frac{1}{2}) \triangle x, (n-\frac{1}{2}) \triangle y) \tag{4.11}$$

In addition, electric permittivity is the numerical domain:

$$[P_x]_k = \epsilon_{rx}((m-\frac{1}{2}) \triangle x, (n-1) \triangle y) \tag{4.12}$$

$$[P_y]_k = \epsilon_{ry}((m-1) \triangle x, (n-\frac{1}{2}) \triangle y) \tag{4.13}$$

$$[P_z]_k = \epsilon_{rz}((m-1) \triangle x, (n-1) \triangle y) \tag{4.14}$$

## 4.2 TE Polarization

Previously it has been presented the obtaining of TE modes in unidimensional problems. Now likewise, it will be explained the manner of getting TE modes but in case of two dimensions, Let us look at Figure 4.2 to understant the concept.

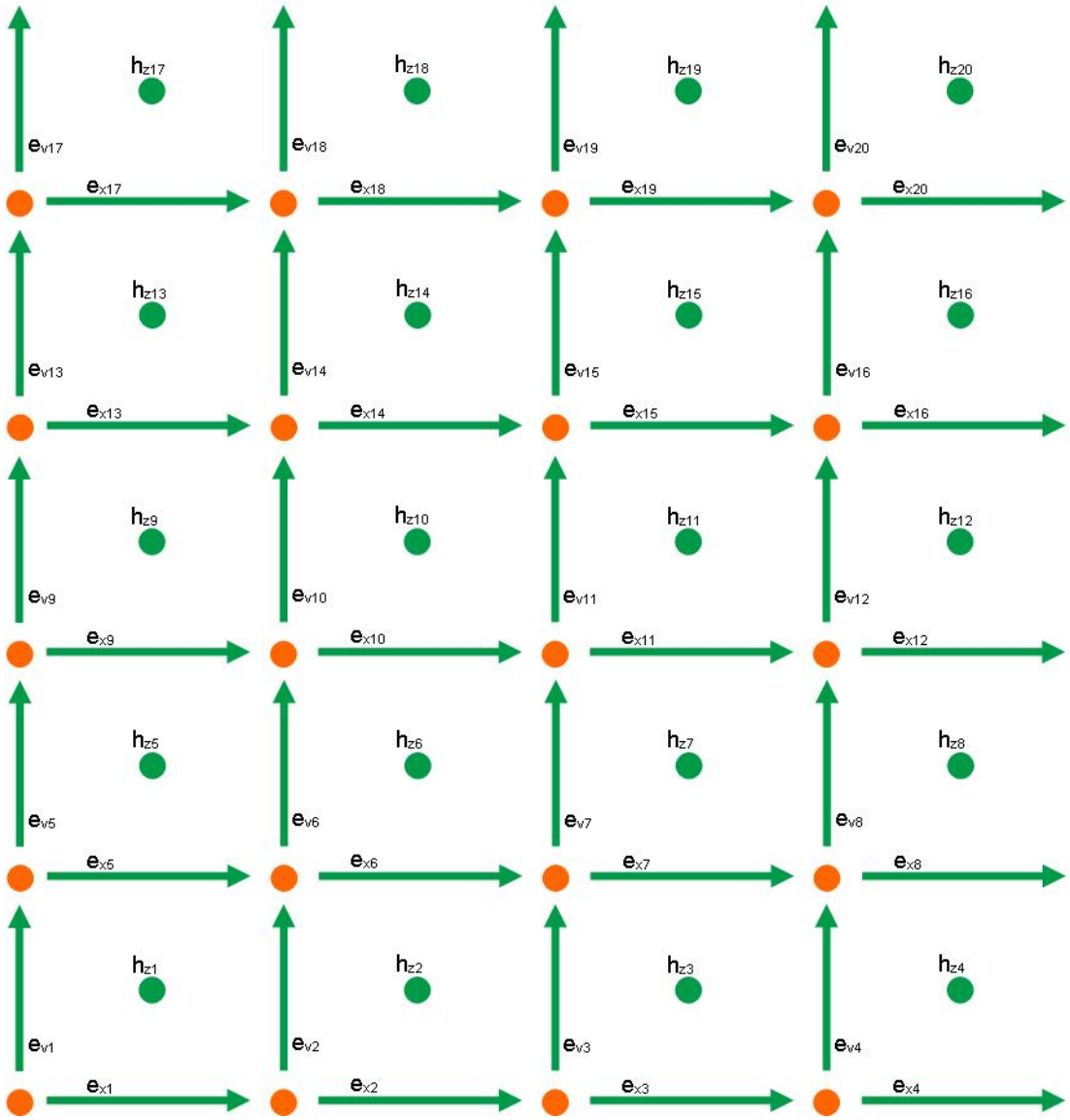


Figure 4.2: The set of points, which are sampled the electric field

We assume $E_z = 0$ ($E_y \neq 0$, $E_x \neq 0$ and $H_z \neq 0$). Therefore, from equations (4.1) and (4.2) are obtained: From equations (4.1) and (4.2):

$$\begin{cases} \gamma E_y = -j\omega\mu_0 H_z \\ -\gamma E_x = -j\omega\mu_0 H_z \\ -\frac{\partial E_x}{\partial y} + \frac{\partial E_y}{\partial x} = -j\omega\mu_0 H_z \end{cases} \tag{4.15}$$

and

$$\begin{cases} \frac{\partial H_z}{\partial y} = (-\frac{\gamma^2}{j\omega\mu_0} + j\omega\epsilon_0\epsilon_x)E_x \\ -\frac{\partial H_z}{\partial x} = -(\frac{\gamma^2}{j\omega\mu_0} + j\omega\epsilon_0\epsilon_y)E_y \end{cases} \tag{4.16}$$

As it was metioned previously, the acceptable fields for TE modes are $E_x$, $E_y$ and $H_z$.

On the one hand, operating the electric field, the equation obtained is

$$-\frac{\partial E_x}{\partial y}+\frac{\partial E_y}{\partial x}=-j\omega\mu_0 H_z \tag{4.17}$$

If the equation (4.17) is solved and it is used the approximation (3.6), it will be obtained briefly:

$$-\frac{E_{x5}-E_{x1}}{\triangle y}+\frac{E_{y2}-E_{y1}}{\triangle x}=-j\omega\mu_0 H_{z1} \tag{4.18}$$

$$-\frac{E_{x6}-E_{x2}}{\triangle y}+\frac{E_{y3}-E_{y2}}{\triangle x}=-j\omega\mu_0 H_{z2} \tag{4.19}$$

$$-\frac{E_{x7}-E_{x3}}{\triangle y}+\frac{E_{y4}-E_{y3}}{\triangle x}=-j\omega\mu_0 H_{z3} \tag{4.20}$$

$$-\frac{E_{x8}-E_{x4}}{\triangle y}+\frac{E_{y5}-E_{y4}}{\triangle x}=-j\omega\mu_0 H_{z4} \tag{4.21}$$

which is associated with equation (4.17) in the way,

$$C_{zt}^{(e)}e_t=-j\omega\mu_0 h_z \tag{4.22}$$

where $C_{zt}^{(e)}$ can be divided in $C_{zx}^{(e)}$ and $C_{zy}^{(e)}$, therefore the equation (4.22) will be defined as,

$$\begin{bmatrix}C_{zx}^{(e)} & C_{zy}^{(e)}\end{bmatrix}\begin{bmatrix}e_x\\ e_y\end{bmatrix}=-j\omega\mu_0 h_z \tag{4.23}$$

These equations are obtained by the electric field but they are examples due to the number of these equations will be variable depending of K (MxN). As a result, it can be defined one matrix for each matrix $C_{zx}^{(e)}$ and $C_{zy}^{(e)}$ as:

$$[C_{zx}^{(e)}]_{mn}=\triangle y^{-1}\begin{cases}-1, m=n,\\ 1, m=n+1,\\ 0, rest\end{cases} \tag{4.24}$$

$$[C_{zy}^{(e)}]_{mn}=\triangle x^{-1}\begin{cases}-1, m=n,\\ 1, m=n+1,\\ 0, rest\end{cases} \tag{4.25}$$

where graphically it can be seen as,

$$C_{zx}^{(e)}=-\frac{1}{\triangle Y}\begin{bmatrix}-1 & 0 & 0 & 0 & 1 & 0 & \dots & 0\\ 0 & -1 & 0 & 0 & 0 & 1 & \dots & 0\\ 0 & 0 & -1 & 0 & 0 & 0 & \dots & 0\\ 0 & 0 & 0 & -1 & 0 & 0 & \dots & 0\\ 0 & 0 & 0 & 0 & -1 & 0 & \dots & 0\\ \vdots & & & & & & & \\ 0 & 0 & 0 & 0 & 0 & 0 & 0 & -1\end{bmatrix} \tag{4.26}$$

$$C_{zy}^{(e)}=\frac{1}{\triangle X}\begin{bmatrix}-1 & 1 & 0 & 0 & 0 & 0 & \dots & 0\\ 0 & -1 & 1 & 0 & 0 & 0 & \dots & 0\\ 0 & 0 & -1 & 1 & 0 & 0 & \dots & 0\\ 0 & 0 & 0 & -1 & 1 & 0 & \dots & 0\\ 0 & 0 & 0 & 0 & -1 & 1 & \dots & 0\\ \vdots & & & & & & & \\ 0 & 0 & 0 & 0 & 0 & 0 & 0 & -1\end{bmatrix} \tag{4.27}$$

It is taken into account the negative signe in the equation (4.26), the main diagonal will be changed as

$$C_{zx}^{(e)} = -\frac{1}{\triangle Y}\begin{bmatrix} 1 & 0 & 0 & 0 & -1 & 0 & \dots & 0 \\ 0 & 1 & 0 & 0 & 0 & -1 & \dots & 0 \\ 0 & 0 & 1 & 0 & 0 & 0 & \dots & 0 \\ 0 & 0 & 0 & 1 & 0 & 0 & \dots & 0 \\ 0 & 0 & 0 & 0 & 1 & 0 & \dots & 0 \\ \vdots & & & & & & & \\ 0 & 0 & 0 & 0 & 0 & 0 & 0 & 1 \end{bmatrix} \tag{4.28}$$

On the other hand, if we focus on equation (4.2), it is necessary to obtain the equations of magnetic field solving the equation (4.2):

$$\begin{cases} \frac{\partial H_z}{\partial y} = (-\frac{\gamma^2}{j\omega\mu_0} + j\omega\epsilon_0\epsilon_x)E_x \\ -\frac{\partial H_z}{\partial x} = -(\frac{\gamma^2}{j\omega\mu_0} + j\omega\epsilon_0\epsilon_y)E_y \end{cases} \tag{4.29}$$

Solving the first equation on equation (4.29) and using the approximation (3.4),

$$\frac{\partial H_z}{\partial y} = (-\frac{\gamma^2}{j\omega\mu_0} + j\omega\epsilon_0\epsilon_x)E_x \tag{4.30}$$

it will be obtained this group of equations:

$$\frac{H_{z5} - H_{z1}}{\triangle y} = (-\frac{\gamma^2}{j\omega\mu_0} + j\omega\epsilon_0\epsilon_x)E_{x1} \tag{4.31}$$

$$\frac{H_{z6} - H_{z2}}{\triangle y} = (-\frac{\gamma^2}{j\omega\mu_0} + j\omega\epsilon_0\epsilon_x)E_{x2} \tag{4.32}$$

$$\frac{H_{z7} - H_{z3}}{\triangle y} = (-\frac{\gamma^2}{j\omega\mu_0} + j\omega\epsilon_0\epsilon_x)E_{x3} \tag{4.33}$$

$$\frac{H_{z8} - H_{z4}}{\triangle y} = (-\frac{\gamma^2}{j\omega\mu_0} + j\omega\epsilon_0\epsilon_x)E_{x4} \tag{4.34}$$

If it is solved the second equation on (4.29)

$$-\frac{\partial H_z}{\partial x} = -(\frac{\gamma^2}{j\omega\mu_0} + j\omega\epsilon_0\epsilon_y)E_y \tag{4.35}$$

In the same way,

$$-\frac{H_{z1} - H_{z0}}{\triangle x} = -(\frac{\gamma^2}{j\omega\mu_0} + j\omega\epsilon_0\epsilon_y)E_{y1} \tag{4.36}$$

$$-\frac{H_{z2} - H_{z1}}{\triangle x} = -(\frac{\gamma^2}{j\omega\mu_0} + j\omega\epsilon_0\epsilon_y)E_{y2} \tag{4.37}$$

$$-\frac{H_{z3} - H_{z2}}{\triangle x} = -(\frac{\gamma^2}{j\omega\mu_0} + j\omega\epsilon_0\epsilon_y)E_{y3} \tag{4.38}$$

$$-\frac{H_{z4} - H_{z3}}{\triangle x} = -(\frac{\gamma^2}{j\omega\mu_0} + j\omega\epsilon_0\epsilon_y)E_{y4} \tag{4.39}$$

In the same way that electric field, it will be got,

$$C_{tz}^{(h)} h_z = j\omega\epsilon_0 P e_t \tag{4.40}$$

where P is the permittivity matrix but it wll be explained subsequently and $C_{tz}^{(h)}$ will be divided in two equations $C_{xz}^{(h)}$ and $C_{yz}^{(h)}$ as:

$$\begin{bmatrix} C_{xz}^{(h)} \\ C_{yz}^{(h)} \end{bmatrix} \begin{bmatrix} h_z \end{bmatrix} = j\omega\epsilon_0 \begin{bmatrix} \epsilon_x & 0 \\ 0 & \epsilon_y \end{bmatrix} \begin{bmatrix} e_x \\ e_y \end{bmatrix} \tag{4.41}$$

The number of equations (4.31) to (4.34) and (4.36) to (4.39), as we commented previously, will be depending on K (number of samples). And in the same way that electric field can be associated one matrix for each group of equations. In case of $C_{xz}^{(h)}$ and $C_{yz}^{(h)}$,

$$C_{xz}^{(h)} = \frac{1}{\triangle Y} \begin{bmatrix} 1 & 0 & 0 & 0 & 0 & 0 & \dots & 0 \\ 0 & 1 & 0 & 0 & 0 & 0 & \dots & 0 \\ 0 & 0 & 1 & 0 & 0 & 0 & \dots & 0 \\ 0 & 0 & 0 & 1 & 0 & 0 & \dots & 0 \\ -1 & 0 & 0 & 0 & 1 & 0 & \dots & 0 \\ 0 & -1 & 0 & 0 & 0 & 1 & \dots & 0 \\ \vdots & & & & & & & \\ 0 & 0 & 0 & -1 & 0 & 0 & 0 & 1 \end{bmatrix} \tag{4.42}$$

$$C_{yz}^{(h)} = \frac{1}{\triangle X} \begin{bmatrix} -1 & 0 & 0 & 0 & 0 & 0 & \dots & 0 \\ 1 & -1 & 0 & 0 & 0 & 0 & \dots & 0 \\ 0 & 1 & -1 & 0 & 0 & 0 & \dots & 0 \\ 0 & 0 & 1 & -1 & 0 & 0 & \dots & 0 \\ 0 & 0 & 0 & 1 & -1 & 0 & \dots & 0 \\ 0 & 0 & 0 & 0 & 1 & -1 & \dots & 0 \\ \vdots & & & & & & & \\ 0 & 0 & 0 & 0 & 0 & 0 & 0 & -1 \end{bmatrix} \tag{4.43}$$

Theoretically, it is possible to realize that $C_{tz}^{(h)} = C_{zt}^{(e)^T}$ so in the Matlab environmental it will not be necessary to create matrices (4.42) and (4.43). Finally, if we base on equation (4.29), it will be obtained by above matrices.

$$\frac{1}{\triangle Y} \begin{bmatrix} 1 & 0 & 0 & 0 & 0 & 0 & \dots & 0 \\ 0 & 1 & 0 & 0 & 0 & 0 & \dots & 0 \\ 0 & 0 & 1 & 0 & 0 & 0 & \dots & 0 \\ 0 & 0 & 0 & 1 & 0 & 0 & \dots & 0 \\ -1 & 0 & 0 & 0 & 1 & 0 & \dots & 0 \\ 0 & -1 & 0 & 0 & 0 & 1 & \dots & 0 \\ \vdots & & & & & & & \\ 0 & 0 & 0 & -1 & 0 & 0 & 0 & 1 \end{bmatrix} \begin{bmatrix} H_{z1} \\ H_{z2} \\ H_{z3} \\ H_{z4} \\ H_{z5} \\ H_{z6} \\ \vdots \\ H_{zK} \end{bmatrix} = \begin{bmatrix} E_{x1} \\ E_{x2} \\ E_{x3} \\ E_{x4} \\ E_{x5} \\ E_{x6} \\ \vdots \\ E_{xK} \end{bmatrix} \tag{4.44}$$

$$\frac{1}{\triangle X}\begin{bmatrix} -1 & 0 & 0 & 0 & 0 & 0 & \dots & 0 \\ 1 & -1 & 0 & 0 & 0 & 0 & \dots & 0 \\ 0 & 1 & -1 & 0 & 0 & 0 & \dots & 0 \\ 0 & 0 & 1 & -1 & 0 & 0 & \dots & 0 \\ 0 & 0 & 0 & 1 & -1 & 0 & \dots & 0 \\ 0 & 0 & 0 & 0 & 1 & -1 & \dots & 0 \\ \vdots & & & & & & & \\ 0 & 0 & 0 & 0 & 0 & 0 & 0 & -1 \end{bmatrix}\begin{bmatrix} H_{z1} \\ H_{z2} \\ H_{z3} \\ H_{z4} \\ H_{z5} \\ H_{z6} \\ \vdots \\ H_{zK} \end{bmatrix} = \begin{bmatrix} E_{y1} \\ E_{y2} \\ E_{y3} \\ E_{y4} \\ E_{y5} \\ E_{y6} \\ \vdots \\ E_{yK} \end{bmatrix} \tag{4.45}$$

If the equations (4.22) and (4.40) are associated, it will be obtained the same problem that in one dimension as,

$$\begin{cases} C_{zt}^{(e)} e_t = j\omega\mu_0 h_z \\ C_{tz}^{(h)} h_z = (-\frac{\gamma^2}{j\omega\mu_0} + j\omega\epsilon_0 P_t) e_t \end{cases} \tag{4.46}$$

where

$$C_{zt}^{(e)} = \left[ C_{zx}^{(e)} C_{zy}^{(e)} \right] \tag{4.47}$$

$$C_{tz}^{(h)} = \begin{bmatrix} C_{xz}^{(h)} \\ C_{yz}^{(h)} \end{bmatrix} \tag{4.48}$$

Likewise in one dimension, it is possible to organise the equations and obtaining the eigenvalue problem for determining the propagation characteristics of TE modes as:

$$[C_{zt}^{(e)} C_{tz}^{(h)} - \omega^2\mu_0\epsilon_0 P] = \gamma^2 e \tag{4.49}$$

or in case of $\gamma = 0$, the cutoff frequency would be obtained in this way,

$$[\mu_0^{-1}\epsilon_0^{-1} P^{-1} C_{zt}^{(e)} C_{tz}^{(h)}] e = \omega^2 e \tag{4.50}$$

In both cases (equations (4.49) and (4.50)) it does not take into account the boundary conditions so far as they are necessary to complete the formulation of the problem.

## 4.3 Boundary conditions for TE polarization

On the one hand, previously mentioned, that equations which will be used to obtain the cutoff frequencies but not taking into account the boundary conditions. The next equations will be changed by boundary conditions. The equations can be transformed in such a way that calculation time will be fewer. Taking into account $e_t = T_t^e \tilde{e}$ and $h_z = T_z^h \tilde{h_z}$, if we remember in unidimensional problem, the equation (4.46) will be changed as,

$$\begin{cases} C_{zt}^{(e)} T_t^e \tilde{e_t} = -j\omega\mu_0 T_z^h \tilde{h_z} \\ C_{tz}^{(h)} T_z^h \tilde{h} = j\omega\epsilon_0 P T_t^e \tilde{e_t} \end{cases} \tag{4.51}$$

If the equation (4.51) is calculated,

$$\begin{cases} T_h^T C_{zt}^{(e)} T_t^e \tilde{e_t} = -j\omega\mu_0 \tilde{h_z} \\ T_e^T C_{tz}^{(h)} T_z^h \tilde{h_z} = j\omega\epsilon_0 T_e^T P T_e \tilde{e_t} \end{cases} \tag{4.52}$$

Finally, it will be obtained the next equations,

$$\begin{cases} \tilde{C}_{zt}^{(e)}\tilde{e_t} = -j\omega\mu_0\tilde{h_z} \\ \tilde{C}_{tz}^{(h)}\tilde{h_z} = j\omega\epsilon_0\tilde{P}_t\tilde{e_t} \end{cases} \tag{4.53}$$

where $\tilde{C}_{zt}^{(e)} = T_z^{h^T} C_{zt}^{(e)} T_t^e$, $\tilde{C}_{tz}^{(h)} = T_t^{e^T} C_{tz}^{(h)} T_h$ and $\tilde{P} = T_t^{e^T} P T_t^e$, which is the permittivity matrix.

On the other hand, it can not be forgot that boundary conditions $e_t = T_t^e \tilde{e}_t$ and $h_z = T_z^h \tilde{h}_z$ in turn will be changed by other matrices. These new matrices are based on the Figure 4.3 which the boundary conditions must be imposed inside on field.

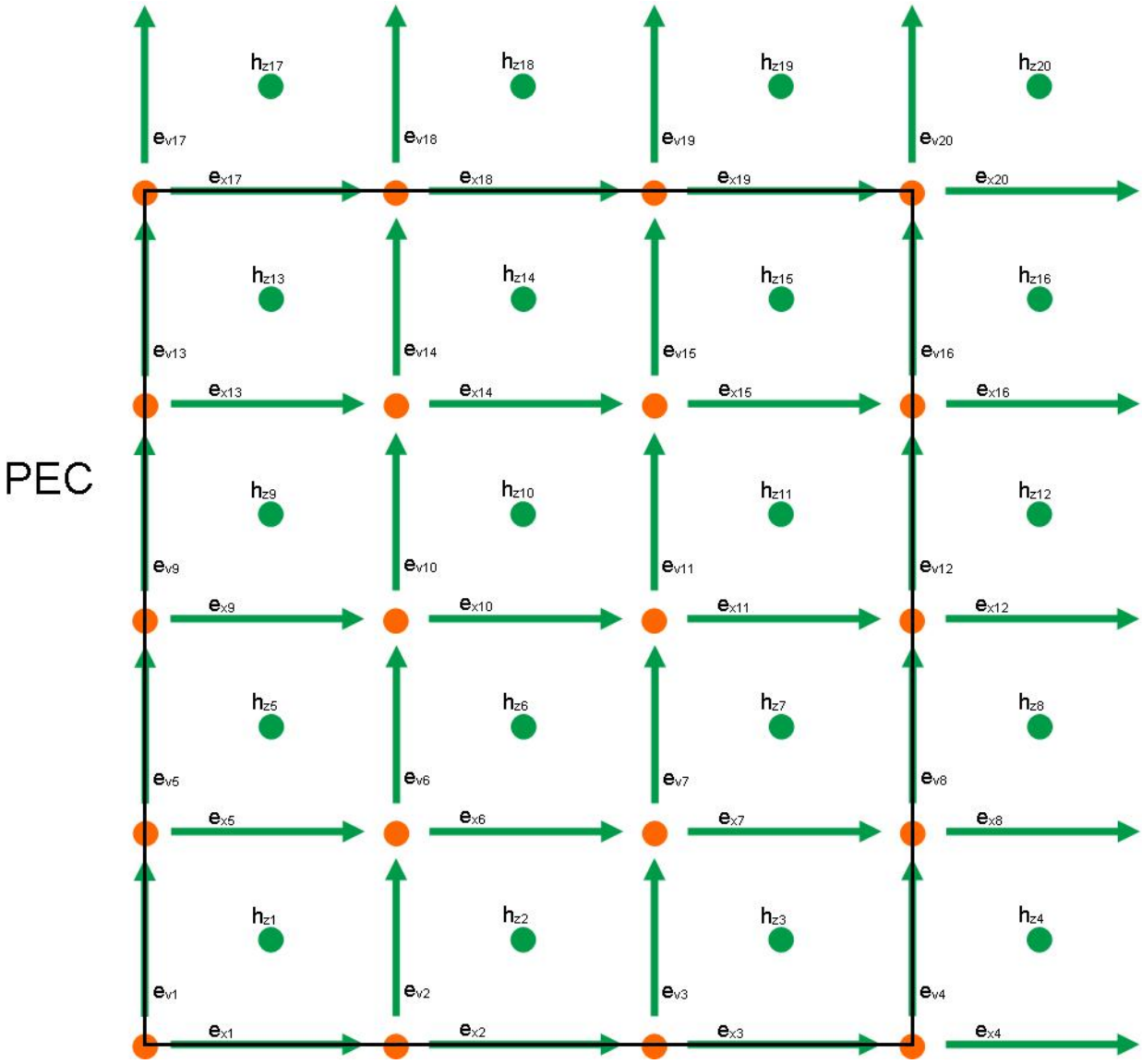


Figure 4.3: The set of points which will be taken into account to get the boundary conditions

In case shown in Figure 4.3, $T_t^e$ and $T_z^h$ can be obtained using extra matrices:

$$R_x^e = \begin{bmatrix} 1 & 0 & 0 & 0 & 1 \\ 1 & 0 & 0 & 0 & 1 \\ 1 & 0 & 0 & 0 & 1 \\ 1 & 1 & 1 & 1 & 1 \end{bmatrix} \tag{4.54}$$

where reshape of $R_x^e = \begin{bmatrix} 1 & 1 & 1 & 1 & 0 & 0 & 0 & 1 & 0 & 0 & 0 & 1 & 1 & 1 & 1 & 1 \end{bmatrix}$

$$R_y^e = \begin{bmatrix} 1 & 1 & 1 & 1 & 1 \\ 0 & 0 & 0 & 0 & 1 \\ 0 & 0 & 0 & 0 & 1 \\ 1 & 1 & 1 & 1 & 1 \end{bmatrix} \tag{4.55}$$

where reshape of $R_y^e = \begin{bmatrix} 1 & 0 & 0 & 1 & 1 & 0 & 0 & 1 & 1 & 0 & 0 & 1 & 1 & 1 & 1 & 1 \end{bmatrix}$

$$R_z^h = \begin{bmatrix} 0 & 0 & 0 & 0 & 1 \\ 0 & 0 & 0 & 0 & 1 \\ 0 & 0 & 0 & 0 & 1 \\ 1 & 1 & 1 & 1 & 1 \end{bmatrix} \tag{4.56}$$

where reshape of $R_z^e = \begin{bmatrix} 0 & 0 & 0 & 1 & 0 & 0 & 0 & 1 & 0 & 0 & 0 & 1 & 1 & 1 & 1 & 1 \end{bmatrix}$

In that way, the above equations and $\tilde{e}_t$ and $\tilde{h}_z$ is representing boundary conditions where $T_t^e$ and $T_z^h$ are,

$$T_z^h = \begin{pmatrix} 1 & 0 & 0 & 0 & 0 & 0 & 0 & 0 & 0 & 0 & 0 & 0 \\ 0 & 1 & 0 & 0 & 0 & 0 & 0 & 0 & 0 & 0 & 0 & 0 \\ 0 & 0 & 1 & 0 & 0 & 0 & 0 & 0 & 0 & 0 & 0 & 0 \\ 0 & 0 & 0 & 0 & 0 & 0 & 0 & 0 & 0 & 0 & 0 & 0 \\ 0 & 0 & 0 & 1 & 0 & 0 & 0 & 0 & 0 & 0 & 0 & 0 \\ 0 & 0 & 0 & 0 & 1 & 0 & 0 & 0 & 0 & 0 & 0 & 0 \\ 0 & 0 & 0 & 0 & 0 & 1 & 0 & 0 & 0 & 0 & 0 & 0 \\ 0 & 0 & 0 & 0 & 0 & 0 & 0 & 0 & 0 & 0 & 0 & 0 \\ 0 & 0 & 0 & 0 & 0 & 0 & 1 & 0 & 0 & 0 & 0 & 0 \\ 0 & 0 & 0 & 0 & 0 & 0 & 0 & 1 & 0 & 0 & 0 & 0 \\ 0 & 0 & 0 & 0 & 0 & 0 & 0 & 0 & 1 & 0 & 0 & 0 \\ 0 & 0 & 0 & 0 & 0 & 0 & 0 & 0 & 0 & 0 & 0 & 0 \\ 0 & 0 & 0 & 0 & 0 & 0 & 0 & 0 & 0 & 1 & 0 & 0 \\ 0 & 0 & 0 & 0 & 0 & 0 & 0 & 0 & 0 & 0 & 1 & 0 \\ 0 & 0 & 0 & 0 & 0 & 0 & 0 & 0 & 0 & 0 & 0 & 1 \\ 0 & 0 & 0 & 0 & 0 & 0 & 0 & 0 & 0 & 0 & 0 & 0 \\ 0 & 0 & 0 & 0 & 0 & 0 & 0 & 0 & 0 & 0 & 0 & 0 \\ 0 & 0 & 0 & 0 & 0 & 0 & 0 & 0 & 0 & 0 & 0 & 0 \\ 0 & 0 & 0 & 0 & 0 & 0 & 0 & 0 & 0 & 0 & 0 & 0 \\ 0 & 0 & 0 & 0 & 0 & 0 & 0 & 0 & 0 & 0 & 0 & 0 \end{pmatrix} \tag{4.57}$$

$$T_t^e = \begin{pmatrix}
0&0&0&0&0&0&0&0&0&0&0&0&0&0&0&0&0\\
1&0&0&0&0&0&0&0&0&0&0&0&0&0&0&0&0\\
0&1&0&0&0&0&0&0&0&0&0&0&0&0&0&0&0\\
0&0&1&0&0&0&0&0&0&0&0&0&0&0&0&0&0\\
0&0&0&0&0&0&0&0&0&0&0&0&0&0&0&0&0\\
0&0&0&1&0&0&0&0&0&0&0&0&0&0&0&0&0\\
0&0&0&0&1&0&0&0&0&0&0&0&0&0&0&0&0\\
0&0&0&0&0&1&0&0&0&0&0&0&0&0&0&0&0\\
0&0&0&0&0&0&0&0&0&0&0&0&0&0&0&0&0\\
0&0&0&0&0&0&1&0&0&0&0&0&0&0&0&0&0\\
0&0&0&0&0&0&0&1&0&0&0&0&0&0&0&0&0\\
0&0&0&0&0&0&0&0&1&0&0&0&0&0&0&0&0\\
0&0&0&0&0&0&0&0&0&0&0&0&0&0&0&0&0\\
0&0&0&0&0&0&0&0&0&0&0&0&0&0&0&0&0\\
0&0&0&0&0&0&0&0&0&0&0&0&0&0&0&0&0\\
0&0&0&0&0&0&0&0&0&0&0&0&0&0&0&0&0\\
0&0&0&0&0&0&0&0&0&1&0&0&0&0&0&0&0\\
0&0&0&0&0&0&0&0&0&0&1&0&0&0&0&0&0\\
0&0&0&0&0&0&0&0&0&0&0&0&0&0&0&0&0\\
0&0&0&0&0&0&0&0&0&0&0&0&0&0&0&0&0\\
0&0&0&0&0&0&0&0&0&0&0&1&0&0&0&0&0\\
0&0&0&0&0&0&0&0&0&0&0&0&1&0&0&0&0\\
0&0&0&0&0&0&0&0&0&0&0&0&0&0&0&0&0\\
0&0&0&0&0&0&0&0&0&0&0&0&0&0&0&0&0\\
0&0&0&0&0&0&0&0&0&0&0&0&0&1&0&0&0\\
0&0&0&0&0&0&0&0&0&0&0&0&0&0&1&0&0\\
0&0&0&0&0&0&0&0&0&0&0&0&0&0&0&0&0\\
0&0&0&0&0&0&0&0&0&0&0&0&0&0&0&0&0\\
0&0&0&0&0&0&0&0&0&0&0&0&0&0&0&1&0\\
0&0&0&0&0&0&0&0&0&0&0&0&0&0&0&0&1\\
0&0&0&0&0&0&0&0&0&0&0&0&0&0&0&0&0\\
0&0&0&0&0&0&0&0&0&0&0&0&0&0&0&0&0\\
0&0&0&0&0&0&0&0&0&0&0&0&0&0&0&0&0
\end{pmatrix} \tag{4.58}$$

## 4.4 Dielectric permitivity

In the above section it was not introduced a dielectric inside on waveguide. This was not introduced due to it had to be understand the general concept. Now, it will be explained how to introduce it, taking into account we have a problem in two dimensions. The introduction of dielectric will be by a polygon and staircase is applied $\epsilon_x$ and $\epsilon_y$ must be shifted by $\frac{\triangle x}{2}$ and $\frac{\triangle y}{2}$. But on the one hand, it should be known that $\epsilon_x$ and $epsilon_y$ is depending on TE modes due to in this polarization, it is taken into account $E_x \neq 0$, $E_y \neq 0$ and $H_z \neq 0$. Therefore, depending on electric fields $E_x$ and $E_y$ it will have a different permittivity.

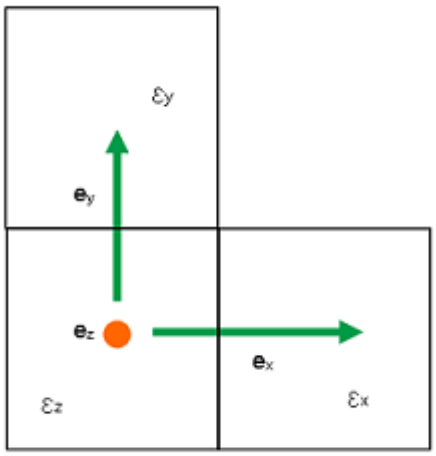


Figure 4.4: Dielectric permittivity in two dimensions

On the other hand, in case of TM polarization, it will not take into account the permittivity of x and y because in case of TM modes we have the conditions $H_x \neq 0$, $H_y \neq 0$ and $E_z \neq 0$, thus in case of TM, it will have a permittivity in the other direction $\epsilon_z$.

## 4.5 TM Polarization

Previously, it has been explained how to obtain TM modes in unidimensional problems. Likewise in TE modes, it will be introduced the obtaining of TM modes but in case of two dimensions. We assume $H_z = 0$ ($H_x \neq 0$, $H_y \neq 0$ and $E_z \neq 0$). Therefore, from equations (4.1) and (4.2) it will be obtained:

Thus, from equations (4.2) and (4.1):

$$\begin{cases} \gamma H_y = j\omega\epsilon_0\epsilon_z E_z \\ -\gamma H_x = j\omega\epsilon_0\epsilon_z E_z \\ -\frac{\partial H_x}{\partial y} + \frac{\partial H_y}{\partial x} = j\omega\epsilon_0 P E_z \end{cases} \tag{4.59}$$

and

$$\begin{cases} \frac{\partial E_z}{\partial y} = (P_y^{-1}\frac{\gamma^2}{j\omega\epsilon_0} - j\omega\mu_0)H_x \\ -\frac{\partial E_z}{\partial x} = (P_x^{-1}\frac{\gamma^2}{j\omega\epsilon_0} - j\omega\mu_0)H_y \end{cases} \tag{4.60}$$

It should be known that TM modes are based on three field components $H_x$, $H_y$ and $E_z$.

On the one hand,

$$-\frac{\partial H_x}{\partial y} + \frac{\partial H_y}{\partial x} = j\omega\epsilon_0 P E_z \tag{4.61}$$

Operating the equation (4.59) and using the approximation (3.4), it will be obtained briefly:

$$-\frac{H_{x5} - H_{x1}}{\triangle y} + \frac{H_{y5} - H_{y4}}{\triangle x} = j\omega\epsilon_0 P_z E_{z5} \tag{4.62}$$

$$-\frac{H_{x6}-H_{x2}}{\triangle y}+\frac{H_{y6}-H_{y5}}{\triangle x}=j\omega\epsilon_0 P_z E_{z6} \tag{4.63}$$

$$-\frac{H_{x7}-H_{x3}}{\triangle y}+\frac{H_{y7}-H_{y6}}{\triangle x}=j\omega\epsilon_0 P_z E_{z7} \tag{4.64}$$

$$-\frac{H_{x8}-H_{x4}}{\triangle y}+\frac{H_{y8}-H_{y7}}{\triangle x}=j\omega\epsilon_0 P_z E_{z8} \tag{4.65}$$

where P is the permittivity matrix depending on z-direction, thus it will be known as $P_z = \epsilon_z$ and equation (4.60) is associated with

$$C_{zt}^{(h)} h_t = j\omega\epsilon_0 P_z e_t \tag{4.66}$$

where $C_{zt}^{(h)}$ can be divided in two matrices $C_{zx}^{(h)}$ and $C_{zy}^{(h)}$, therefore the equation (4.66) can be defined as,

$$\left[C_{zx}^{(h)} C_{zy}^{(h)}\right]\begin{bmatrix}h_x\\h_y\end{bmatrix}=j\omega\epsilon_0 P e_z \tag{4.67}$$

These equations are obtained by magnetic field but they are examples due to number of these equations will be variable depending on K= M x M. As a result and in the same way that in TE modes, it can be defined one matrix for each matrix $C_{zx}^{(h)}$ and $C_{zy}^{(h)}$ as,

$$[C_{zx}^{(h)}]_{mn} = \triangle y^{-1}\begin{cases}-1, m=n,\\ 1, m=n+1,\\ 0, rest\end{cases} \tag{4.68}$$

$$[C_{zy}^{(h)}]_{mn} = \triangle x^{-1}\begin{cases}-1, m=n,\\ 1, m=n+1,\\ 0, rest\end{cases} \tag{4.69}$$

where graphically can be shown as,

$$C_{zx}^{(h)} = -\frac{1}{\triangle Y}\begin{bmatrix}-1&0&0&0&0&0&\dots&0\\0&-1&0&0&0&0&\dots&0\\0&0&-1&0&0&0&\dots&0\\0&0&0&-1&0&0&\dots&0\\1&0&0&0&-1&0&\dots&0\\0&1&0&0&0&-1&\dots&0\\\vdots&&&&&&&\\0&0&0&1&0&0&0&-1\end{bmatrix}\begin{bmatrix}H_{x1}\\H_{x2}\\H_{x3}\\H_{x4}\\H_{x5}\\H_{x6}\\\vdots\\H_{xK}\end{bmatrix} \tag{4.70}$$

$$C_{zy}^{(h)} = \frac{1}{\triangle X}\begin{bmatrix}-1&0&0&0&0&0&\dots&0\\1&-1&0&0&0&0&\dots&0\\0&1&-1&0&0&0&\dots&0\\0&0&1&-1&0&0&\dots&0\\0&0&0&1&-1&0&\dots&0\\0&0&0&0&1&-1&\dots&0\\\vdots&&&&&&&\\0&0&0&0&0&0&1&-1\end{bmatrix}\begin{bmatrix}H_{y1}\\H_{y2}\\H_{y3}\\H_{y4}\\H_{y5}\\H_{y6}\\\vdots\\H_{yK}\end{bmatrix} \tag{4.71}$$

On the other hand, if we focus on equation (4.1), it is necessary to obtain the equations of electric field solving the equation (4.1):

$$\begin{cases} \frac{\partial E_z}{\partial y} = (P_y^{-1}\frac{\gamma^2}{j\omega\epsilon_0} - j\omega\mu_0)H_x \\ -\frac{\partial E_z}{\partial x} = (P_x^{-1}\frac{\gamma^2}{j\omega\epsilon_0} - j\omega\mu_0)H_y \end{cases} \tag{4.72}$$

Solving the first equation on equation (4.70) and using the approximation (3.4),

$$\frac{\partial E_z}{\partial y} = (P_y^{-1}\frac{\gamma^2}{j\omega\epsilon_0} - j\omega\mu_0)H_x \tag{4.73}$$

it will be obtained this group of equations:

$$\frac{E_{z5} - E_{z1}}{\triangle y} = (P_y^{-1}\frac{\gamma^2}{j\omega\epsilon_0} - j\omega\mu_0)H_{x1} \tag{4.74}$$

$$\frac{E_{z6} - E_{z2}}{\triangle y} = (P_y^{-1}\frac{\gamma^2}{j\omega\epsilon_0} - j\omega\mu_0)H_{x2} \tag{4.75}$$

$$\frac{E_{z7} - E_{z3}}{\triangle y} = (P_y^{-1}\frac{\gamma^2}{j\omega\epsilon_0} - j\omega\mu_0)H_{x3} \tag{4.76}$$

$$\frac{E_{z8} - E_{z4}}{\triangle y} = (P_y^{-1}\frac{\gamma^2}{j\omega\epsilon_0} - j\omega\mu_0)H_{x4} \tag{4.77}$$

If it is solved the second equation on (4.70)

$$-\frac{\partial E_z}{\partial x} = (P_x^{-1}\frac{\gamma^2}{j\omega\epsilon_0} - j\omega\mu_0)H_y \tag{4.78}$$

In the same way,

$$-\frac{E_{z1} - E_{z0}}{\triangle x} = (P_x^{-1}\frac{\gamma^2}{j\omega\epsilon_0} - j\omega\mu_0)H_{y1} \tag{4.79}$$

$$-\frac{E_{z2} - E_{z1}}{\triangle x} = (P_x^{-1}\frac{\gamma^2}{j\omega\epsilon_0} - j\omega\mu_0)H_{y2} \tag{4.80}$$

$$-\frac{E_{z3} - E_{z2}}{\triangle x} = (P_x^{-1}\frac{\gamma^2}{j\omega\epsilon_0} - j\omega\mu_0)H_{y3} \tag{4.81}$$

$$-\frac{E_{z4} - E_{z3}}{\triangle x} = (P_x^{-1}\frac{\gamma^2}{j\omega\epsilon_0} - j\omega\mu_0)H_{y4} \tag{4.82}$$

In the same way that electric field, it will be got,

$$C_{tz}^{(e)}e_z = (P_t^{-1}\frac{\gamma^2}{j\omega\epsilon_0} - j\omega\mu_0)h_t \tag{4.83}$$

where $C_{tz}^{(e)}$ will be divided in two matrices $C_{xz}^{(e)}$ and $C_{yz}^{(e)}$ as:

$$\begin{bmatrix} C_{xz}^{(e)} \\ C_{yz}^{(e)} \end{bmatrix} \begin{bmatrix} e_z \end{bmatrix} = (P_t^{-1}\frac{\gamma^2}{j\omega\epsilon_0} - j\omega\mu_0) \begin{bmatrix} h_x \\ h_y \end{bmatrix} \tag{4.84}$$

If equations are representated graphically,

$$C_{xz}^{(e)} = \frac{1}{\triangle Y} \begin{bmatrix} -1 & 0 & 0 & 0 & 1 & 0 & \dots & 0 \\ 0 & -1 & 0 & 0 & 0 & 1 & \dots & 0 \\ 0 & 0 & -1 & 0 & 0 & 0 & \dots & 0 \\ 0 & 0 & 0 & -1 & 0 & 0 & \dots & 1 \\ 0 & 0 & 0 & 0 & -1 & 0 & \dots & 0 \\ 0 & 0 & 0 & 0 & 0 & -1 & \dots & 0 \\ \vdots & & & & & & & \\ 0 & 0 & 0 & 1 & 0 & 0 & 0 & -1 \end{bmatrix} \begin{bmatrix} E_{z1} \\ E_{z2} \\ E_{z3} \\ E_{z4} \\ E_{z5} \\ E_{z6} \\ \vdots \\ E_{zK} \end{bmatrix} \tag{4.85}$$

$$C_{yz}^{(e)} = \frac{1}{\triangle X} \begin{bmatrix} 1 & -1 & 0 & 0 & 0 & 0 & \dots & 0 \\ 0 & 1 & -1 & 0 & 0 & 0 & \dots & 0 \\ 0 & 0 & 1 & -1 & 0 & 0 & \dots & 0 \\ 0 & 0 & 0 & 1 & -1 & 0 & \dots & 0 \\ 0 & 0 & 0 & 0 & 1 & -1 & \dots & 0 \\ 0 & 0 & 0 & 0 & 0 & 1 & \dots & 0 \\ \vdots & & & & & & & \\ 0 & 0 & 0 & 0 & 0 & 0 & 0 & 1 \end{bmatrix} \begin{bmatrix} E_{z1} \\ E_{z2} \\ E_{z3} \\ E_{z4} \\ E_{z5} \\ E_{z6} \\ \vdots \\ E_{zK} \end{bmatrix} \tag{4.86}$$

Finally, it will be obtained these equations,

$$\begin{cases} C_{zt}^{(h)} h_t = j\omega\epsilon_0 P_z e_z \\ C_{tz}^{(e)} e_z = (P_t^{-1} \frac{\gamma^2}{j\omega\epsilon_0} - j\omega\mu_0) h_t \end{cases} \tag{4.87}$$

where

$$C_{zt}^{(h)} = \left[ C_{zx}^{(h)} C_{zy}^{(h)} \right] \tag{4.88}$$

and

$$C_{tz}^{(e)} = \begin{bmatrix} C_{xz}^{(e)} \\ C_{yz}^{(e)} \end{bmatrix} \tag{4.89}$$

Likewise in one dimension, it is possible to organise the equations and obtaining the eigenvalue problem for determining the propagation characteristics of TM polarization as:

$$[C_{zt}^{(h)} C_{tz}^{(e)} - \omega^2 \mu_0 \epsilon_0 P_z] = \gamma^2 e \tag{4.90}$$

or in case of $\gamma = 0$, the cutoff frequency would be obtained in this way,

$$[\mu_0^{-1} \epsilon_0^{-1} P_z^{-1} C_{tz}^{(e)} C_{zt}^{(h)} - \omega^2] e = \gamma^2 e \tag{4.91}$$

In both cases (equations (4.88) and (4.89)) it does not take into account the boundary conditions so far as they are necessary to complete the formulation of the problem.

## 4.6 Boundary conditions for TM polarization

On the one hand, previously mentioned, that equations which will be used to obtain the cutoff frequencies but not taking into account the boundary conditions. The next equations will be changed by boundary conditions but the final results will not be modified. The equations can be

transformed in such a way that calculation time will be fewer. If we remember in unidimensional problem and we take into account $e_z = T_z^e \tilde{e}$ and $h_t = T_t^h \tilde{h}$, the equation (4.87 )will be changed as,

$$\begin{cases} C_{tz}^{(e)} T_z^e \tilde{e} = -j\omega\mu_0 T_t^h \tilde{h} \\ C_{zt}^{(h)} T_t^h \tilde{h} \tilde{h} = j\omega\epsilon_0 P_z T_z^e \tilde{e} \end{cases} \tag{4.92}$$

calculating,

$$\begin{cases} {T_t^h}^T C_{tz}^{(e)} T_z^e \tilde{e} = -j\omega\mu_0 \tilde{h} \\ {T_z^e}^T C_{zt}^{(h)} T_t^h \tilde{h} = j\omega\epsilon_0 T_e^T P_z T_z^e \tilde{e} \end{cases} \tag{4.93}$$

Finally, it will be obtained the new equations as,

$$\begin{cases} \tilde{C}_{tz}^{(e)} \tilde{e} = -j\omega\mu_0 \tilde{h} \\ \tilde{C}_{zt}^{(h)} \tilde{h} = j\omega\epsilon_0 \tilde{P}_z \tilde{e} \end{cases} \tag{4.94}$$

where $\tilde{C}_{tz}^{(e)} = {T_t^h}^T C^{(e)} T_z^e$, $\tilde{C}_{zt}^{(h)} = {T_z^e}^T C^{(h)} T_t^h$ and $\tilde{P}_z = {T_z^e}^T P_z T_z^e$. As it is possible to see, the equations which have been obtained are coincidents with equations in TE polarization but in case of TM $T_e$ and $T_h$ will be obtained by extra equations that will be different to TE polarization.

On the other hand, it can not be forgot that boundary conditions $T_e$ and $T_h$ will be changed by extra matrices. These extra matrices are based on the Figure 4.5 which the boundary conditions must be imposed inside on field.

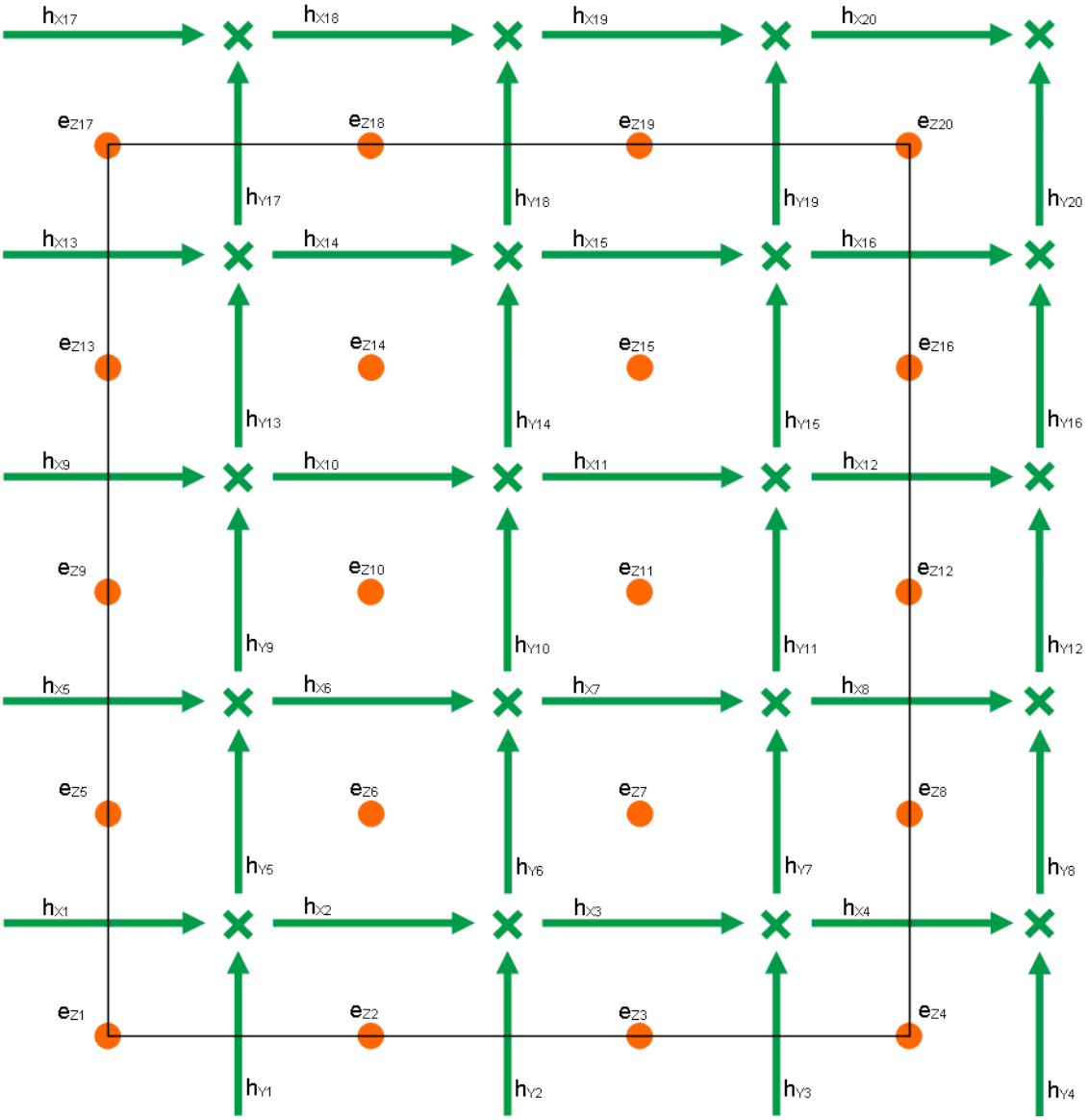


Figure 4.5: The set of points which will be taken into account to get the boundary conditions

In case of TM modes, it should not be forgot that not all fields are valids, only $H_x$, $H_y$ and $E_z$, thus it will be obtained one matrix for each valid field depending on the mesh (Figure 4.4):

$$R_x^h = \begin{bmatrix} 1 & 1 & 1 & 1 & 1 \\ 0 & 0 & 0 & 0 & 1 \\ 0 & 0 & 0 & 0 & 1 \\ 1 & 1 & 1 & 1 & 1 \end{bmatrix} \tag{4.95}$$

where reshape of $R_x^h = \begin{bmatrix} 1 & 0 & 0 & 1 & 1 & 0 & 0 & 1 & 1 & 0 & 0 & 1 & 1 & 1 & 1 \end{bmatrix}$

$$R_y^h = \begin{bmatrix} 1 & 0 & 0 & 0 & 1 \\ 1 & 0 & 0 & 0 & 1 \\ 1 & 0 & 0 & 0 & 1 \\ 1 & 1 & 1 & 1 & 1 \end{bmatrix} \tag{4.96}$$

where reshape of $R_y^h = [\,1\;1\;1\;1\;0\;0\;0\;1\;0\;0\;0\;1\;1\;1\;1\;1\,]$

$$R_z^h = \begin{bmatrix} 1 & 1 & 1 & 1 & 1 \\ 1 & 0 & 0 & 0 & 1 \\ 1 & 0 & 0 & 0 & 1 \\ 1 & 1 & 1 & 1 & 1 \end{bmatrix} \tag{4.97}$$

where reshape of $R_z^h = [\,1\;1\;1\;1\;1\;0\;0\;1\;1\;0\;0\;1\;1\;1\;1\;1\,]$

In that way, the above equations $\tilde{e}_z$ and $\tilde{h}_t$ is representing boundary conditions where $T_z^e$ and $T_t^h$ are,

$$T_t^h = \begin{pmatrix}
0&0&0&0&0&0&0&0&0&0&0&0&0&0&0&0&0\\
1&0&0&0&0&0&0&0&0&0&0&0&0&0&0&0&0\\
0&1&0&0&0&0&0&0&0&0&0&0&0&0&0&0&0\\
0&0&0&0&0&0&0&0&0&0&0&0&0&0&0&0&0\\
0&0&0&0&0&0&0&0&0&0&0&0&0&0&0&0&0\\
0&0&1&0&0&0&0&0&0&0&0&0&0&0&0&0&0\\
0&0&0&1&0&0&0&0&0&0&0&0&0&0&0&0&0\\
0&0&0&0&0&0&0&0&0&0&0&0&0&0&0&0&0\\
0&0&0&0&0&0&0&0&0&0&0&0&0&0&0&0&0\\
0&0&0&0&1&0&0&0&0&0&0&0&0&0&0&0&0\\
0&0&0&0&0&1&0&0&0&0&0&0&0&0&0&0&0\\
0&0&0&0&0&0&0&0&0&0&0&0&0&0&0&0&0\\
0&0&0&0&0&0&0&0&0&0&0&0&0&0&0&0&0\\
0&0&0&0&0&0&1&0&0&0&0&0&0&0&0&0&0\\
0&0&0&0&0&0&0&1&0&0&0&0&0&0&0&0&0\\
0&0&0&0&0&0&0&0&0&0&0&0&0&0&0&0&0\\
0&0&0&0&0&0&0&0&0&0&0&0&0&0&0&0&0\\
0&0&0&0&0&0&0&0&0&0&0&0&0&0&0&0&0\\
0&0&0&0&0&0&0&0&0&0&0&0&0&0&0&0&0\\
0&0&0&0&0&0&0&0&0&0&0&0&0&0&0&0&0\\
0&0&0&0&0&0&0&0&0&0&0&0&0&0&0&0&0\\
0&0&0&0&0&0&0&0&0&0&0&0&0&0&0&0&0\\
0&0&0&0&0&0&0&0&1&0&0&0&0&0&0&0&0\\
0&0&0&0&0&0&0&0&0&1&0&0&0&0&0&0&0\\
0&0&0&0&0&0&0&0&0&0&1&0&0&0&0&0&0\\
0&0&0&0&0&0&0&0&0&0&0&0&0&0&0&0&0\\
0&0&0&0&0&0&0&0&0&0&0&1&0&0&0&0&0\\
0&0&0&0&0&0&0&0&0&0&0&0&1&0&0&0&0\\
0&0&0&0&0&0&0&0&0&0&0&0&0&1&0&0&0\\
0&0&0&0&0&0&0&0&0&0&0&0&0&0&0&0&0\\
0&0&0&0&0&0&0&0&0&0&0&0&0&0&1&0&0\\
0&0&0&0&0&0&0&0&0&0&0&0&0&0&0&1&0\\
0&0&0&0&0&0&0&0&0&0&0&0&0&0&0&0&1
\end{pmatrix} \tag{4.98}$$

$$T_z^e = \begin{pmatrix} 0 & 0 & 0 & 0 & 0 & 0 \\ 0 & 0 & 0 & 0 & 0 & 0 \\ 0 & 0 & 0 & 0 & 0 & 0 \\ 0 & 0 & 0 & 0 & 0 & 0 \\ 0 & 0 & 0 & 0 & 0 & 0 \\ 1 & 0 & 0 & 0 & 0 & 0 \\ 0 & 1 & 0 & 0 & 0 & 0 \\ 0 & 0 & 0 & 0 & 0 & 0 \\ 0 & 0 & 0 & 0 & 0 & 0 \\ 0 & 0 & 1 & 0 & 0 & 0 \\ 0 & 0 & 0 & 1 & 0 & 0 \\ 0 & 0 & 0 & 0 & 0 & 0 \\ 0 & 0 & 0 & 0 & 0 & 0 \\ 0 & 0 & 0 & 0 & 1 & 0 \\ 0 & 0 & 0 & 0 & 0 & 1 \\ 0 & 0 & 0 & 0 & 0 & 0 \\ 0 & 0 & 0 & 0 & 0 & 0 \\ 0 & 0 & 0 & 0 & 0 & 0 \\ 0 & 0 & 0 & 0 & 0 & 0 \\ 0 & 0 & 0 & 0 & 0 & 0 \end{pmatrix} \tag{4.99}$$

## 4.7 Propagation characteristics

### 4.7.1 Propagation characteristics for TE polarization

In case of TE, propagation characteristics can be obtained from the following eigenproblem by equation (4.50),

$$AX = \lambda X \tag{4.100}$$

where $A = C_{tz}^{(h)} C_{zt}^{(e)} - \omega^2 \mu_0 \epsilon_0 P$ and $\lambda = \gamma^2$ which represents the propagation coefficients.

### 4.7.2 Propagation characteristics for TM polarization

In case of TM modes the equation, we will take into account the equation (4.89) and by eigenproblem, it will be possible to calculate the propagation charascteristics.

$$AX = \lambda X \tag{4.101}$$

where $A = C_{zt}^{(h)} C_{tz}^{(e)} - \omega^2 \mu_0 \epsilon_0 P_z$ and $\lambda = \gamma^2$ which represents the propagation coefficients.

## 4.8 Numerical tests

During the project, many tests have been done with the goal of comparing or demostrating that this method is acceptable. It has been carried out by Matlab environmental. As a result it will be exposed the different results for each polarization TE and TM. On the one hand, it will be exposed the results for cutoff frequency and on the other hand the propagation characteristics.

To verify that method, it will be introduce one dielectric of permittivity $\epsilon_{r1} = 9$. At first, it was decided to use the parallel-plate waveguide of width a = 22.86mm and heigth b=10.16mm.

The next figure presents the dielectric which has been introduce in the waveguide.

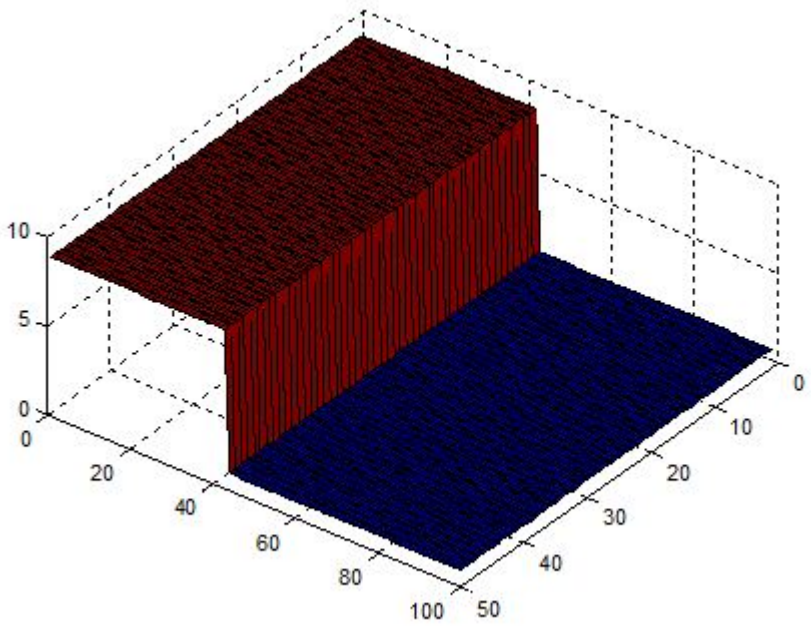


Figure 4.6: Dielectric introduced in the waveguide

As it is shown in Figure 4.5, it has one dielectric with a permittivity of $\epsilon_{r1} = 9$ and the rest of waveguide empty $\epsilon_{r2} = 1$.

It must be remembered that $\epsilon_r$ will be,

$$P_t = \begin{bmatrix} \epsilon_x & 0 \\ 0 & \epsilon_y \end{bmatrix} \tag{4.102}$$

and

$$P_z = \begin{bmatrix} \epsilon_z \end{bmatrix} \tag{4.103}$$

### 4.8.1 TE Polarization

**Obtaining cutoff frequencies in two dimensions**

In case of unidimensional problem, it was obtained the value of cutoff frequency with a dielectric inside of waveguide. In this case, it will be obtained the cutoff frequencies for TE modes without dielectric and, afterwards, it will be got the results with permittivity ($\epsilon_r = 9$) for comparison of TE modes in one and two dimensions which will be simultaneous. Previously, it has been explained how to obtain the propagation coefficients and cutoff frequencies in equations (4.49) and (4.50). Now, we are going to obtain the cutoff frequencies in some conditions which are $\epsilon_0 = 8.854187818 \cdot 10^{-12}$ and $c \simeq 3 \cdot 10^8$ m/s. All results have been obtained by Matlab environment.

Obtaining cutoff frequencies, we focus on equation (4.50) and eigenproblem explained previously,

$$AX = \lambda X \tag{4.104}$$

where $A = \tilde{C}_{tz}^{(h)} \tilde{C}_{zt}^{(e)}$ and $\lambda = \omega^2 \mu_0 \epsilon_0$.

### Empty waveguide

All this thesis is worked by Matlab envirnoment, thus the cutoff frequencies which have been explained previously are exposed in the Table 4.1. In the table, the first five modes have been shown for different meshes but these results have been obtained without dielectric inside on waveguide given. Firstly, a little mesh was used and afterwards the mesh was increased and the results were better. In this way, we were studying the changes of different fields and their progresses.

| | | | TE10 | TE20 | TE01 | TE11 | TE21 |
|---|---|---|---|---|---|---|---|
| | M | N | fc1(GHz) | fc2(GHz) | fc3(GHz) | fc4(GHz) | fc5(GHz) |
| Numerical | 23 | 10 | 6,556 | 13,079 | 14,689 | 16,086 | 19,668 |
| Error(%) | | | 0,09 | 0,33 | 0,50 | 0,43 | 0,43 |
| Numerical | 46 | 20 | 6,5603 | 13,113 | 14,747 | 16,140 | 19,734 |
| Error(%) | | | 0,02 | 0,07 | 0,11 | 0,09 | 0,09 |
| Numerical | 92 | 40 | 6,5614 | 13,121 | 14,760 | 16,152 | 19,749 |
| Error(%) | | | 0,009 | 0,01 | 0,02 | 0,02 | 0,02 |
| Numerical | 184 | 80 | 6,561 | 13,123 | 14,763 | 16,155 | 19,752 |
| Error(%) | | | 0,006 | 0 | 0,006 | 0,006 | 0,005 |
| Analytical | | | 6,562 | 13,123 | 14,764 | 16,156 | 19,753 |

Table 4.1: Frequency data table for $TE_m n$ modes in two dimensions

As it is shown in the Table 4.1 the results have been compared with analytical results by error to verify that we have got good solutions. Analytical solutions have been exposed in appendix B.

Graphically, it is shown the obtained fields in the next images. Firstly, it has been obtained the $TE_{10}$, $TE_{20}$ $TE_{01}$, $TE_{11}$ and $TE_{21}$ modes. That images have been included to demostrate our study. The graphic representation has been made for a differente mesh, M=100 and N=50. This mesh was used due to in one dimension it used a mesh of N=100 points, therefore to compare both results it was necessary having the same size.

It should be known that $TE_{m0}$ or $TE_{0n}$ fields always will have a nul component due to a electric and magnetic fields. In case of $TE_{m0}$ the nul component will be $E_x$ and in case of $TE_{0n}$ will be $E_y$. This is possible to verify by analytical studies in appendix B.

In the following cases, it is possible to see that nule components explained prevously, for example in $TE_{10}$, $TE_{20}$ and $TE_{01}$.

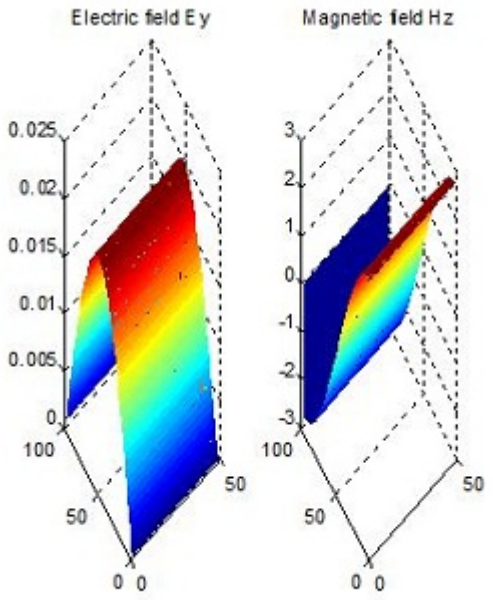


Figure 4.7: Representation TE10 mode in two dimensions

In case of $TE_{10}$ mode, it can be verified that in one and two dimensions the cutoff frecuency is the same. It has been obtained a value of $f_{c10} = 6,5614$ GHz.

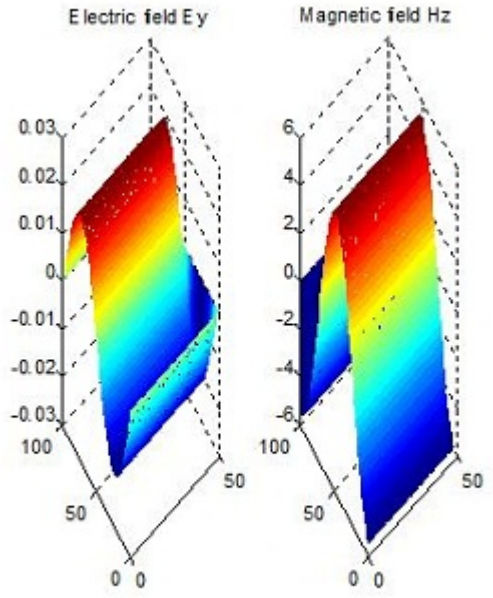


Figure 4.8: Representation TE20 mode in two dimensions

In case of $TE_{20}$ the obtained cutoff frequency is 13,121 GHz.

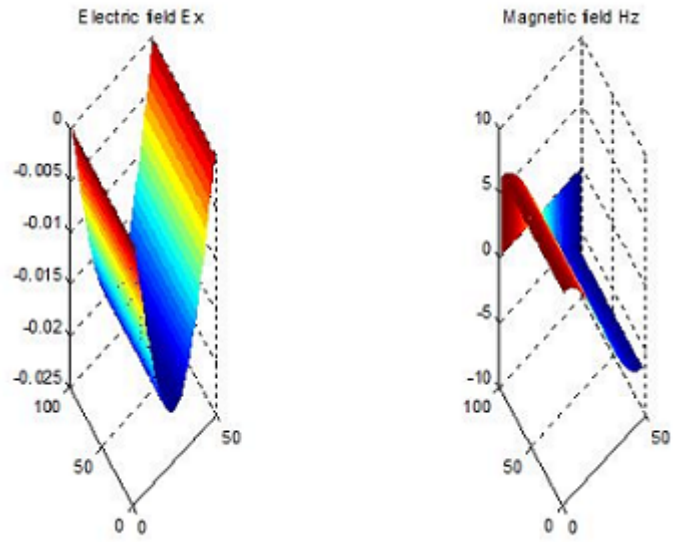


Figure 4.9: Representation TE01 mode in two dimensions

In case of $TE_{01}$ the obtained cutoff frequency is 14,761 GHz.

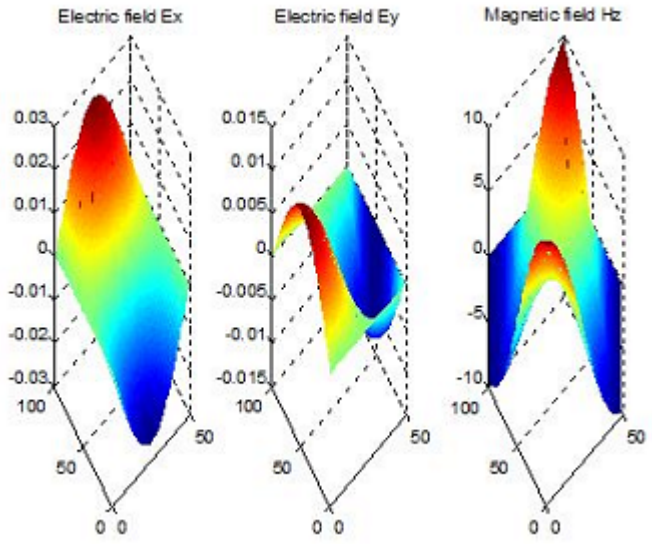


Figure 4.10: Representation TE11 mode in two dimensions

In case of $TE_{11}$ the obtained cutoff frequency is 16,154 GHz.

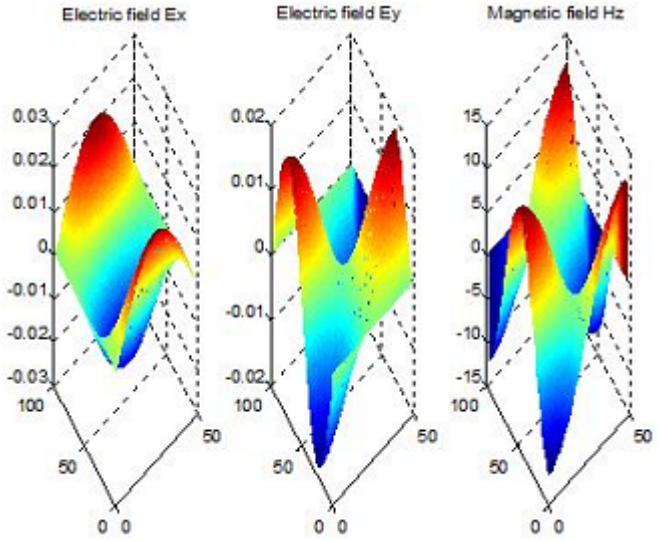


Figure 4.11: Representation TE21 mode in two dimensions

In case of $TE_{21}$ the obtained cutoff frequency is 19,750 GHz.

### Dielectric slab with rectangular waveguide

Subsequently, it was obtained the different fields for TE modes in two dimensions in case of dielectric inside on waveguide. It was included a dielectric which had the same characteristics that in unidimensional problem with the goal of comparing the results of one and two dimensions. The dielectric has a value $\epsilon_{r1} = 9$ and the rest $\epsilon_{r2} = 1$. It has been the three first modes as in previously case.

The cutoff frequencies obtained for each mode have been shown in the Table (4.4). Likewise, we are increasing the mesh and we see that the results are more accuracy.

| | | TE10 | TE20 | TE11 | TE21 |
|---|---|---|---|---|---|
| M | N | fc1(GHz) | fc2(GHz) | fc3(GHz) | fc4(GHz) |
| 23 | 10 | 3,0123 | 7,297 | 8,6718 | 9,9538 |
| 46 | 20 | 3,0097 | 7,3210 | 8,7240 | 10,104 |
| 92 | 40 | 3,0074 | 7,321 | 8,7369 | 10,137 |
| 184 | 80 | 2,9819 | 7,2516 | 8,6806 | 10,138 |

Table 4.2: Frequency data table for $TE_mn$ modes in two dimensions

The following pictures have been obtained for a mesh M=100 and N=50.

The Figure 4.12 represents the $TE_{10}$ mode with a dielectric $\epsilon_{r1} = 9$ inside on waveguide, and the cutoff frequency which has been obtained is 2.9838 GHz. It can be compared that in one and two dimensions the values are coincidents. In this case, it is not shown the electric field in x-direction ($E_x$) due to we are showing the $TE_{10}$ and the electric field in x-direction will be zero. This is explained in analytical solutions for TE modes in appendix B.

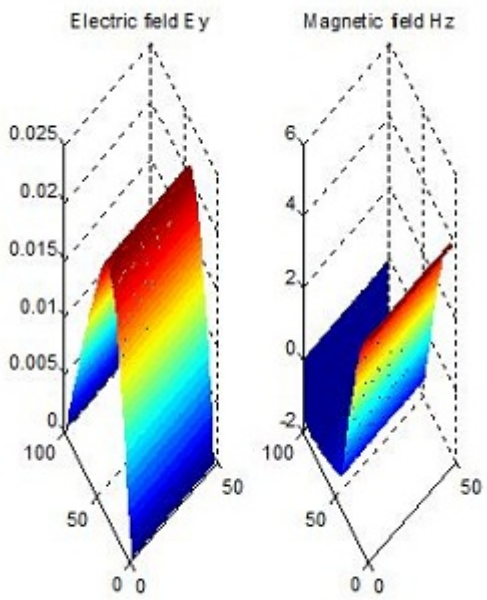


Figure 4.12: Representation TE10 mode in two dimensions with permittivity

In the Figure 4.13 represents $TE_{20}$ and in the same case, it is not shown the electric field in x-direction ($E_x$) due to we are showing the $TE_{20}$ and the electric field in x-direction is zero. This is explained in analytical solutions for TE modes in appendix B.

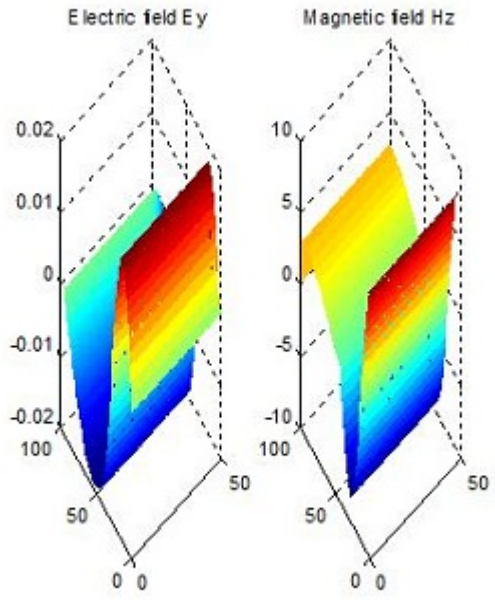


Figure 4.13: Representation TE20 mode in two dimensions with permittivity

In the same way, it can be seen that the cutoff frequencies are coincidents in one and two dimensions with dielectric inside on waveguide.

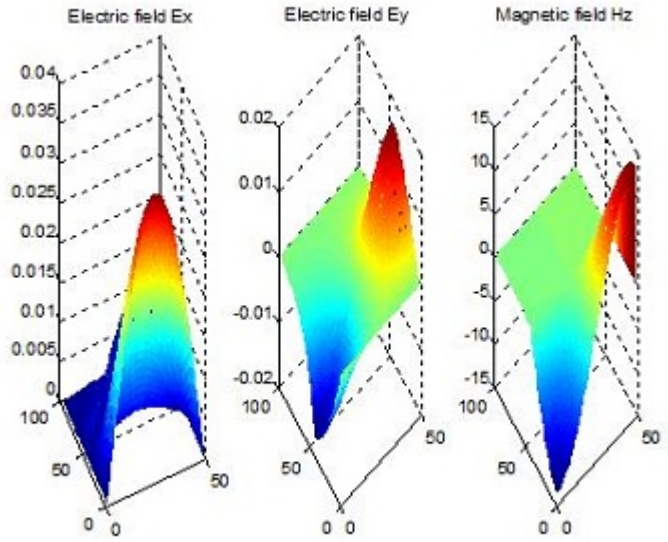


Figure 4.14: Representation TE11 mode in two dimensions with permittivity

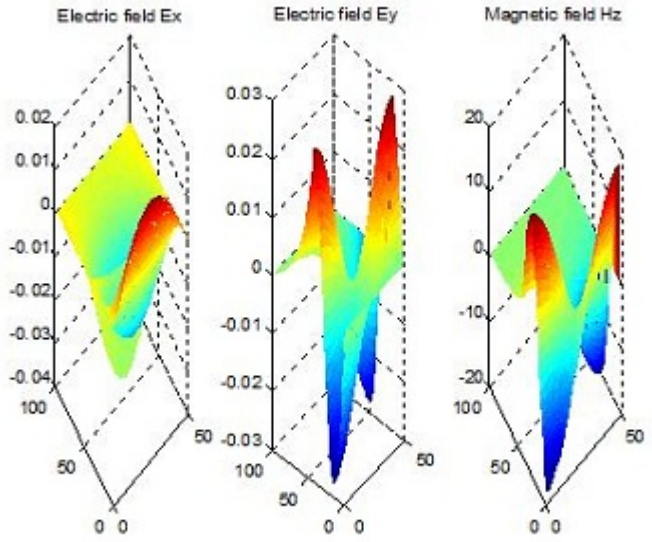


Figure 4.15: Representation TE21 mode in two dimensions with permittivity

Finally, the last mode which has been shown before, TE21 with dielectric.

### Results of propagation characteristics TE modes in two dimensions

As it was explained in unidimensional problem, an important issue for each mode is the frequency which from that point on a mode will be able to propagate by the waveguide. Propagation factor in the general case a complex number, which can be written as:

$$\gamma_{mn} = \alpha_{mn} + j\beta_{mn} \tag{4.105}$$

where $\alpha_{mn}$ is a damping coefficient and $\beta mn$ is a phase factor. The index m and n are the wave number of different modes which propagate.

Programming in Matlab environment, if the TE and TM equations are organised, it is possible to obtain the propagation coefficients such as it was made for the structure in one dimension.

By equation (4.49), it will be obtained the eigenvalue problem to get propagation coefficients.

$$AX = \lambda X \tag{4.106}$$

As we know, when we have an empty waveguide the cutoff frequencies of TE and TM modes are the same in case of $m = 1, 2, 3, \ldots$ and $n = 1, 2, 3, \ldots$. Therefore, the propagation constant for an empty waveguide are the same in TE and TM modes. Analytically, it is possible to verify,

$$\gamma_{mn} = \sqrt{p^2 - \omega^2\mu\epsilon} \tag{4.107}$$

where $c = \frac{1}{\sqrt{\mu\epsilon}}$ and $p = \sqrt{(\frac{m\pi}{a})^2 + (\frac{n\pi}{b})^2}$ and therefore,

$$\gamma_{mn} = \sqrt{p^2 - (\frac{\omega}{c})^2} \tag{4.108}$$

It will have to take into acount next equations to obtain the propagation coefficients will be based on boundary conditions, therefore in case of TE and TM polarization only will be changed the matrices.

First of all, previously it was commented for an empty waveguide the cutoff frequencies in TE and TM modes should be the same in case of $TE_{mn}$ and $TM_{mn}$ where $m = 1, 2 \ldots$ and $n = 1, 2, \ldots$, thus, the propagation coefficients in that cases should be the same in each different mode. Therefore we could verify the validity of that. For a mesh of M=100 and N=50 and $\epsilon_r = 1$, it will be obtained the next propagation coefficients for 20GHz of frequency:

| | n m | 0 | 1 | 2 | 3 |
|---|---|---|---|---|---|
| Numerical | 0 | - | 395,9j | 316,39j | 75,01j |
| Error (%) | | | 0,05 | 0,08 | 0,13 |
| Numerical | 1 | 282,91j | 247,30j | 66,23j | 299,68 |
| Error (%) | | 0,09 | 0,13 | 0,29 | 0,08 |
| | n m | 0 | 1 | 2 | 3 |
| Analytical | 0 | - | 395,70j | 316,13j | 74,907j |
| Analytical | 1 | 282,63j | 246,97j | 66,033j | 299,94 |

Table 4.3: Numerical propagation coefficients compared with analytical coefficients for TE in two dimensions

These values have been compared with analytical results which are shown in the Table 4.3 and they have been obtained by appendix B.

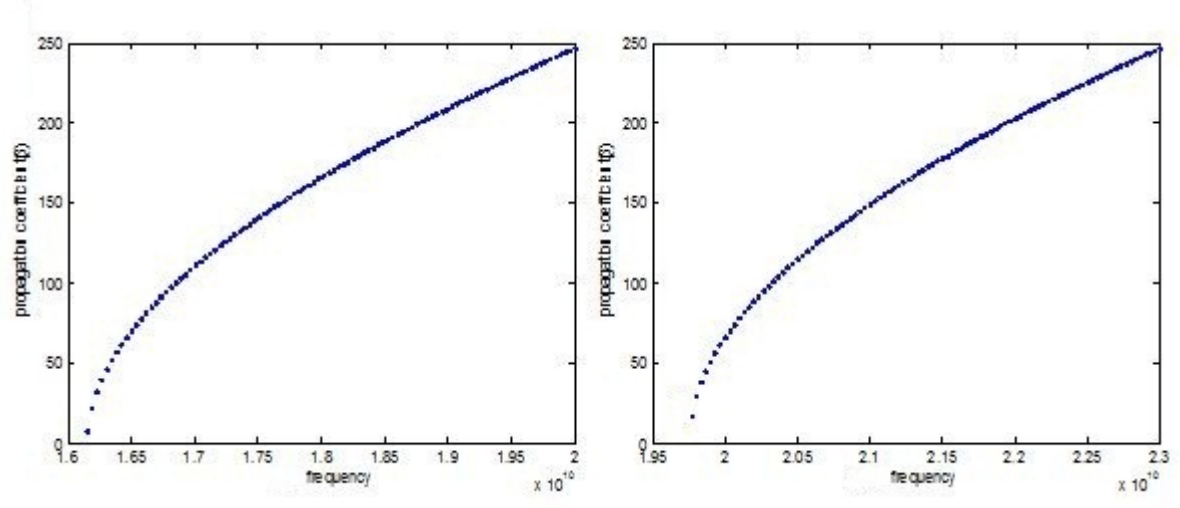


Figure 4.16: Representation of dispersion characteristics of $TE_{11}$ and $TE_{21}$ modes in two dimensions

In this case, we can see the dispersion chacteristics depending on cutoff frequency of the obtained mode. In this case $TE_{11}$ and $TE_{21}$.

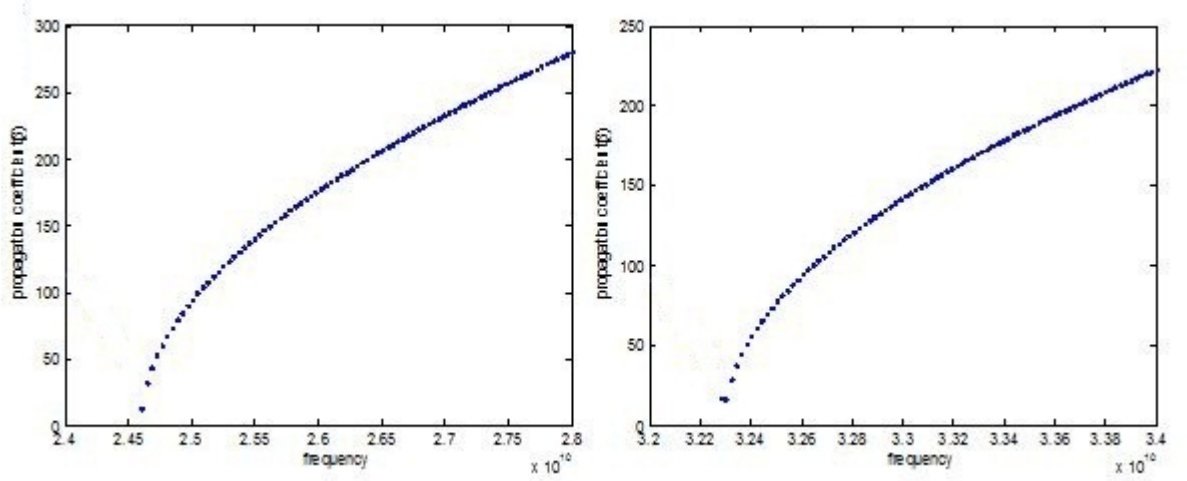


Figure 4.17: Representation of dispersion characteristics of $TE_{31}$ and $TE_{22}$ modes in two dimensions

In this case, we can see the dispersion chacteristics depending on cutoff frequency of the obtained mode. In this case $TE_{31}$ and $TE_{22}$.

In all these pictures, the dispersion characteristics shown the imaginary part of $\gamma$.

### 4.8.2 TM Polarization

#### Obtaining cutoff frequencies in two dimensions

Obtaining cutoff frequencies, we focus on equation (4.84) and by eigenproblem it will be obtained the propagation coefficients as,

$$AX = \lambda X \tag{4.109}$$

where $A = \tilde{C}_{zt}^{(h)} \tilde{C}_{tz}^{(e)}$ and $\lambda = \omega^2 \mu_0 \epsilon_0$.

### Empty waveguide

Likewise, it has been studied the result of different cutoff frequencies for each TM mode. In next table is shown the results with different mesh in order from smallest to largest. In this case, it has not been introduced any dielectric, as we commented to understand the general concept, but subsequently it wil be shown different images with the fields which hav been obtained in Matlab environment.

| | | | TM11 | TM21 | TM31 | TM41 | TM22 |
|---|---|---|---|---|---|---|---|
| | M | N | fc1(GHz) | fc2(GHz) | fc3(GHz) | fc4(GHz) | fc5(GHz) |
| Numerical | 23 | 10 | 16,086 | 19,668 | 24,441 | 29,768 | 31,750 |
| Error(%) | | | 0,43 | 0,43 | 0,67 | 1,15 | 1,74 |
| Numerical | 46 | 20 | 16,140 | 19,734 | 24,567 | 30,032 | 32,185 |
| Error(%) | | | 0,09 | 0,09 | 0,15 | 0,27 | 0,39 |
| Numerical | 92 | 40 | 16,152 | 19,749 | 24,597 | 30,094 | 32,282 |
| Error(%) | | | 0,02 | 0,02 | 0,03 | 0,06 | 0,09 |
| Numerical | 184 | 80 | 16,155 | 19,752 | 24,604 | 30,109 | 32,305 |
| Error(%) | | | 0,006 | 0,005 | 0,008 | 0,01 | 0,02 |
| Analytical | | | 16,156 | 19,753 | 24,606 | 30,114 | 30,248 |

Table 4.4: Frequency data table for $TM_m n$ modes in two dimensions

These results are obtained by different mesh. In addition, each one has been compared with analytical solutions which have been exposed in appendix B.

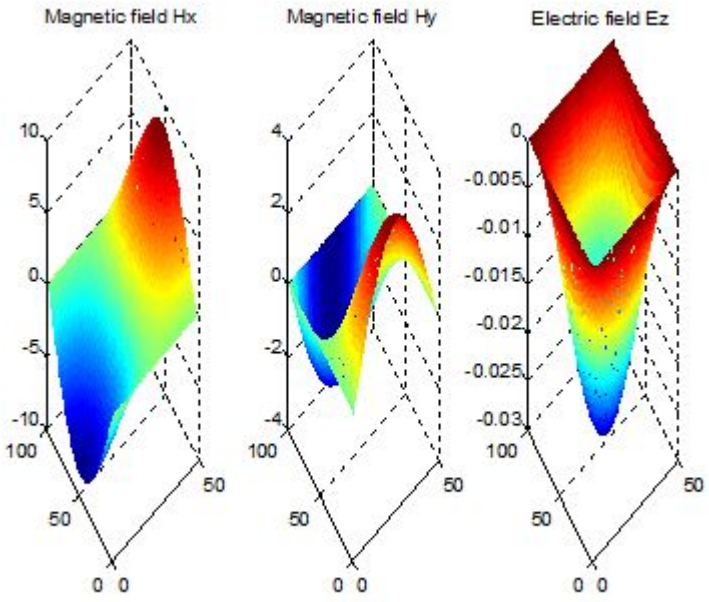


Figure 4.18: Representation TM11 mode in two dimensions

For TM11 mode is obatined a cutoff frequency $fc_{11} = 16,154$ GHz.

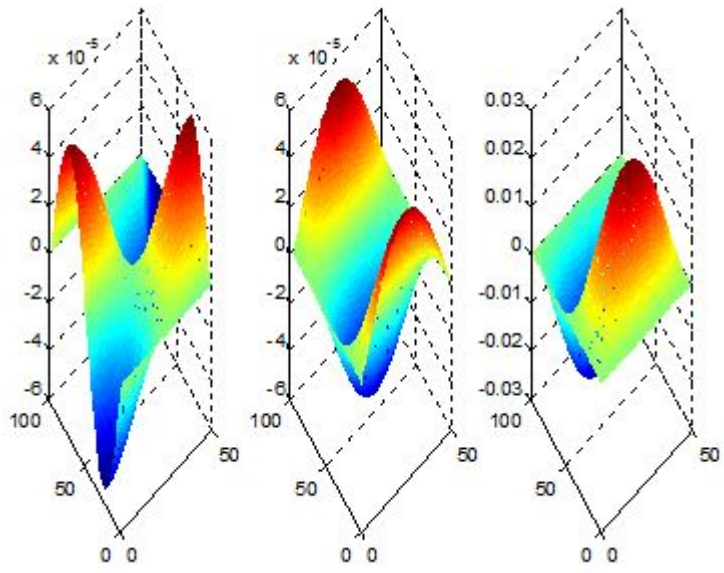


Figure 4.19: Representation TM21 mode in two dimensions

For TM21 mode is obatined a cutoff frequency $fc_{21} = 19,750$ GHz.

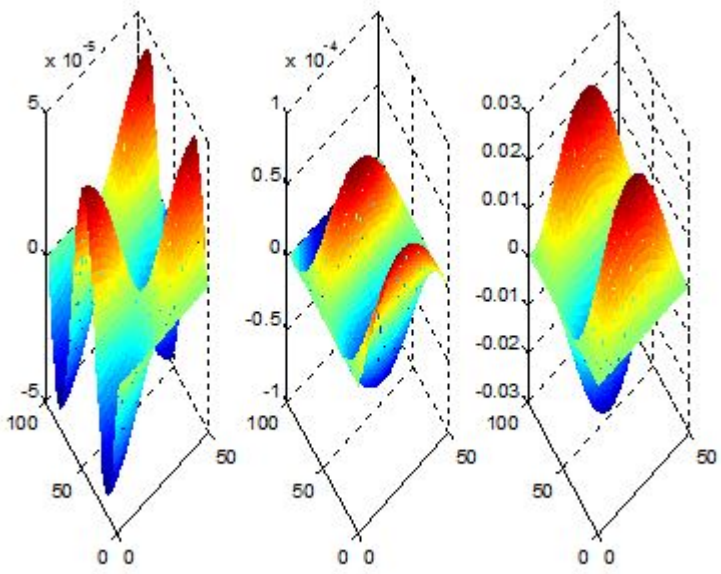


Figure 4.20: Representation TM31 mode in two dimensions

For TM31 mode is obatined a cutoff frequency $fc_{31} = 24,599$ GHz.

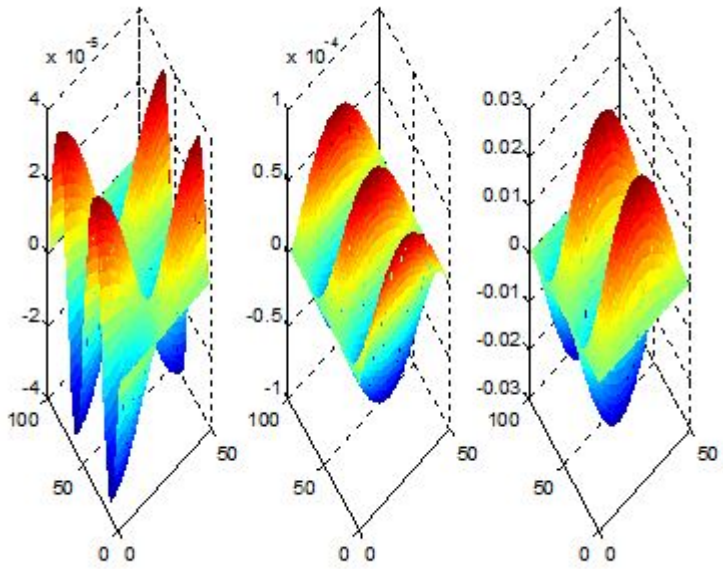


Figure 4.21: Representation TM41 mode in two dimensions

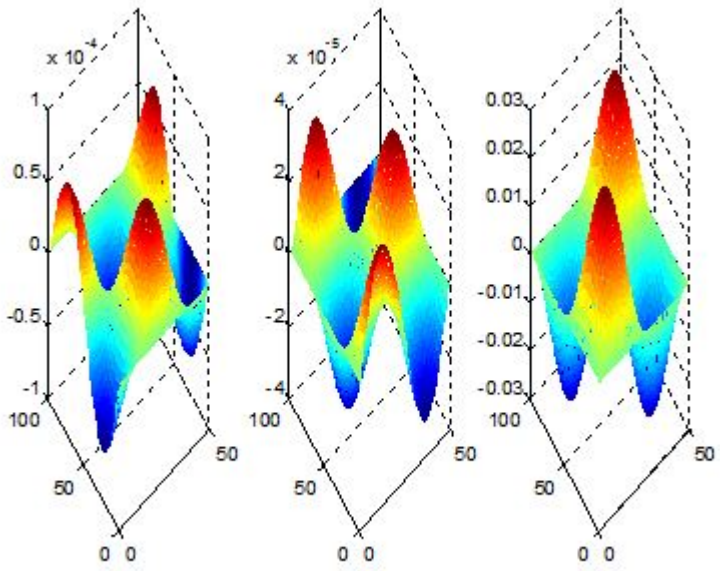


Figure 4.22: Representation TM22 mode in two dimensions

### Dielectric slab with rectangular waveguide

Likewise, it has been introduced a dielectric inside on waveguide with value $\epsilon_{r1} = 9$ and $\epsilon_{r2} = 1$ and the results of cutoff frequencies are shown in the Table 4.6. All results have been obtained by Matlab environment.

| | | TM11 | TM21 | TM12 | TM22 |
|---|---|---|---|---|---|
| M | N | fc1(GHz) | fc2(GHz) | fc3(GHz) | fc4(GHz) |
| 23 | 10 | 6,2481 | 9,5203 | 10,558 | 12,971 |
| 46 | 20 | 6,2678 | 9,5850 | 10,710 | 13,160 |
| 92 | 40 | 6,2705 | 9,5946 | 10,742 | 13,199 |
| 184 | 80 | 6,2459 | 9,5155 | 10,731 | 13,140 |

Table 4.5: Frequency data table for $TE_mn$ modes in two dimensions

We are going to show the same fields but in this case, the mesh which has been used is M=100 and N=50:

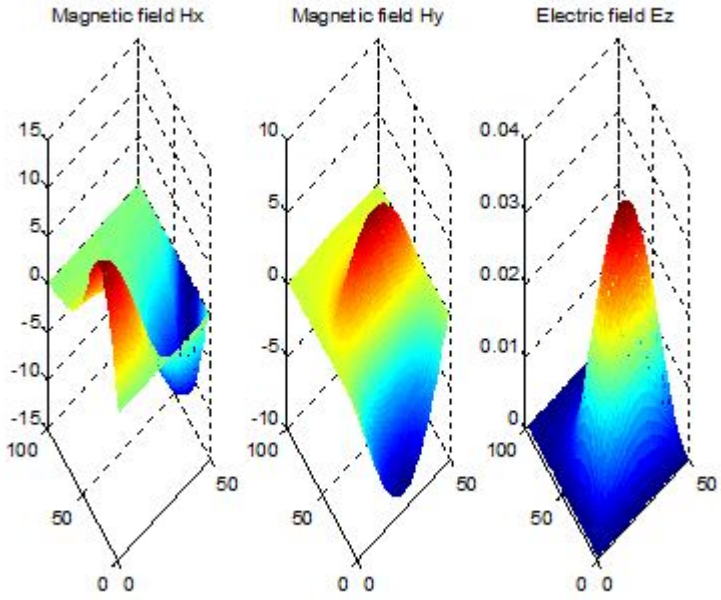


Figure 4.23: Representation TM11 mode in two dimensions with dielectric

In case of $TM_{11}$, the cutoff frequency will be $f_{c11} = 6,2472$ GHz.

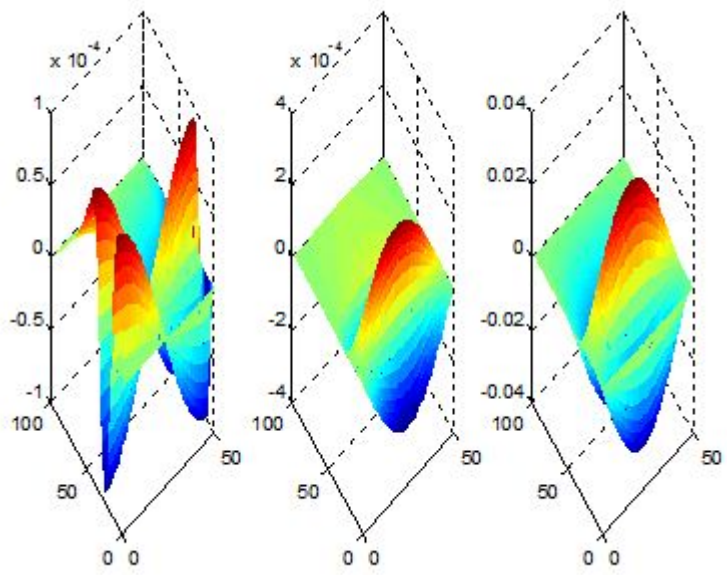


Figure 4.24: Representation TM21 mode in two dimensions with dielectric

In case of $TM_{21}$, the cutoff frequency will be $f_{c21} = 9,5190$ GHz.

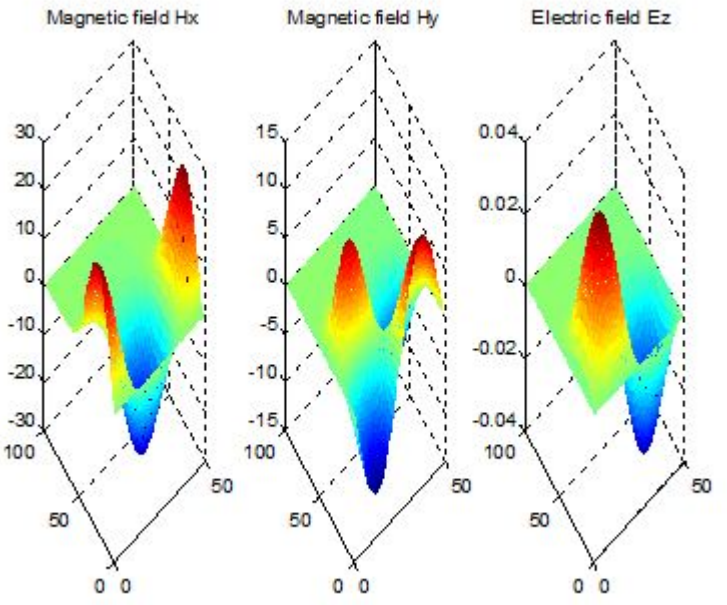


Figure 4.25: Representation TM12 mode in two dimensions with dielectric

In case of $TM_{12}$, the cutoff frequency will be $f_{c12} = 13,606$ GHz.

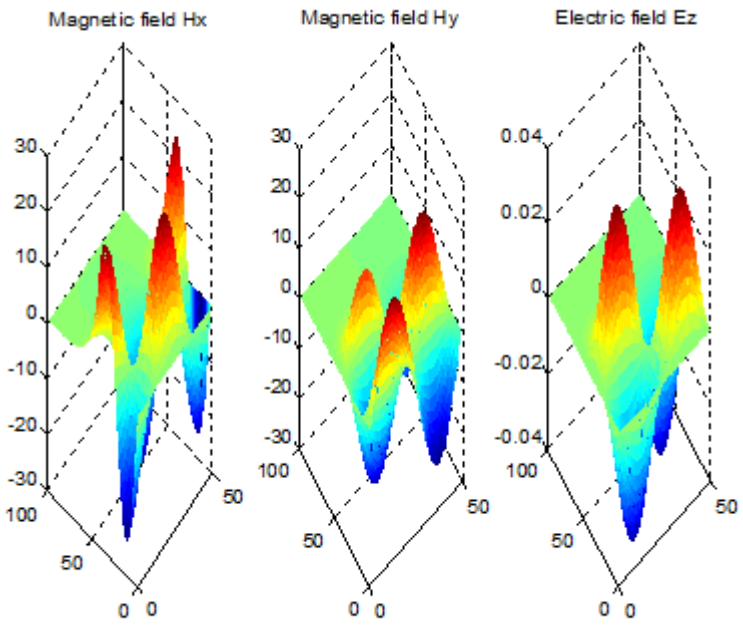


Figure 4.26: Representation TM22 mode in two dimensions with dielectric

In case of $TM_{22}$, the cutoff frequency will be $f_{c22} = 13,139$ GHz.

### Results of propagation characteristics TM modes in two dimensions

As it was explained in unidimensional problem, an important issue for each mode is the frequency which from that point on a mode will be able to propagate by the waveguide. Propagation factor in the general case a complex number, which can be written as:

$$\gamma_{mn} = \alpha_{mn} + j\beta_{mn} \tag{4.110}$$

where $\alpha_{mn}$ is a damping coefficient and $\beta mn$ is a phase factor. The index m and n are the wave number of different modes which propagate.

Programming in Matlab environment, if the TE and TM equations are organised, it is possible to obtain the propagation coefficients such as it was made for the structure in one dimension. It will be the same equation for each mode. If we base on equation (4.84) can be obtained propagation coefficients by eigenproblem.

$$AX = \lambda X \tag{4.111}$$

As we know, when we have an empty waveguide the cutoff frequencies of TE and TM modes are the same in case of $m = 1, 2, 3, \ldots$ and $n = 1, 2, 3, \ldots$. Therefore, the propagation constant for an empty waveguide are the same in TE and TM modes. Analytically, it is possible to verify,

$$\gamma_{mn} = \sqrt{p^2 - \omega^2\mu\epsilon} \tag{4.112}$$

where $c = \frac{1}{\sqrt{\mu\epsilon}}$ and $p = \sqrt{(\frac{m\pi}{a})^2 + (\frac{n\pi}{b})^2}$ and therefore,

$$\gamma_{mn} = \sqrt{p^2 - (\frac{\omega}{c})^2} \tag{4.113}$$

First of all, previously it was commented for an empty waveguide the cutoff frequencies in TE and TM modes should be the same in case of $TE_{mn}$ and $TM_{mn}$ where $m = 1, 2 \ldots$ and $n = 1, 2, \ldots$, thus, the propagation coefficients in that cases should be the same in each different mode. Therefore we could verify the validity of that. For a mesh of M=100 and N=50 and $\epsilon_r = 1$, it will be obtained the next propagation coefficients for a frequency of 20GHz:

These valued can be compared with analytical results in the Table 4.6 and analytical results have been obtained by appendix B.

| | n m | 0 | 1 | 2 | 3 |
|---|---|---|---|---|---|
| Numerical Error (%) | 0 | - | - | - | - |
| Numerical Error (%) | 1 | - | 247,30j 0,13 | 66,23j 0,29 | 299,68 0,08 |
| Numerical Error (%) | 2 | - | 474,54 0,03 | 530,87 0,02 | 613,31 0,02 |
| | n m | 0 | 1 | 2 | 3 |
| Analytical | 0 | - | - | - | - |
| Analytical | 1 | - | 246,97j | 66,03j | 299,94 |
| Analytical | 2 | - | 474,09 | 531,02 | 613,44 |

Table 4.6: Numerical propagation coefficients compared with analytical coefficients for TM in two dimensions

After trying different meshes, we could understand that whenever were increasing the mesh, the propagation coefficients were more accuracy.

Now, we are going to show the dispersion characteristics of $TM_{11}$, $TM_{21}$, $TM_{31}$ and $TM_{22}$ modes. In this way, we can show the different results depending on cutoff frequency and propagation charcateristics of these propagation modes.

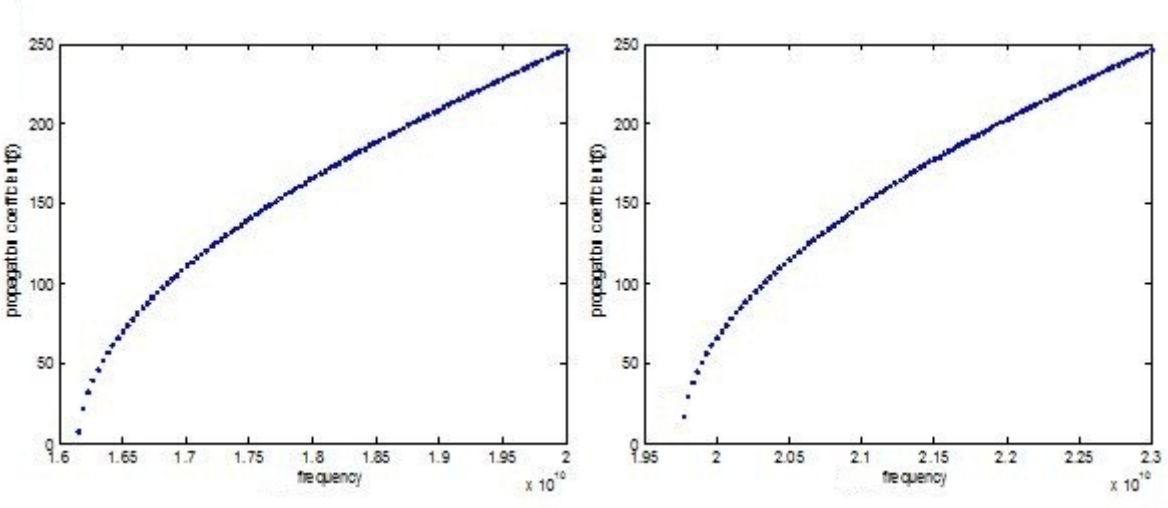


Figure 4.27: Representation of dispersion characteristics of $TM_{11}$ and $TM_{21}$ modes in two dimensions

In this case, we can see the dispersion chacteristics depending on cutoff frequency of the obtained mode. In this case $TM_{11}$ and $TM_{21}$.

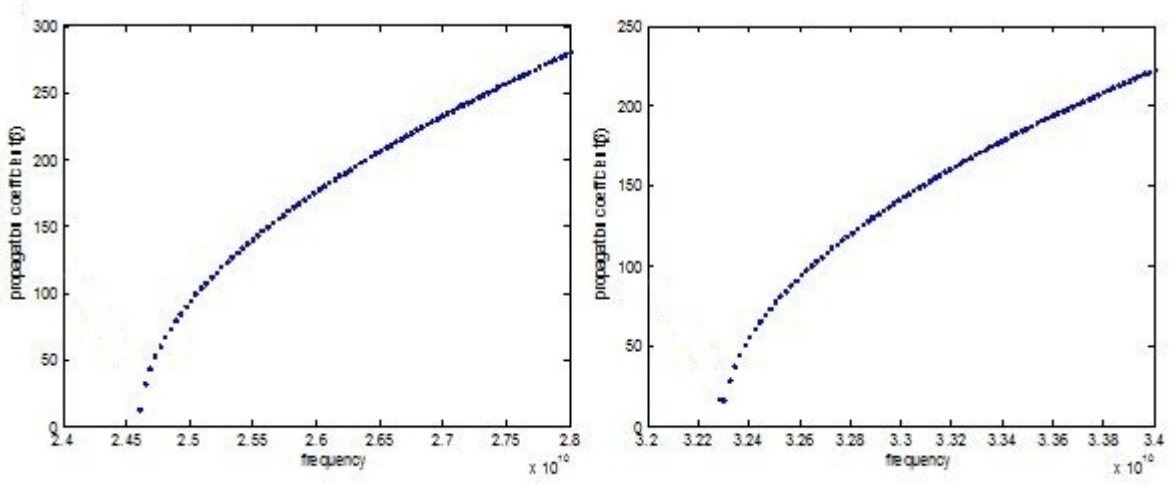


Figure 4.28: Representation of dispersion characteristics of $TM_{31}$ and $TM_{22}$ modes in two dimensions

In this case, we can see the dispersion chacteristics depending on cutoff frequency of the obtained mode. In this case $TM_{31}$ and $TM_{22}$.

Now, we are going to show the propagation coefficients of TM modes which have been obtained with some conditions as the size of mesh M =100 and N=50, $\epsilon_0 = 8.85 \cdot 10^{-12}$ F/m, $\mu_0 = 4\pi \cdot 10^{-7} N/A^2$ and with a permittivy $\epsilon_{r1} = 9$ and $\epsilon_{r2} = 1$.

The results of this table can be compared with analytical solutions to check that all results are correct. In this way to compare these results, it is possible to check appendix B.

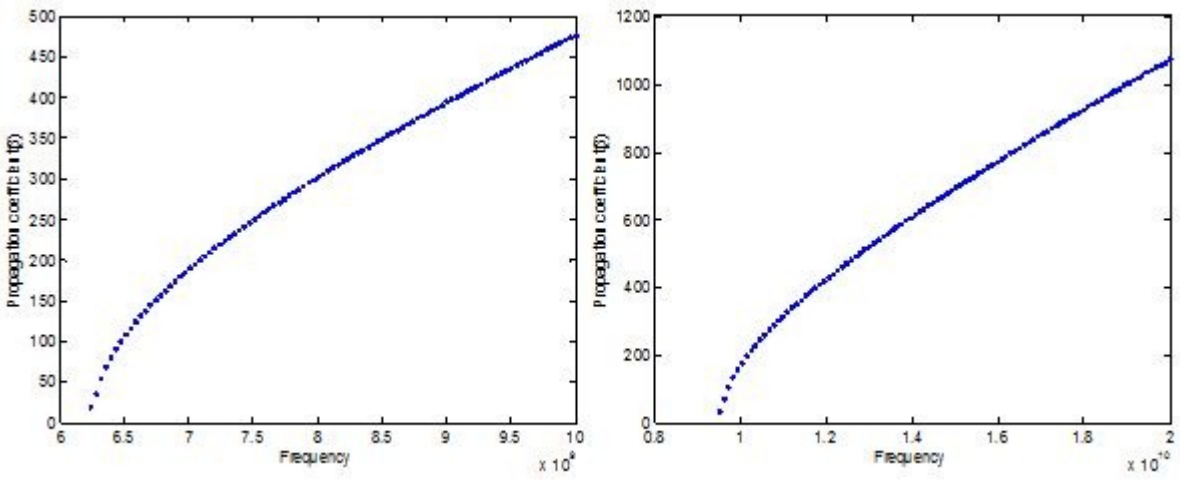


Figure 4.29: Representation of dispersion characteristics of first two modes with permittivity $\epsilon_r = 9$.

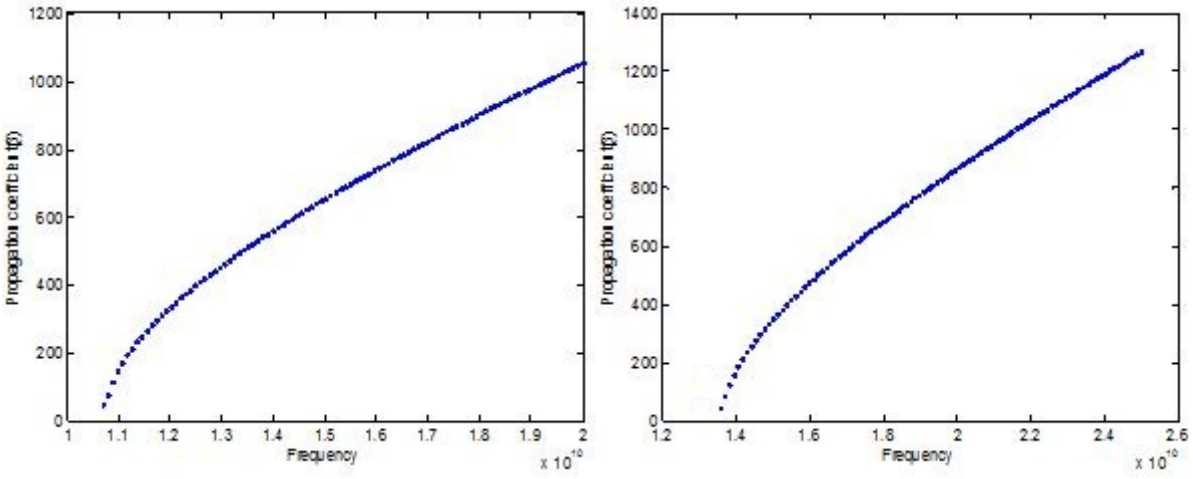


Figure 4.30: Representation of dispersion characteristics of $TM_{12}$ and $TM_{22}$ modes with permittivity $\epsilon_r = 9$.

Likewise in unidimensional problem, it is obtained the propagation characteristics for each mode which indicates when the modes are propagated.

In all the above pictures, the dispersion characteristics shown the imaginary part of $\gamma$.

# Chapter 5

# Hybrid modes (all components)

## 5.1 Introduction

Analysis methods for the determination of the electromagnetic fields in dielectric-loaded waveguides and cavity resonators have received considerable attention. Among the methods being developed are techniques based on field expansions in terms of eigenmodes of the guiding structure, the resonators and enclosures, and on surface integral equations. The results of these approaches provide quantitative design information that can help in the development of new microwave and millimeter- wave components. Pictorial display of the transverse fields of various hybrid modes in the cross section of a dielectric-loaded waveguide gives significant insight about the field structure. Such a display can help in the design of devices using these modes by indicating the locations of strong fields, their directions, etc., so that this information can be used to decide the locations of tuning obstacles to adjust the resonant frequencies of cavities, coupling irises or probes to excite these modes, of discontinuities to suppress or avoid the excitation of spurious modes. Kobayashi and Tanaka calculated the field patterns for hybrid modes for the case of a dielectric rod without an exterior boundary. They presented the field patterns only inside the dielectric rod, except for the HEII mode, where portions of the fields outside the dielectric were displayed.

In some cases, however, it will be impossible to satisfy all the necessary boundary conditions with only TE- or TM-type modes, and a hybrid combination of both types of modes may be required.

Rigorous electromagnetic methods are applied to calculate the propagation constants and the fields of the allowed guided modes in uniaxial slab waveguides for an arbitrary orientation of the optic axis. In addition to the familiar TE and TM modes, there are hybrid guided modes. These hybrid guided modes can be divided into three distinct types: homogeneous pure guided modes, inhomogeneous pure guided modes, and leaky guided modes. The conditions for the existence of these pure guided and leaky guided modes are derived. A quantitative method of classifying the hybrid modes in terms of the limiting decoupled TE and TM cases within that mode where the ordinary and extraordinary polarizations propagate independently is introduced. For each mode the propagation constant has a continuous band of allowed values as a function of optic axis orientation. Metalindiffused positive-birefringent (lithium tantalate) and metal-indiffused and proton-exchange negative-birefringent (lithium niobate) planar waveguides are treated for illustration. This analysis of hybridguided modes is important, not only for the design and use of anisotropic waveguides, but also suggests a new class of waveguide devices based on material birefringence.

In this chapter, it will be studied the hybrid modes which are a combination of TE and TM modes. This type of modes can be found in all waveguides as rectangular waveguides, cavity resonators, optical fiber, etc. Firstly, it will be explained how did that problem by eigenproblem. Afterwards, it will be presented some structures to verify that this method is valid for many

complex structures.

## 5.2 TE and TM Hybrid Modes

Firstly, it neccesary to review the maxwell equations for fields in two dimensions:

$$\begin{bmatrix} 0 & \gamma & \frac{\partial}{\partial y} \\ -\gamma & 0 & -\frac{\partial}{\partial x} \\ -\frac{\partial}{\partial y} & \frac{\partial}{\partial x} & 0 \end{bmatrix} \begin{bmatrix} E_x \\ E_y \\ E_z \end{bmatrix} = -j\omega\mu_0 \begin{bmatrix} H_x \\ H_y \\ H_z \end{bmatrix} \tag{5.1}$$

$$\begin{bmatrix} 0 & \gamma & \frac{\partial}{\partial y} \\ -\gamma & 0 & -\frac{\partial}{\partial x} \\ -\frac{\partial}{\partial y} & \frac{\partial}{\partial x} & 0 \end{bmatrix} \begin{bmatrix} H_x \\ H_y \\ H_z \end{bmatrix} = j\omega\epsilon_0 \begin{bmatrix} \epsilon_x & 0 & 0 \\ 0 & \epsilon_y & 0 \\ 0 & 0 & \epsilon_z \end{bmatrix} \begin{bmatrix} E_x \\ E_y \\ E_z \end{bmatrix} \tag{5.2}$$

$$\begin{bmatrix} \frac{\partial}{\partial x} & \frac{\partial}{\partial y} - \gamma \end{bmatrix} \begin{bmatrix} \epsilon_x & 0 & 0 \\ 0 & \epsilon_y & 0 \\ 0 & 0 & \epsilon_z \end{bmatrix} \begin{bmatrix} E_x \\ E_y \\ E_z \end{bmatrix} = 0 \tag{5.3}$$

$$\begin{bmatrix} \frac{\partial}{\partial x} & \frac{\partial}{\partial y} - \gamma \end{bmatrix} \begin{bmatrix} H_x \\ H_y \\ H_z \end{bmatrix} = 0 \tag{5.4}$$

Then, using the approximation (3.6), equations (5.1) - (5.4) can be stored in the form of a matrix. However, not all of these equations are needed to formulate the eigenvalue problem for the propagation velocity. Considering, therefore, the following set of relationships:

$$\gamma \mathbf{C}_{tt}^{(e)} \mathbf{e}_t + \mathbf{C}_{tz}^{(e)} \mathbf{e}_z = -j\omega\mu_0 \mathbf{h}_t \tag{5.5}$$

$$\mathbf{C}_{zt}^{(e)} \mathbf{e}_t = -j\omega\mu_0 \mathbf{h}_z \tag{5.6}$$

$$\gamma \mathbf{C}_{tt}^{(h)} \mathbf{h}_t + \mathbf{C}_{tz}^{(h)} \mathbf{h}_z = j\omega\epsilon_0 \mathbf{P}_t \mathbf{e}_t \tag{5.7}$$

$$\mathbf{C}_{zt}^{h} \mathbf{h}_t = j\omega\epsilon_0 \mathbf{P}_z \mathbf{e}_z \tag{5.8}$$

where $\mathbf{e}_t = [e_x e_y]^T$, $\mathbf{h}_t = [h_x h_y]^T$ and

$$\mathbf{C}_{tt}^{(e)} = \mathbf{C}_{tt}^{(h)} = \begin{bmatrix} 0_{KxK} & I_{KxK} \\ -I_{KxK} & 0_{KxK} \end{bmatrix} \tag{5.9}$$

$$\mathbf{C}_{tz}^{(e)} = \mathbf{C}_{zt}^{(h)^T} = \begin{bmatrix} \mathbf{C}_{zx}^{(e)} \\ -\mathbf{C}_{zy}^{(e)} \end{bmatrix} \tag{5.10}$$

$$\mathbf{C}_{zt}^{(e)} = \mathbf{C}_{tz}^{(h)^T} = \begin{bmatrix} -\mathbf{C}_{zx}^{(e)} \mathbf{C}_{zy}^{(e)} \end{bmatrix} \tag{5.11}$$

where, $\mathbf{C}_{zy}^{(e)}$ and $\mathbf{C}_{zx}^{(e)}$ are defined by equation (4.25) and (4.26) as

$$[C_{zx}^{(e)}]_{m,n} = \triangle y^{-1} \begin{cases} -1, m = n, \\ 1, m = n + M, \\ 0, rest \end{cases} \tag{5.12}$$

$$[C_{zy}^{(e)}]_{m,n} = \triangle x^{-1} \begin{cases} -1, m = n, \\ 1, m = n + M, \\ 0, rest \end{cases} \tag{5.13}$$

These equations are the same matrices which have been explained in chapter four. These equations will be used for equations (5.5) to (5.8).

Likewise in above chapters, it has been obtained the cutoff frequencies and the propagation characteristics in one and two dimensions in TE and TM modes. Therefore, eliminating from the equation (5.7) the tangential component (5.5) and the longitudinal component of magnetic field (5.6) and a component of the electric field (5.8), it will be obtained the relationship:

$$\mathbf{F}^{(h)}\mathbf{h}_t = -\gamma \mathbf{e}_t \tag{5.14}$$

$$\mathbf{F}^{(e)}\mathbf{e}_t = -\gamma \mathbf{h}_t \tag{5.15}$$

where

$$\mathbf{F}^{(h)} = \mathbf{C}_{tt}^{(e^{-1})}\mathbf{T}_t^{e^{-1}}(j\omega\mu_0\mathbf{I} + \frac{1}{j\omega\epsilon_0}\mathbf{T}_t^e\mathbf{C}_{tz}^{(e)}\mathbf{P}_z^{-1}\mathbf{T}_z^h\mathbf{C}_{zt}^h) \tag{5.16}$$

and

$$\mathbf{F}^{(e)} = \mathbf{C}_{tt}^{(h^{-1})}\mathbf{T}_t^{h^{-1}}(j\omega\epsilon_0\mathbf{P}_t + \frac{1}{j\omega\mu_0}\mathbf{T}_t^h\mathbf{C}_{tz}^{(h)}\mathbf{T}_z^e\mathbf{C}_{zt}^e) \tag{5.17}$$

It should be noted that $\mathbf{T}_t^e$ and $\mathbf{T}_t^h$ are diagonal matrices, so inversion is not expensive numerically. The matrices $\mathbf{C}_{tt}^{(h)}$ and $\mathbf{C}_{tt}^{(e)}$, however, are orthogonal, and therefore their inverses can be replaced by transposition. Using one equation (5.14) or (5.15), it can be used to obtain the propagation coefficients. The first is only for electric fields and the second for magnetic fields. In the same way, by eigenproblem it will be able to obtain $\gamma$.

Interesting is that it was found that there is a limit to the number modes that can be used in the system of equations before ill conditioning occurs in the form of rank deficiency (MATLAB gives a warning if the matrix is rank deficient). This is due to the very large numbers that occur when trigonometric functions are evaluated for imaginary arguments. In effect, the computer runs out of sufficient decimal places to accurately cover the range of the size of numbers in the equation matrix. However, the number of modes required for sufficient accuracy is well below this limit. Once the coefficients are found, they can then be substituted into the field equations so that the field components can be determined from the sum of the basic functions at a number of spatial grid points, and the resultant field in the structure can be plotted as a superposition of all the components.

The eigenvalues are the propagation coefficients of the modes of the structure. These modes can be propagating, evanescent, complex, or backward wave types and there is considerable current interest in the production of guided electromagnetic waves having phase velocities equal to or less than the speed of light in free space. Such phase velocities can be obtained conveniently by partially loading a rectangular waveguide with dielectric material. To determine that the propagation coefficients found are physically sensible, and also to find the type of mode each represents, it is essential to calculate the unknown coefficients and plot the field patterns. A selected coefficient is chosen as unity or some appropriate factor.

Both of these issues are based on a problem of their own matrix which its solution presents the propagation coefficients. It should be clear that the problems discussed above does not involve any boundary condition yet. Therefore, the boundary conditions must be imposed wholly within the field of computing, and their implementation, as in the one-dimensional case requires a reset or delete the corresponding rows and columns in the matrix operators.

## 5.3 Boundary conditions

As it was commented, the above matrices have been created without boundary conditions, but it necessary to obtain them to get our results. Hybrid modes is the combination of TE and TM modes thus, the boundary conditions will be the same used in TE (equations 4.55 to 4.57) and TM (equations 4.95 to 4.97) polarizations. In this way, it will be changed each equation from (5.5) to (5.8) which will be form by boudary conditions:

If we focus on equation (5.5),

$$\gamma \mathbf{C}_{tt}^{(e)} \mathbf{e}_t + \mathbf{C}_{tz}^{(e)} \mathbf{e}_z = -j\omega\mu_0 \mathbf{h}_t \tag{5.18}$$

$$\gamma \mathbf{C}_{tt}^{(e)} \mathbf{T}_t^e \mathbf{E}_t + \mathbf{C}_{tz}^{(e)} \mathbf{T}_z^e \mathbf{E}_z = -j\omega\mu_0 \mathbf{T}_t^h \mathbf{H}_t \tag{5.19}$$

and use $\mathbf{e}_t = \mathbf{T}_t^e \mathbf{E}_t$, $\mathbf{e}_z = \mathbf{T}_z^e \mathbf{E}_z$ and $\mathbf{h}_t = \mathbf{T}_t^h \mathbf{H}_t$ which are the boundary conditions, we obtain

$$\gamma {\mathbf{T}_t^h}^T \mathbf{C}_{tt}^{(e)} \mathbf{T}_t^e \mathbf{E}_t + {\mathbf{T}_t^h}^T \mathbf{C}_{tz}^{(e)} \mathbf{T}_z^e \mathbf{E}_z = -j\omega\mu_0 \mathbf{H}_t \tag{5.20}$$

Finally, we have a simple equation but with boundary conditions:

$$\gamma \tilde{\mathbf{C}}_{tt}^{(e)} \mathbf{E}_t + \tilde{\mathbf{C}_{tz}}^{(e)} \mathbf{e}_z = -j\omega\mu_0 \mathbf{H}_t \tag{5.21}$$

where $\tilde{\mathbf{C}}_{tt}^{(e)} = {\mathbf{T}_t^h}^T \mathbf{C}_{tt}^{(e)} \mathbf{T}_t^e$ and $\tilde{\mathbf{C}_{tz}}^{(e)} = {\mathbf{T}_t^h}^T \mathbf{C}_{tz}^{(e)} \mathbf{T}_z^e$.
In case of equation (5.6), we have

$$\mathbf{C}_{zt}^{(e)} \mathbf{T}_t^e \mathbf{E}_t = -j\omega\mu_0 \mathbf{T}_z^h \mathbf{H}_z \tag{5.22}$$

Calculating,

$$ {\mathbf{T}_z^h}^T \mathbf{C}_{zt}^{(e)} \mathbf{T}_t^e \mathbf{E}_t = -j\omega\mu_0 \mathbf{H}_z \tag{5.23}$$

Finally, the equation (5.6) with boundary conditions will be:

$$\tilde{\mathbf{C}}_{zt}^{(e)} \mathbf{E}_t = -j\omega\mu_0 \mathbf{H}_z \tag{5.24}$$

where $\tilde{\mathbf{C}}_{zt}^{(e)} = {\mathbf{T}_z^h}^T \mathbf{C}_{zt}^{(e)} \mathbf{T}_t^e$
In case of equation (5.7),

$$\gamma \mathbf{C}_{tt}^{(h)} \mathbf{T}_t^h \mathbf{H}_t + \mathbf{C}_{tz}^{(h)} \mathbf{T}_z^h \mathbf{H}_z = j\omega\epsilon_0 \mathbf{P}_t \mathbf{T}_t^e \mathbf{E}_t \tag{5.25}$$

Operating,

$$\gamma {\mathbf{T}_t^e}^T \mathbf{C}_{tt}^{(h)} \mathbf{T}_t^h \mathbf{H}_t + {\mathbf{T}_t^e}^T \mathbf{C}_{tz}^{(h)} \mathbf{T}_z^h \mathbf{H}_z = j\omega\epsilon_0 {\mathbf{T}_t^e}^T \mathbf{P}_t \mathbf{T}_t^e \mathbf{E}_t \tag{5.26}$$

Finally, the equation (5.7) will be,

$$\gamma \tilde{\mathbf{C}}_{tt}^{(h)} \mathbf{H}_t + \tilde{\mathbf{C}}_{tz}^{(h)} \mathbf{H}_z = j\omega\epsilon_0 \tilde{\mathbf{P}}_t \mathbf{E}_t \tag{5.27}$$

where $\tilde{\mathbf{C}}_{tt}^{(h)} = {\mathbf{T}_t^e}^T \mathbf{C}_{tt}^{(h)} \mathbf{T}_t^h$, $\tilde{\mathbf{C}}_{tz}^{(h)} = {\mathbf{T}_t^e}^T \mathbf{C}_{tz}^{(h)} \mathbf{T}_z^h$ and $\tilde{P}_t = {\mathbf{T}_t^e}^T \mathbf{P}_t \mathbf{T}_t^e$.
At the sime time, the last equation will be changed by:

$$\mathbf{C}_{zt}^{(h)}\mathbf{T}_{t}^{(h)}\mathbf{H}_t = j\omega\epsilon_0\mathbf{P}_z\mathbf{T}_{z}^{(e)}\mathbf{E}_z \tag{5.28}$$

Operating,

$$\mathbf{T}_{z}^{(e)^T}\mathbf{C}_{zt}^{(h)}\mathbf{T}_{t}^{(h)}\mathbf{H}_t = j\omega\epsilon_0\mathbf{T}_{z}^{(e)^T}\mathbf{P}_z\mathbf{T}_{z}^{(e)}\mathbf{E}_z \tag{5.29}$$

Finally, the equation (5.8) will be transformed by

$$\tilde{\mathbf{C}}_{zt}^{(h)}\mathbf{H}_t = j\omega\epsilon_0\tilde{\mathbf{P}}_z\mathbf{E}_z \tag{5.30}$$

where $\tilde{\mathbf{C}}_{zt}^{(h)} = \mathbf{T}_{z}^{(e)^T}\mathbf{C}_{zt}^{(h)}\mathbf{T}_{t}^{(h)}$ and $\tilde{\mathbf{P}}_z = \mathbf{T}_{z}^{e^T}\mathbf{P}_z\mathbf{T}_{z}^{e}$.
If we join these equations,

$$\begin{cases} \gamma\tilde{\mathbf{C}}_{tt}^{(e)}\mathbf{E}_t + \tilde{\mathbf{C}_{tz}}^{(e)}\mathbf{E}_z = -j\omega\mu_0\mathbf{H}_t \\ \tilde{\mathbf{C}}_{zt}^{(e)}\mathbf{E}_t = -j\omega\mu_0\mathbf{H}_z \\ \gamma\tilde{\mathbf{C}}_{tt}^{(h)}\mathbf{H}_t + \tilde{\mathbf{C}}_{tz}^{(h)}\mathbf{H}_z = j\omega\epsilon_0\tilde{\mathbf{P}}_t\mathbf{E}_t \\ \tilde{\mathbf{C}}_{zt}^{(h)}\mathbf{H}_t = j\omega\epsilon_0\tilde{\mathbf{P}}_z\mathbf{E}_z \end{cases} \tag{5.31}$$

From here on, it is possible to obtain the propagation characteristics for Hybrid modes taking into account the group of equations (5.31). It should be known that with this approximation it will be obtained only the propagation characteristics.

## 5.4 Numerical tests

A few structures has been analyzed and the results were verified. To show the efficiency of the algorithm proposed in this paper we have analyzed three structures. In the numerical tests we used the boundary conditions for modeling of open space. All calculations have been performed in the MATLAB environment.

The first structure is changing the size and position of dielectric and the dimensions of the waveguide and the last structure will be an optical fiber.

All these structures are to verify that the Finite Difference Method is valied for all structures.

### 5.4.1 Dielectric slab shielded with rectangular waveguide

The first structure which have been studied in the book *Guided electromagnetic waves* by Michal Mrozowski [12].

This waveguide has a dimension of a=15.8mm and b=7.9mm. It has been introduced a dielectric on the bottom of the rectangular waveguide with dimensions 6.32mm (weight) and 3.16mm (height). The value of permittivity is $\epsilon_r = 9$.

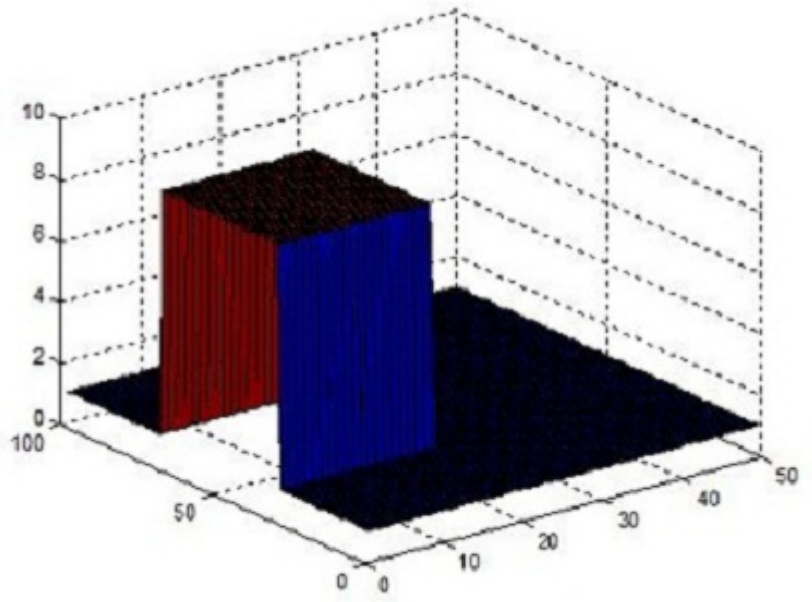


Figure 5.1: Dielectric introduced in the rectangular waveguide

By the previous study, it has been obtained the propagation characteristics to get the Hybrid modes of this structure. We have been able to verify that this method is correct due to we have obtained the same curves and values. In addition, it should be known that in this structure is possible to obtain complex modes. The complex modes have been studied in many structures which are particularly sensitive to perturbations. Numerical investigations carried out by various researchers prove that no complex waves ocurr unless a high permittivity rod is used. The weak perturbation theory also predicts that in a rectangular waveguide we should expect complex waves even when the inhomogeneity seems to be small.

As it was commented previously, we are going to obtain the propagation coefficients and dispersion characteristics of some modes where it will be seen the correct solutions which have been compared with the above study of *Michal Mrozowski* by the Figure 5.2. In this picture, it is possible to see the different modes which are propagated and some complex modes.

From equation (5.14) or (5.15), it will be obtained the propagation characteristics by the eigenvalue problem in the same way that in above chapters. It will be taken into account the equations (5.31) which have included the boundary conditions.

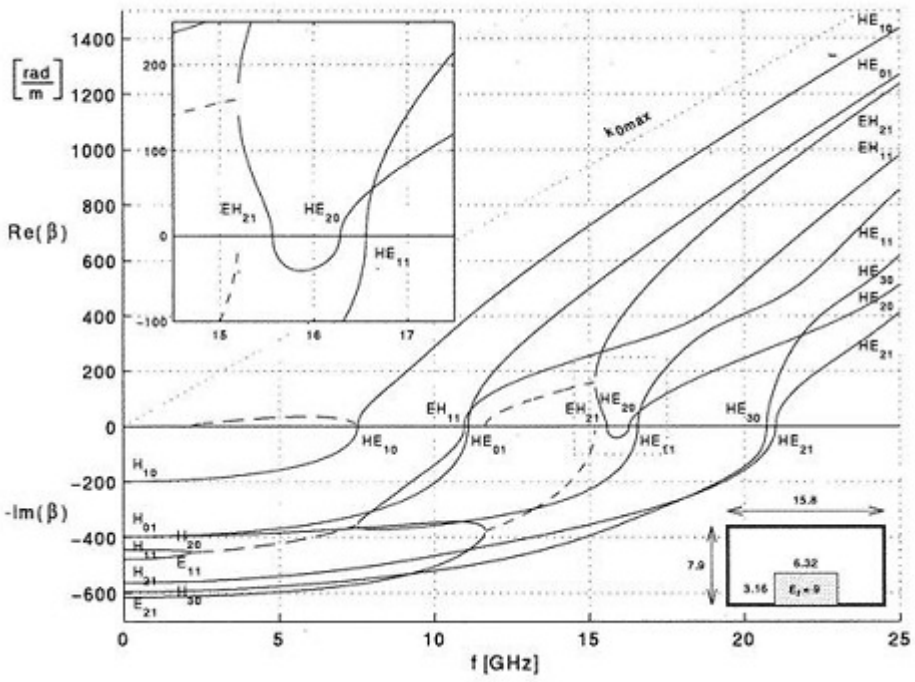


Figure 5.2: Dispersion characteristics of a rectangular waveguide

In the Figure can be seen the results which have been obtained by Matlab environment:

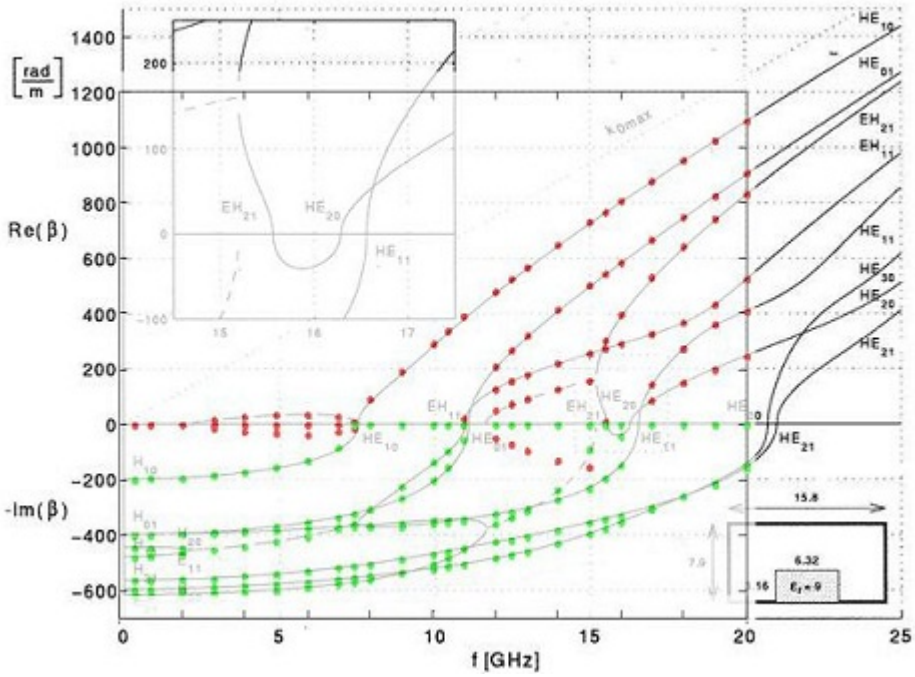


Figure 5.3: Points obtained by Matlab environment

### 5.4.2 Optical fiber

As it has been shown, Finite Differences technique is one of the most popular method of electromagnetic problems analysis. Its flexibility, versatility, and rich spectrum of capabilities causes it is often applied in commercial software. In spite of numerous advantages of the algorithm, some drawbacks are evident. The major one is as a huge number of the variables required for a discretization of the entire computational domain, which results in time-consuming analysis. The second one concerns an analysis of unshielded structures located in free space. When the domain is unbounded, the Boundary Condition (BC) for modeling of open space must by enforced.

To verify this method, it has been chosen an optical fiber which has been studied in PhD *Efektywna analiza światłowodów fotonicznych metodą różnic skończonych w dziedzinie częstotliwości* by Piotr Kowalczyk.

Due to a lach of absorbing or radiating boundary condition only guiding properties have been analyzed.

As we know, the simplest form of an optical waveguide consists of a light-conducting fiber core with the refractive index $n_1$ and a fiber cladding with the refractive index $n_2$, which is $n_2 < n_1$, where the difference is about a few percent or even lower. It will be used a frequency range, aproximately of $[3 \cdot 10^{14}, 6 \cdot 10^{14}]$ Hz due to optical guided communications.

During the project, our objective has been to obtain the propagation constants to see the performace of the different modes that are propagated by the waveguides. To analyze an example of a circular waveguide, it will be imposed $n_1 = 8,4$, $n_2 = 2,4025$, $a = 0,5\mu m$, and it will be shielded with a square waveguide with the dimension of the side $3\mu m$.

The Figure 5.3 represents the dielectric which has been introduced.

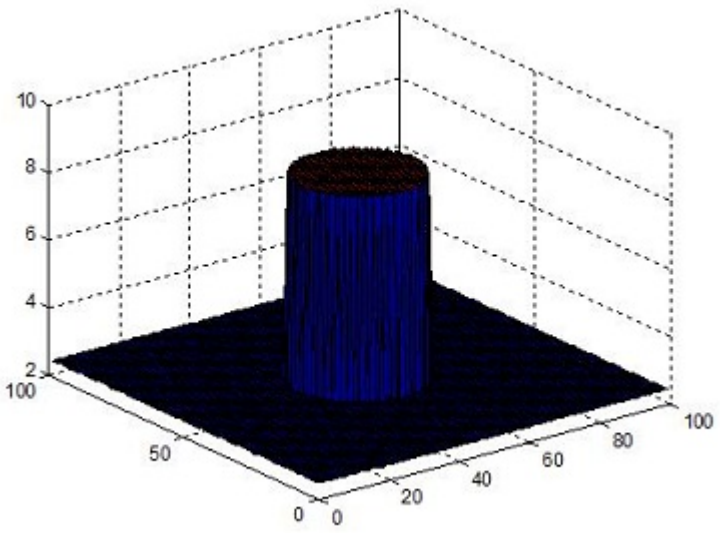


Figure 5.4: Dielectric inside on optical fiber

To obtain the propagation constants, it will be used the equation (5.14) or (5.15) which are based on group of equations (5.31) which are depending on boundary conditions.

On the one hand, it should be known that in an optical fiber, propagation coefficient is commonly replaced by $n_{eff}$

$$n_{eff} = \frac{\gamma}{jk_o} \tag{5.32}$$

Therefore, to verify that the program works, it has been used the results in the doctoral thesis which is named *Effective analysis of photonic optical fibers by finite difference method in frequency domain* by Piotr Kowalczyk. In the Figure 5.8, it is shown some modes which were obtained.

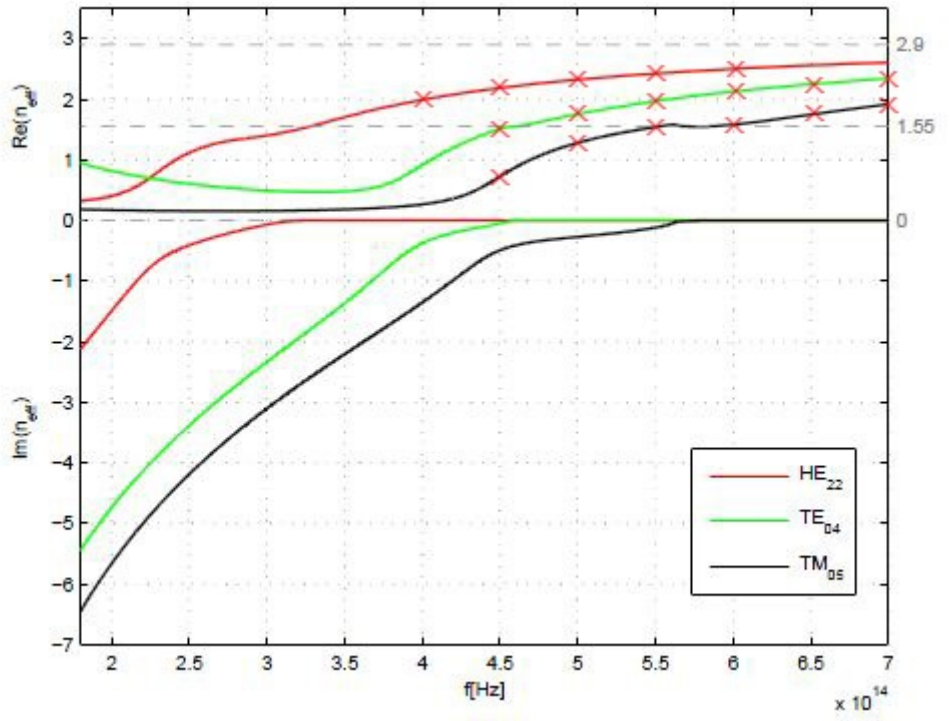


Figure 5.5: Dispersion characteristics for some hybrid modes of the circular waveguide

We have obtained some points to verify that our program works. The points which have been obtained are from $HE_{22}$ and with a frequency range of $4 \cdot 10^{14}$ to $6 \cdot 10^{14}$ Hz. In the following table, it possible to see the different values of $n_{eff}$ in the different frequency which are analogous to $HE_{22}$ mode.

| f (GHz) | $4{\cdot}10^{14}$ | $4,5{\cdot}10^{14}$ | $5{\cdot}10^{14}$ | $5,5{\cdot}10^{14}$ | $6{\cdot}10^{14}$ |
|---|---|---|---|---|---|
| $n_{eff_1}$ | 1,9909 | 2,1873 | 2,258 | 2,4270 | 2,5034 |
| $n_{eff_2}$ | 1,9860 | 2,1844 | 2,3239 | 2,4258 | 2,5025 |

Table 5.1: Propagation coefficients of $HE_{22}$

It should be know that for each mode which is propagated, it will have two modes $HE$ and $EH$. In this case, it will be $HE_{22}$ and $EH_{22}$. The value of $n_eff$ are similar.

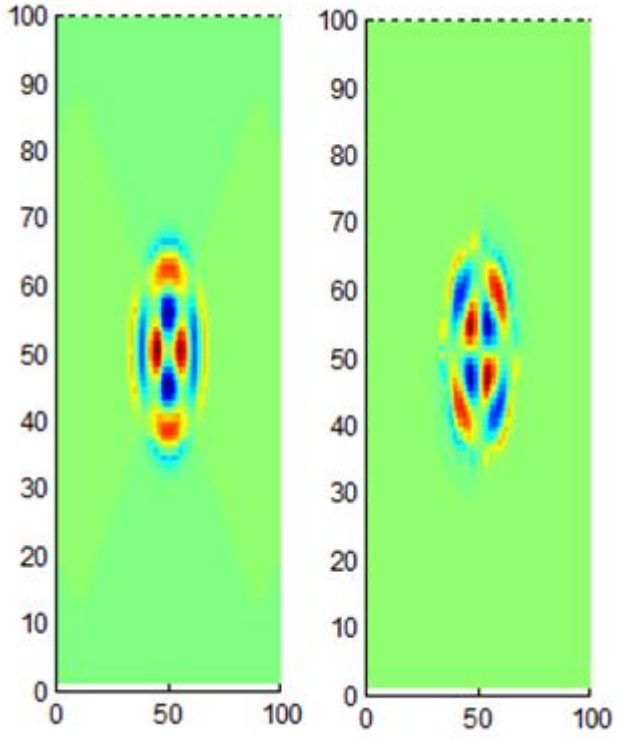


Figure 5.6: Field distribution of $HE_{22}$ hybrid mode

The Figure 5.9 shows the field distribution of $HE_{22}$ mode which has been obtained previously. The Table 5.2 shows the $n_{eff}$ which have been obtained for $TE_{04}$ mode:

| f (GHz) | $5 \cdot 10^{14}$ | $5,5 \cdot 10^{14}$ | $6 \cdot 10^{14}$ | $6,5 \cdot 10^{14}$ | $7 \cdot 10^{14}$ |
|---|---|---|---|---|---|
| $n_{eff_1}$ | 1,6813 | 1,8921 | 2,0667 | 2,2103 | 2,3056 |

Table 5.2: Propagation coefficients of $TE_{04}$

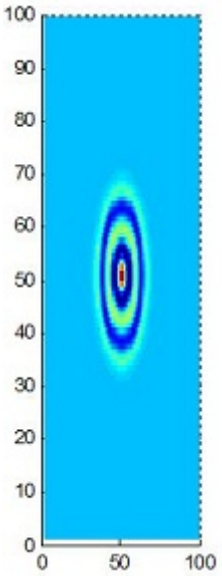


Figure 5.7: Field distribution of $TE_{04}$ hybrid mode

Finally, we show the results for $TM_{05}$

| f (GHz) | $5 \cdot 10^{14}$ | $5,5 \cdot 10^{14}$ | $6 \cdot 10^{14}$ | $6,5 \cdot 10^{14}$ | $7 \cdot 10^{14}$ |
|---|---|---|---|---|---|
| $n_{eff_1}$ | 1,3539 | 1,5501 | 1,6710 | 1,7905 | 1,9585 |

Table 5.3: Propagation coefficients of $TM_{05}$

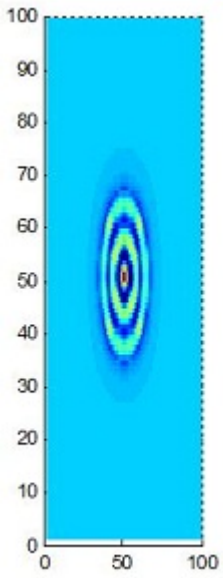


Figure 5.8: Field distribution of $TM_{05}$ hybrid mode

# Chapter 6

# Conclusions

FDM has been successfully implemented in Matlab environment. A numerical verification has been performed for different structure types and the validity of the procedures has been confirmed. Thus, the main educational goal of this project was achieved. It has been shown that FDM is a useful and easy to implement for solving problems which behave according to Maxwell's equations. Also the flexibility of the algorithm has been presented - changing the geometry of the analyzed device does not affect the main structure of the algorithm. It has been shown that this method can be very accurate if a proper mesh density is applied (depending on dimensions of the analyzed structures).

In addition, such studies can be used to improve one's skills in the commercial programs: their limitations, error sources and possibilities of more efficient use. Finally, the knowledge about this type of numerical methods is necessary to create a wide variety of specific software tools which can be perfectly adapted to needs of any specific project (in comercial programs access to some variables is limited).

The future studies will be focused on techniques which improve efficiency of FDM. For instance, the computational domain can be divided into subregions where different mesh densities is applied [1,2]. In some sensitive areas the mesh must be dense, but in some others such mesh generates redundant variables. This approach can significantly increase the efficiency of the calculations by reduction of large number of variables without losing accuracy of the results.

# Appendix A

# Analytical solutions for one dimensional problem

On the other hand, the cuttof frequencies are obtained in the numerical way but to compare that the numerical cutoff frequencies are correct, we can calculate them by analytical way.

It should be known that in case of cutoff frequency ($\gamma = 0$), we have

$$p^2 = \omega^2 \mu\epsilon \tag{A.1}$$

$$p = \omega\sqrt{\mu\epsilon} \tag{A.2}$$

where $\omega = 2\pi f$ and $\frac{1}{c} = \sqrt{\mu\epsilon}$. If the equation (3.70) is solved,

$$f = \frac{p}{2\pi\sqrt{\mu\epsilon}} \tag{A.3}$$

Besides, p is the value of the different modes in the waveguide, due to this,

$$p = \sqrt{(\frac{m\pi}{a})^2 + (\frac{n\pi}{b})^2} \tag{A.4}$$

As consequence to get TE modes which are the main modes $TE_{m0}$, being $n = 0$,

$$p = \sqrt{\frac{m\pi^2}{a}} \tag{A.5}$$

$$p = \frac{m\pi}{a} \tag{A.6}$$

Then,

$$f = \frac{cm}{2a} \tag{A.7}$$

Due to there is a dielectric inside rectangular waveguide, the equation (3.76) will be

$$f = \frac{cm}{2a\sqrt{\epsilon_r}} \tag{A.8}$$

## A.1 Analytical solutions of cutoff frequencies for $TE_{m0}$

As we know, the geometry of a rectangular waveguide is shown in Figure 2.6, where it is assumed that the guide is filled with a material of permittivity $\epsilon$ and permeability $\mu$, as we have seen above.

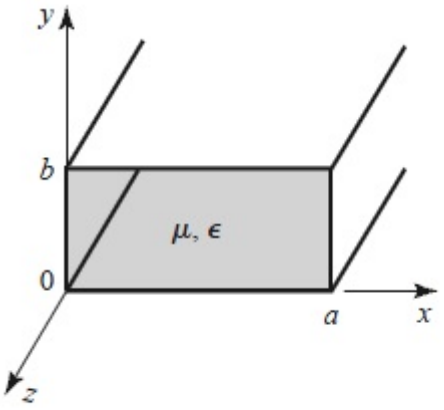


Figure A.1: Geometry of a rectangular waveguide

It is standard convention to have the longest side of the waveguide along the x-axis, so that $a > b$. TE waveguide modes are characterized by fields with $E_z = 0$ and $H_z$ and satisfy by

$$(\frac{\partial^2}{\partial x^2} + \frac{\partial^2}{\partial y^2} + k_c^2)h_z(x, y) = 0, \tag{A.9}$$

with $H_z(x, y, z) = h_z(x, y)e^- j\beta z$ ; here $k_c = sqrtk^2 - \beta^2$ is the cuttof wave number. The partial differential equation (2.52) can be solved by the method of separation of variables by letting

$$h_z(x, y) = X(x)Y(y) \tag{A.10}$$

and substituting into (2.49) to obtain

$$\frac{1}{X}\frac{d^2X}{dx^2} + \frac{1}{Y}\frac{d^2Y}{dy^2} + k_c^2 = 0 \tag{A.11}$$

Then, by the usual separation-of-variables argument, each of the terms must be equal to a constant. If we focus on equations (2.25) and we want to obtain the analytical cuttof frequencies,

$$\frac{\partial^2 E_y}{\partial x^2} = -j\omega\mu\frac{\partial H_z}{\partial x} \tag{A.12}$$

$$\frac{\partial^2 E_y}{\partial x^2} = -j\omega\mu(-j\omega\epsilon E_y) \tag{A.13}$$

$$\frac{d^2 E_y}{dx^2} + \omega^2\mu\epsilon E_y = 0 \tag{A.14}$$

Thus, it is necessary to take into account that there are two mediums inside waveguide, as it is shown in the Figure 2.7.

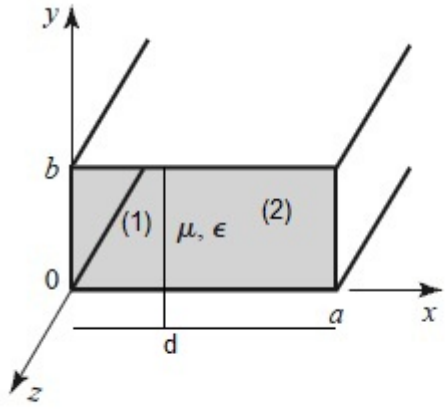


Figure A.2: Two mediums in a rectangular waveguide

Therefore, the equations which will be analysed are in the first medium:

$$\begin{cases} E_y^{(1)}(x) = A^{(1)}\cos\left(k^{(1)}x\right) + B^{(1)}\sin\left(k^{(1)}x\right) \\ H_z^{(1)}(x) = -\frac{1}{j\omega\mu}\frac{\partial E_y}{\partial x} = -\frac{1}{j\omega\mu}(-A^{(1)}k^{(1)}\sin\left(k^{(1)}x\right) + B^{(1)}k^{(1)}\cos\left(k^{(1)}x\right)) \end{cases} \tag{A.15}$$

$$\begin{cases} E_y^{(1)}(x) = A^{(1)}\cos\left(k^{(1)}x\right) + B^{(1)}\sin\left(k^{(1)}x\right) \\ H_z^{(1)}(x) = \frac{1}{j\omega\mu}A^{(1)}k^{(1)}\sin\left(k^{(1)}x\right) - \frac{1}{j\omega\mu}B^{(1)}k^{(1)}\cos\left(k^{(1)}x\right) \end{cases} \tag{A.16}$$

And in case of second medium,

$$\begin{cases} E_y^{(2)}(x) = A^{(2)}\cos\left(k^{(2)}x\right) + B^{(2)}\sin\left(k^{(2)}x\right) \\ H_z^{(2)}(x) = \frac{1}{j\omega\mu}A^{(2)}k^{(2)}\sin\left(k^{(2)}x\right) - \frac{1}{j\omega\mu}B^{(2)}k^{(2)}\cos\left(k^{(2)}x\right) \end{cases} \tag{A.17}$$

If $x = 0$ means that it is in the first medium,

$$\begin{cases} E(x=0) = 0 \dashrightarrow E_y^{(1)}(x=0) = A^{(1)}\cos\left(k^{(1)}0\right) + B^{(1)}\sin\left(k^{(1)}0\right) = 0 \\ A^{(1)} = 0 \end{cases} \tag{A.18}$$

If $x = a$, it is in the second medium,

$$E(x=a) = 0 \dashrightarrow E_y^{(2)}(x=a) = A^{(2)}\cos\left(k^{(2)}(x=a)\right) + B^{(2)}\sin\left(k^{(2)}(x=a)\right) = 0 \tag{A.19}$$

and in the last case, it is found between two mediums then it will take into account $x = d$,

$$\begin{cases} E^{(1)}(x=d) = E^{(2)}(x=d) \\ A^{(1)}\cos\left(k^{(1)}(x=d)\right) + B^{(1)}\sin\left(k^{(1)}(x=d)\right) = A^{(2)}\cos\left(k^{(2)}(x=d) + B^{(2)}\sin\left(k^{(2)}(x=d)\right)\right) \end{cases} \tag{A.20}$$

In case of magnetic field,

$$\begin{cases} H^{(1)}(x=d) = H^{(2)}(x=d) \\ -B^{(1)}(\cos\left(k^{(1)}d\right)) = A^{(2)}k^{(2)}(\sin\left(k^{(2)}d\right)) - B^{(2)}k^{(2)}(\cos\left(k^{(2)}d\right)) \end{cases} \tag{A.21}$$

where in our case, we have two dielectrics so it will have $k_1$ and $k_2$ and if $k = 2\pi\lambda$,

$$\begin{cases} k = 2\pi\lambda \\ \lambda = cf\sqrt{\epsilon_r} \\ k = \frac{2\pi f\sqrt{\epsilon_r}}{c} \end{cases} \tag{A.22}$$

where $\omega = 2\pi f$, we have these k values of first and second dielectric:

$$\begin{cases} k_1 = \frac{\omega\sqrt{\epsilon_{r1}}}{c} \\ k_2 = \frac{\omega\sqrt{\epsilon_{r2}}}{c} \end{cases} \tag{A.23}$$

Finally, using a matrix which is composed of this equations,

$$\begin{bmatrix} 0 & \cos(k^{(2)}a) & \sin(k^{(2)}a) \\ -\sin(k^{(1)}d) & \cos(k^{(2)}d) & \sin(k^{(2)}d) \\ k^{(1)}\cos(k^{(1)}d) & k^{(2)}\sin(k^{(2)}d) & -k^{(2)}\cos(k^{(2)}d) \end{bmatrix} \begin{bmatrix} B^{(1)} \\ A^{(2)} \\ B^{(2)} \end{bmatrix} = 0$$

it is possible to get the analytical frequencies and compare with numerical frequencies. In other way, it would have another way to obtain these analytical frequency, because we know $\gamma = \sqrt{-\omega^2\mu\epsilon + p^2}$.

## A.2 Analytical solutions of cutoff frequencies for $TM_{m0}$

Through these equations, it is possible to get the cuttof of frequencies using the equation (2.43). And the same way that TE modes, it is necessary to compare that the obtained results are correct. Therefore, it is interesting to get the analytical cuttof frequencies, which are obtained with separation-of-variables method. However, we should remember that inside waveguide we have a dielectric as in TE mode thus, the waveguide will have two different mediums which are composed by one dielectric of value $\epsilon_r = 9$ and the second medium will be filled by air $\epsilon_r = 1$. The new equations to solve the cuttof frequency problem in the analytical way will be based on equation (2.76) being

$$H_y = \frac{1}{j\omega\mu}\frac{\partial E_z}{\partial x} \tag{A.24}$$

Sustituting,

$$\frac{\partial}{\partial x}\left(\frac{1}{j\omega\mu}\frac{\partial E_z}{\partial x}\right) = j\omega\epsilon E_z \tag{A.25}$$

$$\frac{d^2E_z}{dx^2} + \omega^2\mu\epsilon E_z = 0 \tag{A.26}$$

By separation-of-variables method and taking into account the two mediums inside waveguide,

$$\begin{cases} E_z^{(1)}(x) = A^{(1)}\cos(k^{(1)}x) + B^{(1)}\sin(k^{(1)}x) \\ H_y^{(1)}(x) = \frac{1}{j\omega\mu}\frac{\partial E_z}{\partial x} = \frac{1}{j\omega\mu}(-A^{(1)}k^{(1)}\sin(k^{(1)}x) + B^{(1)}k^{(1)}\cos(k^{(1)}x)) \end{cases} \tag{A.27}$$

$$\begin{cases} E_z^{(1)}(x) = A^{(1)}\cos(k^{(1)}x) + B^{(1)}\sin(k^{(1)}x) \\ H_y^{(1)}(x) = -\frac{1}{j\omega\mu}A^{(1)}k^{(1)}\sin(k^{(1)}x) + \frac{1}{j\omega\mu}B^{(1)}k^{(1)}\cos(k^{(1)}x) \end{cases} \tag{A.28}$$

And in case of second medium,

$$\begin{cases} E_z^{(2)}(x) = A^{(2)}\cos\left(k^{(2)}x\right) + B^{(2)}\sin\left(k^{(2)}x\right) \\ H_y^{(2)}(x) = -\frac{1}{j\omega\mu}A^{(2)}k^{(2)}\sin\left(k^{(2)}x\right) + \frac{1}{j\omega\mu}B^{(2)}k^{(2)}\cos\left(k^{(2)}x\right) \end{cases} \tag{A.29}$$

If $x = 0$ means that is in the first medium,

$$\begin{cases} E^{(1)}(x=0) = 0 \dashrightarrow E_z^{(1)}(x=0) = A^{(1)}\cos\left(k^{(1)}0\right) + B^{(1)}\sin\left(k^{(1)}0\right) = 0 \\ A^{(1)} = 0 \end{cases} \tag{A.30}$$

If $x = a$, it is in the second medium,

$$E^{(2)}(x=a) = 0 \dashrightarrow E_z^{(2)}(x=a) = A^{(2)}\cos\left(k^{(2)}(x=a)\right) + B^{(2)}\sin\left(k^{(2)}(x=a)\right) = 0 \tag{A.31}$$

and in the last case which is found between two mediums then it will take into account $x = d$,

$$\begin{cases} E^{(1)}(x=d) = E^{(2)}(x=d) \\ B^{(1)}\sin\left(k^{(1)}d\right) = A^{(2)}\cos\left(k^{(2)}d\right) + B^{(2)}\sin\left(k^{(2)}d\right) \end{cases} \tag{A.32}$$

In case of magnetic field,

$$\begin{cases} H^{(1)}(x=d) = H^{(2)}(x=d) \\ B^{(1)}(\cos\left(k^{(1)}d\right)) = -A^{(2)}k^{(2)}(\sin\left(k^{(2)}d\right)) + B^{(2)}k^{(2)}(\cos\left(k^{(2)}d\right)) \end{cases} \tag{A.33}$$

where in our case, we have two dielectrics so it will have $k_1$ and $k_2$ and if $k = 2\pi\lambda$,

$$\begin{cases} k = 2\pi\lambda \\ \lambda = cf\sqrt{\epsilon_r} \\ k = \frac{2\pi f\sqrt{\epsilon_r}}{c} \end{cases} \tag{A.34}$$

where $\omega = 2\pi f$, we have these k values of first and second dielectric:

$$\begin{cases} k_1 = \frac{\omega\sqrt{\epsilon_{r1}}}{c} \\ k_2 = \frac{\omega\sqrt{\epsilon_{r2}}}{c} \end{cases} \tag{A.35}$$

Finally, using a matrix which is composed of this equations,

$$\begin{bmatrix} 0 & \cos\left(k^{(2)}a\right) & \sin\left(k^{(2)}a\right) \\ -\sin\left(k^{(1)}d\right) & \cos\left(k^{(2)}d\right) & \sin\left(k^{(2)}d\right) \\ -k^{(1)}\cos\left(k^{(1)}d\right) & -k^{(2)}\sin\left(k^{(2)}d\right) & k^{(2)}\cos\left(k^{(2)}d\right) \end{bmatrix} \begin{bmatrix} B^{(1)} \\ A^{(2)} \\ B^{(2)} \end{bmatrix} = 0$$

As a result of this and using Matlab environmental, we can compare the numerical and analytical cuttof frequencies.

## A.3 Analytical solutions of propagation coefficients for TE and TM modes

### A.3.1 Propagation characteristics in TE modes

A very important issue for each mode is the frequency which from that point on a mode will be able to propagate by the waveguide. To find this value, we must focus on equation (2.106) that determines the propagation constant $\gamma_n$ for each $TE_m mode$.

$$\begin{cases} \gamma_m^2 = k_{cm}^2 - k^2 \\ \gamma_m = \pm\sqrt{k_{cm}^2 - k^2} \end{cases} \tag{A.36}$$

It can be seen in this equation that $\gamma_m$ is a square root which value will be positive or negative depending on function of $k_{cm}$ value and the frequency.

The value will be negative as long as $k^2 = \omega^2\mu\epsilon > k_{cm}$, when the frequency becomes sufficiently high for $k$ becomes larger than the cutoff wavenumber. In this case, the propagation constant is imaginary and it can be expressed as:

$$k_c < k \rightarrow \gamma = j\beta \rightarrow \beta = \sqrt{k^2 - k_c^2} \tag{A.37}$$

The field components are proportional to the term $e^{-j\beta z}$, consequently achieves that $k^2 = \omega^2\mu\epsilon < k_{cm}$. In this case, the propagation constant will be a real value which can be expressed as:

$$k_c > k \rightarrow \gamma = \alpha \rightarrow \beta = \sqrt{k_c^2 - k^2} \tag{A.38}$$

In contrast the above case, all field components will be proportional to $e^{-\alpha z}$, therefore the fields will not be propagated by the waveguide. As a consequency, these fields will be atenuated at the same time advance by $z$. The modes which determine that conditions will be named as ' the cut '.

Related to cutoff wavenumber of mode exists a frequency limit up to there is not propagation, and from that point this mode will be propagated. This frequency is named as cutoff frequency of mode and its value is:

$$f_c = \frac{k_{cm}}{2\pi\sqrt{\mu\epsilon}} \tag{A.39}$$

As it is shown, the cutoff frequency depends on electric and magnetic permittivity of medium and the mode which is considered.In case of it had some losses still would exist propagation, but in turn would decrease the field amplitudes due to these losses.

As a conclusion, it will have two intervals which will be known $f < f_c$ and $f > f_c$,

$$f < f_c \rightarrow \gamma = \alpha \tag{A.40}$$

$$f > f_c =\rightarrow \gamma = j\beta \tag{A.41}$$

### A.3.2 Propagation characteristics in TM modes

Likewise in TE modes, it must be explained that each TM mode shows a different cutoff wavenumber, and thus, its constant and propagation velocity differs from one mode to another.

$$\begin{cases} \gamma_m^2 = k_{cm}^2 - k^2 \\ \gamma_m = \pm\sqrt{k_{cm}^2 - k^2} \end{cases} \tag{A.42}$$

In the same way, it can be made the study of cutoff frequency for TM modes. To obtain this value, we must focus on equation (2.112) which defines the propagation constant $\gamma_m$ for each $TM_m$ mode. It can be appreciated in that equation, $\gamma_m$ is a square root which will be positive or negative depending on $k_{cm}$ and frequency.

Again, if $k^2 = \omega^2\mu\epsilon > k_{cm}$ the propagation constant is imaginary and it can be expressed as:

$$k_c < k \rightarrow \gamma = j\beta \rightarrow \beta = \sqrt{k^2 - k_c^2} \tag{A.43}$$

In this case, the field components are proportional to the term $e^{-j\beta z}$, consequently these components will not be attenuated but they will have an oscillatory behaviour with the distance.

However, when $k^2 = \omega^2\mu\epsilon < k_{cm}$ the propagation constant will be a real value and can be expressed as

$$k_c > k \rightarrow \gamma = \alpha \rightarrow \alpha = \sqrt{k_c^2 - k^2} \tag{A.44}$$

In contrast the above case, all field components will be proportional to $e^{-\alpha z}$, therefore the fields will not be propagated by the waveguide. As a consequency, these fields will be atenuated at the same time advance by $z$. The modes which determine that conditions will be named as ' the cut '.

The point, where starts the propagation or attenuation of a TM mode is named cutoff frequency of the mode and its value is:

$$f_c = \frac{k_{cm}}{2\pi\sqrt{\mu\epsilon}} \tag{A.45}$$

As it is shown, this equation is defined the same way that in TE modes. The cutoff frequency depends on electric and magnetic permittivity of medium and the mode which is considered.

As a conclusion, it will have two intervals which will be known $f < f_c$ and $f > f_c$,

$$f < f_c \rightarrow \gamma = \alpha \tag{A.46}$$

$$f > f_c =\rightarrow \gamma = j\beta \tag{A.47}$$

# Appendix B

# Analytical solutions for two dimensional problems

## B.1 Analytical solutions of cutoff frequencies for TE and TM modes in two dimensions

When the waveguide is rectangular signal by allowing to guide the type of TE and TM, the cross-section of the waveguide has a rectangular shape of dimensions a x b where $a > b$. Mostly waveguide is not filled with any other material, thus the waveguide is called air, but in general may comprise any material. Due to the geometry of the structure analysis of this guide is convenient to lead in a rectangular pattern. Consider the following issues, in which we determine the distributions of fields in rectangular waveguide for the TE and TM types.

Calculating field distributions, in rectangular waveguide exits the Helmholtz equation, which is written (Cartesian) in the form of:

$$\frac{\partial^2 \hat{E}_z}{\partial x^2} + \frac{\partial^2 \hat{E}_z}{\partial y^2} + p^2 \hat{E}_z = 0 \tag{B.1}$$

An important thing to solve the above equation is the separation-of-variables method in the form $\hat{E}_z(x, y) = X(x)Y(y)$:

$$Y\frac{\partial^2 X}{\partial x^2} + X\frac{\partial^2 Y}{\partial y^2} + p^2 XY = 0 \tag{B.2}$$

therefore

$$\frac{1}{X}\frac{\partial^2 X}{\partial x^2} + \frac{1}{Y}\frac{\partial^2 Y}{\partial y^2} + p^2 = 0 \tag{B.3}$$

Having x value as a contant,

$$\frac{1}{X}\frac{\partial^2 X}{\partial x^2} = -\beta_x^2 \tag{B.4}$$

Thus,

$$-\beta_x^2 - \beta_y^2 + p^2 = 0 \tag{B.5}$$

The variability of x,

$$\frac{\partial^2 X}{\partial x^2} + \beta_x^2 = 0 \tag{B.6}$$

$$X(x) = C_1 \sin \beta_x x + C_2 \cos \beta_x x \tag{B.7}$$

By boundary conditions, it is obtained

$$X(0) = 0 \Longrightarrow C_2 = 0 X(a) = 0 \Longrightarrow C_1 \sin \beta_x a = 0 \Longrightarrow \beta_x = \frac{m\pi}{a} \tag{B.8}$$

Thus,

$$X(x) = C_1 \sin \frac{m\pi x}{a}, m = 1, 2, \ldots, \infty \tag{B.9}$$

In case of y,

$$\frac{\partial^2 Y}{\partial y^2} + \beta_x^2 Y = 0 \tag{B.10}$$

$$X(x) = C_3 \sin \beta_y y + C_4 \cos \beta_y y \tag{B.11}$$

Calculating in the same way,

$$Y(0) = 0 \Longrightarrow C_4 = 0 Y(b) = 0 \Longrightarrow C_3 \sin \beta_y b = 0 \Longrightarrow \beta_y = \frac{n\pi}{b} \tag{B.12}$$

Therefore,

$$Y(y) = C_3 \sin \frac{n\pi x}{b}, n = 1, 2, \ldots, \infty \tag{B.13}$$

The transverse wave number for a rectangular waveguide becomes:

$$p_{mn} = \sqrt{(\frac{m\pi}{a})^2 + (\frac{n\pi}{b})^2} m, n = 1, 2, \ldots, \infty \tag{B.14}$$

Finally, the component $\hat{E}_z(x, y)$ is described as,

$$\hat{E}_{z(mn)}(x, y, z) = C_5 \sin (\frac{m\pi x}{a}) + \sin (\frac{n\pi y}{b}) \tag{B.15}$$

If we focus on the wave propagation in the z-direction:

$$\hat{E}_{z(mn)}(x, y, z) = E_{o(mn)} \sin (\frac{m\pi x}{a}) + \sin (\frac{n\pi y}{b}) e^{-\gamma_{mn} z} \tag{B.16}$$

Using electromagnetic relations,

$$\hat{\vec{E}}_{t(mn)}(x, y, z) = -\frac{\gamma_{mn}}{p_{mn}^2} [E_{o(mn)} \frac{m\pi}{a} \cos (\frac{m\pi x}{a}) \sin (\frac{n\pi y}{b}) e^{-\gamma_{mn} z}, E_{o(mn)} \frac{n\pi}{b} \sin (\frac{m\pi x}{a}) \cos (\frac{n\pi y}{b}) e^{-\gamma_{mn} z}, 0] \tag{B.17}$$

Therefore, the total electric field intensity for the kind of TM has the form:

$$\hat{\vec{E}}_{(mn)}(x,y,z) = -[E_{o(mn)}\frac{m\pi}{a}\frac{\gamma_{mn}}{p_{mn}^2}\frac{m\pi}{a}\cos(\frac{m\pi x}{a})\sin(\frac{n\pi y}{b})e^{-\gamma_{mn}z} - E_{o(mn)}\frac{\gamma_{mn}}{p_{mn}^2}\frac{n\pi}{b}\sin(\frac{m\pi x}{a})\cos(\frac{n\pi y}{b})e^{-\gamma_{mn}z}, E_o \tag{B.18}$$

and obtaining the magnetic field for TE,

$$\hat{\vec{H}}_{(mn)}(x,y,z) = [E_{o(mn)}\frac{n\pi}{b}\frac{j\omega\epsilon}{p_{mn}^2}\sin(\frac{m\pi x}{a})\cos(\frac{n\pi y}{b})e^{-\gamma_{mn}z}, -E_{o(mn)}\frac{j\omega\epsilon}{p_{mn}^2}\frac{m\pi}{a}\cos(\frac{m\pi x}{a})\cos(\frac{n\pi y}{b})e^{-\gamma_{mn}z}, 0] \tag{B.19}$$

Similarly to the types of the TM to the rectangular waveguide equation is written in the form of:

$$\frac{\partial^2\hat{H}_z}{\partial x^2} + \frac{\partial^2\hat{H}_z}{\partial y^2} + p^2\hat{H}_z = 0 \tag{B.20}$$

Using the separation- of- variables method described in the above problem,

$$\hat{H}_{z(mn)}(x,y,z) = H_{o(mn)}\cos(\frac{m\pi x}{a}) + \cos(\frac{n\pi y}{b})e^{-\gamma_{mn}z} \tag{B.21}$$

then,

$$p_{mn} = \sqrt{(\frac{m\pi}{a})^2 + (\frac{n\pi}{b})^2}m, n = 1, 2, \ldots, \infty \tag{B.22}$$

Following an analogous procedure, it will be obtained the total magnetic field intensity for TE modes in the form,

$$\hat{\vec{H}}_{(mn)}(x,y,z) = [H_{o(mn)}\frac{m\pi}{a}\frac{\gamma_{mn}}{p_{mn}^2}\sin(\frac{m\pi x}{a})\cos(\frac{n\pi y}{b})e^{-\gamma_{mn}z}, H_{o(mn)}\frac{\gamma_{mn}}{p_{mn}^2}\frac{n\pi}{b}\cos(\frac{m\pi x}{a})\sin(\frac{n\pi y}{b})e^{-\gamma_{mn}z}, H_{o(mn)}\,c \tag{B.23}$$

and the total electric field for TE mode,

$$\hat{\vec{E}}_{(mn)}(x,y,z) = [H_{o(mn)}\frac{n\pi}{b}\frac{j\omega\mu}{p_{mn}^2}\cos(\frac{m\pi x}{a})\sin(\frac{n\pi y}{b})e^{-\gamma_{mn}z}, -H_{o(mn)}\frac{j\omega\mu}{p_{mn}^2}\frac{m\pi}{a}\sin(\frac{m\pi x}{a})\cos(\frac{n\pi y}{b})e^{-\gamma_{mn}z}, 0] \tag{B.24}$$

With the above solutions for TE and TM modes, it will be obtained the different cutoff frequencies in the analytical for to compare if our numerical results are correct. It should be obtained TE and TM modes in the form $TE_10$, $TE_20$, $TE_01$, $TE_11$, ... and the same for por TM case.

## B.2 Analytical solutions of propagation characteristics for TE and TM modes in two dimensions

Using all equations (4.66) and (4.67), it must be obtained the cutoff frequencies without dielectric inside on waveguide. As it was exposed in unidimensional problems, it is possible to verify if the cutoff frequencies which have been obtained by Matlab environment are correct and it will be possible with analytical cutoff frequencies. The propagation constant can be defined as

$$\beta = \sqrt{k^2 - k_c^2} = \sqrt{k^2 - (\frac{m\pi}{a}^2) - (\frac{n\pi}{b}^2)} \tag{B.25}$$

which is seen to be real, corresponding to a propagation mode when

$$k > k_c = \sqrt{(\frac{m\pi}{a})^2 - (\frac{n\pi}{b})^2} \tag{B.26}$$

Each mode (each combination of m and n) has a cutoff frequency $fc_{mn}$ given by

$$fc_{mn} = \frac{k_c}{2\pi\sqrt{\mu\epsilon}} = \frac{1}{2\pi\sqrt{\mu\epsilon}}\sqrt{(\frac{m\pi}{a})^2 - (\frac{n\pi}{b})^2} \tag{B.27}$$

The mode with the lowest cutoff frequency is called the dominant mode; because we have to assumed $a > b$, the lowest cutoff frequency occurs for the $TE_{10}$ (m=e, n=0) mode which was obtained in unidimensional problem:

$$fc_{10} = \frac{1}{2a\sqrt{\mu\epsilon}} \tag{B.28}$$

Thus the $TE_{10}$ mode is the dominant TE mode and, as we know, the overall dominant mode of the rectangular waveguide. As it was exposed, at a given operating frequency f only those modes having $f > f_c$ will propagate; modes with $f < f_c$ will lead to an imaginary $\beta$ (or real $\alpha$), meaning that all field components will decay exponentially away from the soruce excitation. Such modes are referred to as cutoff modes, or evanescent modes.

All this thesis is worked by Matlab envirnoment, thus the cutoff frequencies which have been explained previously are exposed in the Table 4.1. In the table shows different resuts of cutoff frequency for first five modes for different mesh. Firslty, a little mesh and afterwards the mesh is increased and the results are better.

# List of Figures

# List of Tables

# Bibliography


[1] Piotr Kowalczyk, M. Wiktor and M. Mrozowski, member IEEE. *"Efficient finite difference analysis of microstructured optical fibers"* Opt. Express 13(25) 10349-10359 (2005)

[2] Piotr Kowalczyk, L. kulas and Michal Mrozowski, member IEEE. *"Analysis of microstructured optical fibers using compact macromodels"* Opt. Express 19(20), 19354-19364 (2011)

[3] Mathew N. O. Sadiku. Ph.D. *"Numerical Techniques in Electromagnetics"*. Second edition, 2000.

[4] David M. Pozar. *"Microwave Engineering"*. Fourth edition, 2011.

[5] Antonio P. *"Aplicación del método de las diferencias finitas en el dominio del tiempo a la resolución de cavidades resonantes"* Proyecto Final de Carrera, Septiembre 2010.

[6] G. Mur. *"A Finite Difference Method for the Solution of Electromagnetic Waveguide Discontinuity Problems"*. Third edition, Microwave Conference,1973.

[7] Karlheinz Bierwirth, Norbert Schulz, and Fritz Arndt, Senior Member, IEEE. *"Finite-Difference Analysis of Rectangular Dielectric Waveguide Structrures"* Volume 34, 1986

[8] K. Pontoppidan *"Numerical Solutions of Waveguide Problems using Finite Difference Methods"* Microwave conference, 1969

[9] Colin G. and James A. R. Ball., Members IEEE *"Mode-Matching Analysis of a Shiefield Rectangular Dielectric-Rod Waveguide"* Volumen 53, October 2005

[10] P. H. Vartantan, W. P. Ayrest, and A. L. Helgesson, IEEE. *"Propagation in Dielectric Slab Loaded Rectangular Waveguide"* Microwave techniques, 1958

[11] N. Kaneda, B. Houshmand, T. Itoh, IEEE. *"FDTD Analysis of Dielectric Resonators with Curved Surfaces"* Volumen 45, 1997

[12] Kawthar A. Zaki, senior member IEEE and Chunming Chen, studen member IEEE. *"Intensity and Distribution of Hybrid-Mode Fields in Dielectric-Loaded Waveguides"* Microwave Techniques, December 1985

[13] A. Knoesen, member IEEE, T. K. Gaylord, Fellow IEEE, and M. G. Moharam, senior member, IEEE. *"Hybrid Guided Modes in Uniaxial Dielectric Planar Waveguides"* Volumen 6, June 1988

[14] Michal Mrozowski, member IEEE. *"Guided Electromagnetics Waves- Properties and Analysis"* 1997

[15] Lukasz Kulas and Michal Mrozowski, member IEEE. *"Reduced-Order Models in FDTD"* Volumen 11, October 2001

[16] Piotr Kowalczyk, Michal Mrozowski, member IEEE. *"Hybrid Accurate Finite Difference Analysis of Leaky, Guided and Complex Waves in Photonic Optical Fibers and Dielectric Waveguiding Structures"* 2011/2012

**Politechnika Gdańska**

**Wydział Elektroniki,
Telekomunikacji i Informatyki**

| | |
|---|---|
| **Katedra:** | Departamento de Técnicas de Antena y Microondas |
| **Imię i nazwisko dyplomanta:** | Ana Hernández Martínez |
| **Nr albumu:** | 159138 |
| **Forma i poziom studiów:** | Título de Ingeniería de Telecomuniación |
| **Kierunek studiów:** | Informatyka |

# Praca dyplomowa magisterska

**Temat pracy:**
Método de las Diferencias Finitas en problemas electromagnéticos

**Kierujący pracą:**
dc.ing. Piotr Kowalczyk

**Zakres pracy:**
Teoría Electromagnética

Gdańsk, 2014-15

# Índice general

# Capítulo 1

# Introducción

## 1.1. Historia y origen de este proyecto

Este documento se constituye como proyecto fin de carrera de la titulación de Ingeniería de Telecomunicación.

El problema que se presenta se centra en el método de diferencias finitas (FDM). Este método es una de las técnicas más flexibles y generales, por lo que se utiliza comúnmente en el análisis y diseño de microondas y dispositivos ópticos (también en software comercial).

En primer lugar, es importante saber que el campo de electromagnetismo es muy amplio, y cada región del mismo es estudiada con unas herramientas determinadas. Aunque deberíamos seguir un orden a la hora de explicar cada tipo de onda electromagnética, vamos a ver lo que realmente nos interesa, el concepto de microondas. El campo de frecuencia de radio (RF) y la ingeniería de microondas generalmente cubre el comportamiento de las señales de corriente alterna con frecuencias en la gama de 100 MHz a 1.000 GHz. Frecuencias de RF se extienden de muy alta frecuencia (VHF) (30-300 MHz) a frecuencia ultra alta (UHF) (300-3000 MHz), mientras que el término microondas se utiliza normalmente.

Para realizar una breve descripción de lo que es ese tipo de análisis, el análisis numérico es una rama de las matemáticas cuyos límites no son del todo precisos. De una forma rigurosa, se puede definir como la disciplina ocupada de describir, analizar y crear algoritmos numéricos que nos permitan resolver problemas matemáticos, en los que estén involucradas cantidades numéricas, con una precisión determinada.

En el contexto del cálculo numérico, un algoritmo es un procedimiento que nos puede llevar a una solución aproximada de un problema mediante un número finito de pasos que pueden ejecutarse de manera lógica. En algunos casos, se les da el nombre de métodos constructivos a estos algoritmos numéricos. El análisis numérico cobra especial importancia con la llegada de los ordenadores. Los ordenadores son útiles para cálculos matemáticos extremadamente complejos, pero en última instancia operan con números binarios y operaciones matemáticas simples.

Existen diferentes métodos numéricos, entre los que cabe destacar los siguientes:

- Método de los momentos:

  El método de los momentos (MoM) es uno de los más usados en la actualidad para determinar los campos emitidos o recibidos por estructuras radiantes.

- Método de la matriz de líneas de transmisión (TLM del inglés Transmission Line Matrix):

  Este método fue desarrollado en la década de 1970 para analizar problemas de propagación de ondas acústicas y electromagnéticas. Se trata de un método simple, intuitivo e incondicionadamente estable para la modelización de la propagación de ondas, debido a que el modelo

está fuertemente relacionado con el proceso físico de la propagación.

- Método de Elementos Finitos (MEF en castellano, FEM en inglés):

  El método de elementos finitos es un método numérico general para la aproximación de soluciones de ecuaciones diferenciales parciales muy utilizado en diversos problemas de ingeniería y física.

- Método de las Diferencias Finitas (DF en castellano, FD en inglés):

  Entre todas las técnicas numéricas que resuelven las ecuaciones de Maxwell con ayuda de un ordenador, ésta es una de las más antiguas y posiblemente la que menor contenido analítico tiene. En esencia, la aplicación de este método consiste en calcular la solución del problema diferencial original en un conjunto discreto de puntos, que suelen asociarse con los nodos de una red.

## 1.2. Objetivos

El objetivo de este proyecto es presentar el método numérico de diferencias finitas, así como sus propiedades numéricas. En primer lugar, será demostrado la validez del método para analizar guías de onda y cavidades resonantes de varias geometrías y formadas por materiales diferentes. En el presente trabajo se analizan y comparan diferentes alternativas para resolver problemas electromagnéticos mediante el método de las Diferencias Finitas.

Así, el plan de este proyecto se puede especificar en los siguientes puntos:

- Repasar los conceptos de las ecuaciones de Maxwell.
- Implementación del método en problemas de una y dos dimensiones usando el entorno Matlab.
- Verificación de los algoritmos para algunas estructuras (frecuencias de resonancia, frecuencias de corte, características de dispersión, etc.).
- Análisis de posibilidades de aceleración del método en algunos casos especiales.

Objetivos:

- Comprensión de fenómenos electromagnéticos en las estructuras de microondas y ópticas debido a la solución directa de las ecuaciones de Maxwell, por ejemplo, en FDM.
- Acceso completo a todas las variables y procedimientos.
- Posibilidad de modificaciones arbitrarias del método ( los software pueden ser más rápidos y precisos que el comercial).

## 1.3. Descripción del modelo

### 1.3.1. Introducción

En la actualidad, el software comercial para la simulación de problemas electromagnéticos aplicados es una herramienta importante para los diseñadores de cualquier circuito o dispositivo eléctrico o de alta velocidad óptica. De hecho, su uso va en gran medida por el tiempo de progreso y permite un ahorro de recursos, ya que, en el pasado, los prototipos se tuvieron que hacer al mismo tiempo que se realizaron numerosas pruebas experimentales.

La importancia del conocimiento acerca de este tipo de métodos numéricos está vinculada a la capacidad de crear una amplia variedad de herramientas de software específicos que pueden ser

perfectamente adaptados a las necesidades de cualquier proyecto debido a programas comerciales que, por lo general, no están realcionados con problemas de características muy particulares.

El método de las Diferencias Finitas permite resolver de forma intuitiva las ecuaciones que gobiernan la mayor parte del comportamiento físico, en mecánica y electromagnética. El objetivo de este proyecto es resolver las ecuaciones algebraicas que quedan después de la aplicación del método, y de esa manera, lograr los resultados que proporciona la solución que se puede utilizar para resolver diferentes magnitudes electromagnéticas, tales como el campo eléctrico.

### 1.3.2. Aplicaciones en ingeniéria óptica y de microondas

El método de este proyecto es una técnica general que puede ser aplicado para resolver diferentes estructuras electromagnéticas como pueden ser: cilíndrica, guía de ondas rectangular, fibras ópticas y resonadores.

Entre las guías de onda óptica, sólo algunas estructuras como fibras ópticas de salto de índice y guías de onda se pueden resolver analíticamente. Para las estructuras de guía de ondas más complejas, se han propuesto métodos numéricos rigurosos incluyendo tanto los métodos de elementos finitos y el método de las diferencias finitas (FD).

Por ejemplo, la propagación de la luz a través de fibra óptica se rige por ecuaciones diferenciales parciales (PDE). FDM, impulsado por su simplicidad se considera como uno entre los métodos populares disponibles para la solución numérica de los PDE. Pero esta técnica no logra producir mejor resultado en problemas como la propagación de pulsos de luz en un medio de fibras, debido a la presencia de la variación brusca de la intensidad de la luz sobre una pequeña sección de la fibra.

Una clase de estructuras de guía de onda dieléctrica utilizando una tira dieléctrica rectangular con uno o más dieléctricos se analiza con un método de diferencias finitas formulado directamente en términos de la ecuación de onda para los componentes transversales del campo magnético. Esto lleva a un problema de valores propios. Por otra parte, el análisis incluye efectos de conversión de modo híbrido, tales como las ondas complejas, en las frecuencias donde los modos aún no están completamente unidos al núcleo, así como a frecuencias por debajo de la de corte. Ejemplos de dispersión característica se calculan en estructuras adecuadas para circuitos integrados ópticos, tales como, líneas de imagen dieléctricas de ondas milimétricas, guías de onda dieléctrica, etc.

FDM se basa directamente en las ecuaciones de Maxwell,ya que, es muy flexible y universal, por lo que, es comúnmente utilizado también en el software comercial. Por otra parte, el aspecto educativo de este método no puede ser omitido.

# Capítulo 2

# Concepto fundamental del método de las Diferencias Finitas

## 2.1. Introduction

Es raro que los problemas electromagnéticos de la vida real puedan ser resueltos por los métodos de análisis presentados en el capítulo anterior. Enfoques clásicos pueden fallar si:

- El PDE no es lineal y no se puede linealizar sin afectar seriamente al resultado.
- La región de solución es compleja.
- Las condiciones de contorno son de varios tipos.
- El medio es inhomogéneo o anisótropo.

Cada vez que surge un problema con tal complejidad, soluciones numéricas deben ser empleadas. De todos los métodos numéricos para la resolución de las PDE, el método de las diferencias finitas es más fácil de entender, más utilizado, y más universalmente aplicable que cualquier otro. Este método fue desarrollado por primera vez por A. Thom en la década de 1920 bajo el título de .el método de los cuadrados"para resolver ecuaciones hidrodinámicas no lineales. Desde entonces, el método ha encontrado aplicaciones en la resolución de diferentes problemas de campo. Una solución de diferencias finitas básicamente consta de tres pasos:

1. División de la región de solución en una malla de nodos.
2. La aproximación de la ecuación diferencial dada mediante las diferencias finitas que relaciona la variable dependiente en un punto en la región solución con sus valores en los puntos vecinos.
3. Resolución de las ecuaciones diferenciales sujeta a las condiciones de contorno y / o las condiciones iniciales.

Antes de encontrar las soluciones de diferencias finitas a PDE específicos, vamos a ver cómo se construye aproximaciones en diferencias finitas para una ecuación diferencial dada. Dada una función f (x), podemos aproximar su derivada como,

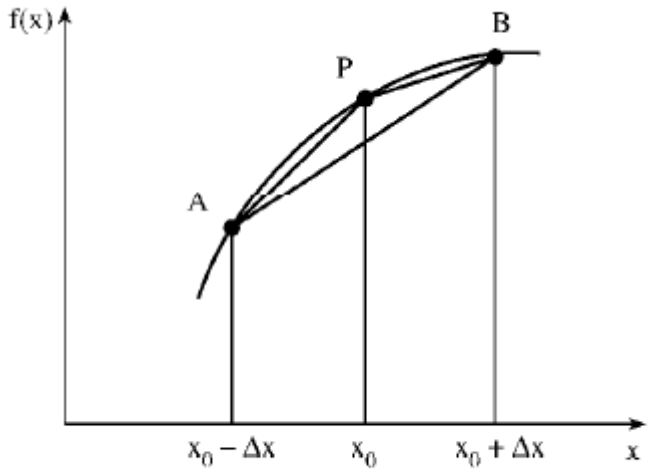


Figura 2.1: Estimates for the derivative of f(x) at P using forward, backward, and central differences

$$f'(x_o) \simeq \frac{f(x_o + \triangle x) - f(x_o)}{\triangle x} \tag{2.1}$$

Cualquier aproximación de una derivada en un conjunto discreto de puntos se llama aproximación de diferencia finita.

El enfoque utilizado anteriormente en la obtención de aproximaciones en diferencias finitas es bastante intuitivo. Un enfoque más general está utilizando series de Taylor. De acuerdo a la expansión bien conocido,

$$f(x_o + \triangle x) = f(x_o) + \triangle x f'(x_o) + \frac{1}{2!}(\triangle x)^2 f"(x_o) + \dots \tag{2.2}$$

## 2.2. Ecuaciones de Maxwell para las amplitudes de los armónicos

Como sabemos, los métodos de diferencias finitas se basan en las ecuaciones de Maxwell. En esta tesis se aplican las ecuaciones de Maxwell para amplitudes armónicas.

Los campos electromagnéticos, que varían con respecto al tiempo y la frecuencia $\omega$, $\vec{F}(x, y, z, t)$ o $\vec{F}(\vec{r}, t)$ se puede expresar como,

$$\vec{F}(\vec{r}, t) = Re[\vec{F}_s(\vec{r})e^{j\omega t}] \tag{2.3}$$

donde $\vec{F}_s = \vec{F}_s(x, y, z)$ es el fasor de F(r,t) y es, en general, complejo. Además, $\omega$ es la frecuencia angular (en rad / s) de la excitación sinusoidal. Las cantidades de campos electromagnéticos pueden ser representados en notación fasorial como

$$\begin{bmatrix} E(r,t) \\ D(r,t) \\ H(r,t) \\ B(r,t) \end{bmatrix} = Re\left( e^{j\omega t} \begin{bmatrix} E_s(r) \\ D_s(r) \\ H_s(r) \\ B_s(r) \end{bmatrix} \right)$$

Por lo que, las ecuaciones de Maxwell en forma sinusoidal serán:

$$\nabla \cdot \vec{D}_s(r) = \rho_{vs} \tag{2.4}$$

$$\nabla \cdot \vec{B}_s(r) = 0 \tag{2.5}$$

$$\nabla \times \vec{E}_s(r) = -j\omega\vec{B}_s(r) \tag{2.6}$$

$$\nabla \times \vec{H}_s(r) = \vec{J}_s(r) + j\omega\vec{D}_s(r) \tag{2.7}$$

donde $\vec{D}_s(r) = \epsilon\vec{E}_s(r)$ y $\vec{B}_s(r) = \mu\vec{H}_s(r)$.

Lo que se consigue es eliminar la dependencia del tiempo de las ecuaciones de Maxwell, reduciendo con ello la dependencia tiempo-espacio para solamente tener espacio. Si eliminamos la dependecia con el tiempo de la ecuación de onda por $(j\omega)^2$, la ecuación de onda en representación fasorial será:

$$\nabla^2\psi + k^2\psi = 0 \tag{2.8}$$

donde k es la constante de propagación (en rad/m), dada por

$$k = \frac{\omega}{u} = \frac{2\pi f}{u} = \frac{2\pi}{\lambda} \tag{2.9}$$

A partir de la forma general de la ecuación de onda,

$$\nabla^2\psi + k^2\psi = g \tag{2.10}$$

Nos damos cuenta que la ecuación de Helmholtz se reduce a

1. Ecuación de Poisson:

$$\nabla^2\psi = g \tag{2.11}$$

   donde k = 0.

2. Ecuación de Laplace:

$$\nabla^2\psi = 0 \tag{2.12}$$

   donde k = 0 = g.

En este trabajo, el concepto de campo eléctrico o magnético que se entiende, a menudo, es sólo la amplitud armónica. Aunque esta convención es ampliamente aceptada, vale la pena señalar una vez más que el escenario físico frente al campo se deriva del producto de la parte real de la amplitud del armónico factor de $e^{j\omega t}$. En el sistema de coordenadas cartesianas, las ecuaciones de Maxwell $\triangle \cdot \vec{D} = \rho_v$ y $\triangle \cdot \vec{B} = 0$ se puede escribir de la forma:

$$\begin{bmatrix} 0 & -\frac{\partial}{\partial z} & \frac{\partial}{\partial y} \\ \frac{\partial}{\partial z} & 0 & -\frac{\partial}{\partial x} \\ -\frac{\partial}{\partial y} & \frac{\partial}{\partial x} & 0 \end{bmatrix} \begin{bmatrix} E_x \\ E_y \\ E_z \end{bmatrix} = -j\omega\mu_0 \begin{bmatrix} \mu_x & 0 & 0 \\ 0 & \mu_y & 0 \\ 0 & 0 & \mu_z \end{bmatrix} \begin{bmatrix} H_x \\ H_y \\ H_z \end{bmatrix} \tag{2.13}$$

$$\begin{bmatrix} 0 & -\frac{\partial}{\partial z} & \frac{\partial}{\partial y} \\ \frac{\partial}{\partial z} & 0 & -\frac{\partial}{\partial x} \\ -\frac{\partial}{\partial y} & \frac{\partial}{\partial x} & 0 \end{bmatrix} \begin{bmatrix} H_x \\ H_y \\ H_z \end{bmatrix} = j\omega\epsilon_0 \begin{bmatrix} \epsilon_x & 0 & 0 \\ 0 & \epsilon_y & 0 \\ 0 & 0 & \epsilon_z \end{bmatrix} \begin{bmatrix} E_x \\ E_y \\ E_z \end{bmatrix} + \begin{bmatrix} J_x \\ J_y \\ J_z \end{bmatrix} \tag{2.14}$$

Las ecuaciones anteriores (2.13) y (2.14) son el punto de partida para la aplicación del método de diferencias finitas.

# Capítulo 3

# Método de las Diferencias Finitas en una dimensión

En primer lugar, es posible suponer que la placa dieléctrica es $\epsilon(x)$, una es la $\mu(x)$ magnético. El sistema de acuerdo con las condiciones de contorno impuestas puede ser tratada ya sea como guía de ondas plano-paralelo y una fibra óptica planar. Por otro lado, también se supondrá que la volatilidad de los campos en este sentido representa un factor de $e^{\gamma z}$, donde $\gamma = \alpha + j\beta$ ($\alpha$ factor de amortiguamiento y $\beta$ coeficiente de propagación).

Postulando la falta de variación en los campos en los que no fluyen corrientes de conducción ($\sigma = 0$), partiremos de las matrices (2.13) y (2,14) como:

$$\begin{bmatrix} 0 & \gamma & 0 \\ -\gamma & 0 & -\frac{\partial}{\partial x} \\ 0 & \frac{\partial}{\partial x} & 0 \end{bmatrix} \begin{bmatrix} E_x \\ E_y \\ E_z \end{bmatrix} = -j\omega\mu_0 \begin{bmatrix} \mu_x & 0 & 0 \\ 0 & \mu_y & 0 \\ 0 & 0 & \mu_z \end{bmatrix} \begin{bmatrix} H_x \\ H_y \\ H_z \end{bmatrix} \tag{3.1}$$

$$\begin{bmatrix} 0 & \gamma & 0 \\ -\gamma & 0 & -\frac{\partial}{\partial x} \\ 0 & \frac{\partial}{\partial x} & 0 \end{bmatrix} \begin{bmatrix} H_x \\ H_y \\ H_z \end{bmatrix} = j\omega\epsilon_0 \begin{bmatrix} \epsilon_x & 0 & 0 \\ 0 & \epsilon_y & 0 \\ 0 & 0 & \epsilon_z \end{bmatrix} \begin{bmatrix} E_x \\ E_y \\ E_z \end{bmatrix} \tag{3.2}$$

Por lo que, tendremos un sistema de ecuaciones diferenciales que son separadas en dos sistemas independientes en lo que se incluye polarización TE y TM. En el caso de la polarización TE se tendrá en cuenta que $E_z = 0$ y, en el caso, de TM se tendrá en cuenta que $H_z = 0$, por lo que, podemos obtener estas ecuaciones a partir de (2.13) y (2.14):

- $E_x$, $H_x$ y $H_z$ $(TE)$

$$\begin{cases} -\gamma E_y = -j\omega\mu_0\mu_x H_x \\ \frac{\partial E_y}{\partial x} = -j\omega\mu_0\mu_z H_z \\ -\gamma H_x - \frac{\partial H_z}{\partial x} = j\omega\epsilon_0\epsilon_y E_y \end{cases} \tag{3.3}$$

- $E_x$, $E_z$ y $H_y$ $(TM)$

$$\begin{cases} -\gamma E_x - \frac{\partial E_z}{\partial x} = -j\omega\mu_0\mu_z H_y \\ \gamma H_y = j\omega\epsilon_0\epsilon_x E_x \\ \frac{\partial H_y}{\partial x} = j\omega\epsilon_0\epsilon_z E_z \end{cases} \tag{3.4}$$

En ambos casos, el problema se reduce a resolver sus problemas de valores propios de operador diferencial de segundo orden. A veces es posible resolverlo analíticamente. Sin embargo, en el caso

general, cuando $\epsilon(x)$ es arbitrario, el método de diferencias finitas se puede utilizar. Hay una gran cantidad de aplicaciones de este método en el análisis de la guía de ondas, cavidades resonantes, etc (características de dispersión, de corte y frecuencias de resonancia ($\gamma = 0$), distribuciones de campo).

## 3.1. Polarización TE

Con el fin de presentar los supuestos básicos del método de las diferencias finitas, es necesario, considerar un caso especial de los temas tratados en el párrafo anterior. Suponiendo que el material es no-magnético, la solución de los campos TE generados en la estructura son considerados por la eliminación de la componente $H_x$ del sistema anterior. De esta manera las ecuaciones (3.3) serán:

$$\begin{cases} \frac{\partial E_y}{\partial x} = -j\omega\mu_0 H_z \\ -\frac{\partial H_z}{\partial x} = (-\frac{\gamma^2}{j\omega\mu_0} + j\omega\epsilon_0\epsilon_y)E_y \end{cases} \tag{3.5}$$

La primera etapa del método se basa en el cálculo de diferencia de discretización espacio finito. Por lo que, nos centraremos en la Figura 3.1, donde la distancia entre los sucesivos puntos de discretización del campo se llamará, paso de discretización. Este concepto fue propuesto por primera vez en 1966 por KS Yee.

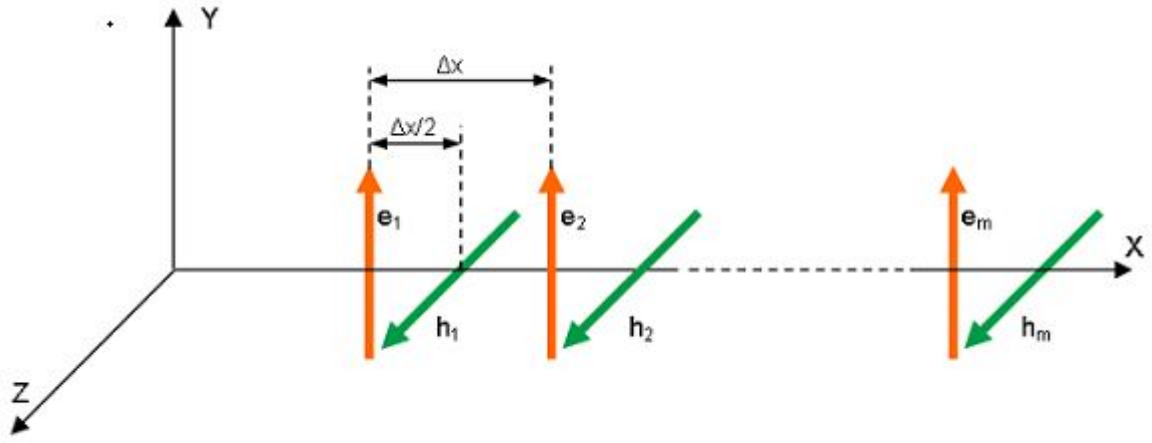


Figura 3.1: Field distribution for TE mode

La esencia de este método es la aproximación de la aproximación a la derivada de la función. Por lo que, para una función dada f(x) tendremos,

$$f'(x_o) \simeq \frac{f(x_o + \triangle x/2) - f(x_o - \triangle x/2)}{\triangle x}, \triangle x << 1 \tag{3.6}$$

En primer lugar, si se tiene en cuenta la ecuación (3.5) y nos fijamos en la Figura 3.1, es posible introducir la siguiente notación utilizando el algoritmo anterior:

$$\frac{E_{m+1} - E_m}{\triangle x} = -j\omega\mu H_m \tag{3.7}$$

donde m corresponderá al número de campo en el que nos encontremos. Por otro lado, en el caso de $H_z = 0$ las ecuaciones serán:

$$-\frac{H_m - H_{m-1}}{\triangle x} = (-\frac{\gamma^2}{j\omega\mu_0} + j\omega\epsilon_0 P_m)E_m \tag{3.8}$$

donde $P_m = \epsilon_y(M \triangle x)$ cuando m=1, 2, .... $P_m$ será la permitividad dieléctrica de nuestro medio.

Si nos basamos en las ecuaciones (3.7) y (3.8) tendremos la siguiente relación:

$$\begin{cases} C_{zy}^{(e)}\mathbf{e} = -j\omega\mu_0\mathbf{h} \\ C_{yz}^{(h)}\mathbf{h} = (-\frac{\gamma^2}{j\omega\mu_0} + j\omega\epsilon_0 P)\mathbf{e} \end{cases} \tag{3.9}$$

donde $C_{zy}^{(e)}$ , $C_{yz}^{(h)}$ y P son matrices cuadradas de dimensión M x M, las cuales de pueden definir de la siguiente manera:

$$[C_{zy}^{(e)}]_{mn} = \triangle x^{-1} \begin{cases} -1, m = n, \\ 1, m = n+1, \\ 0, rest \end{cases} \tag{3.10}$$

$$C_{zy}^{(h)} = C_{zy}^{(e)^T} \tag{3.11}$$

$$P = diag[P_1, \ldots, P_M] \tag{3.12}$$

donde P es definida como la matriz de permitividad $P_m = \epsilon_r((m-1) \triangle x)$ y se muestra como:

$$P_m = \begin{bmatrix} \epsilon_r((m-1) \triangle x) & 0 & 0 & \ldots & 0 \\ 0 & \epsilon_r((m-1) \triangle x) & 0 & \ldots & 0 \\ 0 & 0 & \epsilon_r((m-1) \triangle x) & \ldots & 0 \\ \vdots & & & & \\ 0 & 0 & 0 & \ldots & \epsilon_r((m-1) \triangle x) \end{bmatrix} \tag{3.13}$$

y los vectores **e** y **h** son

$$\mathbf{e} = \begin{bmatrix} E_1 \\ E_2 \\ \vdots \\ E_M \end{bmatrix} \mathbf{h} = \begin{bmatrix} H_1 \\ H_2 \\ \vdots \\ H_M \end{bmatrix}$$

Si nos fijamos en las ecuaciones (3.10) y (3.11), las matrices de la ecuación (3.9) pueden ser presentadas como:

$$C_{zy}^{(e)} = \frac{1}{\triangle X} \begin{bmatrix} -1 & 1 & 0 & 0 & 0 & \ldots \\ 0 & -1 & 1 & 0 & 0 & \ldots \\ 0 & 0 & -1 & 1 & 0 & \ldots \\ 0 & 0 & 0 & -1 & 1 & \ldots \\ \vdots & & & & \ddots & \\ 0 & 0 & 0 & 0 & 0 & -1 \end{bmatrix} \tag{3.14}$$

$$C_{yz}^{(h)} = \frac{1}{\triangle Y} \begin{bmatrix} 1 & 0 & 0 & 0 & 0 & \dots \\ -1 & 1 & 0 & 0 & 0 & \dots \\ 0 & -1 & 1 & 0 & 0 & \dots \\ 0 & 0 & -1 & 1 & 0 & \dots \\ \vdots & & & & \ddots & \\ 0 & 0 & 0 & 0 & -1 & 1 \end{bmatrix} \tag{3.15}$$

Las ecuaciones (3.9) pueden ser reorganizadas para obtener el problema de valores propios con el fin de determinar las constantes de propagación de los modos TE.

$$[C_{yz}^{(h)} C_{zy}^{(e)} - \omega^2 \mu_0 \epsilon_0 P] e = \gamma^2 e \tag{3.16}$$

o en caso de $\gamma = 0$ las frecuencias de corte de una guía de onda (o frecuencia de resonancia de una cavidad) pueden ser obtenidas con una ecuación análoga a la anterior:

$$[\mu_0^{-1} \epsilon_0^{-1} P^{-1} C_{yz}^{(h)} C_{zy}^{(e)}] e = \omega^2 e \tag{3.17}$$

En ambos casos, no tiene en cuenta las condiciones de contorno hasta el momento, sin embargo, son necesarios para completar la formulación del problema. La implementación más simple de la pared, es forzando a cero la componente tangencial, respectivamente, de los campos eléctricos o magnéticos. En la práctica, esto significa restaurar o extraer la columna de la matriz $C_{zy}^{(e)}$ y (o fila $C_{yz}^{(h)}$) para la pared eléctrica (PEC). Simultáneamente, las columnas $C_{zy}^{(h)}$ (o fila $C_{yz}^{(e)}$), en el caso de la pared magnética (PMC).

Es necesario mencionar que los problemas (3.16) y (3.17) se implementan de forma natural con las condiciones de contorno que son para la pared magnética $x = -\frac{1}{2} \triangle x$ y para la pared eléctrica $x = M \triangle x$.

## 3.2. Condiciones de contorno

Debido a las condiciones de contorno, se crearán matrices de transformación que reducen el tiempo de cómputo mediante la eliminación de algunas muestras de campo. Estos cambios no afectarán al resultado final. Por lo tanto, la ecuación (3.9) será modificada de forma que $e = T_e \tilde{e}$ y $h = T_h \tilde{h}$,

$$\begin{cases} C^e T_e \tilde{e} = -j\omega\mu T_h \tilde{h} \\ C^h T_h \tilde{h} = j\omega\epsilon P \tilde{e} \end{cases} \tag{3.18}$$

donde teniendo en cuenta la condición de conductor eléctrico perfecto en caso de $T_e$, ésta será la matriz identidad con la eliminación de la primera y útlima columna.

$$T_e = \begin{bmatrix} 0 & 0 & 0 & \dots & 0 \\ 1 & 0 & 0 & \dots & 0 \\ 0 & 1 & 0 & \dots & 0 \\ 0 & 0 & 1 & \dots & 0 \\ \vdots & & & & \\ 0 & 0 & 0 & \dots & 1 \\ 0 & 0 & 0 & \dots & 0 \end{bmatrix} \tag{3.19}$$

y, en caso de $T_m$, será eliminada la última columna,

$$T_h = \begin{bmatrix} 1 & 0 & 0 & 0 & \dots & 0 \\ 0 & 1 & 0 & 0 & \dots & 0 \\ 0 & 0 & 1 & 0 & \dots & 0 \\ 0 & 0 & 0 & 1 & \dots & 0 \\ \vdots & & & & & \\ 0 & 0 & 0 & 0 & \dots & 1 \\ 0 & 0 & 0 & 0 & \dots & 0 \end{bmatrix} \tag{3.20}$$

Tomando $T_h^T \cdot T_h = I$ y $T_e^T \cdot T_e = I$, la ecuación modificada es:

$$\begin{cases} T_h^T C^e T_e \tilde{e} = -j\omega\mu\tilde{h} \\ T_e^T C^h T_h \tilde{h} = j\omega\epsilon T_e^T P T_e \tilde{e} \end{cases} \tag{3.21}$$

o de una forma más corta,

$$\begin{cases} \tilde{C}^e \tilde{e} = -j\omega\mu\tilde{h} \\ \tilde{C}^h \tilde{h} = j\omega\epsilon\tilde{P}\tilde{e} \end{cases} \tag{3.22}$$

donde $\tilde{C}^e = T_h^T C^e T_e$, $\tilde{C}^h = T_e^T C^h T_h$ y $\tilde{P} = T_e^T P T_e$.

## 3.3. Permitividad dieléctrica

Hay muchas técnicas diferentes de aplicación permitividad dieléctrica en DF. En esta tesis la aproximación más simple se aplica como la ecuación (3.13), pero se puede simplemente actualizar a algoritmos más complejos. Resultados más precisos pueden ser obtenidos mediante el uso de la aproximación de Kaneda, Itoh [11].

## 3.4. Polarización TM

De forma similar a los modos TE, los modos TM serán resuesto de la misma manera pero nos centraremos en otro grupo de ecuaciones. Si recordamos el concepto principal de la polarización TM, en el que $H_z = 0$, el grupo de ecuaciones a tratar será:

$$\begin{cases} \frac{\partial H_y}{\partial x} = j\omega\epsilon E_z \\ -\frac{\partial E_z}{\partial x} = (-\frac{\gamma^2}{j\omega\epsilon_0\epsilon_x} + j\omega\mu_0\mu_z)H_y \end{cases} \tag{3.23}$$

Como en el caso de TE, en la representación de los modos TM se tiene en cuenta que el campo magnético es transversal a la dirección de propagación z.

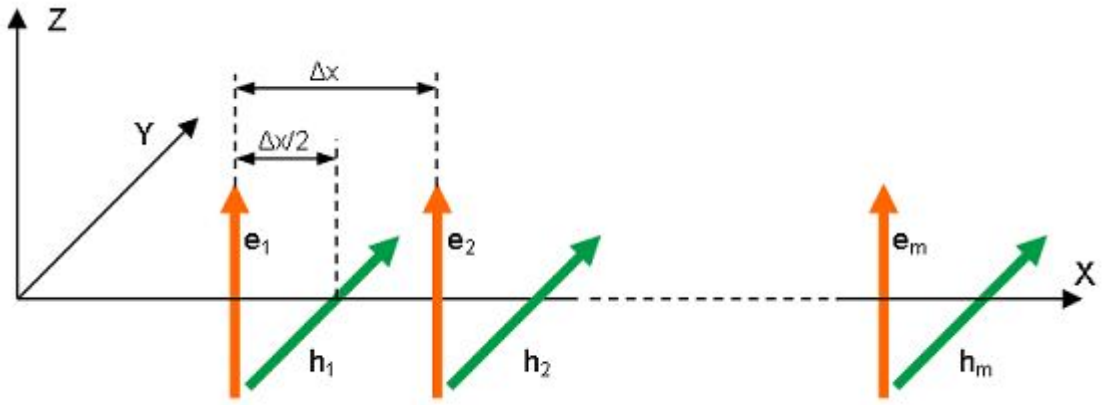


Figura 3.2: Field distribution for TM mode

Basándonos en la ecuación (3.23) para el campo eléctrico tendremos,

$$-\frac{E_{m+1}-E_m}{\triangle x} = (-\frac{\gamma^2}{j\omega\epsilon_0}P^{-1} + j\omega\mu_0\mu_z)H_m \tag{3.24}$$

y, para el campo magnético,

$$-\frac{H_m - H_{m-1}}{\triangle x} = -j\omega\mu E_m \tag{3.25}$$

Las ecuaciones, en este caso, serán agrupadas de la siguiente forma:

$$\begin{cases} C_{yz}^{(e)}\mathbf{e} = (-\frac{\gamma^2}{j\omega\epsilon} + j\omega\mu_z)\mathbf{h} \\ C_{zy}^{(h)}\mathbf{h} = j\omega\epsilon\mathbf{e} \end{cases} \tag{3.26}$$

donde $C_{zy}^{(e)}$, $C_{yz}^{(h)}$ y P matrices cuadradas de dimensión M x M. Estas ecuaciones son definidas como,

$$[C_{yz}^{(e)}]_{mn} = \triangle x^{-1} \begin{cases} -1, m = n, \\ 1, m = n+1, \\ 0, rest \end{cases} \tag{3.27}$$

$$C_{zy}^{(h)} = C_{yz}^{(e)^T} \tag{3.28}$$

$$P = diag[P_1, \ldots, P_M] \tag{3.29}$$

donde P, como en la polarización TE es definida como la matriz de permitividad $P_m = \epsilon_r((m-1) \triangle x$ y puede ser mostrada como:

$$P_m = \begin{bmatrix} \epsilon_r((m-1)\triangle x) & 0 & 0 & \ldots & 0 \\ 0 & \epsilon_r((m-1)\triangle x) & 0 & \ldots & 0 \\ 0 & 0 & \epsilon_r((m-1)\triangle x) & \ldots & 0 \\ \vdots & & & & \\ 0 & 0 & 0 & \ldots & \epsilon_r((m-1)\triangle x) \end{bmatrix} \tag{3.30}$$

Las incógnitas $C_{yz}^{(e)}$ y $C_{zy}^{(h)}$ son presentadas en forma de matriz como,

$$C_{yz}^{(e)} = -\frac{1}{\triangle X}\begin{bmatrix} -1 & 0 & 0 & \dots & \\ 1 & -1 & 0 & \dots & \\ 0 & 1 & -1 & 0 & \\ 0 & 0 & 1 & -1 & \\ \vdots & & & & \\ 0 & 0 & 0 & 1 & \dots \end{bmatrix} \tag{3.31}$$

$$C_{zy}^{(h)} = -\frac{1}{\triangle Y}\begin{bmatrix} 1 & 0 & 0 & 0 & \dots \\ -1 & 1 & 0 & 0 & \dots \\ 0 & -1 & 1 & 0 & \dots \\ 0 & 0 & -1 & 1 & \dots \\ \vdots & & & & \\ \dots & 0 & 0 & -1 & 1 \end{bmatrix} \tag{3.32}$$

De la misma manera que anteriormente, se obtendrán las características de propagación para la polarizacion TM, por lo que, si la ecuación (3.26) es reorganizada, se obtendrá el problema de valores propios con el fin de determinar las constantes de propagación:

$$[C_{zy}^{(h)} C_{yz}^{(e)} - \omega^2 \mu_0 \epsilon_0 P]e = \gamma^2 e \tag{3.33}$$

o en caso de $\gamma = 0$ se obtendrán las frecuencias de corte de una guía de onsa o frecuencias de resonancia de una cavidad mediante la ecuación:

$$[\mu_0^{-1} \epsilon_0^{-1} P^{-1} C_{zy}^{(h)} C_{yz}^{(e)}]e = \omega^2 e \tag{3.34}$$

En las ecuaciones anteriores no están incluídas las condiciones de contorno pero serán necesarias para completar la formulación del problema. Se forzará a cero la componente tangencial, respectivamente, de los campos eléctricos o magnéticos. Esto significa, la restauración (o eliminación) de la columna de la matriz $C_{yz}^{(e)}$ y (o fila $C_{zy}^{(h)}$) de la pared eléctrica.

Las condiciones de contorno aquí aplicadas son las mismas que para los modos TE, explicadas en la sección 3.2.

## 3.5. Resultados numéricos

Durante el proyecto, se han realizado numerosas pruebas y comparaciones para demostrar que éste método es válido. Todas estas pruebas se han llevado a cabo en el entorno de Matlab. Como resultado se han expuesto diferentes pruebas para cada polarización TE y TM. Por un lado, serán expuestos los resultados obtenidos de las frecuencias de corte y, por otro lado, las características de dispersión.

Con el objetivo de verificar el método, será introducido un dieléctrico en el medio de permitividad $\epsilon_{r1} = 9$. Tendremos unas placas paralelas con una anchura de a = 22.86mm.

Se debe recordar que $\epsilon_r$ pertenece a la matriz P que será una matriz cuadrada M x M. De esta forma la nueva matriz P estará formado por una diagonal de valores de diferentes dieléctricos.

$$P = \begin{bmatrix} 9 & 0 & \dots & 0 & 0 & 0 & 0 \\ 0 & 9 & \dots & 0 & 0 & 0 & 0 \\ \vdots & & \ddots & 0 & 0 & 0 & \vdots \\ 0 & 0 & 0 & 9 & 0 & 0 & \dots \\ 0 & 0 & 0 & 0 & 1 & 0 & \dots \\ \vdots & 0 & 0 & 0 & 0 & \ddots & \\ 0 & 0 & 0 & 0 & 0 & 0 & 1 \end{bmatrix}$$

En la guía de onda, en función de la distancia que ha sido tomado por el dieléctrico, la diagonal de la matriz tendrá más o menos valores de la permitividad. En nuestro caso, se decidió que la distancia sería de 10 mm y el resto de la guía, aire.

### 3.5.1. Polarización TE

#### Obtención de las frecuencias de corte en una dimensión

En primer lugar, obtendremos las frecuencias de corte para los modos TE. Las condiciones que se han utilizado son $\epsilon_0 = 8{,}854187818 \cdot 10^{-12}$ , $c = 299792458$ m/s $\simeq 3 \cdot 10^8$ m/s. En este caso, $\gamma = 0$, por lo que, será utilizada la ecuación (3.17) que hace referencia al problema de valores propios.

Combinando los términos de la ecuación (3.17), tendremos el siguiente problema,

$$AX = \lambda X \tag{3.35}$$

donde $A = \frac{1}{\mu_0 \epsilon_0} P^{-1} C_{yz}^{(h)} C_{zy}^{(e)}$, $\lambda = \omega^2$ que representa la frecuencia de corte y el vector X representa la correspodiente distribución de campo.

#### Resultados de los modos $TE_{m0}$ en la guía de onda WR90

La tabla siguiente muestra las frecuencias de corte de los primeros cinco modos de la polarización TE. En esta tabla se muestran los resultados numéricos obtenidos a través de Matlab comparados con los resultados analíticos que han sido expuestos en el apéndice A.

| | TE10 | TE20 | TE30 | TE40 | TE50 |
|---|---|---|---|---|---|
| Value | fc1(GHz) | fc2(GHz) | fc3(GHz) | fc4(GHz) | fc5(GHz) |
| Numerical N=10 | 3,1952 | 7,5269 | 10,279 | 11,585 | 19,106 |
| Error( %) | 6,76 | 3,35 | 5,6 | 13,6 | 9,18 |
| Numerical N=100 | 2,9838 | 7,2558 | 10,883 | 13,378 | 17,398 |
| Error( %) | 0,29 | 0,37 | 0,10 | 0,30 | 0,58 |
| Numerical N=1000 | 2,9949 | 7,2891 | 10,897 | 13,426 | 17,515 |
| Error( %) | 0,07 | 0,08 | 0,01 | 0,04 | 0,08 |
| Numerical N=10000 | 2,9929 | 7,2835 | 10,895 | 13,420 | 17,501 |
| Error( %) | 0,007 | 0,008 | 0,0009 | 0,04 0,003 | 0,008 |
| Analytical | 2,9927 | 7,2829 | 10,895 | 13,420 | 17,500 |

Cuadro 3.1: Cutoff frequency data table for $TE_m0$ obtained for different meshes

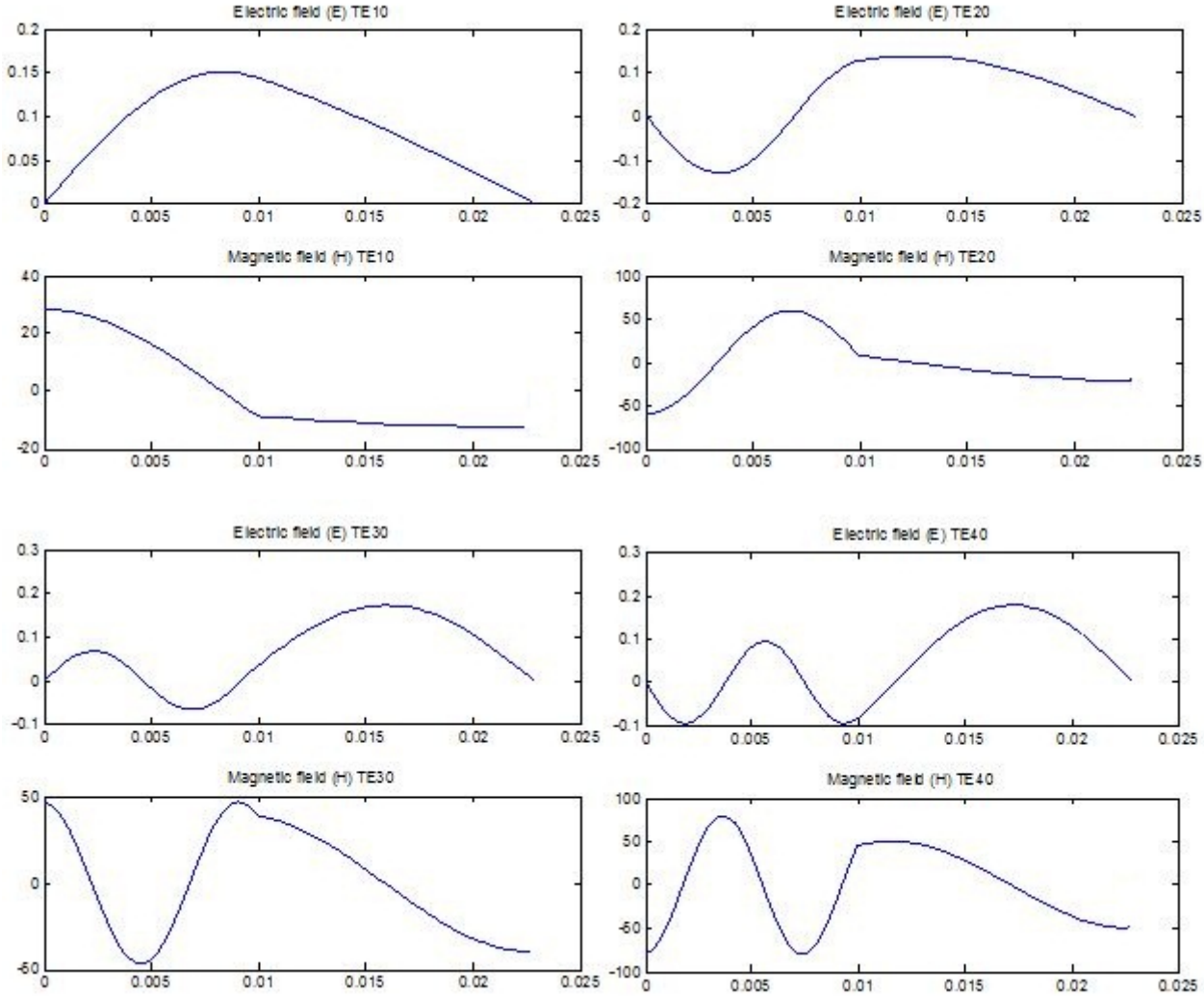


Figura 3.3: Representation of cutoff frequencies for TE modes in one dimension

En la figura 3.4, se muestran la variación de los campos magnético y eléctricos de los primeros cuatro modos. Estos resultados se han obtenido para una malla de N=100.

### Resultados de las características de propagación de los modos TE

Ahora será utilizada la ecuación (3.16), ya que, se tiene en cuenta que ahora $\gamma \neq 0$, por lo que, de nuevo tendremos un problema de valores propios por la ecuación (3.16)

$$AX = \lambda X \tag{3.36}$$

donde $A = C_{zy}^{(h)} C_{zy}^{(e)} - \omega^2 \mu_0 \epsilon_0 P$, $\lambda = \gamma^2$ y X representa la distribución de campo correspondiente con el coeficiente de propagación $\gamma$.

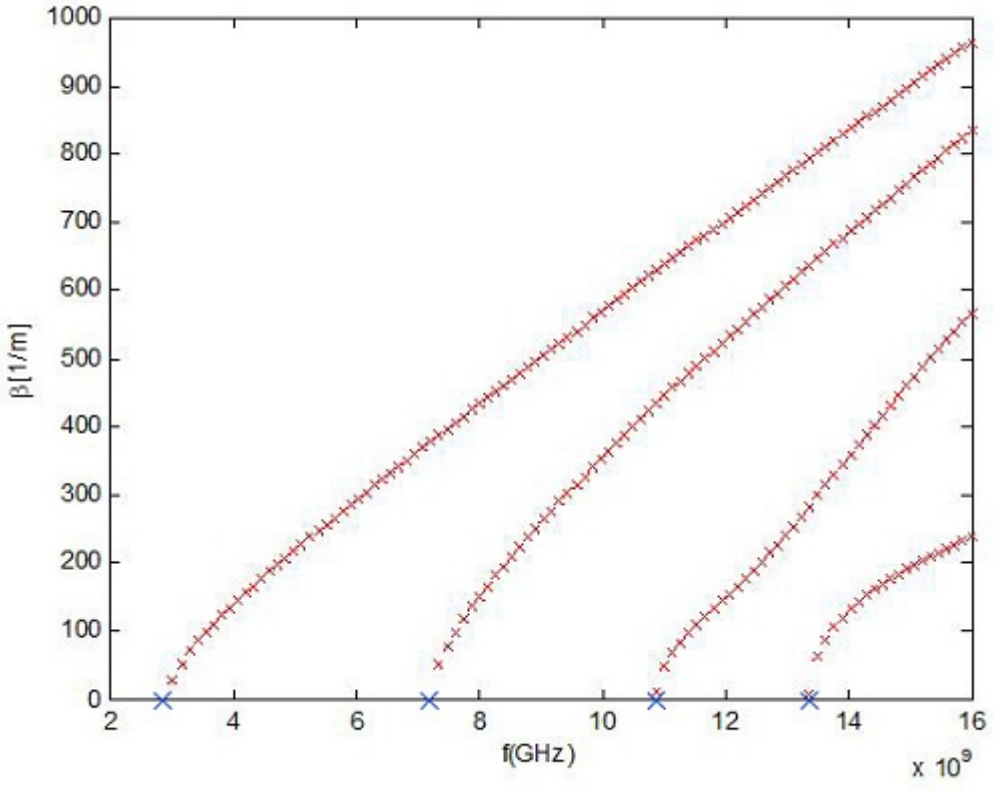


Figura 3.4: Propagation coefficients for $TE_{m0}$ modes

La figura 3.4 muestra los características de propagación de los modos TE para los primeros cuatro modos. Si la frecuencia del modo es más baja que la de corte, será obtenida la constante de propagación real.

### 3.5.2. Polarización TM

#### Obtención de las frecuencias de corte en una dimensión

Serán utilizadas las mismas condiciones que en los modos TE para la obtención de las frecuencias de corte. De la misma forma, partiendo de la ecuación (3.34), y teniendo en cuenta que $\gamma = 0$, mediante el problema de valores propios podremos conseguir las frecuencias de corte.

$$AX = \lambda X \tag{3.37}$$

donde $A = \frac{1}{\mu_0 \epsilon_0} C_{zy}^{(h)} C_{yz}^{(e}$, $\lambda = \omega^2$, que representa las frecuencias de corte y el vector X la distribución de campo, análoga a la polarización TE.

#### Resultados de los modos $TM_{m0}$ en ña guía de onda WR90

Se utilizará una guía de onda de dimensiones $a = 22{,}86mm$ y permitividades $\epsilon_{r1} = 9$ y $\epsilon_{r2} = 1$ que se corresponde con el aire.

En la tabla 3.2 se muestran las diferentes frecuencias de corte que han sido obtenidas mediante el entorno Matlab. Éstas han sido comparadas con los resultados analíticos, como indica la tabla,

que han sido expuestos en el apéndice A.

| | TM10 | TM20 | TM30 | TM40 | TM50 |
|---|---|---|---|---|---|
| Value | fc1 | fc2 | fc3 | fc4 | fc5 |
| Numerical N10 | 3,1952 | 7,5269 | 10,279 | 11,585 | 19,106 |
| Error( %) | 6,76 | 3,35 | 5,6 | 13,6 | 9,18 |
| Numerical N100 | 2,9838 | 7,2558 | 10,883 | 13,378 | 17,398 |
| Error( %) | 0,30 | 0,36 | 0,11 | 0,30 | 0,57 |
| Numerical N1000 | 2,9949 | 7,2891 | 10,897 | 13,426 | 17,515 |
| Error( %) | 0,07 | 0,08 | 0,01 | 0,05 | 0,09 |
| Numerical N10000 | 2,9929 | 7,2835 | 10,895 | 13,420 | 17,501 |
| Error( %) | 0,003 | 0,01 | 0,001 | 0,04 0,007 | 0,01 |
| Analytical | 2,9928 | 7,2827 | 10,895 | 13,419 | 17,499 |

Cuadro 3.2: Cutoff frequency data table for $TM_m0$ obtained for different meshes

La figura 3.5, por tanto, muestra la distribución de los campos eléctricos y magnéticos para los primeros cuatro modos de propagación.

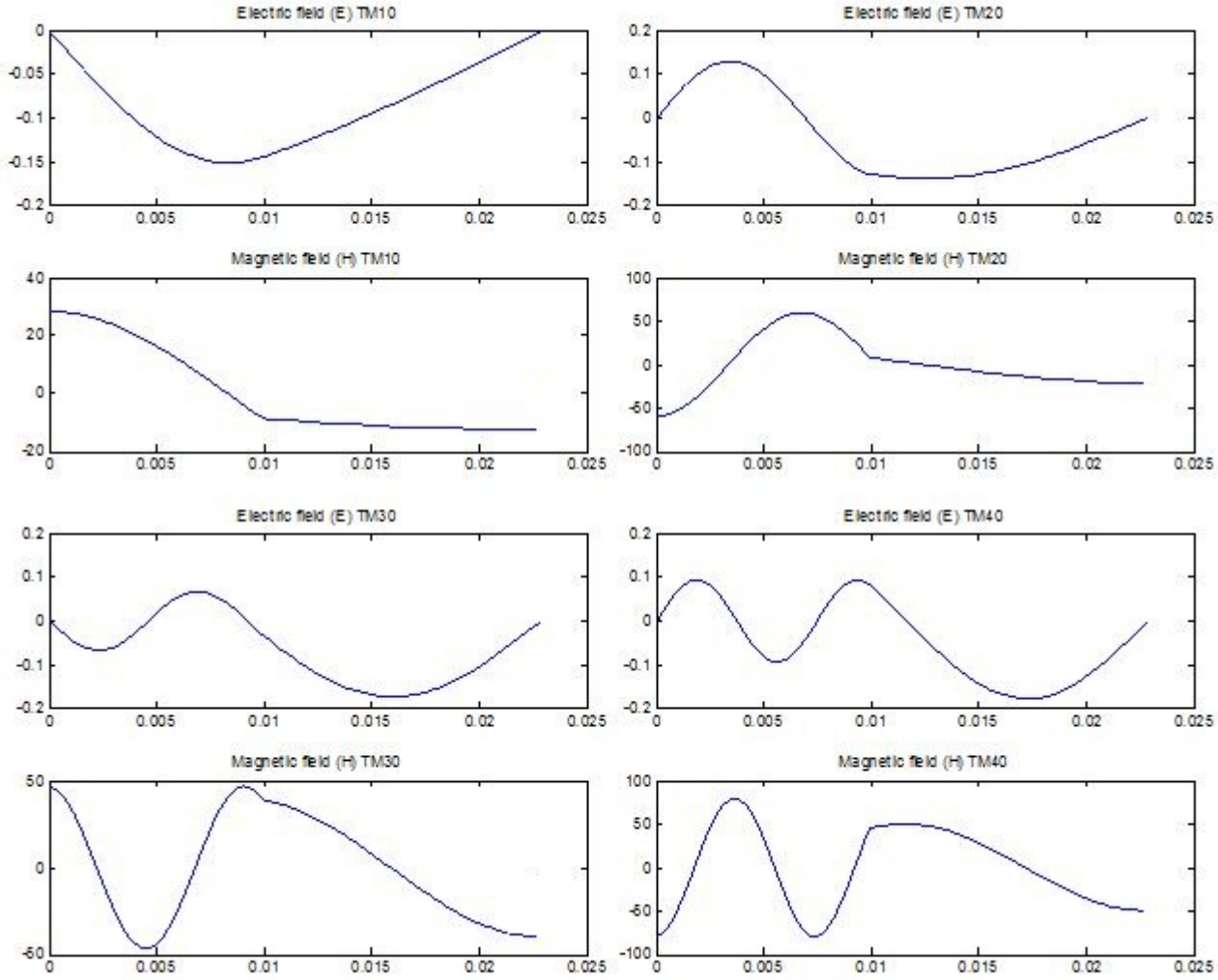


Figura 3.5: Representation of cutoff frequencies for TM modes in one dimension

### Resultados de las características de propagación de los modos TM

Por el problema de valores propios, igual que en los modos TE, se han obtenido las características de propagación de los modos TM, por lo que, centrándonos en la ecuación (3.33) tendremos que,

$$AX = \lambda X \tag{3.38}$$

donde $A = C_{zy}^{(h)} C_{zy}^{(e)} - \omega^2 \mu_0 \epsilon_0 P$ y $\lambda = \gamma^2$.

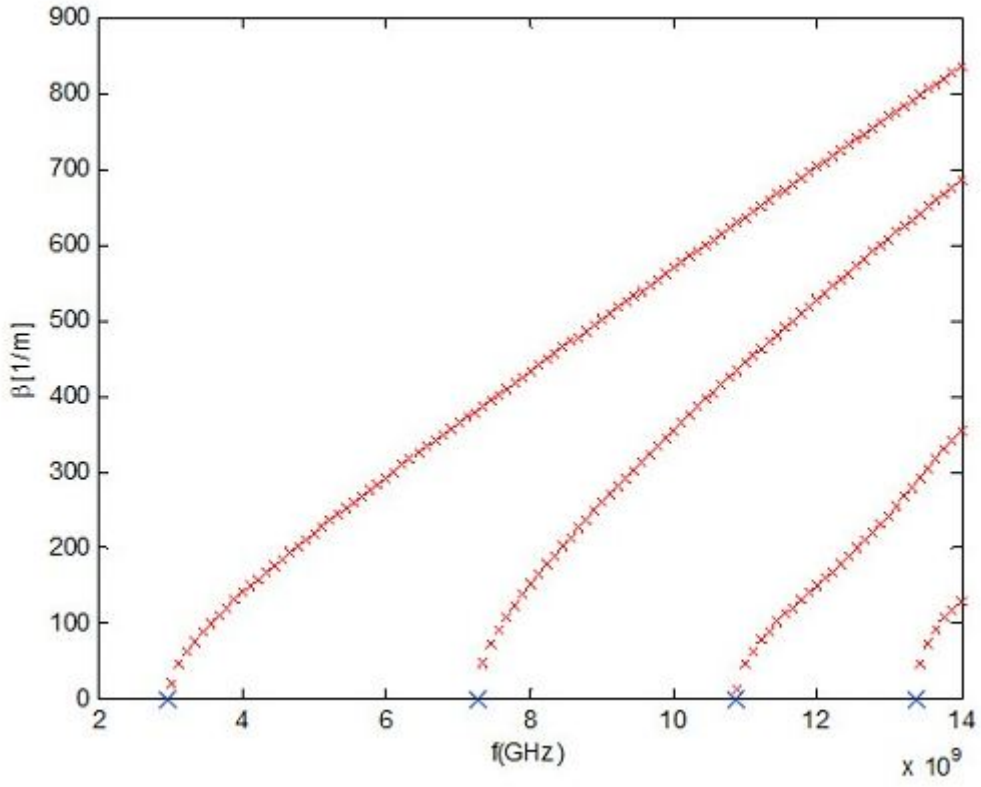


Figura 3.6: Propagation coefficients for $TM_{m0}$ modes

Por último, la figura 3.5 muestra los coeficientes de propagación de los primeros cuatro modos TM en los que esos puntos en la gráfica representan las frecuencias de corte para esos modos.

# Capítulo 4

# Método de las Diferencias Finitas en dos dimensiones

En la sección anterior, se ha presentado un análisis de tan sólo un grupo particular de superficie cerrada. Este tipo de estructuras tienen una aplicación práctica más bien estrecha, sin embargo, su análisis ayuda a entender la idea del método de diferencias finitas.

## 4.1. Ecuaciones de Maxwell en problemas de dos dimensiones

En el caso general, es necesario incluir todos los componentes de los campos eléctricos y magnéticos. Suponiendo que la estructura relevante es uniforme a lo largo del eje z, es posible asumir que cada uno de los componentes de ambos campos está representado por la variación en la dirección z por el factor $e^{-\gamma z}$. Además, suponiendo que es un medio no magnético en el que no hay corrientes de flujo ($\sigma = 0$) y la densidad de carga es igual a cero ($\rho_v = 0$), partiremos entonces de las siguientes ecuaciones:

$$\begin{bmatrix} 0 & \gamma & \frac{\partial}{\partial y} \\ -\gamma & 0 & -\frac{\partial}{\partial x} \\ -\frac{\partial}{\partial y} & \frac{\partial}{\partial x} & 0 \end{bmatrix} \begin{bmatrix} E_x \\ E_y \\ E_z \end{bmatrix} = -j\omega\mu_0 \begin{bmatrix} H_x \\ H_y \\ H_z \end{bmatrix} \tag{4.1}$$

$$\begin{bmatrix} 0 & \gamma & \frac{\partial}{\partial y} \\ -\gamma & 0 & -\frac{\partial}{\partial x} \\ -\frac{\partial}{\partial y} & \frac{\partial}{\partial x} & 0 \end{bmatrix} \begin{bmatrix} H_x \\ H_y \\ H_z \end{bmatrix} = j\omega\epsilon_0 \begin{bmatrix} \epsilon_x & 0 & 0 \\ 0 & \epsilon_y & 0 \\ 0 & 0 & \epsilon_z \end{bmatrix} \begin{bmatrix} E_x \\ E_y \\ E_z \end{bmatrix} \tag{4.2}$$

$$\begin{bmatrix} \frac{\partial}{\partial x} & \frac{\partial}{\partial y} - \gamma \end{bmatrix} \begin{bmatrix} \epsilon_x & 0 & 0 \\ 0 & \epsilon_y & 0 \\ 0 & 0 & \epsilon_z \end{bmatrix} \begin{bmatrix} E_x \\ E_y \\ E_z \end{bmatrix} = 0 \tag{4.3}$$

$$\begin{bmatrix} \frac{\partial}{\partial x} & \frac{\partial}{\partial y} - \gamma \end{bmatrix} \begin{bmatrix} H_x \\ H_y \\ H_z \end{bmatrix} = 0 \tag{4.4}$$

El sistema de ecuaciones descrito anteriormente puede ser analizado de forma similar al caso del problema unidimensional. Los conjuntos de puntos, en los que se muestrean las componentes de los campos eléctricos magnéticos transversales se muestran en la Figura 4.1.

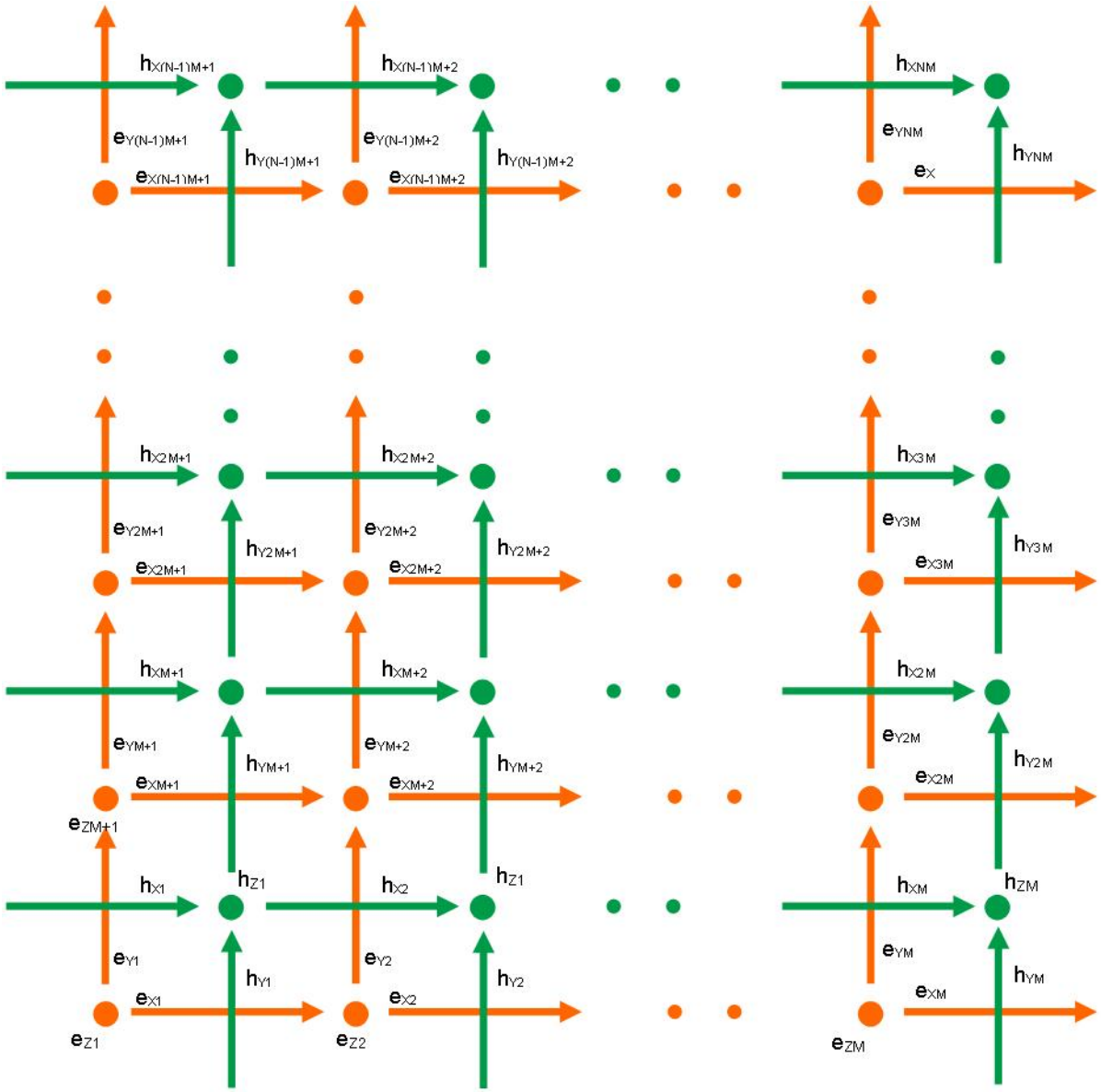


Figura 4.1: The set of points, which are sampled electric and magnetic fields

Se llamará M al número de muestras en la dirección X y N al número de muestras en la dirección Y, por lo que, el conjunto de puntos K será $K = M \cdot N$ para cada componente de campo. Podemos simplificar de manera que:

$$k = (n-1)M + m \tag{4.5}$$

where k=1,..., K, m=1,..., M and n=1,..., N. The vector $\mathbf{e}_i$ which contains the samples of the i-th component of the electric field can be written as:

$$[e_x]_k = E_x((m - \frac{1}{2}) \triangle x, (n-1) \triangle y) \tag{4.6}$$

$$[e_y]_k = E_y((m-1) \triangle x, (n - \frac{1}{2}) \triangle y) \tag{4.7}$$

$$[e_z]_k = E_z((m-1) \triangle x, (n-1) \triangle y) \tag{4.8}$$

and in case of $h_i$ elements:

$$[h_x]_k = E_x((m-1) \triangle x, (n-\frac{1}{2}) \triangle y) \tag{4.9}$$

$$[h_y]_k = E_y((m-\frac{1}{2}) \triangle x, (n-1) \triangle y) \tag{4.10}$$

$$[h_z]_k = E_z((m-\frac{1}{2}) \triangle x, (n-\frac{1}{2}) \triangle y) \tag{4.11}$$

In addition, electric permittivity is the numerical domain:

$$[P_x]_k = \epsilon_{rx}((m-\frac{1}{2}) \triangle x, (n-1) \triangle y) \tag{4.12}$$

$$[P_y]_k = \epsilon_{ry}((m-1) \triangle x, (n-\frac{1}{2}) \triangle y) \tag{4.13}$$

$$[P_z]_k = \epsilon_{rz}((m-1) \triangle x, (n-1) \triangle y) \tag{4.14}$$

## 4.2. Polarización TE

Seguiremos asumiendo que $E_z = 0$ ($E_y \neq 0$, $E_x \neq 0$ y $H_z \neq 0$), por lo que, partiendo de las ecuaciones (4.1) y (4.2) se obtiene:

$$\begin{cases} \gamma E_y = -j\omega\mu_0 H_z \\ -\gamma E_x = -j\omega\mu_0 H_z \\ -\frac{\partial E_x}{\partial y} + \frac{\partial E_y}{\partial x} = -j\omega\mu_0 H_z \end{cases} \tag{4.15}$$

and

$$\begin{cases} \frac{\partial H_z}{\partial y} = (-\frac{\gamma^2}{j\omega\mu_0} + j\omega\epsilon_0\epsilon_x)E_x \\ -\frac{\partial H_z}{\partial x} = -(\frac{\gamma^2}{j\omega\mu_0} + j\omega\epsilon_0\epsilon_y)E_y \end{cases} \tag{4.16}$$

Por un lado, si operamos con respecto al campo eléctrico, tendremos

$$-\frac{\partial E_x}{\partial y} + \frac{\partial E_y}{\partial x} = -j\omega\mu_0 H_z \tag{4.17}$$

y puede ser asociada, de igual manera que en el caso de una dimensión, a una ecuación basada en matrices como:

$$C_{zt}^{(e)} e_t = -j\omega\mu_0 h_z \tag{4.18}$$

donde $C_{zt}^{(e)}$ puede ser separada en $C_{zx}^{(e)}$ y $C_{zy}^{(e)}$, por lo tanto la ecuación (4.18) será definida como,

$$\begin{bmatrix} C_{zx}^{(e)} & C_{zy}^{(e)} \end{bmatrix} \begin{bmatrix} e_x \\ e_y \end{bmatrix} = -j\omega\mu_0 h_z \tag{4.19}$$

El número de ecuaciones obtenidas a partir de la ecuación (4.17) dependerá del número de muestras que sean escogidas ($K = MxN$). Como resultado tendremos para cada matriz $C_{zx}^{(e)}$, $C_{zy}^{(e)}$:

$$[C_{zx}^{(e)}]_{mn} = \triangle y^{-1} \begin{cases} -1, m = n, \\ 1, m = n+1, \\ 0, rest \end{cases} \tag{4.20}$$

$$[C_{zy}^{(e)}]_{mn} = \triangle x^{-1} \begin{cases} -1, m = n, \\ 1, m = n+1, \\ 0, rest \end{cases} \tag{4.21}$$

donde gráficamente puede ser representadas como:

$$C_{zx}^{(e)} = -\frac{1}{\triangle Y} \begin{bmatrix} -1 & 0 & 0 & 0 & 1 & 0 & \dots & 0 \\ 0 & -1 & 0 & 0 & 0 & 1 & \dots & 0 \\ 0 & 0 & -1 & 0 & 0 & 0 & \dots & 0 \\ 0 & 0 & 0 & -1 & 0 & 0 & \dots & 0 \\ 0 & 0 & 0 & 0 & -1 & 0 & \dots & 0 \\ \vdots & & & & & & & \\ 0 & 0 & 0 & 0 & 0 & 0 & 0 & -1 \end{bmatrix} \tag{4.22}$$

$$C_{zy}^{(e)} = \frac{1}{\triangle X} \begin{bmatrix} -1 & 1 & 0 & 0 & 0 & 0 & \dots & 0 \\ 0 & -1 & 1 & 0 & 0 & 0 & \dots & 0 \\ 0 & 0 & -1 & 1 & 0 & 0 & \dots & 0 \\ 0 & 0 & 0 & -1 & 1 & 0 & \dots & 0 \\ 0 & 0 & 0 & 0 & -1 & 1 & \dots & 0 \\ \vdots & & & & & & & \\ 0 & 0 & 0 & 0 & 0 & 0 & 0 & -1 \end{bmatrix} \tag{4.23}$$

Por otro lado, si tenemos en cuenta la ecuación (4.2) es necesario obtener las ecuaciones de l campo magnético,

$$\begin{cases} \frac{\partial H_z}{\partial y} = (-\frac{\gamma^2}{j\omega\mu_0} + j\omega\epsilon_0\epsilon_x)E_x \\ -\frac{\partial H_z}{\partial x} = -(\frac{\gamma^2}{j\omega\mu_0} + j\omega\epsilon_0\epsilon_y)E_y \end{cases} \tag{4.24}$$

Si resolvemos las dos ecuaciones anteriores, se obtendrá una ecuación dependiente de las dos ecuaciones anteriores:

$$C_{tz}^{(h)} h_z = j\omega\epsilon_0 P e_t \tag{4.25}$$

donde P es la matriz de permitvidad, que será explicada posteriormente y $C_{tz}^{(h)}$ será dividida en dos ecuacioneso $C_{xz}^{(h)}$ y $C_{yz}^{(h)}$ como:

$$\begin{bmatrix} C_{xz}^{(h)} \\ C_{yz}^{(h)} \end{bmatrix} \begin{bmatrix} h_z \end{bmatrix} = j\omega\epsilon_0 \begin{bmatrix} \epsilon_x & 0 \\ 0 & \epsilon_y \end{bmatrix} \begin{bmatrix} e_x \\ e_y \end{bmatrix} \tag{4.26}$$

De igual forma que en el campo eléctrico, es asociado una matriz para cada $C_{xz}^{(h)}$ and $C_{yz}^{(h)}$ como:

$$C_{xz}^{(h)} = \frac{1}{\triangle Y}\begin{bmatrix} 1 & 0 & 0 & 0 & 0 & 0 & \dots & 0 \\ 0 & 1 & 0 & 0 & 0 & 0 & \dots & 0 \\ 0 & 0 & 1 & 0 & 0 & 0 & \dots & 0 \\ 0 & 0 & 0 & 1 & 0 & 0 & \dots & 0 \\ -1 & 0 & 0 & 0 & 1 & 0 & \dots & 0 \\ 0 & -1 & 0 & 0 & 0 & 1 & \dots & 0 \\ \vdots & & & & & & & \\ 0 & 0 & 0 & -1 & 0 & 0 & 0 & 1 \end{bmatrix} \tag{4.27}$$

$$C_{yz}^{(h)} = \frac{1}{\triangle X}\begin{bmatrix} -1 & 0 & 0 & 0 & 0 & 0 & \dots & 0 \\ 1 & -1 & 0 & 0 & 0 & 0 & \dots & 0 \\ 0 & 1 & -1 & 0 & 0 & 0 & \dots & 0 \\ 0 & 0 & 1 & -1 & 0 & 0 & \dots & 0 \\ 0 & 0 & 0 & 1 & -1 & 0 & \dots & 0 \\ 0 & 0 & 0 & 0 & 1 & -1 & \dots & 0 \\ \vdots & & & & & & & \\ 0 & 0 & 0 & 0 & 0 & 0 & 0 & -1 \end{bmatrix} \tag{4.28}$$

Teóricamente es posible darse cuenta que $C_{tz}^{(h)} = C_{zt}^{(e)^T}$, por lo que, en la práctica no será necesario crear las matrices (4.27) y (4.28).

Si las ecuaciones (4.18) y (4.25) son asociadas, obtendremos el mismo problema que en una dimension tal que,

$$\begin{cases} C_{zt}^{(e)} e_t = j\omega\mu_0 h_z \\ C_{tz}^{(h)} h_z = (-\frac{\gamma^2}{j\omega\mu_0} + j\omega\epsilon_0 P_t) e_t \end{cases} \tag{4.29}$$

donde

$$C_{zt}^{(e)} = \left[C_{zx}^{(e)} C_{zy}^{(e)}\right] \tag{4.30}$$

$$C_{tz}^{(h)} = \begin{bmatrix} C_{xz}^{(h)} \\ C_{yz}^{(h)} \end{bmatrix} \tag{4.31}$$

De la misma manera que en el capítulo anterior, podemos reorganizar las ecuaciones y obtener las características de propagación y las frecuencias de corte para la polarización TE en dos dimensiones. En caso de las características de propagación:

$$[C_{zt}^{(e)} C_{tz}^{(h)} - \omega^2\mu_0\epsilon_0 P] = \gamma^2 e \tag{4.32}$$

o en caso $\gamma = 0$, las frecuencias de corte se obtendrán:

$$[\mu_0^{-1}\epsilon_0^{-1} P^{-1} C_{zt}^{(e)} C_{tz}^{(h)}] e = \omega^2 e \tag{4.33}$$

En ambos casos, no se tienen en cuenta las condiciones de corto, pero serán importantes para completar la formulación del problema.

## 4.3. Condiciones de contorno para la polarización TE

Las ecuaciones se pueden transformar de una manera de tal forma que no modifiquen el resultado final pero el tiempo de cálculo será menor. Teniendo en cuenta que $e_t = T_T^e \tilde{e}$ y $h_z = T_z^h \tilde{h_z}$, si recordamos en el problema unidimensional, la ecuación (4.31) se modificará como,

$$\begin{cases} C_{zt}^{(e)} T_t^e \tilde{e_t} = -j\omega\mu_0 T_z^h \tilde{h_z} \\ C_{tz}^{(h)} T_z^h \tilde{h} = j\omega\epsilon_0 P T_t^e \tilde{e_t} \end{cases} \tag{4.34}$$

Si se opera la ecuación (4.36),

$$\begin{cases} T_h^T C_{zt}^{(e)} T_t^e \tilde{e_t} = -j\omega\mu_0 \tilde{h_z} \\ T_e^T C_{tz}^{(h)} T_z^h \tilde{h_z} = j\omega\epsilon_0 T_e^T P T_e \tilde{e_t} \end{cases} \tag{4.35}$$

Por lo que, finalmente se obtendrán las siguientes ecuaciones:

$$\begin{cases} \tilde{C}_{zt}^{(e)} \tilde{e_t} = -j\omega\mu_0 \tilde{h_z} \\ \tilde{C}_{tz}^{(h)} \tilde{h_z} = j\omega\epsilon_0 \tilde{P_t} \tilde{e_t} \end{cases} \tag{4.36}$$

donde $\tilde{C}_{zt}^{(e)} = {T_z^h}^T C_{zt}^{(e)} T_t^e$, $\tilde{C}_{tz}^{(h)} = {T_t^e}^T C_{tz}^{(h)} T_h$ y $\tilde{P} = {T_t^e}^T P T_t^e$, que es la matriz de permitividad.

Por otro lado, no se puede olvidar que las condiciones de contorno $e_t = T_t^e \tilde{e}_t$ and $h_z = T_z^h \tilde{h}_z$ son cambiadas por otras matrices. Estas matrices nuevas están basadas en la Figura 4.3 que representa las condiciones de contorno que deben ser impuestas en el campo.

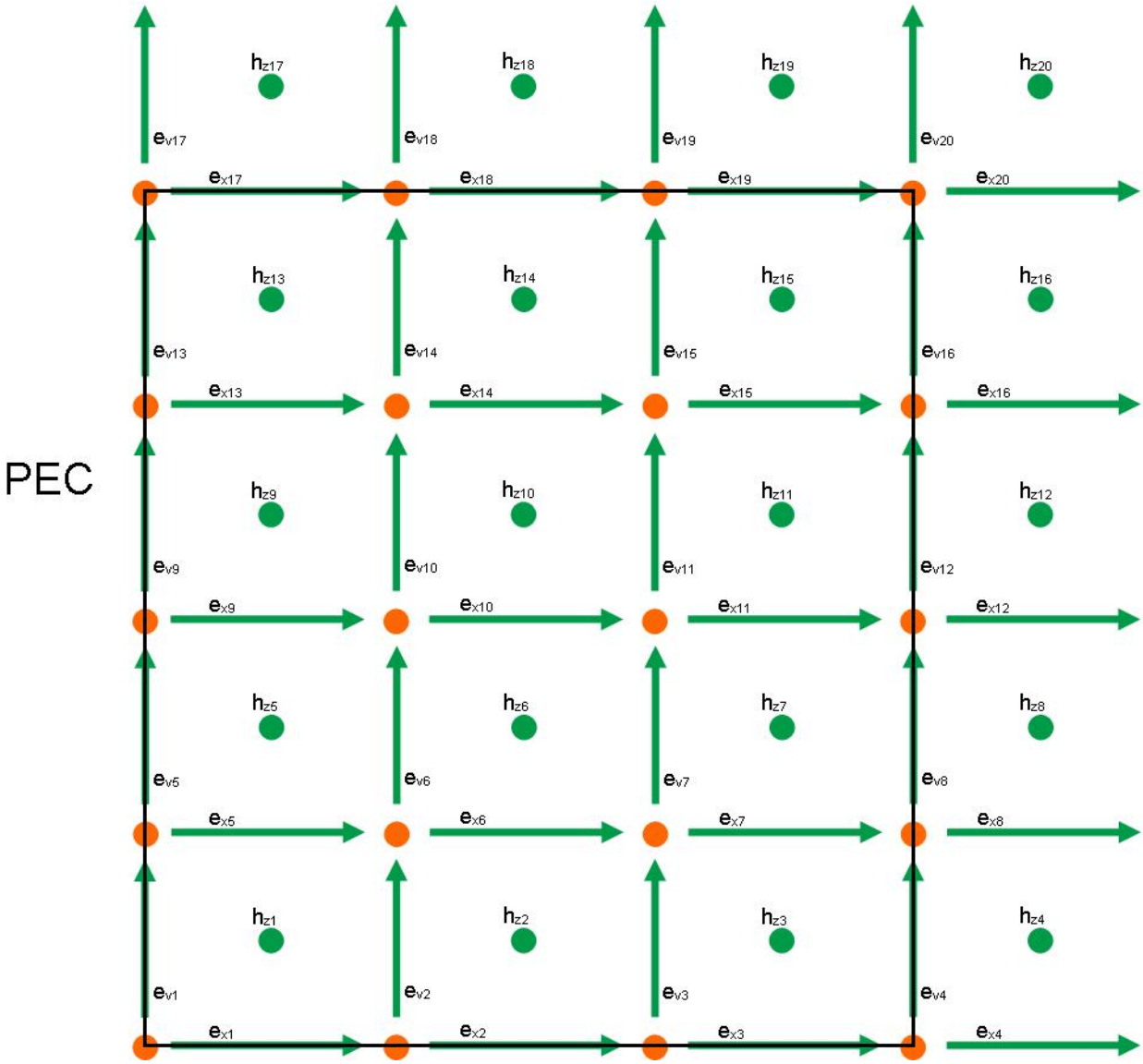


Figura 4.2: Conjunto de puntos en los que se impondrán las condiciones de contorno

En caso de la Figure 4.3, $T_t^e$ y $T_z^h$ pueden obtenerse usando unas matrices extra:

$$R_x^e = \begin{bmatrix} 1 & 0 & 0 & 0 & 1 \\ 1 & 0 & 0 & 0 & 1 \\ 1 & 0 & 0 & 0 & 1 \\ 1 & 1 & 1 & 1 & 1 \end{bmatrix} \tag{4.37}$$

donde mediante el comando *reshape* (remodelación) de $R_x^e = [\,1\;1\;1\;1\;0\;0\;0\;1\;0\;0\;0\;1\;1\;1\;1\,]$

$$R_y^e = \begin{bmatrix} 1 & 1 & 1 & 1 & 1 \\ 0 & 0 & 0 & 0 & 1 \\ 0 & 0 & 0 & 0 & 1 \\ 1 & 1 & 1 & 1 & 1 \end{bmatrix} \tag{4.38}$$

donde mediante el comando *reshape* (remodelación) de $R_y^e = [\,1\;0\;0\;1\;1\;0\;0\;1\;1\;0\;0\;1\;1\;1\;1\,]$

$$R_z^h = \begin{bmatrix} 0 & 0 & 0 & 0 & 1 \\ 0 & 0 & 0 & 0 & 1 \\ 0 & 0 & 0 & 0 & 1 \\ 1 & 1 & 1 & 1 & 1 \end{bmatrix} \tag{4.39}$$

donde mediante el comando *reshape* (remodelación) de $R_z^e = [\,0\;0\;0\;1\;0\;0\;0\;1\;0\;0\;0\;1\;1\;1\;1\;1\,]$

De esa forma, las ecuaciones anteriores y $\tilde{e}_t$ y $\tilde{h}_z$ representan las condiciones de contorno donde $T_t^e$ y $T_z^h$ son:

$$T_z^h = \begin{pmatrix} 1 & 0 & 0 & 0 & 0 & 0 & 0 & 0 & 0 & 0 & 0 & 0 \\ 0 & 1 & 0 & 0 & 0 & 0 & 0 & 0 & 0 & 0 & 0 & 0 \\ 0 & 0 & 1 & 0 & 0 & 0 & 0 & 0 & 0 & 0 & 0 & 0 \\ 0 & 0 & 0 & 0 & 0 & 0 & 0 & 0 & 0 & 0 & 0 & 0 \\ 0 & 0 & 0 & 1 & 0 & 0 & 0 & 0 & 0 & 0 & 0 & 0 \\ 0 & 0 & 0 & 0 & 1 & 0 & 0 & 0 & 0 & 0 & 0 & 0 \\ 0 & 0 & 0 & 0 & 0 & 1 & 0 & 0 & 0 & 0 & 0 & 0 \\ 0 & 0 & 0 & 0 & 0 & 0 & 0 & 0 & 0 & 0 & 0 & 0 \\ 0 & 0 & 0 & 0 & 0 & 0 & 1 & 0 & 0 & 0 & 0 & 0 \\ 0 & 0 & 0 & 0 & 0 & 0 & 0 & 1 & 0 & 0 & 0 & 0 \\ 0 & 0 & 0 & 0 & 0 & 0 & 0 & 0 & 1 & 0 & 0 & 0 \\ 0 & 0 & 0 & 0 & 0 & 0 & 0 & 0 & 0 & 0 & 0 & 0 \\ 0 & 0 & 0 & 0 & 0 & 0 & 0 & 0 & 0 & 1 & 0 & 0 \\ 0 & 0 & 0 & 0 & 0 & 0 & 0 & 0 & 0 & 0 & 1 & 0 \\ 0 & 0 & 0 & 0 & 0 & 0 & 0 & 0 & 0 & 0 & 0 & 1 \\ 0 & 0 & 0 & 0 & 0 & 0 & 0 & 0 & 0 & 0 & 0 & 0 \\ 0 & 0 & 0 & 0 & 0 & 0 & 0 & 0 & 0 & 0 & 0 & 0 \\ 0 & 0 & 0 & 0 & 0 & 0 & 0 & 0 & 0 & 0 & 0 & 0 \\ 0 & 0 & 0 & 0 & 0 & 0 & 0 & 0 & 0 & 0 & 0 & 0 \\ 0 & 0 & 0 & 0 & 0 & 0 & 0 & 0 & 0 & 0 & 0 & 0 \end{pmatrix} \tag{4.40}$$

$$T_t^e = \begin{pmatrix}
0&0&0&0&0&0&0&0&0&0&0&0&0&0&0&0&0\\
1&0&0&0&0&0&0&0&0&0&0&0&0&0&0&0&0\\
0&1&0&0&0&0&0&0&0&0&0&0&0&0&0&0&0\\
0&0&1&0&0&0&0&0&0&0&0&0&0&0&0&0&0\\
0&0&0&0&0&0&0&0&0&0&0&0&0&0&0&0&0\\
0&0&0&1&0&0&0&0&0&0&0&0&0&0&0&0&0\\
0&0&0&0&1&0&0&0&0&0&0&0&0&0&0&0&0\\
0&0&0&0&0&1&0&0&0&0&0&0&0&0&0&0&0\\
0&0&0&0&0&0&0&0&0&0&0&0&0&0&0&0&0\\
0&0&0&0&0&0&1&0&0&0&0&0&0&0&0&0&0\\
0&0&0&0&0&0&0&1&0&0&0&0&0&0&0&0&0\\
0&0&0&0&0&0&0&0&1&0&0&0&0&0&0&0&0\\
0&0&0&0&0&0&0&0&0&0&0&0&0&0&0&0&0\\
0&0&0&0&0&0&0&0&0&0&0&0&0&0&0&0&0\\
0&0&0&0&0&0&0&0&0&0&0&0&0&0&0&0&0\\
0&0&0&0&0&0&0&0&0&0&0&0&0&0&0&0&0\\
0&0&0&0&0&0&0&0&0&1&0&0&0&0&0&0&0\\
0&0&0&0&0&0&0&0&0&0&1&0&0&0&0&0&0\\
0&0&0&0&0&0&0&0&0&0&0&0&0&0&0&0&0\\
0&0&0&0&0&0&0&0&0&0&0&0&0&0&0&0&0\\
0&0&0&0&0&0&0&0&0&0&0&1&0&0&0&0&0\\
0&0&0&0&0&0&0&0&0&0&0&0&1&0&0&0&0\\
0&0&0&0&0&0&0&0&0&0&0&0&0&0&0&0&0\\
0&0&0&0&0&0&0&0&0&0&0&0&0&0&0&0&0\\
0&0&0&0&0&0&0&0&0&0&0&0&0&1&0&0&0\\
0&0&0&0&0&0&0&0&0&0&0&0&0&0&1&0&0\\
0&0&0&0&0&0&0&0&0&0&0&0&0&0&0&0&0\\
0&0&0&0&0&0&0&0&0&0&0&0&0&0&0&1&0\\
0&0&0&0&0&0&0&0&0&0&0&0&0&0&0&0&1\\
0&0&0&0&0&0&0&0&0&0&0&0&0&0&0&0&0\\
0&0&0&0&0&0&0&0&0&0&0&0&0&0&0&0&0\\
0&0&0&0&0&0&0&0&0&0&0&0&0&0&0&0&0\\
0&0&0&0&0&0&0&0&0&0&0&0&0&0&0&0&0
\end{pmatrix} \tag{4.41}$$

## 4.4. Permitividad dieléctrica

La introducción de un dieléctrico, en el caso de dos dimensiones, será mediante un polígono, ya que, se tendrá en cuenta que ahora $\epsilon_r$ tendrá dos direcciones $\epsilon_x$ y $\epsilon_y$ que deben ser desplazadas por $\frac{\triangle x}{2}$ y $\frac{\triangle y}{2}$. Por un lado, es necesario saber que $\epsilon_x$ y $\epsilon_y$ está en función de modos TE debido a que en esta polarización, se tiene en cuenta $E_x \neq 0$, $E_y \neq 0$ y $H_z \neq 0$. Por lo tanto, dependiendo de los campos eléctricos $E_x$ y $E_y$ tendrá una permitividad diferente.

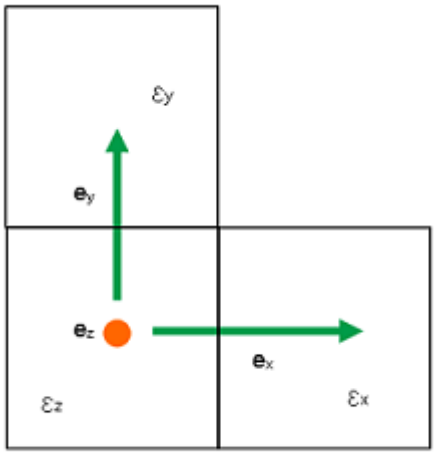


Figura 4.3: Dielectric permittivity in two dimensions

Por otro lado, en el caso de la polarización TM no se tendrá en cuenta la permitividad en dirección x e y, ya que, en este caso las condiciones son $H_x \neq 0$, $H_y \neq 0$ y $E_z \neq 0$, se tendrá en cuenta, entonces la permitividad en la dirección z $\epsilon_z$.

## 4.5. Polarización TM

En este caso, se asume que $H_z = 0$ ($H_x \neq 0$, $H_y \neq 0$ y $E_z \neq 0$). Partiendo de las ecuaciones (4.1) y (4.2) se obtendrá:

$$\begin{cases} \gamma H_y = j\omega\epsilon_0\epsilon_z E_z \\ -\gamma H_x = j\omega\epsilon_0\epsilon_z E_z \\ -\frac{\partial H_x}{\partial y} + \frac{\partial H_y}{\partial x} = j\omega\epsilon_0 P E_z \end{cases} \tag{4.42}$$

y

$$\begin{cases} \frac{\partial E_z}{\partial y} = (P_y^{-1}\frac{\gamma^2}{j\omega\epsilon_0} - j\omega\mu_0)H_x \\ -\frac{\partial E_z}{\partial x} = (P_x^{-1}\frac{\gamma^2}{j\omega\epsilon_0} - j\omega\mu_0)H_y \end{cases} \tag{4.43}$$

Por un lado, tendremos:

$$-\frac{\partial H_x}{\partial y} + \frac{\partial H_y}{\partial x} = j\omega\epsilon_0 P E_z \tag{4.44}$$

donde P es la matriz de permitividad dependiente de la dirección z $P_z = \epsilon_z$ y la ecuación anterior estará asociada con:

$$C_{zt}^{(h)} h_t = j\omega\epsilon_0 P_z e_t \tag{4.45}$$

donde $C_{zt}^{(h)}$ es dividida en dos matrices $C_{zx}^{(h)}$ y $C_{zy}^{(h)}$, por lo que la ecuación (4.47) puede ser definida como,

$$\begin{bmatrix} C_{zx}^{(h)} C_{zy}^{(h)} \end{bmatrix} \begin{bmatrix} h_x \\ h_y \end{bmatrix} = j\omega\epsilon_0 P e_z \tag{4.46}$$

Las matrices $C_{zx}^{(h)}$ y $C_{zy}^{(h)}$ serán:

$$[C_{zx}^{(h)}]_{mn} = \triangle y^{-1} \begin{cases} -1, m = n, \\ 1, m = n+1, \\ 0, rest \end{cases} \tag{4.47}$$

$$[C_{zy}^{(h)}]_{mn} = \triangle x^{-1} \begin{cases} -1, m = n, \\ 1, m = n+1, \\ 0, rest \end{cases} \tag{4.48}$$

donde gráficamente se pueden ver como,

$$C_{zx}^{(h)} = -\frac{1}{\triangle Y} \begin{bmatrix} -1 & 0 & 0 & 0 & 0 & 0 & \dots & 0 \\ 0 & -1 & 0 & 0 & 0 & 0 & \dots & 0 \\ 0 & 0 & -1 & 0 & 0 & 0 & \dots & 0 \\ 0 & 0 & 0 & -1 & 0 & 0 & \dots & 0 \\ 1 & 0 & 0 & 0 & -1 & 0 & \dots & 0 \\ 0 & 1 & 0 & 0 & 0 & -1 & \dots & 0 \\ \vdots & & & & & & & \\ 0 & 0 & 0 & 1 & 0 & 0 & 0 & -1 \end{bmatrix} \begin{bmatrix} H_{x1} \\ H_{x2} \\ H_{x3} \\ H_{x4} \\ H_{x5} \\ H_{x6} \\ \vdots \\ H_{xK} \end{bmatrix} \tag{4.49}$$

$$C_{zy}^{(h)} = \frac{1}{\triangle X} \begin{bmatrix} -1 & 0 & 0 & 0 & 0 & 0 & \dots & 0 \\ 1 & -1 & 0 & 0 & 0 & 0 & \dots & 0 \\ 0 & 1 & -1 & 0 & 0 & 0 & \dots & 0 \\ 0 & 0 & 1 & -1 & 0 & 0 & \dots & 0 \\ 0 & 0 & 0 & 1 & -1 & 0 & \dots & 0 \\ 0 & 0 & 0 & 0 & 1 & -1 & \dots & 0 \\ \vdots & & & & & & & \\ 0 & 0 & 0 & 0 & 0 & 0 & 1 & -1 \end{bmatrix} \begin{bmatrix} H_{y1} \\ H_{y2} \\ H_{y3} \\ H_{y4} \\ H_{y5} \\ H_{y6} \\ \vdots \\ H_{yK} \end{bmatrix} \tag{4.50}$$

Por otr lado, si nos centramos en la ecuación (4.1), será necesario obtener las ecuaciones para el campo eléctrico,

$$\begin{cases} \frac{\partial E_z}{\partial y} = (P_y^{-1} \frac{\gamma^2}{j\omega\epsilon_0} - j\omega\mu_0) H_x \\ -\frac{\partial E_z}{\partial x} = (P_x^{-1} \frac{\gamma^2}{j\omega\epsilon_0} - j\omega\mu_0) H_y \end{cases} \tag{4.51}$$

Si operamos las dos ecuaciones anteriores llegaremos a,

$$C_{tz}^{(e)} e_z = (P_t^{-1} \frac{\gamma^2}{j\omega\epsilon_0} - j\omega\mu_0) h_t \tag{4.52}$$

donde $C_{tz}^{(e)}$ será dividida en dos matrices $C_{xz}^{(e)}$ y $C_{yz}^{(e)}$ como:

$$\begin{bmatrix} C_{xz}^{(e)} \\ C_{yz}^{(e)} \end{bmatrix} [e_z] = (P_t^{-1} \frac{\gamma^2}{j\omega\epsilon_0} - j\omega\mu_0) \begin{bmatrix} h_x \\ h_y \end{bmatrix} \tag{4.53}$$

Si estas matrices son representadas gráficamente,

$$C_{xz}^{(e)} = \frac{1}{\triangle Y} \begin{bmatrix} -1 & 0 & 0 & 0 & 1 & 0 & \dots & 0 \\ 0 & -1 & 0 & 0 & 0 & 1 & \dots & 0 \\ 0 & 0 & -1 & 0 & 0 & 0 & \dots & 0 \\ 0 & 0 & 0 & -1 & 0 & 0 & \dots & 1 \\ 0 & 0 & 0 & 0 & -1 & 0 & \dots & 0 \\ 0 & 0 & 0 & 0 & 0 & -1 & \dots & 0 \\ \vdots & & & & & & & \\ 0 & 0 & 0 & 1 & 0 & 0 & 0 & -1 \end{bmatrix} \begin{bmatrix} E_{z1} \\ E_{z2} \\ E_{z3} \\ E_{z4} \\ E_{z5} \\ E_{z6} \\ \vdots \\ E_{zK} \end{bmatrix} \tag{4.54}$$

$$C_{yz}^{(e)} = \frac{1}{\triangle X} \begin{bmatrix} 1 & -1 & 0 & 0 & 0 & 0 & \dots & 0 \\ 0 & 1 & -1 & 0 & 0 & 0 & \dots & 0 \\ 0 & 0 & 1 & -1 & 0 & 0 & \dots & 0 \\ 0 & 0 & 0 & 1 & -1 & 0 & \dots & 0 \\ 0 & 0 & 0 & 0 & 1 & -1 & \dots & 0 \\ 0 & 0 & 0 & 0 & 0 & 1 & \dots & 0 \\ \vdots & & & & & & & \\ 0 & 0 & 0 & 0 & 0 & 0 & 0 & 1 \end{bmatrix} \begin{bmatrix} E_{z1} \\ E_{z2} \\ E_{z3} \\ E_{z4} \\ E_{z5} \\ E_{z6} \\ \vdots \\ E_{zK} \end{bmatrix} \tag{4.55}$$

Finalmente, obtendremos estas ecuaciones,

$$\begin{cases} C_{zt}^{(h)} h_t = j\omega\epsilon_0 P_z e_z \\ C_{tz}^{(e)} e_z = (P_t^{-1} \frac{\gamma^2}{j\omega\epsilon_0} - j\omega\mu_0) h_t \end{cases} \tag{4.56}$$

donde

$$C_{zt}^{(h)} = \left[ C_{zx}^{(h)} C_{zy}^{(h)} \right] \tag{4.57}$$

y

$$C_{tz}^{(e)} = \begin{bmatrix} C_{xz}^{(e)} \\ C_{yz}^{(e)} \end{bmatrix} \tag{4.58}$$

Igual que en una dimensión, se puede reorganizar estas ecuaciones y mediante el problema de valores propios obtener las características de propagación como:

$$[C_{zt}^{(h)} C_{tz}^{(e)} - \omega^2 \mu_0 \epsilon_0 P_z] = \gamma^2 e \tag{4.59}$$

o en caso de $\gamma = 0$, las frecuencias de corte

$$[\mu_0^{-1} \epsilon_0^{-1} P_z^{-1} C_{tz}^{(e)} C_{zt}^{(h)} - \omega^2] e = \gamma^2 e \tag{4.60}$$

En ambos casos, no están impuestas las condiciones de contorno, pero de deben imponer para completar la formulación del problema.

## 4.6. Condiciones de contorno para la polarización TM

Para imponer las condiones de contorno en el caso de dos dimensiones y para la polarización TM, utilizaremos unas matrices de transformación al igual que en el caso de la polarización TE. Tenemos en cuenta ahora $e_z = T_z^e \tilde{e}$ y $h_t = T_t^h \tilde{h}$, por lo que, la ecuación (4.53) será

$$\begin{cases} C_{tz}^{(e)} T_z^e \tilde{e} = -j\omega\mu_0 T_t^h \tilde{h} \\ C_{zt}^{(h)} T_t^h \tilde{h} \tilde{h} = j\omega\epsilon_0 P_z T_z^e \tilde{e} \end{cases} \tag{4.61}$$

Operando,

$$\begin{cases} {T_t^h}^T C_{tz}^{(e)} T_z^e \tilde{e} = -j\omega\mu_0 \tilde{h} \\ {T_z^e}^T C_{zt}^{(h)} T_t^h \tilde{h} = j\omega\epsilon_0 T_e^T P_z T_z^e \tilde{e} \end{cases} \tag{4.62}$$

Finalmente, se obtendrá esta nueva ecuación,

$$\begin{cases} \tilde{C}_{tz}^{(e)} \tilde{e} = -j\omega\mu_0 \tilde{h} \\ \tilde{C}_{zt}^{(h)} \tilde{h} = j\omega\epsilon_0 \tilde{P}_z \tilde{e} \end{cases} \tag{4.63}$$

donde $\tilde{C}_{tz}^{(e)} = {T_t^h}^T C^{(e)} T_z^e$, $\tilde{C}_{zt}^{(h)} = {T_z^e}^T C^{(h)} T_t^h$ y $\tilde{P}_z = {T_z^e}^T P_z T_z^e$. Las matrices de transformación utilizadas en esta polarización serán ahora $T_e$ y $T_h$, por lo que serán obtenida unas matrices extra diferentes de la polarización TE. Estas matrices extra están basadas en la Figure 4.5 donde las condiciones de contorno son impuestas en el campo.

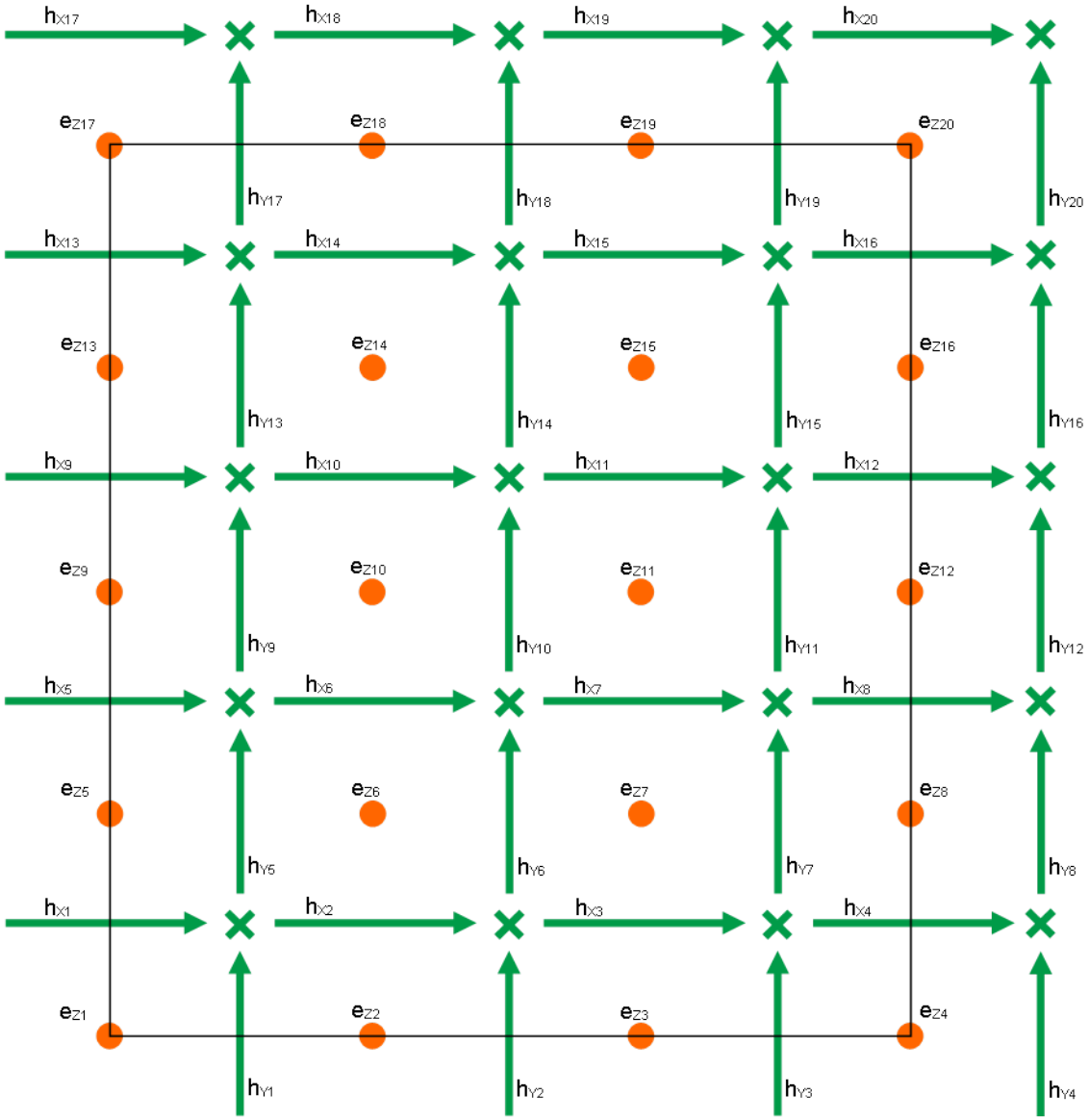


Figura 4.4: The set of points which will be taken into account to get the boundary conditions

$$R_x^h = \begin{bmatrix} 1 & 1 & 1 & 1 & 1 \\ 0 & 0 & 0 & 0 & 1 \\ 0 & 0 & 0 & 0 & 1 \\ 1 & 1 & 1 & 1 & 1 \end{bmatrix} \tag{4.64}$$

donde mediante el comando reshape (remodelación) de $R_x^h = [\,1\,0\,0\,1\,1\,0\,0\,1\,1\,0\,0\,1\,1\,1\,1\,]$

$$R_y^h = \begin{bmatrix} 1 & 0 & 0 & 0 & 1 \\ 1 & 0 & 0 & 0 & 1 \\ 1 & 0 & 0 & 0 & 1 \\ 1 & 1 & 1 & 1 & 1 \end{bmatrix} \tag{4.65}$$

donde mediante el comando reshape (remodelación) de $R_y^h = [\,1\,1\,1\,1\,0\,0\,0\,1\,0\,0\,0\,1\,1\,1\,1\,]$

$$R_z^h = \begin{bmatrix} 1 & 1 & 1 & 1 & 1 \\ 1 & 0 & 0 & 0 & 1 \\ 1 & 0 & 0 & 0 & 1 \\ 1 & 1 & 1 & 1 & 1 \end{bmatrix} \tag{4.66}$$

donde mediante el comando reshape (remodelación) de $R_z^h = [\,1\;1\;1\;1\;1\;0\;0\;1\;1\;0\;0\;1\;1\;1\;1\,]$

De esa manera, las ecuaciones anteriores $\tilde{e}_z$ y $\tilde{h}_t$ representan las condiones de contorno mediante $T_z^e$ y $T_t^h$,

$$T_t^h = \begin{pmatrix}
0&0&0&0&0&0&0&0&0&0&0&0&0&0&0&0&0\\
1&0&0&0&0&0&0&0&0&0&0&0&0&0&0&0&0\\
0&1&0&0&0&0&0&0&0&0&0&0&0&0&0&0&0\\
0&0&0&0&0&0&0&0&0&0&0&0&0&0&0&0&0\\
0&0&0&0&0&0&0&0&0&0&0&0&0&0&0&0&0\\
0&0&1&0&0&0&0&0&0&0&0&0&0&0&0&0&0\\
0&0&0&1&0&0&0&0&0&0&0&0&0&0&0&0&0\\
0&0&0&0&0&0&0&0&0&0&0&0&0&0&0&0&0\\
0&0&0&0&0&0&0&0&0&0&0&0&0&0&0&0&0\\
0&0&0&0&1&0&0&0&0&0&0&0&0&0&0&0&0\\
0&0&0&0&0&1&0&0&0&0&0&0&0&0&0&0&0\\
0&0&0&0&0&0&0&0&0&0&0&0&0&0&0&0&0\\
0&0&0&0&0&0&0&0&0&0&0&0&0&0&0&0&0\\
0&0&0&0&0&0&1&0&0&0&0&0&0&0&0&0&0\\
0&0&0&0&0&0&0&1&0&0&0&0&0&0&0&0&0\\
0&0&0&0&0&0&0&0&0&0&0&0&0&0&0&0&0\\
0&0&0&0&0&0&0&0&0&0&0&0&0&0&0&0&0\\
0&0&0&0&0&0&0&0&0&0&0&0&0&0&0&0&0\\
0&0&0&0&0&0&0&0&0&0&0&0&0&0&0&0&0\\
0&0&0&0&0&0&0&0&0&0&0&0&0&0&0&0&0\\
0&0&0&0&0&0&0&0&0&0&0&0&0&0&0&0&0\\
0&0&0&0&0&0&0&0&0&0&0&0&0&0&0&0&0\\
0&0&0&0&0&0&0&0&1&0&0&0&0&0&0&0&0\\
0&0&0&0&0&0&0&0&0&1&0&0&0&0&0&0&0\\
0&0&0&0&0&0&0&0&0&0&1&0&0&0&0&0&0\\
0&0&0&0&0&0&0&0&0&0&0&0&0&0&0&0&0\\
0&0&0&0&0&0&0&0&0&0&0&1&0&0&0&0&0\\
0&0&0&0&0&0&0&0&0&0&0&0&1&0&0&0&0\\
0&0&0&0&0&0&0&0&0&0&0&0&0&1&0&0&0\\
0&0&0&0&0&0&0&0&0&0&0&0&0&0&0&0&0\\
0&0&0&0&0&0&0&0&0&0&0&0&0&0&1&0&0\\
0&0&0&0&0&0&0&0&0&0&0&0&0&0&0&1&0\\
0&0&0&0&0&0&0&0&0&0&0&0&0&0&0&0&1
\end{pmatrix} \tag{4.67}$$

$$T_z^e = \begin{pmatrix} 0 & 0 & 0 & 0 & 0 & 0 \\ 0 & 0 & 0 & 0 & 0 & 0 \\ 0 & 0 & 0 & 0 & 0 & 0 \\ 0 & 0 & 0 & 0 & 0 & 0 \\ 0 & 0 & 0 & 0 & 0 & 0 \\ 1 & 0 & 0 & 0 & 0 & 0 \\ 0 & 1 & 0 & 0 & 0 & 0 \\ 0 & 0 & 0 & 0 & 0 & 0 \\ 0 & 0 & 0 & 0 & 0 & 0 \\ 0 & 0 & 1 & 0 & 0 & 0 \\ 0 & 0 & 0 & 1 & 0 & 0 \\ 0 & 0 & 0 & 0 & 0 & 0 \\ 0 & 0 & 0 & 0 & 0 & 0 \\ 0 & 0 & 0 & 0 & 1 & 0 \\ 0 & 0 & 0 & 0 & 0 & 1 \\ 0 & 0 & 0 & 0 & 0 & 0 \\ 0 & 0 & 0 & 0 & 0 & 0 \\ 0 & 0 & 0 & 0 & 0 & 0 \\ 0 & 0 & 0 & 0 & 0 & 0 \\ 0 & 0 & 0 & 0 & 0 & 0 \end{pmatrix} \tag{4.68}$$

## 4.7. Resultados numéricos

A la hora de realizar las pruebas numéricas se ha introducido un dieléctrico de permitivida $\epsilon_{r1} = 9$. Se decidión utilizar dimensiones de la guía de anchura a = 22.86mm y altura b=10.16mm.

### 4.7.1. Polarización TE

#### Obtención de las frecuencias de corte en dos dimensiones

Las condiciones y valores utilizados para obtener los resultados son $\epsilon_0 = 8{,}854187818 \cdot 10^{-12}$ y $c \simeq 3 \cdot 10^8$ m/s.

#### Guía de onda vacía

En la siguiente tabla se muestran los primeros cinco modos para diferente malla.

| | | | TE10 | TE20 | TE01 | TE11 | TE21 |
|---|---|---|---|---|---|---|---|
| | M | N | fc1(GHz) | fc2(GHz) | fc3(GHz) | fc4(GHz) | fc5(GHz) |
| Numerical | 23 | 10 | 6,556 | 13,079 | 14,689 | 16,086 | 19,668 |
| Error( %) | | | 0,09 | 0,33 | 0,50 | 0,43 | 0,43 |
| Numerical | 46 | 20 | 6,5603 | 13,113 | 14,747 | 16,140 | 19,734 |
| Error( %) | | | 0,02 | 0,07 | 0,11 | 0,09 | 0,09 |
| Numerical | 92 | 40 | 6,5614 | 13,121 | 14,760 | 16,152 | 19,749 |
| Error( %) | | | 0,009 | 0,01 | 0,02 | 0,02 | 0,02 |
| Numerical | 184 | 80 | 6,561 | 13,123 | 14,763 | 16,155 | 19,752 |
| Error( %) | | | 0,006 | 0 | 0,006 | 0,006 | 0,005 |
| Analytical | | | 6,562 | 13,123 | 14,764 | 16,156 | 19,753 |

Cuadro 4.1: Frequency data table for $TE_mn$ modes in two dimensions

En la Tabla 4.1, se muestran los valores obtenidos, los cuales han sido comparados con los valores analíticos que son expuestos en el apendice B.

Gráficamente, han sido expuestos los campos obtenidos. Esta representación se ha hecho para una malla de M=100 y N=50. Como ejemplos, se muestran los campos obtenidos de los modos $TE_{10}$, $TE_{20}$, $TE_{01}$. Es bueno recordar que los campos $TE_{m0}$ y $TE_{0n}$ siempre tendrán una componente nula debido a los campos eléctricos y magnéticos. En caso de $TE_{m0}$ la componente nula será $E_x$ y en el caso de $TE_{0n}$ la componente nuña será $E_y$. Esto se puede verificar mediante el apéndice B.

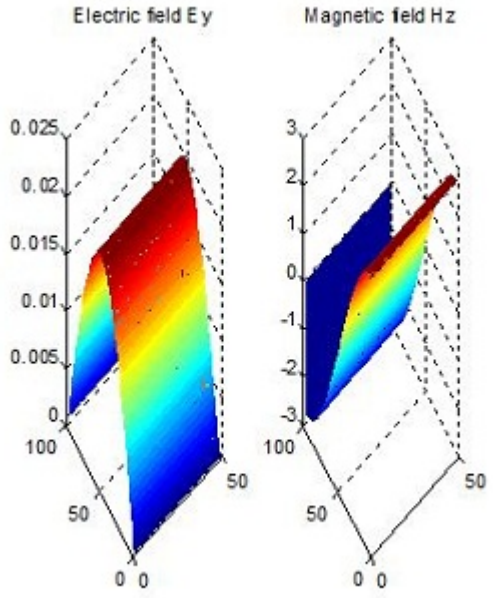


Figura 4.5: Representation TE10 mode in two dimensions

En caso del modo $TE_{10}$ se puede verificar que en una y dos dimensiones la frecuencia de corte es la misma. esto es debido a que estamos en una guía de onda que no está formada por ningún material. La frecuencia de corte obtenida en este caso es de $f_{c10} = 6,5614$ GHz.

### Guía de onda rectangular formada con un material dieléctrico

En este caso, el material tendrá un permitividad dieléctrica de $\epsilon_{r1} = 9$ en una parte de la guía y en la otra parte no tendrá nada, $\epsilon_{r2} = 1$. Por lo que, las frecuencias de corte obtenidas para este caso son recogidas en la Tabla 4.4. De la misma, manera se va incrementando la malla para observar los resultados. Podemos verificar en la Tabla 4.3 y 4.4, que a medida que la malla es mayor los resultados son cda vez más precisos.

| | | TE10 | TE20 | TE11 | TE21 |
|---|---|---|---|---|---|
| M | N | fc1(GHz) | fc2(GHz) | fc3(GHz) | fc4(GHz) |
| 23 | 10 | 3,0123 | 7,297 | 8,6718 | 9,9538 |
| 46 | 20 | 3,0097 | 7,3210 | 8,7240 | 10,104 |
| 92 | 40 | 3,0074 | 7,321 | 8,7369 | 10,137 |
| 184 | 80 | 2,9819 | 7,2516 | 8,6806 | 10,138 |

Cuadro 4.2: Frequency data table for $TE_m n$ modes in two dimensions

Como ejemplos, las siguientes figuras muestran los distintos modos que se han propagado, en los cuales podemos ver el dieléctrico. En primer lugar, se muestra el modo $TE_{10}$ con una $f_{c_{10}} = 2,9838GHz$

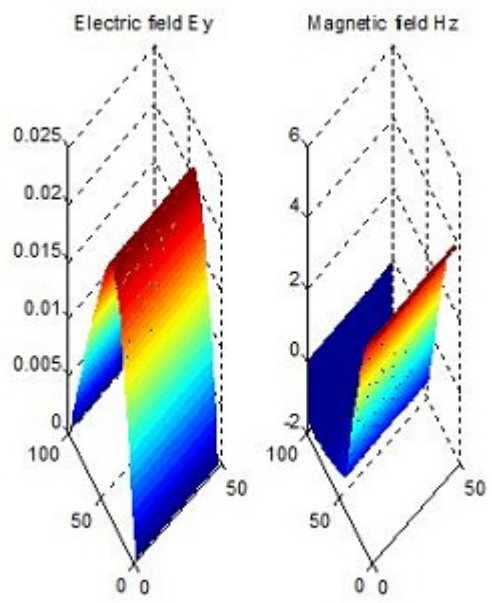


Figura 4.6: Representation TE10 mode in two dimensions with permittivity

En segundo lugar, mostramos el modo $TE_{20}$

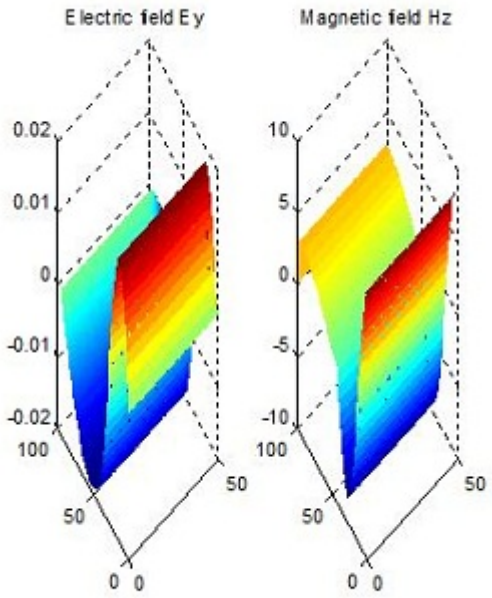


Figura 4.7: Representation TE20 mode in two dimensions with permittivity

### Características de propagación para los modos TE en dos dimensiones

Como se explicó en el problema unidimensional, un tema importante para cada modo, es la frecuencia a partir de la cual un modo comenzará a propagarse por la guía. El factor de propagación, en el caso general, es un número complejo, que puede ser escrita como:

$$\gamma_{mn} = \alpha_{mn} + j\beta_{mn} \tag{4.69}$$

donde $\alpha_{mn}$ es el coeficiente de amoriguamiento y $\beta mn$ factor de fase. El índice m y n hacen referencia al número de onda de los diferentes modos que se propagan.

Mediante la ecuación (4.34) y el problema de valores propios, podrá ser obtenida las características de propagación para este caso. Previamente, se comentó que las frecuencias de corte para los modos $TE_{mn}$ y $TM_{mn}$ donde $m = 1, 2 \ldots$ y $n = 1, 2, \ldots$, debería ser las mismas, por lo que, en el caso de las características de propagación serán las mismas cuando la guía de onda no está formada por un material dieléctrico.

| | n m | 0 | 1 | 2 | 3 |
|---|---|---|---|---|---|
| Numerical | 0 | - | 395,9j | 316,39j | 75,01j |
| Error ( %) | | | 0,05 | 0,08 | 0,13 |
| Numerical | 1 | 282,91j | 247,30j | 66,23j | 299,68 |
| Error ( %) | | 0,09 | 0,13 | 0,29 | 0,08 |
| | n m | 0 | 1 | 2 | 3 |
| Analytical | 0 | - | 395,70j | 316,13j | 74,907j |
| Analytical | 1 | 282,63j | 246,97j | 66,033j | 299,94 |

Cuadro 4.3: Numerical propagation coefficients compared with analytical coefficients for TE in two dimensions

En la tabla 4.3 se muestran los coeficientes de propagación numéricos, obtenidos mediante

Matlab y comparados con los valores analíticos que han sido expuestos en el apéndice B.

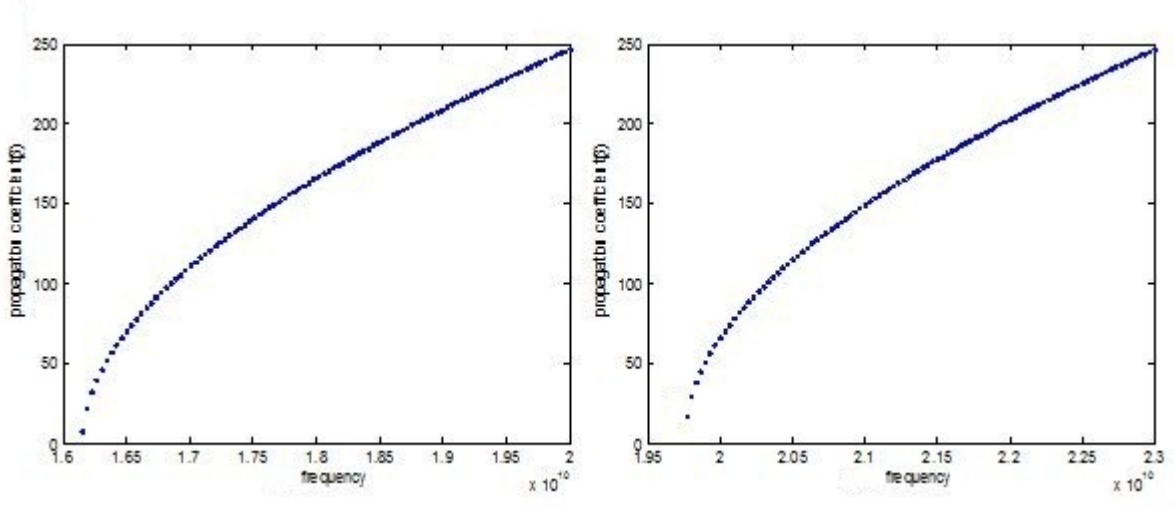


Figura 4.8: Representation of dispersion characteristics of $TE_{11}$ and $TE_{21}$ modes in two dimensions

La característica de dispersión de los modos $TE_{11}$ y $TE_{21}$ es mostrada en la figura anterior. En todas las gráficas se muestra la parte imaginaria de $\gamma$.

### 4.7.2. Polarización TM

#### Obtención de las frecuencias para los modos TM en dos dimensiones

Las condiciones y valores utilizados para obtener los resultados son $\epsilon_0 = 8{,}854187818 \cdot 10^{-12}$ y $c \simeq 3 \cdot 10^8$ m/s.

| | | | TM11 | TM21 | TM31 | TM41 | TM22 |
|---|---|---|---|---|---|---|---|
| | M | N | fc1(GHz) | fc2(GHz) | fc3(GHz) | fc4(GHz) | fc5(GHz) |
| Numerical | 23 | 10 | 16,086 | 19,668 | 24,441 | 29,768 | 31,750 |
| Error( %) | | | 0,43 | 0,43 | 0,67 | 1,15 | 1,74 |
| Numerical | 46 | 20 | 16,140 | 19,734 | 24,567 | 30,032 | 32,185 |
| Error( %) | | | 0,09 | 0,09 | 0,15 | 0,27 | 0,39 |
| Numerical | 92 | 40 | 16,152 | 19,749 | 24,597 | 30,094 | 32,282 |
| Error( %) | | | 0,02 | 0,02 | 0,03 | 0,06 | 0,09 |
| Numerical | 184 | 80 | 16,155 | 19,752 | 24,604 | 30,109 | 32,305 |
| Error( %) | | | 0,006 | 0,005 | 0,008 | 0,01 | 0,02 |
| Analytical | | | 16,156 | 19,753 | 24,606 | 30,114 | 30,248 |

Cuadro 4.4: Frequency data table for $TM_mn$ modes in two dimensions

Como ejemplos, se muestra la distribución de los campos $TM_{11}$ y $TM_{21}$ y sus respectivas frecuencias de corte:

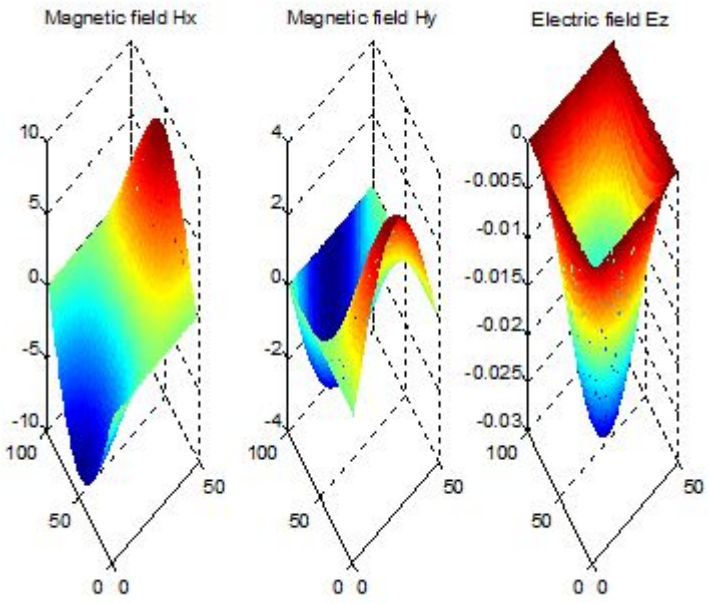


Figura 4.9: Representation TM11 mode in two dimensions

Modo TM11 con una frecuencia de corte de $fc_{11} = 16,154$ GHz.

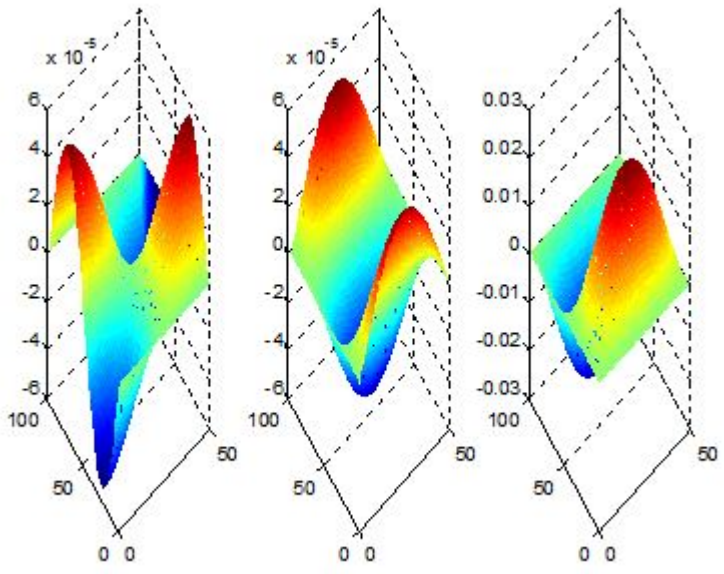


Figura 4.10: Representation TM21 mode in two dimensions

Modo $TM_{21}$ con $fc_{21} = 19,750$ GHz.

### Guía de onda rectangular formada con un material dieléctrico

La siguiente tabla muestra las frecuencias de corte para los modos TM después de haberle introducido el dieléctrico anterior.

| | | TM11 | TM21 | TM12 | TM22 |
|---|---|---|---|---|---|
| M | N | fc1(GHz) | fc2(GHz) | fc3(GHz) | fc4(GHz) |
| 23 | 10 | 6,2481 | 9,5203 | 10,558 | 12,971 |
| 46 | 20 | 6,2678 | 9,5850 | 10,710 | 13,160 |
| 92 | 40 | 6,2705 | 9,5946 | 10,742 | 13,199 |
| 184 | 80 | 6,2459 | 9,5155 | 10,731 | 13,140 |

Cuadro 4.5: Frequency data table for $TE_mn$ modes in two dimensions

En las siguientes figuras se muestran, como ejemplos, las distribuciones de los campos de los modos$TM_{11}$ y $TM_{21}$ con una malla de M=100 y N=50:

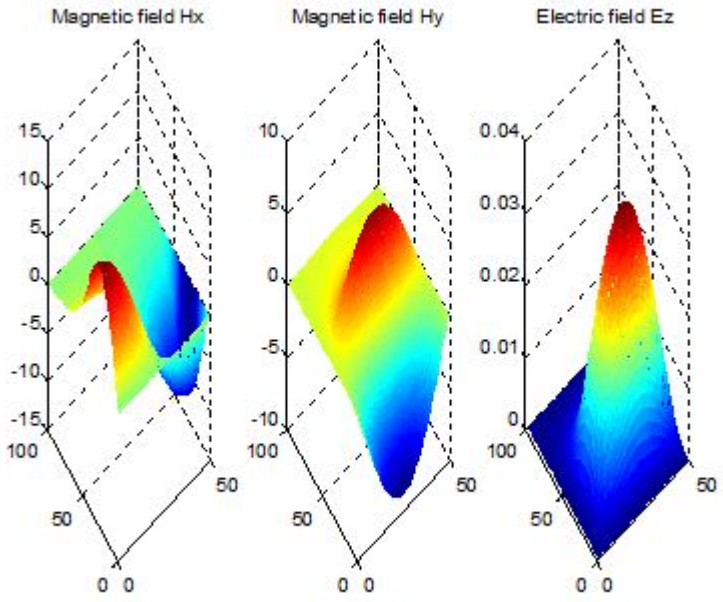


Figura 4.11: Representation TM11 mode in two dimensions with dielectric

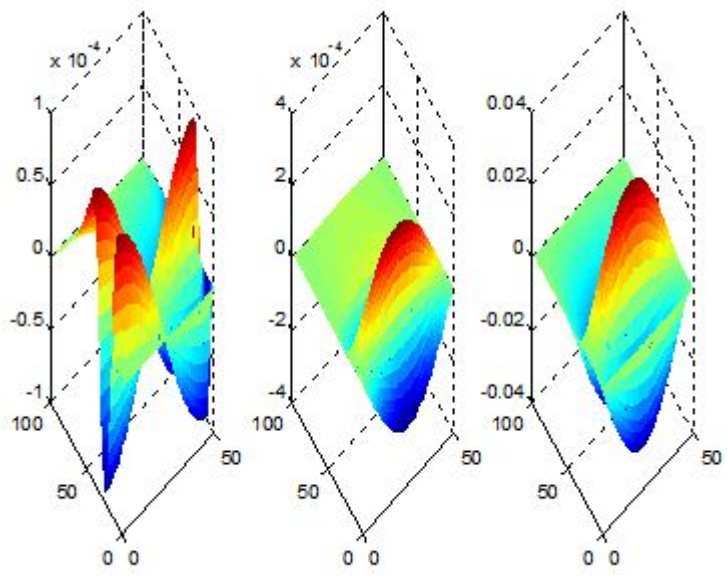


Figura 4.12: Representation TM21 mode in two dimensions with dielectric

### Características de propagación para los modos TM en dos dimensiones

Como se comentó anteriormente, en esta tabla mostramos los resultados numéricos comparados con los analíticos en el caso de una guía de onda que no está formada por ningún material.

| | n m | 0 | 1 | 2 | 3 |
|---|---|---|---|---|---|
| Numerical Error ( %) | 0 | - | - | - | - |
| Numerical Error ( %) | 1 | - | 247,30j 0,13 | 66,23j 0,29 | 299,68 0,08 |
| Numerical Error ( %) | 2 | - | 474,54 0,03 | 530,87 0,02 | 613,31 0,02 |
| | n m | 0 | 1 | 2 | 3 |
| Analytical | 0 | - | - | - | - |
| Analytical | 1 | - | 246,97j | 66,03j | 299,94 |
| Analytical | 2 | - | 474,09 | 531,02 | 613,44 |

Cuadro 4.6: Numerical propagation coefficients compared with analytical coefficients for TM in two dimensions

Después de numerosas pruebas incrementando la malla, nos dimos cuenta que a medida que ibamos aumentándola, los resultados eran más precisos. En las siguientes gráficas, mostramos la dispersión característica de los modos $TM_{11}$ y $TM_{21}$

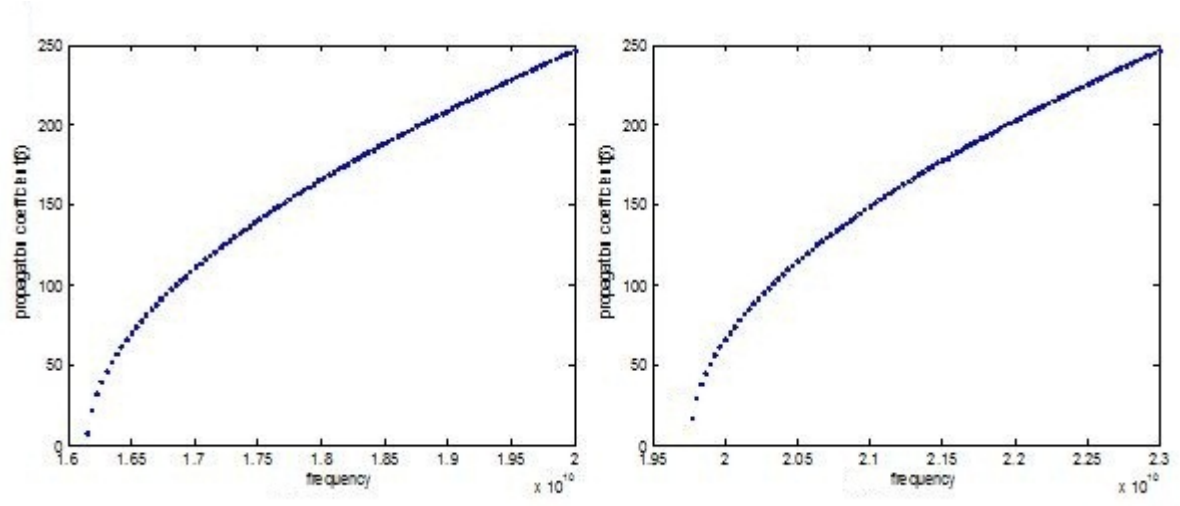


Figura 4.13: Representation of dispersion characteristics of $TM_{11}$ and $TM_{21}$ modes in two dimensions

Ahora, vamos a mostrar los coeficientes de propagación de los modos TM que se han obtenido con algunas condiciones como el tamaño de malla M = 100 y N = 50, $\epsilon_0 = 8{,}85 \cdot 10^{-12}$ F/m, $\mu_0 = 4\pi \cdot 10^{-7} N/A^2$ y una permitividad de $\epsilon_{r1} = 9$ y $\epsilon_{r2} = 1$.

Como ejemplo, motramos las características de dispersión de los modos $TM_{11}$ y $TM_{21}$.

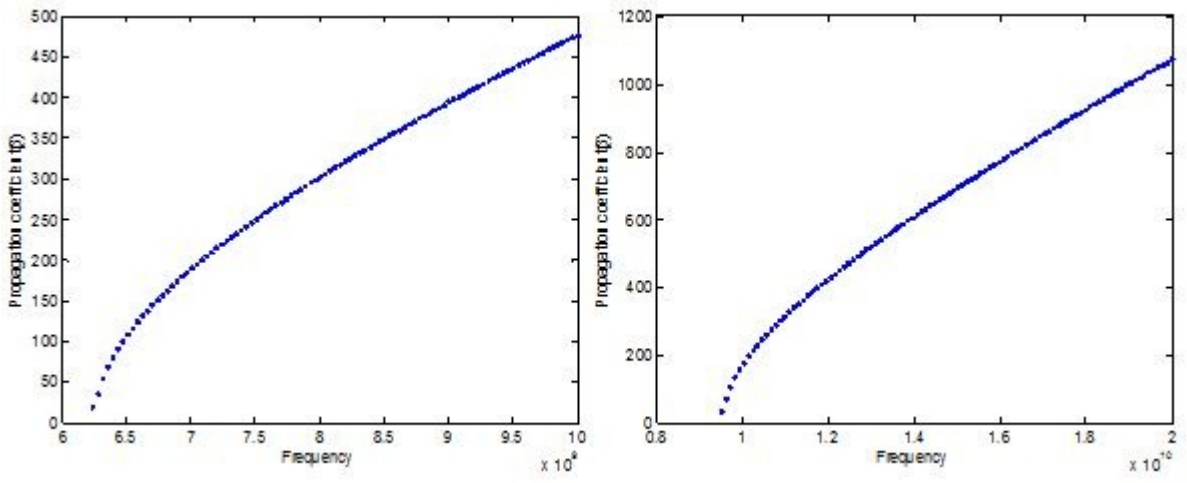


Figura 4.14: Representation of dispersion characteristics of first two modes with permittivity $\epsilon_r = 9$.

# Capítulo 5

# Modos híbridos (todas las componentes)

## 5.1. Introducción

Los métodos de análisis para la determinación de los campos electromagnéticos en guías de onda dieléctricas cargadas y cavidades resonantes han recibido considerable atención. Entre los métodos que se están desarrollando son técnicas basadas en las expansiones de campo en términos de modos propios de la estructura de guía. Los resultados de estos enfoques proporcionan información cuantitativa de diseño que puede ayudar en el desarrollo de nuevos componentes de microondas.

En algunos casos, sin embargo, será imposible satisfacer todas las condiciones de contorno necesarios con sólo modos TE o TM, por lo que, una combinación híbrida de ambos tipos puede ser requerida.

En este capítulo, se estudió los modos híbridos, que son una combinación de los modos TE y TM. Este tipo de modos se puede encontrar en todas las guías de ondas como guía de onda rectangular, cavidades resonantes, fibra óptica, etc. En primer lugar, se explicará cómo hizo ese problema de valores propios y, después, se presentarán algunas estructuras para verificar que este método es válido.

## 5.2. Modos híbridos TE y TM

Partiremos de las mismas ecuaciones que en el capítulo 4, es decir, (4.1), (4.2), (4.3) y (4.4). Por lo que, usando la aproximación (3.6) las ecuaciones anteriores pueden ser trasnformadas a forma de matriz dependiendo del siguiente conjunto de relaciones:

$$\gamma \mathbf{C}_{tt}^{(e)} \mathbf{e}_t + \mathbf{C}_{tz}^{(e)} \mathbf{e}_z = -j\omega\mu_0 \mathbf{h}_t \tag{5.1}$$

$$\mathbf{C}_{zt}^{(e)} \mathbf{e}_t = -j\omega\mu_0 \mathbf{h}_z \tag{5.2}$$

$$\gamma \mathbf{C}_{tt}^{(h)} \mathbf{h}_t + \mathbf{C}_{tz}^{(h)} \mathbf{h}_z = j\omega\epsilon_0 \mathbf{P}_t \mathbf{e}_t \tag{5.3}$$

$$\mathbf{C}_{zt}^{h} \mathbf{h}_t = j\omega\epsilon_0 \mathbf{P}_z \mathbf{e}_z \tag{5.4}$$

donde $\mathbf{e}_t = [e_x e_y]^T$, $\mathbf{h}_t = [h_x h_y]^T$ y

$$\mathbf{C}_{tt}^{(e)} = \mathbf{C}_{tt}^{(h)} = \begin{bmatrix} 0_{KxK} & I_{KxK} \\ -I_{KxK} & 0_{KxK} \end{bmatrix} \tag{5.5}$$

$$\mathbf{C}_{tz}^{(e)} = \mathbf{C}_{zt}^{(h)^T} = \begin{bmatrix} \mathbf{C}_{zx}^{(e)} \\ -\mathbf{C}_{zy}^{(e)} \end{bmatrix} \tag{5.6}$$

$$\mathbf{C}_{zt}^{(e)} = \mathbf{C}_{tz}^{(h)^T} = \begin{bmatrix} -\mathbf{C}_{zx}^{(e)} \mathbf{C}_{zy}^{(e)} \end{bmatrix} \tag{5.7}$$

donde, $\mathbf{C}_{zy}^{(e)}$ y $\mathbf{C}_{zx}^{(e)}$ fueron obtenidas en el capítulo 4.

Asimismo en los capítulos anteriores, se ha obtenido las frecuencias de corte y las características de propagación en una y dos dimensiones en los modos TE y TM. Por lo tanto, la eliminación de la ecuación (5.7) la componente tangencial (5.5) y el componente longitudinal del campo magnético (5.6) y un componente del campo eléctrico (5.8), nos permitirá obtener, de nuevo, las características de propagación:

$$\mathbf{F}^{(h)} \mathbf{h}_t = -\gamma \mathbf{e}_t \tag{5.8}$$

$$\mathbf{F}^{(e)} \mathbf{e}_t = -\gamma \mathbf{h}_t \tag{5.9}$$

donde

$$\mathbf{F}^{(h)} = \mathbf{C}_{tt}^{(e^{-1})} \mathbf{T}_t^{e^{-1}} (j\omega\mu_0 \mathbf{I} + \frac{1}{j\omega\epsilon_0} \mathbf{T}_t^e \mathbf{C}_{tz}^{(e)} \mathbf{P}_z^{-1} \mathbf{T}_z^h \mathbf{C}_{zt}^h) \tag{5.10}$$

y

$$\mathbf{F}^{(e)} = \mathbf{C}_{tt}^{(h^{-1})} \mathbf{T}_t^{h^{-1}} (j\omega\epsilon_0 \mathbf{P}_t + \frac{1}{j\omega\mu_0} \mathbf{T}_t^h \mathbf{C}_{tz}^{(h)} \mathbf{T}_z^e \mathbf{C}_{zt}^e) \tag{5.11}$$

Hay que tener en cuenta que, $\mathbf{T}_t^e$ y $\mathbf{T}_t^h$ son matrices diagonales, por lo que puede ser realizada la inversión de esas matrices. Las matrices $\mathbf{C}_{tt}^{(h)}$ y $\mathbf{C}_{tt}^{(e)}$, sin embargo, son ortogonales, y sus inversas deben ser cambiadas por sus traspuestas. El uso de una ecuación (5.8) o (5.9), puede ser utilizada para obtener los coeficientes de propagación. La primera es sólo para campos eléctricos y lal segundo para los campos magnéticos. De la misma manera, por el problema de valores propios se obtendrá $\gamma$.

## 5.3. Condiciones de contorno

Igualmente, se deberá completar la formulación del problema imponiendo las condiciones de contorno de la siguiente manera:

$$\gamma \mathbf{C}_{tt}^{(e)} \mathbf{e}_t + \mathbf{C}_{tz}^{(e)} \mathbf{e}_z = -j\omega\mu_0 \mathbf{h}_t \tag{5.12}$$

$$\gamma \mathbf{C}_{tt}^{(e)} \mathbf{T}_t^e \mathbf{E}_t + \mathbf{C}_{tz}^{(e)} \mathbf{T}_z^e \mathbf{E}_z = -j\omega\mu_0 \mathbf{T}_t^h \mathbf{H}_t \tag{5.13}$$

y el uso de $\mathbf{e}_t = \mathbf{T}_t^e \mathbf{E}_t$, $\mathbf{e}_z = \mathbf{T}_z^e \mathbf{E}_z$ y $\mathbf{h}_t = \mathbf{T}_t^h \mathbf{H}_t$ que son las condiciones de contorno, obtenemos:

$$\gamma \mathbf{T}_t^{h^T} \mathbf{C}_{tt}^{(e)} \mathbf{T}_t^e \mathbf{E}_t + \mathbf{T}_t^{h^T} \mathbf{C}_{tz}^{(e)} \mathbf{T}_z^e \mathbf{E}_z = -j\omega\mu_0 \mathbf{H}_t \tag{5.14}$$

Finalmente, tendremos unas ecuaciones más simples:

$$\gamma\tilde{\mathbf{C}}_{tt}^{(e)}\mathbf{E}_t + \tilde{\mathbf{C}_{tz}}^{(e)}\mathbf{e}_z = -j\omega\mu_0\mathbf{H}_t \tag{5.15}$$

where $\tilde{\mathbf{C}}_{tt}^{(e)} = \mathbf{T}_t^{h^T}\mathbf{C}_{tt}^{(e)}\mathbf{T}_t^e$ and $\tilde{\mathbf{C}_{tz}}^{(e)} = \mathbf{T}_t^{h^T}\mathbf{C}_{tz}^{(e)}\mathbf{T}_z^e$.

En el caso de la ecuación (5.2), tenemos que,

$$\mathbf{C}_{zt}^{(e)}\mathbf{T}_t^e\mathbf{E}_t = -j\omega\mu_0\mathbf{T}_z^h\mathbf{H}_z \tag{5.16}$$

Operando,

$$\mathbf{T}_z^{h^T}\mathbf{C}_{zt}^{(e)}\mathbf{T}_t^e\mathbf{E}_t = -j\omega\mu_0\mathbf{H}_z \tag{5.17}$$

Finalmente, la ecuación (5.2) será:

$$\tilde{\mathbf{C}}_{zt}^{(e)}\mathbf{E}_t = -j\omega\mu_0\mathbf{H}_z \tag{5.18}$$

where $\tilde{\mathbf{C}}_{zt}^{(e)} = \mathbf{T}_z^{h^T}\mathbf{C}_{zt}^{(e)}\mathbf{T}_t^e$

In case of equation (5.3),

$$\gamma\mathbf{C}_{tt}^{(h)}\mathbf{T}_t^h\mathbf{H}_t + \mathbf{C}_{tz}^{(h)}\mathbf{T}_z^h\mathbf{H}_z = j\omega\epsilon_0\mathbf{P}_t\mathbf{T}_t^e\mathbf{E}_t \tag{5.19}$$

Operando,

$$\gamma\mathbf{T}_t^{e^T}\mathbf{C}_{tt}^{(h)}\mathbf{T}_t^h\mathbf{H}_t + \mathbf{T}_t^{e^T}\mathbf{C}_{tz}^{(h)}\mathbf{T}_z^h\mathbf{H}_z = j\omega\epsilon_0\mathbf{T}_t^{e^T}\mathbf{P}_t\mathbf{T}_t^e\mathbf{E}_t \tag{5.20}$$

La ecuación (5.3) se transformarrá como,

$$\gamma\tilde{\mathbf{C}}_{tt}^{(h)}\mathbf{H}_t + \tilde{\mathbf{C}}_{tz}^{(h)}\mathbf{H}_z = j\omega\epsilon_0\tilde{\mathbf{P}}_t\mathbf{E}_t \tag{5.21}$$

where $\tilde{\mathbf{C}}_{tt}^{(h)} = \mathbf{T}_t^{e^T}\mathbf{C}_{tt}^{(h)}\mathbf{T}_t^h$, $\tilde{\mathbf{C}}_{tz}^{(h)} = \mathbf{T}_t^{e^T}\mathbf{C}_{tz}^{(h)}\mathbf{T}_z^h$ and $\tilde{P}_t = \mathbf{T}_t^{e^T}\mathbf{P}_t\mathbf{T}_t^e$.

La última ecuación, por tanto será:

$$\mathbf{C}_{zt}^{(h)}\mathbf{T}_t^{(h)}\mathbf{H}_t = j\omega\epsilon_0\mathbf{P}_z\mathbf{T}_z^{(e)}\mathbf{E}_z \tag{5.22}$$

Operando,

$$\mathbf{T}_z^{(e)^T}\mathbf{C}_{zt}^{(h)}\mathbf{T}_t^{(h)}\mathbf{H}_t = j\omega\epsilon_0\mathbf{T}_z^{(e)^T}\mathbf{P}_z\mathbf{T}_z^{(e)}\mathbf{E}_z \tag{5.23}$$

$$\tilde{\mathbf{C}}_{zt}^{(h)}\mathbf{H}_t = j\omega\epsilon_0\tilde{\mathbf{P}}_z\mathbf{E}_z \tag{5.24}$$

where $\tilde{\mathbf{C}}_{zt}^{(h)} = \mathbf{T}_z^{(e)^T}\mathbf{C}_{zt}^{(h)}\mathbf{T}_t^{(h)}$ and $\tilde{\mathbf{P}}_z = \mathbf{T}_z^{e^T}\mathbf{P}_z\mathbf{T}_z^e$.

Agrupando las ecuaciones anteriores, tendremos las nuevas ecuaciones basandas en las condiciones de contorno:

$$\begin{cases} \gamma\tilde{\mathbf{C}}_{tt}^{(e)}\mathbf{E}_t + \tilde{\mathbf{C}_{tz}}^{(e)}\mathbf{E}_z = -j\omega\mu_0\mathbf{H}_t \\ \tilde{\mathbf{C}}_{zt}^{(e)}\mathbf{E}_t = -j\omega\mu_0\mathbf{H}_z \\ \gamma\tilde{\mathbf{C}}_{tt}^{(h)}\mathbf{H}_t + \tilde{\mathbf{C}}_{tz}^{(h)}\mathbf{H}_z = j\omega\epsilon_0\tilde{\mathbf{P}}_t\mathbf{E}_t \\ \tilde{\mathbf{C}}_{zt}^{(h)}\mathbf{H}_t = j\omega\epsilon_0\tilde{\mathbf{P}}_z\mathbf{E}_z \end{cases} \tag{5.25}$$

## 5.4. Resultados numéricos

En esta sección, se han analizad dos estructuras distintas con el objetivo de verificar que este método es válido para numerosas estructuras electromagnéticas.

La primera estructura será cambiando la dimensión y la posición del dieléctrico y la segunda estructura será una fibra óptica.

### 5.4.1. Guía de onda rectangular formada por un material con dieléctrico

La primera estructura ha sido estudiada en el libro *Guided electromagnetic waves* por Michal Mrozowski [14]. Esta guía de onda tendrá una anchura de 15.8mm y altura de 7.9mm y el dieléctrico introducido 6.32mm de anchura y 3.16mm de altura. El valor de la permitividad es $\epsilon_r = 9$.

Hemos podido comprobar que este método es correcto debido a que hemos obtenido las mismas curvas y valores. Además, debe saberse que en esta estructura es posible obtener modos complejos. Los modos complejos se han estudiado en muchas estructuras, ya que, son particularmente sensibles a las perturbaciones. Numerosas investigaciones realizadas por varios investigadores prueban que no hay ondas complejas a menos que se utilice una alta permitividad. La teoría de la perturbación débil también predice que en una guía de ondas rectangular debemos esperar ondas complejas, incluso cuando la falta de homogeneidad parece ser pequeña.

Partiendo de las ecuaciones (5.8) o (5.9), es posible obtener las características de propagación de la misma forma que en capítulos anteriores, mediante el problema de valores propios. Por lo que basándonos en una de esas dos ecuaciones y teniendo en cuenta las condiciones de contorno, obtendremos las características de propagación mostradas en la figura 5.1, estudiada por Michal Mrozowski [14].

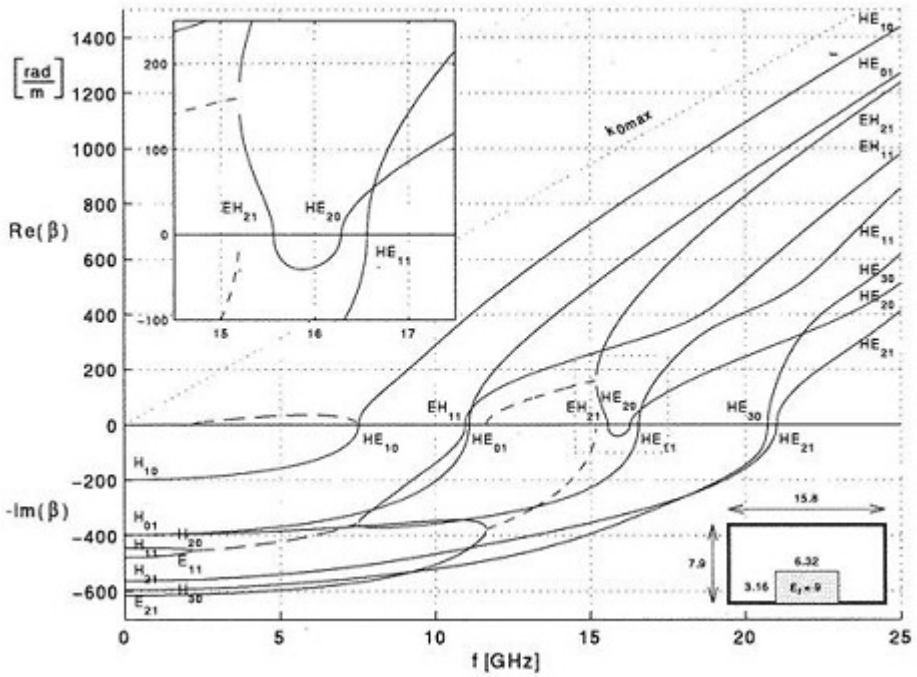


Figura 5.1: Dispersion characteristics of a rectangular waveguide

En la figura 5.2, se puede observar los correctos resultados obtenidos.

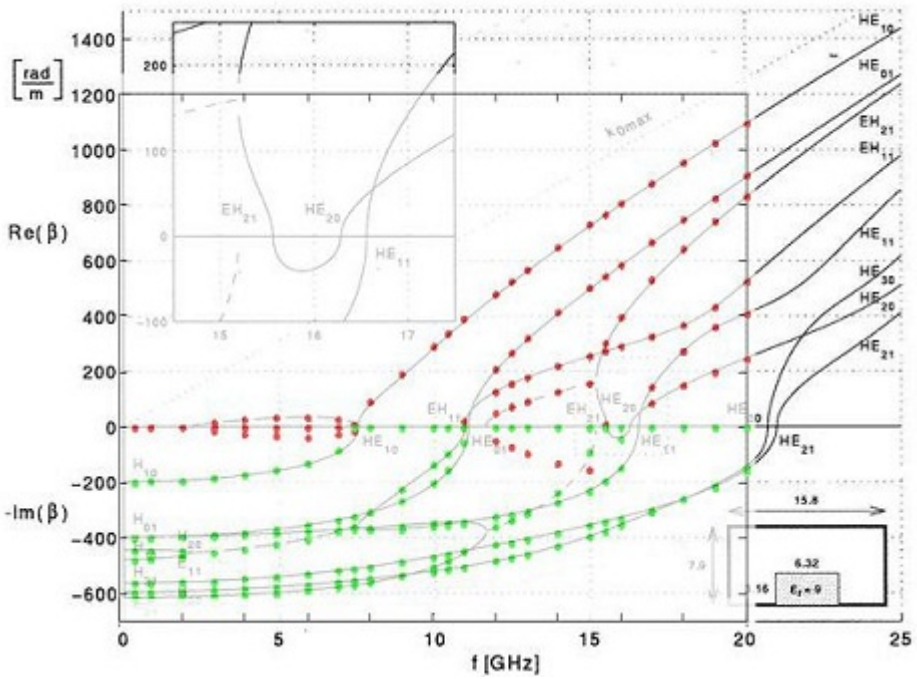


Figura 5.2: Points obtained by Matlab environment

### 5.4.2. Fibra óptica

Otra estructura a analizar ha sido la estudiada en la tesis doctoral de mi supervisor Piotr Kowalczyk llamada *Efektywna analiza światłowodów fotonicznych metodą różnic skończonych w dziedzinie częstotliwości.*

En este caso, los índices de refracción de la fibra serán $n_1 = 8,4$, $n_2 = 2,4025$ y un radio de $a = 0,5\mu m$. Basándonos de nuevo en las ecuaciones (5.8) y (5.9) se obtendrán las características de dispersión pero, en este caso, nos centraremos en el índice de refracción normalizado que depende del coeficiente de propagación.

$$n_{eff} = \frac{\gamma}{jk_o} \tag{5.26}$$

En la figura 5.3, se ven las características de propagación con respecto el índice de refracción de los modos que van a ser estudiados.

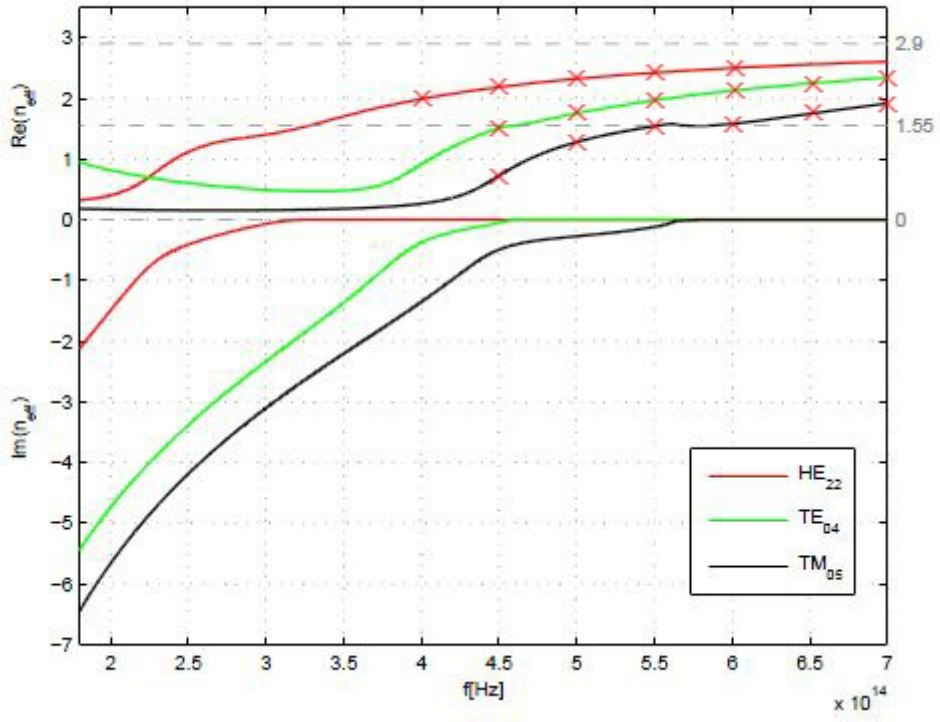


Figura 5.3: Dispersion characteristics for some hybrid modes of the circular waveguide

Se estudiaron los modos $HE_{22}$ $TE_{04}$ y $TM_{05}$, pero pondremos como ejemplo, solo el primer caso. A través del entorno Matlab se consiguió obtener los valores de los índices de refracción que forma la característica de propagación que puede verde en la figura 5.3 para diversas frecuencias. En la siguiente tabla, se muestra los índices de refracción obtenidos que se corresponen con los puntos marcados en la figura 5.3.

| f (GHz) | $4\cdot 10^{14}$ | $4,5\cdot 10^{14}$ | $5\cdot 10^{14}$ | $5,5\cdot 10^{14}$ | $6\cdot 10^{14}$ |
|---|---|---|---|---|---|
| $n_{eff_1}$ | 1,9909 | 2,1873 | 2,258 | 2,4270 | 2,5034 |
| $n_{eff_2}$ | 1,9860 | 2,1844 | 2,3239 | 2,4258 | 2,5025 |

Cuadro 5.1: Propagation coefficients of $HE_{22}$

Y, finalmente, en la figura 5.4, puede verte el modo $HE_{22}$ y $EH_{22}$ obtenido anteriormente.

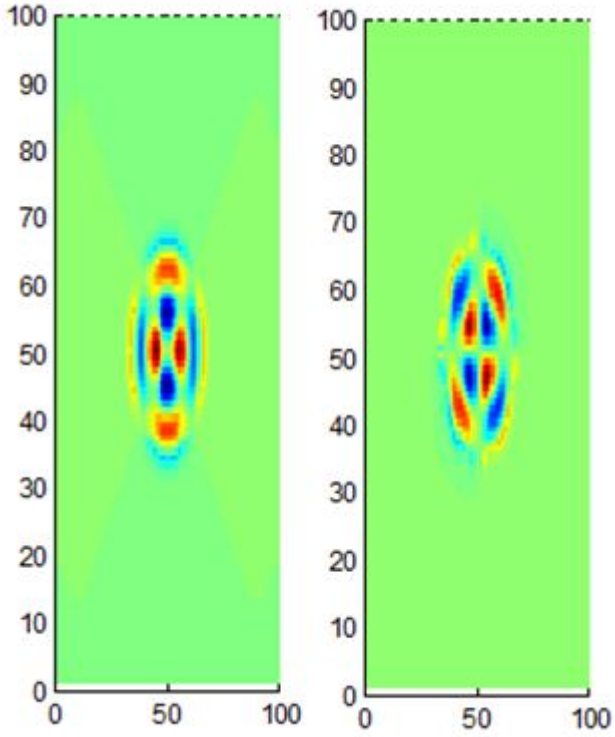


Figura 5.4: Field distribution of $HE_{22}$ hybrid mode

# Capítulo 6

# Conclusiones

FDM se ha aplicado con éxito en el entorno Matlab. Una verificación numérica ha sido realizada para los diferentes tipos de estructura y la validez de los procedimientos ha sido confirmada. De este modo, se logró el objetivo principal de este proyecto educativo. Se ha demostrado que FDM es un método útil y fácil de implementar para resolver los problemas que se comportan de acuerdo con las ecuaciones de Maxwell. También la flexibilidad del algoritmo se ha presentado - el cambio de la geometría del dispositivo analizado no afecta a la estructura principal del algoritmo. Se ha demostrado que este método puede ser muy precisa si se aplica una densidad de malla adecuado (dependiendo de las dimensiones de las estructuras analizadas).

Además, estos estudios pueden utilizarse para mejorar las habilidades de uno de los programas comerciales: sus limitaciones, las fuentes de error y las posibilidades de un uso más eficiente. Por último, es necesario el conocimiento sobre este tipo de métodos numéricos para crear una amplia variedad de herramientas de software específicos que pueden ser perfectamente adaptados a las necesidades de cualquier proyecto específico (los programas de acceso comercial son más limitados).

Los estudios futuros se centrarán sobre las técnicas que mejoran la eficiencia de la FDM. Por ejemplo, el dominio computacional puede ser dividido en subregiones donde se aplican diferentes densidades de malla [1,2]. Algunas áreas de la malla serán más denso, pero en algunos otros la malla genera las variables redundantes. Este enfoque puede significativamente aumentar la eficiencia de los cálculos de reducción de gran número de variables sin perder precisión de los resultados.

# Índice de figuras

# Índice de cuadros

# Bibliografía


[1] Piotr Kowalczyk, M. Wiktor and M. Mrozowski, member IEEE. *"Efficient finite difference analysis of microstructured optical fibers"* Opt. Express 13(25) 10349-10359 (2005)

[2] Piotr Kowalczyk, L. kulas and Michal Mrozowski, member IEEE. *"Analysis of microstructured optical fibers using compact macromodels"* Opt. Express 19(20), 19354-19364 (2011)

[3] Mathew N. O. Sadiku. Ph.D. *"Numerical Techniques in Electromagnetics"*. Second edition, 2000.

[4] David M. Pozar. *"Microwave Engineering"*. Fourth edition, 2011.

[5] Antonio P. *"Aplicación del método de las diferencias finitas en el dominio del tiempo a la resolución de cavidades resonantes"* Proyecto Final de Carrera, Septiembre 2010.

[6] G. Mur. *"A Finite Difference Method for the Solution of Electromagnetic Waveguide Discontinuity Problems"*. Third edition, Microwave Conference,1973.

[7] Karlheinz Bierwirth, Norbert Schulz, and Fritz Arndt, Senior Member, IEEE. *"Finite-Difference Analysis of Rectangular Dielectric Waveguide Structrures"* Volume 34, 1986

[8] K. Pontoppidan *"Numerical Solutions of Waveguide Problems using Finite Difference Methods"* Microwave conference, 1969

[9] Colin G. and James A. R. Ball., Members IEEE *"Mode-Matching Analysis of a Shiefield Rectangular Dielectric-Rod Waveguide"* Volumen 53, October 2005

[10] P. H. Vartantan, W. P. Ayrest, and A. L. Helgesson, IEEE. *"Propagation in Dielectric Slab Loaded Rectangular Waveguide"* Microwave techniques, 1958

[11] N. Kaneda, B. Houshmand, T. Itoh, IEEE. *"FDTD Analysis of Dielectric Resonators with Curved Surfaces"* Volumen 45, 1997

[12] Kawthar A. Zaki, senior member IEEE and Chunming Chen, studen member IEEE. *"Intensity and Distribution of Hybrid-Mode Fields in Dielectric-Loaded Waveguides"* Microwave Techniques, December 1985

[13] A. Knoesen, member IEEE, T. K. Gaylord, Fellow IEEE, and M. G. Moharam, senior member, IEEE. *"Hybrid Guided Modes in Uniaxial Dielectric Planar Waveguides"* Volumen 6, June 1988

[14] Michal Mrozowski, member IEEE. *"Guided Electromagnetics Waves- Properties and Analysis"* 1997

[15] Lukasz Kulas and Michal Mrozowski, member IEEE. *"Reduced-Order Models in FDTD"* Volumen 11, October 2001

[16] Piotr Kowalczyk, Michal Mrozowski, member IEEE. *"Hybrid Accurate Finite Difference Analysis of Leaky, Guided and Complex Waves in Photonic Optical Fibers and Dielectric Waveguiding Structures"* 2011/2012